

https://dspace.org/

Heat Shock Factor (HSF) Expression and Its Effect on Life Table Parameters in the Main African Malaria Vector Anopheles funestus

Bloch, Nerissa Wendy

2024
University of the Witwatersrand, Johannesburg
https://hdl.handle.net/10539/47349

Bloch, Nerissa Wendy. (2024). Heat Shock Factor (HSF) Expression and Its Effect on Life Table Parameters in the Main African Malaria Vector Anopheles funestus [PhD thesis, University of the Witwatersrand, Johannesburg]. WIReDSpace.

Downloaded from a DSpace repository. https://dspace.org/

UNIVERSITY OF THE WITWATERSRAND

HEAT SHOCK FACTOR (*HSF*) EXPRESSION AND ITS EFFECT ON LIFE TABLE PARAMETERS IN THE MAIN AFRICAN MALARIA VECTOR *ANOPHELES FUNESTUS*

Nerissa Wendy Bloch

456102



UNIVERSITY OF THE WITWATERSRAND, JOHANNESBURG

School of Pathology

A Thesis submitted to the Faculty of Health Sciences, University of the Witwatersrand, Johannesburg, in fulfilment of the requirements for the degree of

Doctor of Philosophy

Johannesburg, 2024

DECLARATION

I, Nerissa Wendy Bloch, declare that this Thesis is my own, unaided work. It is being submitted for the Degree of Doctor of Philosophy at the University of the Witwatersrand, Johannesburg. It has not been submitted before for any degree or examination at any other University.



(Signature of candidate)

13th day of July in 2024

DEDICATION

For Lara Gabriella Bloch:

my twin sister, better half, and forever friend.



POSTER PRESENTATION

Bloch, N. W., Dahan-Moss, Y. L. and Koekemoer, L. L. (2019) The role of a sex-limited esterase (*EZ976679*) in *Anopheles funestus* males. Entomology Society of Southern Africa Congress, Umhlanga, KwaZulu- Natal, South Africa, 8- 11 July 2019.

Role: I did all the analysis, interpretation and presented this work in a poster. This was part of a study I did during my PhD. This project was terminated when the gene *EZ976679*, did no amplify consistently and the results were not reproducible. I therefore changed projects to this study.

ORAL PRESENTATION

Bloch, N. W., Dahan-Moss, Y. L. and Koekemoer, L. L. (2024) Heat shock factor transcript abundance and its effect on life table parameters in the main African malaria vector *Anopheles funestus*. Molecular Biosciences Research Thrust, Johannesburg, South Africa, 7 December 2023.

Bloch, N. W., Dahan-Moss, Y. L. and Koekemoer, L. L. (2024) Heat shock factor transcript abundance and its effect on life table parameters in the main African malaria vector *Anopheles funestus*. WITS Research Institute for Malaria (WRIM) Research Day, Johannesburg, South Africa, 25 April 2024.

Role: I did all the analysis and interpretation and presented this work in a 10-minute oral presentation.

PUBLICATIONS

Bloch, N. W., Dahan-Moss, Y. L. and Koekemoer, L. L. (2024) Heat shock factor transcript abundance and its effect on life table parameters in the main African malaria vector *Anopheles funestus*. Insect Molecular Biology, in draft.

Role: I wrote the fifth draft of a paper (awaiting comments from the co-authors) to be submitted to the journal Insect Molecular Biology. I did all the experimental work and analysis.

ABSTRACT

Anopheles funestus is a major malaria vector, which is predominantly responsible for malaria transmission in Africa and this vector needs to be controlled due to the devastation of the disease. Temperatures worldwide are rising steadily, which can affect mosquito distribution and behaviour. Heat shock factor (HSF), a transcription factor, is crucial in these physiological and behavioral processes. This is because HSF has a high degree of functional variability and is temperature dependent, enabling mosquitoes to survive the heat by repairing damaged proteins in the cell. This study aimed to understand the biological role of HSF in the African malaria vector *An. funestus* with regard to *HSF* transcript abundance and its effect on life table parameters. In this work, the *HSF* gene was the target of RNA interference (RNAi). RNAi was implemented using short interfering RNA (siRNA) that was previously synthesised and was performed to understand the role of HSF in *An. funestus*. *HSF* is a poorly understood gene, yet it has been found to have a variety of functions within insects and, more specifically, mosquitoes. Understanding the role of *HSF* in *An. funestus* is important to advance knowledge in this understudied vector. *HSF* transcript abundance was measured using real-time quantitative PCR (qPCR) throughout the four life stages in *An. funestus* in order to assess the average expression levels of HSF at 25°C. The *HSF* transcript abundance was significantly lower during the egg and pupal stages in comparison to the larval and adult stages. Inhibition, via siRNA, of the *HSF* transcript was subsequently used to understand its biological role in *An. funestus.* A system was designed to deliver the siRNA to the adult using the ingestion of sugar water. This was the chosen delivery system due to its ease of use and the potential to replicate this method in the wild because of the sugar-feeding behaviour of the adult mosquitoes. A known reference gene, *RPL19,* was used to evaluate the efficiency of

a “siRNA-sugar feeding delivery system” in *An. funestus.* Results showed this would be an effective system for evaluating transcript inhibition or knockdown. Different concentrations of HSF-siRNA were utilised, 10 ng/µl, 20 ng/µl and 30 ng/µl at three different temperatures of 20°C, 25°C and 30°C, to evaluate the impact of different concentrations and temperatures on the fold change of *HSF* transcript abundance after siRNA treatments. A 20 ng/µl siRNA concentration at 25°C reduced the HSF transcript abundance. Therefore, these conditions were selected to study the phenotypic effect of HSF-siRNA on longevity and reproduction in *An. funestus*. Longevity, fertility, fecundity, and time-to-hatch were all reduced when mosquitoes were treated with HSF-siRNA. In addtion, the impact of decreased survivability in males was more prominent than in females. In conclusion, HSF might regulate vector development and needs to be investigated in the future. Furthermore, this study confirms the pleiotropic effect of HSF in *An. funestus*.

ACKNOWLEDGEMENTS

I would like to acknowledge my supervisor Prof. Lizette Koekemoer. Her knowledge, patience, and assistance wherever possible allowed me to complete this degree. I appreciate her giving me the technical and monetary assistance I needed to acquire the scientific expertise I needed to carry out my research. She also gave me the opportunity to discuss my findings at national conferences, which helped enhance my career as a scientist, and for that I am grateful. It is such an honour to have worked with Lizette and I am forever grateful for what you taught me academically and in other spheres of life. Your emotional support and advice allowed me to get up each day and conduct my research, so thank you.

I would like to thank Dr. Yael Dahan-Moss for her assistance in the project structure and extensive knowledge.

I would like to express my gratitude to Professor Basil Brooke. I am a much better scientist today thanks to the abilities I developed in his department. Thank you for having me as a student in his department at the Vector Reference Laboratory.

I am appreciative for the financial support received for this project from the National Research Foundation (NRF) in the form of the DST/NRF Research Chair Initiative grant awarded to Prof. Koekemoer. This research would not have been able to be accomplished without this help and funding.

Thank you to my fellow staff and students from Vector Reference Laboratory and WITS Institute for Malaria for all your advice, assistance and for being there to listen to my research predicaments and for offering solutions.

I wish to extend my deepest gratitude to my wonderful family. Mom and Dad, thank you for always being there for me through this very tumultuous journey and for your patience and unwavering love over the years it has taken me to complete this degree. Lara (to whom this dissertation is dedicated to), my twin sister and better half, I just want to express my thanks for being my rock, constant and sunshine. I would not be here without you. Thank you for being my continual source of strength.

TABLE OF CONTENTS

Declaration……..ii

Dedication……..iii

Presentations and Publications……iv

Abstract……vi

Acknowledgements……viii

List of Figures……xvi

List of Tables……..xx

List of Abbreviations……...xxi

CHAPTER 1: INTRODUCTION: MALARIA AND THE MAJOR AFRICAN MALARIA VECTOR, *ANOPHELES FUNESTUS*

1.1. Malaria. **1**

1.2. Malaria Vector Control **2**

1.3. *Anopheles funestus* **4**

1.4. Temperature Effects on Mosquitoes **6**

1.4.1. Effect of temperature on mosquito susceptibility to insecticides 6

1.4.2. Effect of temperature on *Plasmodium* infection 7

1.4.3. Effect of temperature on mosquito larvae and adults 8

1.5. Heat Shock Response **10**

1.5.1 Heat shock proteins 12

1.5.2. Heat shock factor (HSF) 14

1.6. Study rationale **17**

1.7. Aim and Objectives **18**

CHAPTER 2: *HSF* TRANSCRIPT ABUNDANCE DURING THE FOUR LIFE STAGES OF *ANOPHELES FUNESTUS*

2.1. Introduction **20**

2.1.1. Aim and objectives 22

2.2. Materials and Methods **23**

2.2.1. Study samples 23

2.2.2. Experimental setup to determine that the designed HSF primers efficiently target the *HSF* gene 24

2.2.2.1. Primer design 24

2.2.2.2. RNA extraction and cDNA synthesis 25

2.2.2.3. Confirmation of HSF primers 26

2.2.3. Experimental setup for assessing *HSF* transcript abundance at different life stages 29

2.2.3.1. Obtaining study samples 29

2.2.3.2. Spermathecal capsule dissection 29

2.2.3.3. Obtaining samples from each life stage 30

2.2.3.4. RNA extraction and cDNA synthesis 34

2.2.3.5. Reference gene selection 34

2.2.3.6. Real-time PCR for quantitative analysis 36

2.2.3.7. Data analysis 36

2.3. Results 37
2.3.1. HSF-designed primers successfully amplified the *HSF* gene 37
2.3.2. Reference gene selection 38
2.3.3. Sequencing confirming reference gene identity 39
2.3.4. *HSF* transcript abundance across the different life stages 40
i. Confirmation of mating 40
ii. HSF transcript abundance 41
2.4. Discussion 42
2.5. Conclusion 46

CHAPTER 3: EXPLORING SUGAR WATER AS A DELIVERY MEDIUM FOR siRNA-MEDIATED GENE KNOCKDOWN AND VALIDATION THROUGH *RPL19* IN *ANOPHELES FUNESTUS*

3.1. Introduction 47
3.1.1. Ribonucleic acid interference (RNAi) 47
3.1.2. Receptor-mediated endocytosis to assist in cell membrane crossing 50
3.1.3. Delivery systems used to introduce dsRNA into an organism 51
3.1.4. Aim and objectives 54
3.2. Materials and Methods 54
3.2.1. Best feeding proportions to maximise feeding success 54
3.2.2. Short Interfering RNA (siRNA) 57
3.2.3. Experimental setup to validate siRNA delivery system using *RPL19* transcript abundance 57
3.2.4. RNA Extraction and cDNA Synthesis 58
3.2.5. *RPL19* sequence identity confirmation 58
3.2.6. Data analysis 59
3.3. Results 59
3.3.1. Feeding optimisation 59
3.3.2. RPL19 sequence identity confirmation 60
3.3.3. Experimental setup to validate siRNA delivery system using *RPL19* 60
3.4. Discussion 62
3.5. Conclusion 63

CHAPTER 4: ACHIEVING KNOCKDOWN OF HEAT SHOCK FACTOR (HSF) IN *ANOPHELES FUNESTUS* VIA SPECIFIC SHORT-INTERFERING RNA (siRNA)

4.1. Introduction 64

4.1.1. Aim and objectives 65

4.2. Materials and methods 65

4.2.1. Confirming that the optimised protocol (described in Chapter 3) could successfully be used to achieve HSF knockdown 65

4.2.1.1. Short interfering RNA 65

4.2.1.2. Experimental setup 66

4.2.2. Determining the effect of siRNA concentration and adult exposure temperatures on *HSF* transcript reduction 67

4.2.2.1. Experimental set up 67

4.3. Results 69

4.3.1. Real-time PCR for quantitative analysis for the optimised protocol (as described in Chapter 3) to assess success in HSF knockdown 69

4.3.2. Determination of the impact of siRNA concentration and specific temperatures on HSF transcript abundance 70

i. Adults housed at 20°C 71

a. 10 ng/µl 71

b. 20 ng/µl 72

c. 30 ng/µl 73

ii. Adults housed at 25°C 73

d. 10 ng/µl 73

e. 20 ng/µl 75

f. 30 ng/µl 76

iii. Adults housed at 30°C 77

g. 10 ng/µl 77

h. 20 ng/µl 78

i. 30 ng/µl 79

j. Effect of siRNA concentration on HSF transcript abundance at a set temperature 80

k. The impact of adult exposure to varying temperature on *HSF* transcript abundance 81

4.4. Discussion 84

4.5. Conclusion 88

CHAPTER 5: THE EFFECT OF siRNA TARGETING THE *HSF* GENE, ON LIFE TABLE PARAMETERS OF *ANOPHELES FUNESTUS*

5.1. Introduction 89

5.1.1. Role of HSF on survival 89

5.1.2. *Anopheles funestus* female reproductive fitness 91

5.1.3. Aim and Objectives 93

5.2. Materials and methods 94

5.2.1. Experimental setup for longevity studies 94

5.2.2. Experimental setup for fecundity studies 95

5.2.3. Experimental setup to determine time-to-hatch and fertility studies . 98

i. Fertility 98

ii. Time-to-hatch 98

5.2.4. Confirmation of siRNA knockdown throughout the experiment 98

5.2.5. RNA Extraction and cDNA Synthesis 100

5.2.6. Real-time PCR for quantitative analysis 100

5.3. Results 100

5.3.1. Effect of HSF knockdown on *An. funestus* longevity 100

5.3.2. Spermathecal capsule dissection 102

5.3.3. Effect of HSF knockdown on *An. funestus* fecundity 103

5.3.4. Effect of HSF knockdown on *An. funestus* fertility and time-to-hatch 104

i. Fertility 104

ii. Time-to-hatch 105

5.3.5. Confirmation of siRNA knockdown throughout the experiment 106

5.4. Discussion 109

CHAPTER 6: CONCLUSION 113

REFERENCES 118

APPENDICES

APPENDIX A: Permission obtained to use Figure 3 167

APPENDIX B: CDNA Dilutions for Determining *HSF* Transcript Abundance in All Four *An. funestus* Life Stages 168

APPENDIX C: Permission obtained to use Figure 6 171

APPENDIX D: Reference Gene Selection CT Values 172

APPENDIX E*:* HSF Sequencing Results 174

APPENDIX F: HSF Transcript Abundance In All Life Stages (Fig 13) 180

APPENDIX G: cDNA Calculations To Validate SiRNA Delivery System Using *RPL19* 186

APPENDIX H: *RPL19* Transcript Abundance 189

APPENDIX I: cDNA Dilutions To Determine The Effect of Concentration and Temperature On HSF Knockdown 192

APPENDIX J*: An. funestus* Treated With HSF-SiRNA..... 196

APPENDIX K: HSF normalised against the control mean values for each treatment 224

APPENDIX L: cDNA Dilutions To Confirm SiRNA Knockdown Throughout The Life Table Parameter Experiment..... 225

APPENDIX M: Change Of Title Of Research..... 227

APPENDIX N: Ethics Clearance Certificate 228

APPENDIX O: Plagiarism Declaration And Turnitin Report 229

APPENDIX P: Publication Draft (awaiting comments from co-authors) 231

LIST OF FIGURES

CHAPTER 1

Figure 1: Heat shock response pathway. 11
Figure 2: Schematic illustration of the typical HSF protein domains. 15
Figure 3: Heat shock response by activation of HSF. 16

CHAPTER 2

Figure 4: The life stages of the anopheline mosquito life cycle 21
Figure 5: *HSF* gene and the position of the primers 24
Figure 6: Complementary DNA (cDNA) synthesis. 26
Figure 7: Flow diagram of the methods involved in determining if the HSF primers that were designed targeted the *HSF* gene 28
Figure 8: Illustration of the oviposition cup. 30
Figure 9: Microscope images showing the four stages of *An. funestus* development 32
Figure 10: Flow diagram of the methods involved in assessing life stage transcript abundance 33
Figure 11: PCR using HSF primer pairs 38
Figure 12: The percentage of mating success in females across three biological replicates 41
Figure 13: The relative *HSF* transcript abundance normalised against the reference genes, *RPS7* and *GAPDH*, across the four life stages of *An. funestus*. 42
Figure 14: Graphical representation of the *HSF* transcript abundance profile 44

CHAPTER 3

Figure 15: Mechanism of siRNA silencing 49
Figure 16: Schematic representation of cell types that form the insect midgut epithelium 51
Figure 17: Illustration showing how the paper cups containing mosquitoes were covered to perform feeding optimisation experiments without siRNA treated sugar water 55
Figure 18: Feeding cups 56

Figure 19: *Anopheles funestus* female adults viewed under a dissecting microscope……... 59
Figure 20: The normalised relative *RPL19* transcript abundance values against the reference genes, *RPS7* and *GAPDH,* in males (A) and females (B) after treatment with 20 ng/µl RPL19-siRNA and 20 ng/µl β2m-siRNA at 25°C.. 61

CHAPTER 4

Figure 21: Flow diagram of the methods involved in determining if the protocol described in chapter 3 can achieve HSF knockdown 67
Figure 22: Flow diagram of the methods involved in determining the level of transcript abundance after siRNA ingestion 68
Figure 23: The relative *HSF* transcript abundance normalised against the reference genes, *RPS7* and *GAPDH*, in males (A) and females (B) at 25°C with treatment of 20 ng/µl siRNA 70
Figure 24: The relative *HSF* transcript abundance normalised against the reference genes, *RPS7* and *GAPDH*, in males (A) and females (B) at 20°C with treatment of 10 ng/µl siRNA 71
Figure 25: The relative *HSF* transcript abundance normalised against the reference genes, *RPS7* and *GAPDH*, in males (A) and females (B) at 20°C with treatment of 20 ng/µl siRNA 72
Figure 26: The relative *HSF* transcript abundance normalised against the reference genes, *RPS7* and *GAPDH*, in males (A) and females (B) at 20°C with treatment of 30 ng/µl siRNA 74
Figure 27: The relative *HSF* transcript abundance normalised against the reference genes, *RPS7* and *GAPDH*, in males (A) and females (B) at 25°C with treatment of 10 ng/µl siRNA 75
Figure 28: The relative *HSF* transcript abundance normalised against the reference genes, *RPS7* and *GAPDH*, in males (A) and females (B) at 25°C with treatment of 20 ng/µl siRNA 76
Figure 29: The relative *HSF* transcript abundance normalised against the reference genes, *RPS7* and *GAPDH*, in males (A) and females (B) at 25°C with treatment of 30 ng/µl siRNA 77

Figure 30: The relative *HSF* transcript abundance normalised against the reference genes, *RPS7* and *GAPDH*, in males (A) and females (B) at 30°C with treatment of 10 ng/µl siRNA 78
Figure 31: The relative *HSF* transcript abundance normalised against the reference genes, *RPS7* and *GAPDH*, in males (A) and females (B) at 30°C with treatment of 20 ng/µl siRNA 79
Figure 32: The relative *HSF* transcript abundance normalised against the reference genes, *RPS7* and *GAPDH*, in males (A) and females (B) at 30°C with treatment of 30 ng/µl siRNA 80
Figure 33: The relative *HSF* transcript abundance normalised against the no-siRNA control in males at 20°C (A), 25°C (B) and 30°C (C) after treatment with 10 ng/µl, 20 ng/µl and 30 ng/µl HSF-siRNA 82
Figure 34: The relative *HSF* transcript abundance normalised against the no-siRNA control in females at 20°C (A), 25°C (B) and 30°C (C) after treatment with 10 ng/µl, 20 ng/µl and 30 ng/µl HSF-siRNA 83
Figure 35: The relative *HSF* transcript abundance normalised against the no-siRNA control in males with an HSF-siRNA concentration of 10 ng/µl (A), 20 ng/µl (B) and 30 ng/µl (C) across all three temperatures 83
Figure 36: The relative *HSF* transcript abundance was normalised against the no-siRNA control in females with an HSF-siRNA concentration of 10 ng/µl (A), 20 ng/µl (B) and 30 ng/µl (C) across all three temperatures. 84

CHAPTER 5

Figure 37: Flow diagram of the methods involved in assessing longevity 95
Figure 38: Flow diagram of the methods involved in assessing fecundity 97
Figure 39: Flow diagram of the methods involved in assessing fertility 99
Figure 40: Kaplan-Meier survival analysis of male *An. funestus* assessed after treatment with siRNA 101
Figure 41: Kaplan-Meier survival analysis of female *An. funestus* assessed after treatment with siRNA 102
Figure 42: Mating success in females across three treatments 103

Figure 43: Kaplan-Meier time-to-event of *An. funestus* fertility (time-to-hatch) assessed after treatment with siRNA. Samples treated with HSF-siRNA in pink; β2m-siRNA in purple and the no-siRNA control in green. ... **Error! Bookmark not defined.**

Figure 44: The normalised relative *HSF* transcript abundance values against the reference genes, *RPS7* and *GAPDH,* in males (A) and females (B) two days post treatment with 20 ng/µl HSF-siRNA and β2m-siRNA at 25°C. 107

Figure 45: The normalised relative *HSF* transcript abundance values at day 10 against the reference genes, *RPS7* and *GAPDH,* in males after treatment with 20 ng/µl HSF- siRNA and β2m-siRNA at 25°C..... 108

LIST OF TABLES

CHAPTER 2

Table 1: Primers sequences and amplicon length of the predicted product.……..24
Table 2: Primers sequences, melting temperatures and amplicon lengths for each reference gene that was evaluated in qPCR. 35
Table 3: Stability values of each reference gene..... 39

CHAPTER 3

Table 4: Primers sequences and amplicon length of RPL19-siRNA and β2m-*siRNA*..... 57

CHAPTER 4

Table 5: Primers sequences and amplicon length for the HSF-siRNA 66

CHAPTER 5

Table 6: Mean fecundity values between the *An. funestus* mosquitoes which ingested three siRNA treatments (HSF, β2m and no-siRNA control)..... 104
Table 7: Mean fertility values between the *An. funestus* mosquitoes which ingested one of three siRNA treatments (HSF, β2m or no-siRNA control). **Error! Bookmark not defined.**

LIST OF ABBREVIATIONS

A260/280	The ratio of absorbance at 260nm and 280nm
A260/230	The ratio of absorbance at 260nm and 230nm
Acp	Accessory gland proteins
Ago	Argonaute protein
ATP	Adenosine triphosphate
ATSB	Attractive toxic sugar bait
Ae.	Aedes
An.	Anopheles
ANOVA	Analysis of variance
β2m	Beta-2 microglobulin
bp	Base pairs
BLAST	Basic local alignment tool
CC	Columnar cells
cDNA	Complementary DNA
Co.	Company
CRISPR-i	Clustered regularly interspaced short palindromic repeats interference
Ct	Quantification cycle
∆Ct	Change in Ct
∆∆Ct	Delta Ct
Cx.	Culex
°C	Degrees Celsius
D.	*Drosophila*
DBD	DNA binding domain
DDT	Dichlorodiphenyltrichloroethane
DF	Degrees of freedom
DNA	Deoxyribonucleic acid
dsDNA	Double-stranded DNA
dsRNA	Double-stranded RNA
EC	Endocrine cells
EMBOSS	European Molecular Biology Open Software Suite
Et al	*Et al*ia
Etc	Et cetera
FANG	A laboratory strain of *An. funestus* mosquitoes originally collected from Angola
FC	Fold change
FUN18S	*Funestus* ribosomal protein 18S
EMBOSS	European Molecular Biology Open Software Suite
FUMOZ	A laboratory strain of *An. funestus* mosquitoes originally collected from Mozambique
g	Grams
GAPDH	Glyceride 3-phosphate dehydrogenase
HSE	Heat shock element

HSD	Honestly significant difference
HSF	Heat shock factor
HSP	Heat shock protein
IGR	Heptad repeat
HR	Insect growth regulator
IPCC	Intergovernmental Panel on Climate Change
IRS	Indoor residual spraying
ITNs	Insecticide-treated nets
Ltd.	Limited
LLINs	Long-lasting insecticide-treated be nets
mRNA	Messenger RNA
µM	Micromolar
µm	Micrometre
µg	Microgram
MV	Microvilli
ng/µl	Nanograms per microlitre
NICD	National Institute for Communicable Diseases
nm	Nanometre
NTC	No template control
%	Percentage
PBO	Pyrethroids with piperonyl-butoxide
P.	*Plasmodium*
PKA	Protein kinase
PCR	Polymerase chain reaction
PAZ	Piwi-Argonaute-Zwille domain
PRRs	Pattern recognition receptors
qPCR	Real-time quantitative PCR
RD	Regulatory domain
RdRP	RNA-dependent RNA polymerase
RPS7	Ribosomal protein S7
RPS26	Ribosomal protein S26
RISC	RNA-induced silencing complex
RNA	Ribonucleic acid
RNAi	RNA mediated interference
RNase III	Ribonuclease III
RPL19	Ribosomal protein L19
SC	Stem cells
SID-1	Systemic RNA interference deficiency-1
SIRT1	Nicotinamide adenine dinucleotide dependent sirtuin
S.D.	Standard deviation
SEM	Standard error of the mean
sHSPs	Small heat shock proteins
siRNA	Short interfering RNA
s.s.	*Sensu stricto*
ssRNA	Single-stranded RNA
SUMO	Small ubiquitin modifying protein
TAD	Trans-activation domain
UPS	Ubiquitin (Ub)-proteosome system
vs	Versus

CHAPTER 1

INTRODUCTION: MALARIA AND THE MAJOR AFRICAN MALARIA VECTOR, *ANOPHELES FUNESTUS*

1.1. Malaria

Malaria is endemic in Africa and the World Health Organization (WHO) reported 249 million cases of malaria worldwide in 2022 with 608 000 deaths (WHO, 2023A). This tropical disease is caused by the transmission of a protozoan, mainly *Plasmodium falciparum* (Rogers and Randolph, 2000). The parasite is transmitted to humans, specifically by female *Anopheles* (Sinka *et al*., 2010). This happens when the *Anopheles* female ingests a blood meal from a human host infected with *Plasmodium* parasites and becomes infected herself. The female then bites a human and infects the human with the parasite (Aly *et al*., 2009). The parasites undergo several developmental stages before moving into the salivary glands of the *Anopheles* female (Sato, 2021). Once the infected female consumes a blood meal, the mature parasites (sporozoites) in the female's salivary glands can spread to the next human host.

Malaria is a devastating disease which has been shown to not only have a huge impact on the health burden but also has big socio-economic implications. Effects such as drastically lower economic growth due to unemployment, contribute to poverty and lower levels of education. This is mainly due to the absence from school (Carrasco-Escobar *et al*., 2021). Households suffer significant costs such as food and medical costs when a household member is sick with malaria. The direct and indirect costs of malaria might be substantial, further impoverishing poor households. The mean direct cost of seeking care for malaria was estimated at 2%–2.9% of household income

(Ricci, 2012). Therefore, every control effort, including the vector control, is necessary to combat this disease.

1.2. Malaria Vector Control

The focus of malaria vector control, using insecticides as one of the ways of control, is to limit or prevent human-vector contact (Sinka *et al*., 2010; WHO, 2020). After World War II, the amount of the organochlorine, dichlorodiphenyltrichloroethane (DDT), used for agricultural and anti-malaria house spraying, increased (Pampana, 1969). However, DDT resistance began to spread throughout different vector populations and prompted the creation and development of substitute insecticides such as pyrethroids, organophosphates, pyrroles, neonicotinoids, broflanilide, and carbamates (WHO, 1997; Govoetchan *et al*., 2022; Ashu *et al*., 2023). Currently, long-lasting insecticide-treated bed nets (LLINs) and indoor residual spraying (IRS) are the main chemical interventions that are widely used to target the malaria vector (Pryce *et al*., 2022).

The insecticide classes approved by the WHO for use in LLINs were historically limited to pyrethroids (Killeen *et al*., 2017). The pesticides are embedded into the nets' fibres, killing or deterring anthropophilic (feeding on humans) and endophilic (resting indoors) vectors from feeding. A new type of insecticide-treated net (ITN) that combines pyrethroids with piperonyl-butoxide (PBO) was subsequently used after a recommendation by WHO in 2017 (WHO, 2017). PBO is a synergist that increases the potency of pyrethroids against monooxygenase metabolic resistant mosquitoes. Recently, two new bed net formulations have been approved for vector control use. The first is pyrethroid-chlorfenapyr nets, a mix of pyrethroid and pyrrole insecticides to increase the killing power of the net (Syme *et al*., 2023). The second net type contains

an insect growth regulator (IGR), pyriproxyfen, and a pyrethroid. The IGR prevents mosquito reproduction and growth (Accrombessi *et al.,* 2023; WHO, 2023B). As mentioned above, another preventive strategy used to reduce human-vector contact is IRS (Brooke *et al.*, 2013; WHO, 2015). Insecticides are sprayed on house walls as part of this preventative treatment to lessen the number of endophilic and endophagic (feeding indoors) malaria vectors.

Both LLINs and IRS have been demonstrated to be efficient and effective when carried out proficiently (WHO, 2022B). However, these treatments are frequently undermined by the target vector populations' rising pesticide (insecticide) resistance rates. The term "insecticide resistance" describes the alteration in an insect's capacity to tolerate or overcome the harmful effects of one or more insecticides as a result of particular characteristics or behaviours that have evolved through natural selection (Zoh *et al.,* 2021; Adams *et al*., 2023). The cumulative use of insecticides for vector control and ongoing use in agriculture has resulted in the selection of resistance in several malaria vector populations (Brooke *et al*., 2013; Ahmed *et al*., 2022; Kahamba *et al*., 2022; Nkya *et al*., 2022; Zinszer and Talisuna, 2022). Agricultural insecticides generally end up in water bodies, which are also the larval breeding sites. Larvae exposure to these agricultural insecticides results in selection for resistance, including adult resistance (Ansari *et al*., 2014). Various samples of malaria vectors were tested for insecticide resistance and 90% of these in the WHO African regions have resistance to at least one of the five pesticide classes, and 32% are known to be resistant to four of the five insecticide classes (WHO, 2022A). This resistance might prevent malaria vectors from being killed by a standard dose of insecticides used in LLINs or IRS implementation (Okal *et al*., 2015; Ugwu, 2023; WHO, 2023C).

South Africa is one of the textbook examples illustrating vector control failure due to insecticide resistance and how this impacted malaria transmission. *Anopheles funestus*, a major malaria vector in Africa, has been eradicated from South Africa since the 1950s owing to vector control measures involving DDT (Olivier, 1950). However, in South Africa, the malaria control program replaced the use of DDT with pyrethroids in 1996 due to increased pressure and concern about its negative effects on people and the environment (Sharp and le Sueur, 1996; Hargreaves *et al*., 2000; Bouwman *et al.,* 2011; Thuy, 2015). Moving away from DDT prompted a malaria outbreak in South Africa. The population of *An. funestus* from southern Mozambique was pyrethroid-resistant, which was unknown then, and *An. funestus* slowly reinvaded South Africa in 1996. In 2000, this led to a malaria pandemic that resulted in almost 65 000 malaria cases (Coetzee *et al*., 2013). This highlighted not only the impact of insecticide resistance on malaria vector control and malaria transmission, but also South Africa's vulnerability to malaria transmission. Insecticide resistance in *An. funestus* and other malaria vector species is a widespread problem in Africa and additional control interventions are necessary to reduce malaria transmission (Liu, 2015; Richards *et al*., 2020; WHO, 2022B; Suh *et al*., 2023). Since *An. funestus* is the focus of this study, it is discussed in more detail below.

1.3. *Anopheles funestus*

Anopheles funestus sensu stricto (*An. funestus s.s.*, called *An. funestus* going forward) is a member of the *An. funestus* group that consists of at least 11 morphologically similar African species, which are distinguished by using molecular and cytogenetic techniques (Gillies and De Meillon, 1968; Gillies and Coetzee, 1987; Koekemoer *et al*., 2002; Cohuet *et al.,* 2003; Spillings *et al.,* 2012). *Anopheles funestus* is a major malaria

vector in Africa (Sinka *et al*., 2010) and the *P. falciparum* infection rates in females range between 11% to 50% as seen in a Tanzanian study (Mapua *et al.,* 2022). *Anopheles funestus* achieves its efficient vector capacity due to its anthropophilic, endophilic and endophagic behaviour (Gillies and De Meillon, 1968; Gillies and Coetzee, 1987; Coetzee and Fontenille, 2004; Charlwood, 2017; Wat'senga *et al*., 2018). This species requires permanent or semi-permanent water bodies with some form of vegetation for larval breeding. However, the use of other non-traditional breeding sites, e.g., irrigated fields, tree holes that catch rainfall, ponds and pools formed by rainfall, have also been reported (Gillies and De Meillon, 1968; Dia *et al.,* 2013; Aikpon, 2017; Djouaka, 2017).

There are several studies relating to insecticide resistance in *An. funestus* (Coetzee and Koekemoer, 2013; Mungezi *et al*., 2022; Ngongang-Yipmo *et al*., 2022; Suh *et al.*, 2023) and the various factors affecting the behaviour and life stages of this species (Ngowo *et al*., 2021; Zengenene *et al.,* 2021A; Felamboahangy *et al.,* 2023). However, the knowledge regarding *An. funestus* physiology and life parameters is still somewhat limited compared to the information available on other main African malaria vector species, such as *Anopheles gambiae.* This is due to the difficulty in colonisation of *An. funestus* in set laboratory or insectary conditions (Gillies and De Meillon, 1968; Nepomichene *et al*., 2017; Ngowo *et al*., 2021). Colonisation difficulty is mainly due to low mating success and this species needs approximately 10 days for optimal mating under laboratory conditions (Maharaj *et al*., 2022). This is much longer than the three days reported for the other African malaria vectors, e.g., *Anopheles arabiensis* (Munhenga *et al*., 2016). It is necessary to increase the biological knowledge of *An. funestus* to advance vector control methods.

Since this study will investigate the heat shock factor (part of the heat shock response), the biological impact of temperature (insecticide susceptibility, parasite development and life table parameters) on mosquito vectors, including *An. funestus*, will be discussed in more detail as background information.

1.4. Temperature Effects on Mosquitoes

1.4.1. Effect of temperature on mosquito susceptibility to insecticides

As mentioned above, insecticide resistance is a big concern for malaria vector control efforts. Insects' metabolism, binding affinity, and chemical uptake of insecticides are impacted by changes in ambient temperature (Whiten and Peterson, 2015). This impacts the capacity of insects to detoxify insecticides and develop metabolic resistance. Changes in insecticide susceptibility in mosquito vector populations are due to the physiological stress induced by temperatures higher than 35°C (Oliver and Brooke, 2017). Few studies have investigated the impact of temperature on *An. funestus* insecticide susceptibility (Glunt *et al*., 2018; Agyekum *et al*., 2021). It has been shown that *An. funestus*, like *An. arabiensis* (another main African malaria vector), has reduced mortality after pyrethroid exposure at high temperatures (30°C) (Glunt *et al*., 2018). Similarly, with rising temperatures, mosquito pyrethroid susceptibility was reduced in *An. gambiae* due to the greater activity of metabolic enzymes at high temperature ranges of 25°C to 40°C (Agyekum *et al*., 2022A). At high temperatures of 30°C to 39°C, insect metabolism is significantly faster than at lower temperatures, which causes the insect to break down pyrethroids quickly, resulting in the pyrethroids losing their effectiveness (Neven, 2000).

Global temperatures are predicted to rise by 1.1°C to 6.4°C, depending on the region, within the next 50 years (Intergovernmental Panel on Climate Change (IPCC), 2022). Higher insecticide resistance in anopheline malaria vectors at elevated temperatures can severely impact current vector control methods and disease transmission (Oliver and Brooke, 2017).

1.4.2. Effect of temperature on *Plasmodium* infection

It has been suggested that by the end of the 21st century, climate change will increase the rate of malaria transmission as well as the mortality in human populations by a predicted 2.6% (Beck-Johnson et al., 2013; Dasgupta, 2018). A reason for this could be due to temperature affecting the incubation time of the *Plasmodium* parasite.Temperature affects the incubation time of the *Plasmodium* parasite and its development within the *Anopheles* female host. At 25°C, the malaria parasite, *P. falciparum*, only requires 12 days to complete its development inside the mosquito host, whereas at 20°C, 30 days are required (Ikemoto, 2008). As an example, the impact of temperature on the sporogonic cycle of *P. falciparum* was examined in the vector *Anopheles stephensi*. Females that were fed a solution containing the parasite were kept at temperatures of 16°C, 18°C, and 23°C to identify the best temperature for parasite development. The temperature for the parasite to develop at a normal rate inside the vector during a period of about 16 days was 18°C, whereas at 26°C, the parasite developed at a much faster rate of 10 days (Waite *et al.,* 2019). Studies pertaining to parasite development have not been investigated in *An. funestus,* again highlighting the gap in the literature relating to this species

1.4.3. Effect of temperature on mosquito larvae and adults

Temperature changes affect many biological parameters in mosquitoes, such as size, growth, fecundity, fertility, genitalia rotation, biting rate and developmental rates, amongst others (Agyekum *et al.,* 2021; Lim *et al*., 2021; Chandra and Mukherjee, 2022). Mosquitoes can adapt to such changes in their environment, which has been highlighted in past studies (Lyons *et al.,* 2012).

Insects have upper and lower thermal limits in which they cannot survive or thrive and the capacity of an organism to endure extreme temperatures is known as thermotolerance. High temperatures such as 50°C can be lethal although insects have mechanisms to respond to temperature change and to overcome stressors, such as heat, which confers an advantage to insects in climate change (Charlwood and Braganca, 2012; Lyons *et al.,* 2016). Most malaria vector larvae tend to be more sensitive to temperature changes, compared to adult mosquitoes, as they live in small pools or bodies of water and cannot remove themselves from unsuitable water conditions (Oliver and Brooke, 2017). A side effect seen in larvae is that they will expend high levels of energy to increase their metabolic rates at high temperatures, which causes less thermotolerance and even death (Dodson *et al*., 2012; Pörtner *et al*., 2017).

Most mosquito larvae are reared in laboratories at 25°C-27°C, which is similar to their natural environment (Davies *et al.,* 2016) and studies have been performed to assess the effects of high temperatures on larval survival. Ezeakacha and Yee (2019) studied the impact of temperature on intraspecific larval competition and changes from larval to adult stages in *Aedes albopictus.* There was a significant interaction between larval

density and temperature whereby at the highest temperature of 34°C, the smallest females took the longest to develop. Higher density also generally accentuated this effect of longer development.

Adults exposed to higher temperatures had bigger variations in fecundity and survival, which were carry-over effects from larvae. A separate study showed *Ae. albopictus* larvae reared at 26°C pupated faster than those reared at 22°C, however, fewer larvae completed ecdysis (adult emergence) at the higher temperature (Alto and Juliano 2001). Additionally, *An. gambiae,* reared in warmer temperatures, lead to faster pupal development but smaller adults based on wing size (Christiansen-Jucht *et al*., 2014). Conversely, lower rearing temperatures resulted in slower development but larger adults (Westbrook *et al.,* 2010). When temperatures are too low (21°C), ecdysis, as well as egg hatching, was also delayed in *Ae. albopictus* as was observed in *Anopheles albitarsis* and *Anopheles aquasalis* (Gonçalvez de Carvalho *et al*., 2002). This temperature impact on mosquito developmental times has also been reported in *Culex tarsalis* (Reisen *et al*., 1984), *Anopheles sergentii* (Beier *et al.,* 1987), *Anopheles dirus*, *Anopheles sawadwongporni* (Phasomkusolsil *et al*., 2011), *An. arabiensis* (Oliver and Brooke, 2017) and *An. gambaie* (Lyimo *et al.*, 1992) to mention but a few. Bayoh and Lindsay (2003) showed that *An. gambiae* larvae exposed to 38°C and then moved to 25°C did not complete development, implying a cumulative effect at increased temperatures. Charlwood *et al.* (2003) showed that wild-caught *An. funestus* female adults' wing size increased when temperature increased from 26°C to 29°C in a Furvela village in southern Mozambique.

Furthermore, species-specific trends regarding temperature survival tolerance have been identified. For example, *An. arabiensis* tends to have higher larval survival

tolerance to high temperatures compared to *An. funestus* or *An. quadriannulatus* (Agyekum *et al*., 2021). *Anopheles funestus* larvae showed mortality when the temperature was low (15°C) and at a high temperature of 35°C (Lyons *et al*. 2013). Another study supports this whereby *An. funestus* larvae survive best at a temperature of 27°C, but when it drops below 18°C and approaches 32°C, it becomes less viable (Kahamba *et al*., 2022). Temperature effects are also gender specific and, in *An. arabiensis* and *An. funestus*, the females were more tolerant to low and high temperatures than males (Lyons *et al.,* 2012). Based on the understanding of how temperature influences survival, it is clear that temperature changes can potentially affect the success of mosquito vector populations and, thus, the spread of malaria. Only a few studies investigated the effect of temperature on *An. funestus* and additional studies from different geographical locations are urgently needed

1.5. Heat Shock Response

Heat, as well as cold, are stressors for mosquitoes, and this is mitigated by the heat shock response (HSR). The HSR is instigated by the heat shock factor, which in turn is involved in cell regulation in response to stress (Tintó-Font and Cortés, 2022). Although the HSR is not only related to heat stress, the bulk of the literature relates to temperature. The HSR is described as the rapid process associated with the synthesis of heat shock proteins (HSPs) provoked by stress from heat (Bowler, 2005). The first description of HSR and the molecular changes that occur was described in *Drosophila melanogaster* by Ritossa (1962), whereby a HSR was initiated upon a shift in temperature from 20°C to 37°C. It was not until 1973 that it was discovered that the heat shock response was also accompanied by the production of several HSPs (Tissieres *et al*., 1974).

The HSR is initiated within minutes when an organism is exposed to a stressor and is a useful indicator of stress in organisms (Lindquist and Craig,1988). Cellular stress, such as heat, can cause proteins in the cell to misfold and aggregate (Zhao and Jones, 2012; Chang *et al*., 2018). Accumulation of damaged proteins in the cell is mitigated by the HSR pathway (Figure 1). The HSR is regulated by a transcription factor called the heat shock factor (HSF). The HSF exists mainly in a sequestrated and inactive state as a monomer, which is inhibited by its association with HSPs (Hightower, 1991). The HSPs break away from HSF during cellular stresses and bind to misfolded proteins (Gross *et al.,* 2009). Thus, HSPs act as molecular chaperones, which assist the organism to acclimate to stress and are required in huge amounts. Unbound HSF undergoes trimerisation, which allows it to be activated and act as a transcription factor (Sivan *et al.,* 2017). The HSPs and HSF (relevant to this study) will be discussed further in more detail.

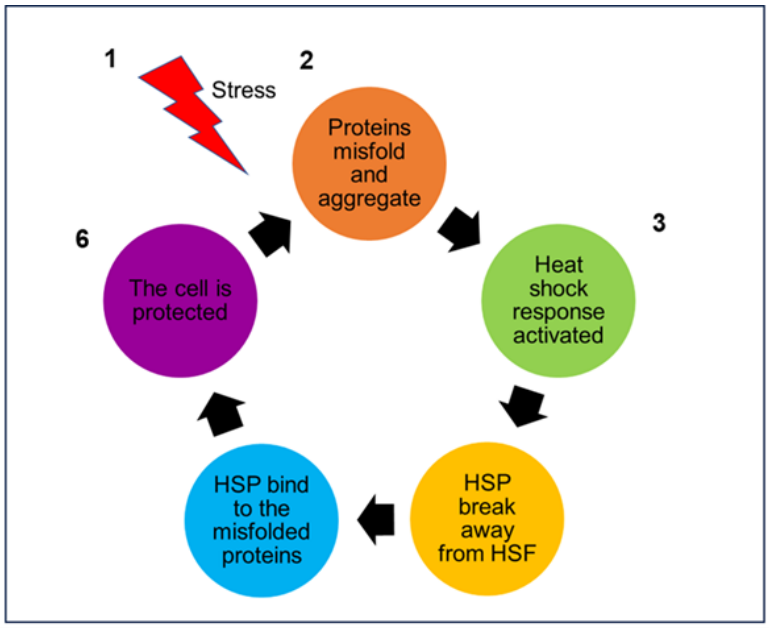


Figure 1: Heat shock response pathway. The cell undergoes a stress (1) which causes proteins in the cells to misfold and aggregate (2). The stressor activates the heat shock response (3). Heat shock factor (HSF) remains in a sequestered state by HSPs. These HSPs break away from the HSF (4) and bind to the misfolded and aggregated proteins (5). The HSPs either repair the misfolding or they destroy the damaged proteins. Thus, the cell and its proteins remain protected (6).

1.5.1 Heat shock proteins

The HSPs are required for everyday cell survival, preservation cell homeostasis, and play a role in protein folding and normal development and makeup 1% to 2% of all proteins in all organisms (Stephanou and Latchman, 2011; Barna *et al.*, 2018; Chen *et al*., 2018A). For example, the Antarctic midge, *Belgica antarctica*, consistently expresses HSP70 and HSP90 regardless of cold stress, suggesting HSPs are required for survival (Lopez-Martinez *et al*., 2008). HSPs are required for the survival of all organisms, whereby HSPs break away allowing HSF to be translocated to the nucleus to activate its function as a transcription factor. It is this continual loop that allows these two components to work together.

As mentioned above, many HSPs act as molecular chaperones to prevent or reverse misfolded proteins and provide a more suitable environment for correct protein folding (Richter *et al*., 2010). The insect's HSPs are divided into four families based on molecular weight, function, and amino acid sequence (King and MacRae, 2015). HSPs can be divided into either small heat shock proteins (sHSPs) or larger heat shock proteins (HSPs). The sHSPs are adenosine triphosphate (ATP) independent, while HSPs (HSP60, HSP70, HSP90 and HSP100) are ATP dependent. HSPs are numbered according to their molecular weight ranging from 10 to 110 kilodaltons (Hu *et al*., 2022).

When a stressor is introduced, the first line of defence is sHSPs, which assist in preventing the irreversible damage to proteins. If proteins cannot be protected and conserved, sHSPs promote protein degradation through either the ubiquitin (Ub)-proteosome system (UPS) or the autophagy-lysosome system (Ciechanover and

Kwon, 2017). The larger HSPs then interact with the proteins by protein folding. This influences protein integrity and cell metabolism (King and MacRae, 2015). HSPs work by collapsing the hydrophobic chains of misfolded proteins to expose and bind to the interactive surfaces of the protein, by working on forces such as electrostatic forces and hydrogen bonds (Hartl, 1996; Hu *et al.*, 2022).

HSP70 is the most prominent and well-studied HSP upon cell stress and has two domains (Mayer and Bukau, 2005; Kurashova *et al.*, 2020). The N-terminal is the most conserved across species and has a high affinity to ATP. The C-terminal is less conserved and is responsible for binding to proteins. In *Drosophila* species, HSP70 is undetectable in non-stressed cells, but upon heat, it is expressed 1 000-fold (Benedict *et al*., 1993). HSP60 is highly sensitive to damaged proteins and proteolytic digestion by exposing the core of the protein. That being said, HSP70 and HSP60 are less specific in their interactions with proteins than HSP90. HSP90 is associated with only particular proteins, and these interactions are usually long-lived and are important regulatory features (Parsell and Lindquist, 1993).

HSPs in adult *Aedes aegypti* mosquitoes are linked to egg production, dehydration tolerance and water balance maintenance, which is important in vector control as water behaviour is linked to habitat preferences (Benoit *et al*., 2010). *Aedes aegypti* and *An. gambiae* adult females take a hot blood meal, initiating the heat shock response (Sivan *et al*., 2017). However, when the HSPs are suppressed via interfering RNA (RNAi), fewer eggs are produced, suggesting that HSPs are required for egg production (Benoit *et al*., 2011). A study involving *Ae. aegypti, Cx. pipiens* and *An. gambiae* showed a direct link between *HSP70* and HSP90 transcript abundance and dehydration tolerance. In all three species, dehydration induced the transcript

abundance of *HSP70*, but only *Cx. pipiens* maintained this transcript following rehydration. Except for *Cx. pipiens*, whose transcript abundance was not observed during rehydration, HSP90 was constitutively expressed and its levels remained largely consistent during dehydration and rehydration (Benoit *et al.,* 2010; Pereira *et al*., 2017).

1.5.2. Heat shock factor (HSF)

HSF is a DNA-binding transcription factor with conserved structure and function across various organisms including humans (Kregel, 2002). *HSF*'s transcript abundance and function may differ between organisms (Feder and Hofmann, 1999; Si *et al*., 2019). HSFs are commonly divided into four types, including HSF1, HSF2, HSF3 and HSF4 in vertebrates, whereby HSF1 is considered the main regulator of heat shock protein transcript abundance. HSF1 is the only HSF present in Diptera and yeast. The fundamental structure of HSF consists of a helix-turn-helix DNA binding domain, one or more hydrophobic coiled-coil regions essential for the stability and regulation of homotrimer formation, and a carboxyl-terminal trans-activation domain (TAD) (Hahn *et al.*, 2004). TAD is responsible for transcriptional activation whereby a regulatory domain (RD) modulates TAD activity. The coiled regions are made up of HR-A/B oligomerisation domains, which include heptad repeat (HR) A (HR-A) and HR-B leucine-zipper domains, that mediate HSF trimerisation. HR-C heptad repeat domain keeps HSF in a monomeric form, due to its interaction with the HR-A/B domain (Figure 2).

HSF, most importantly, acts as an activator of the HSPs during times of cellular stresses such as heat, radiation, hypoxia, infection, introduction of dsRNA and toxicity

caused by heavy metals (Åkerfelt *et al.,* 2010; Vihervaara and Sistonen, 2014). Once the HSPs have dissociated from HSF monomers, HSF trimerises and translocates to the cell nucleus where the HSF trimer binds to with heat shock elements (HSE) to activate the transcription of heat shock genes (Hightower, 1991; Gomez-Pastor *et al*., 2018). HSEs consist of 10 base pair sequence repeats of 5'-nGAAn-3' (where 'n' indicates any nucleotide) in alternating orientations (Nagao *et al*., 1990).

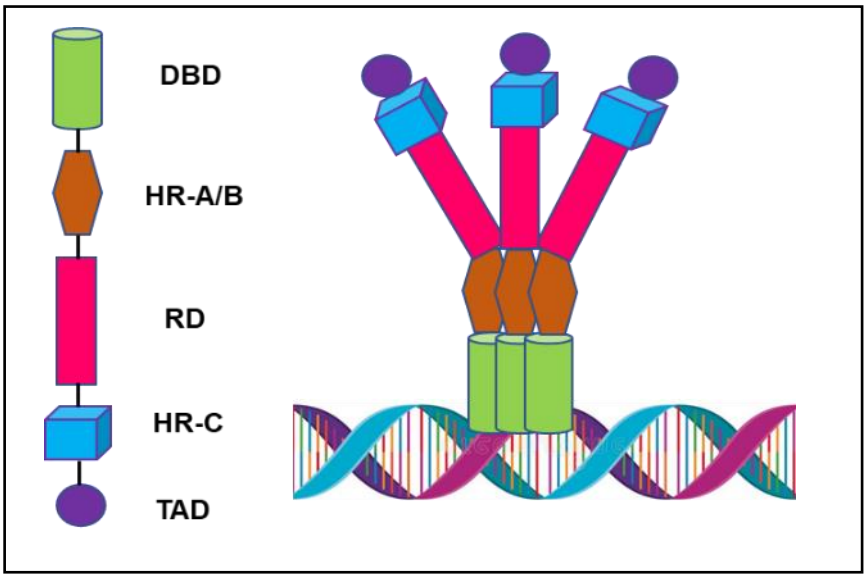


Figure 2 : Schematic illustration of the typical HSF protein domains. DBD: DNA binding domain, which binds the consensus HSE (heat shock elements) sequence; HR-A/B oligomerisation domain: The HR-A and HR-B leucine-zipper domains mediate the trimerisation of HSF1. RD: regulatory domain, which modulates TAD activity. The HR-C heptad repeat domain keeps HSF1 in a monomeric form due to its interaction with the HR-A/B domain. TAD: transactivation domain is responsible for transcriptional activation.

HSF undergoes phosphorylation on serine and threonine residues once it is activated by the release of HSPs upon a stressor. The HSF activity can be inhibited when phosphorylation on serine residues 121, 303, 307 and 363 occurs. In comparison, phosphorylation on serine residues 320 and 326 by kinase A results in activation (Chou *et al*., 2012) (Figure 3). Phosphorylation of serine 326 leads to a secondary post-translational modification in which lysine 298 is sumoylated (Gabriel *et al*., 2023). In

the sumoylation process, small ubiquitin modifying proteins (SUMO) are covalently bound to particular lysine residues in the target proteins, controlling a variety of elements of protein function, including transcription, subcellular localisation, DNA repair and cell cycle (Zhang *et al*., 2021). Kinase A is a regulator of cell metabolism and consists of two subunits, namely PKAc and PKAr. PKAc α-form binds to HSF and initiates phosphorylation of serine residue 320 by activating the promoter site, activating transcription (Moreno *et al*., 2021). The trimerisation of HSF, after the HSR is produced, enables domains previously hidden to be phosphorylated. The HSR attenuation occurs when HSF is converted from a trimer to an inactive monomer via deactylation by the NAD+-dependent sirtuin (SIRT1) deactylase (Stephanou and Latchman, 2011). Attenuation occurs proportionally to the intensity of the stress to return to the control conditions (Shi *et al*., 1998; Voellmy and Boellmann, 2007).

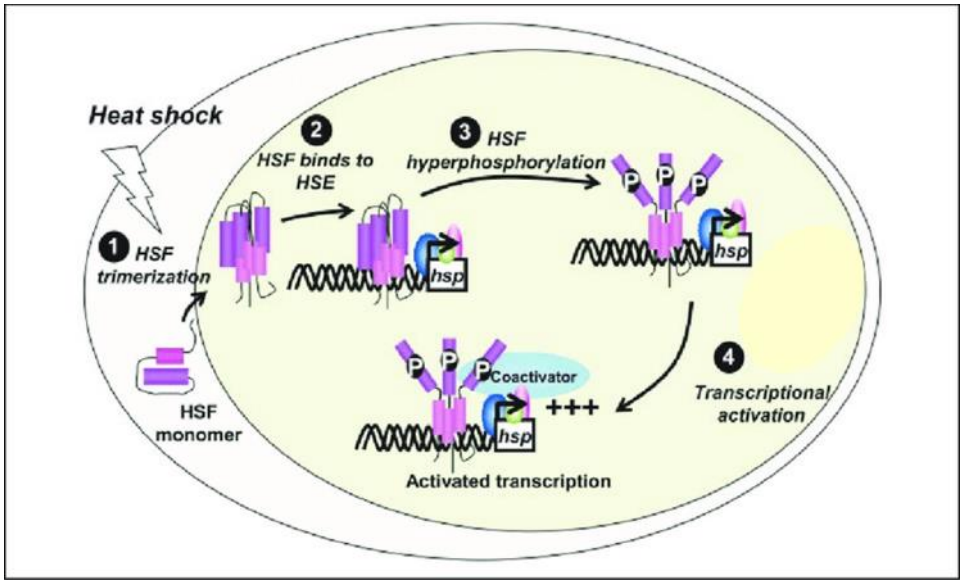


Figure 3: Heat shock response by activation of HSF. The heat shock factor exists as an inert monomer and attains its transcriptional activity stepwise upon exposure to heat shock. (1): HSF accumulates in the nucleus and oligomerises into a DNA-binding competent trimer. (2): trimeric HSF binds to heat HSE sequences (inverted repeats of nGAAn) present in the promoters of target genes. (3): HSF becomes hyperphosphorylated. (4): the hyperphosphorylated HSF attains complete transcriptional activity by Kinase A (coactivator), resulting in the induction of heat shock protein gene transcription. The outer circle represents the cell, whereas the inner circle represents the nucleus (Permission obtained from Westerheide *et al*., 2006; Appendix A).

HSF transcriptionally activates genes that encode components needed for protein folding, processing, targeting, and degradation. HSF is also involved in responding to stresses related to cell growth and differentiation as well as normal physiological processes and this is becoming more evident, although their role in thermotolerance and the activation of gene expression in response to environmental stress has been thoroughly studied (Morano and Thiele, 1999; Garbuz *et al*., 2003; Nielsen *et al*., 2005). In addition to its role in stress response, the HSF is also required during normal, unstressed growth in the single-celled yeasts *Saccharomyces cerevisiae* and *Schizosaccharomyces pombe* (Gallo *et al*., 1993). Little is known about the unstressed growth aspect of HSF biology, although the requirement is likely to reflect a need for HSF in the basal transcription of various target genes. This highlights the need for HSF investigation as there is a large gap in knowledge of HSF function outside of temperature in mosquitoes, specifically in *An. funestus*.

Vectors can expand their geographical range because of global warming (Li and Managi, 2022). Therefore, it is important to look at global warming in vectors although it is not directly going to be used to control vectors currently. Understanding how vector physiology and molecular mechanisms change and the mechanism around the HSR is important to give biological insight into the vector that needs to be controlled. It is important to know what impacts its fertility, fecundity and longevity.

1.6. Study rationale

Insecticide resistance is a major threat to vector control, and stakeholders are investigating novel genetic approaches to supplement current vector control interventions. However, the lack of understanding of complex molecular pathways and

systems limits the expansion and development of supplementary approaches. This is also true for *An. funestus* and although it is responsible for a substantial number of malaria cases in Africa, it remains understudied compared to the other main African malaria vectors (Ngowo *et al*., 2021; Kahamba *et al*., 2022). In order to study HSF under stressed conditions, this study prioritised to understand and gain knowledge of HSF under non-stressed conditions. Thus, this study is a stepping stone for further studies. In order to improve our understanding of the molecular and biological systems of *An. funestus*, the current study aims to better understand the biological role of HSF in this species.

1.7. Aim and Objectives

This study aimed to understand the biological role of HSF in the African malaria vector *An. funestus* with regard to *HSF* transcript abundance and its effect on life table parameters.

The following objectives, with sub-objectives, were used to achieve the aim:

1.7.1. To evaluate *HSF* transcript abundance during all *An. funestus* life stages (egg, larvae, pupae, and adults) (Chapter 2).

- Since HSP*s* are essential for survival (Åkerfelt *et al.*, 2010), it is hypothesised that *HSF* transcripts will be present throughout all developmental stages.

1.7.2. To determine if siRNA fed via sugar water can be used as a delivery system to achieve target gene knockdown of *RPL19* (Chapter 3).

- *RPL19* is a positive control and the evaluation of *RPL19* knockdown before testing HSF knockdown was performed to assess that the delivery method of siRNA was suitable. Given that it is non-invasive and incorporates siRNA into an energy source

(sucrose solution), it is hypothesised that this technique can be used to deliver siRNA to female *An. funestus* mosquitoes.

1.7.3. To achieve knockdown of HSF via siRNA targeting the *HSF* gene (Chapter 4).

- It is hypothesised that sugar feeding of siRNA will decrease *HSF* transcript abundance.

1.7.4. To evaluate the HSF knockdown effect at the phenotypic level (longevity, fecundity, fertility, and time-to-hatch) in adults (Chapter 5).

- It is hypothesised that HSF knockdown will affect longevity, fecundity, fertility, and time-to-hatch of *An. funestus*.

CHAPTER 2

HSF TRANSCRIPT ABUNDANCE DURING THE FOUR LIFE STAGES OF *ANOPHELES FUNESTUS*

2.1. Introduction

Anopheles funestus was discussed in Chapter 1 and has a life cycle similar to that of other anophelines. Mosquitoes have four separate life stages, namely eggs, larvae, pupae, and adults (Figure 4). The life cycle of mosquitoes is interdependent, whereby internal and environmental factors from one stage affect the development of the other stages (Childs *et al*., 2016). *Anopheles funestus* females usually lay around 60 elongated eggs at a time, individually directly onto the water surface (Clements, 2000; Zengenene *et al*., 2021B; Felamboahangy *et al.*, 2022). The eggs are 0.44-0.51 mm in length and 0.13-0.17 mm in breadth, and they have floats with 14-18 air chambers in order to float on the water surface (Gillies and De Meillon, 1968). *Anopheles funestus* eggs hatch into larvae after about three days (Gillies and De Meillon, 1968; Ngowo *et al.,* 2021), after which the larvae grow and undergo four growth stages called instars (Rozendaal, 1997). The larval stage is the longest of the three juvenile stages and is the only juvenile stage that feeds (Beck-Johnson *et al*., 2013). The first instar larvae measure around 1.5 mm long, whereas the fourth instar measures about 8 mm, depending on the species (Schaper and Hernandez-Chavarria, 2006). Larvae (anophelines specifically) feed on particulate matter using mouth brushes by anchoring to the water's surface (Clements, 2000). They usually rest and feed parallel to the water surface (Rozendaal, 1997)

A study by Zengenene *et al.* (2021A) showed that *An. funestus* larval development time to pupation ranged from 16- 21 days under laboratory conditions (25°C). In warmer climates of 30°C, the larval period of other anophelines can last four to seven days, after which they develop into non-feeding pupae. Once the pupa matures after about two to five days, the pupal case splits open and the adult mosquito emerges (eclosion) (Williams and Pinto, 2012). The newly emerged adult requires rest to allow for the cuticle to harden. Males and females feed on nectar as an energy source, but the female requires blood to develop her eggs post-mating. In the wild, a female requires a blood meal every two days in order to lay eggs. This life cycle from egg to adult lasts about 21 to 30 days in optimal conditions in *An. funestus* (Ngowo *et al.,* 2021).

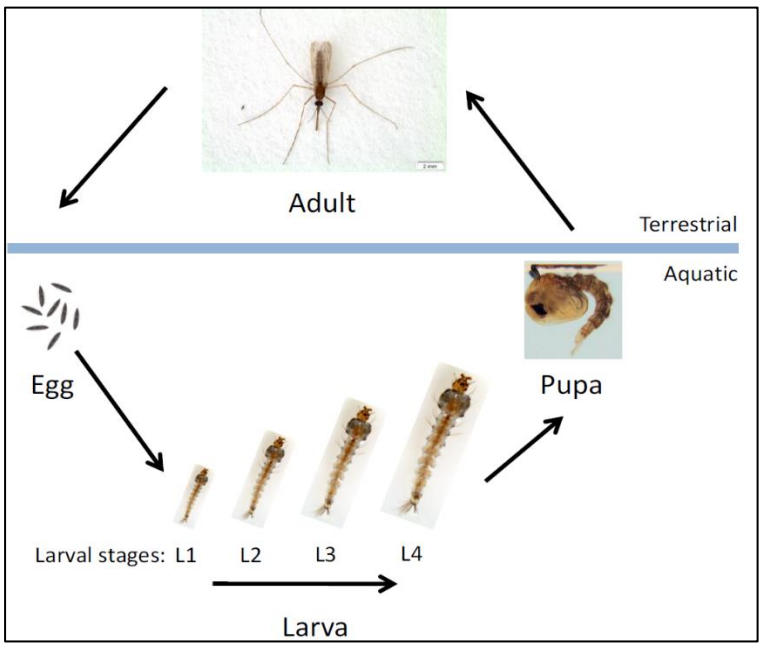


Figure 4: The life stages of the anopheline mosquito life cycle. There are three aquatic life stages: eggs, larvae, and pupae. The one terrestrial life stage is adults. The larvae undergo four stages called instars, which increase in size (Williams and Pinto, 2012).

In a stress-free environment, HSF activity and associated gene transcript abundance have been linked to developmental stages. For example, *Caenorhabditis elegans*, a

model organism, shows a sudden decline of *HSF* transcript abundance during the first 24 hours of adulthood, just as sexual maturity is reached, suggesting a developmental role in addition to a HSR role (Chen *et al*., 2018B). During diapause, all of the HSF splice variants identified in the study by Chen *et al*. (2018B) were up-regulated in pupae of *Helicoverpa armigera* (cotton bollworm). In addition, even the synthesis of HSPs, which are transcriptionally activated by HSF, in *An. stephensi* was linked to morphological and physiological events during pupal development (Gakhar and Shandilya, 1999).

HSF is the main interest of this study. Before determining its biological role in *An. funestus*, its transcript abundance at the different developmental stages in a stress-free environment was investigated.

2.1.1. Aim and objectives

The aim of the study described in this chapter was to determine the transcript abundance of *HSF* during all life stages in the major malaria vector, *An. funestus*. The following objectives were formulated:

2.1.1.1. Optimising real-time quantitative PCR (qPCR) protocol and analysis procedures.

2.1.1.2. Confirmation that experimental mosquito cage setup with male and female adults in a 1:1 ratio will produce mated females (mating was allowed for 10 days) for downstream life stage analysis studies for objective 2.1.1.3.

- It is expected the majority of females will be mated due to the optimal mating time of 10 days (for *An. funestus*) being used (Maharaj *et al*., 2022).

2.1.1.3. Assess *HSF* transcript abundance level in eggs, larvae, pupae, and adults using qPCR

- It is hypothesised that *HSF* transcripts will be present in all life stages but will vary between life stages.

2.2. Materials and Methods

2.2.1. Study samples

Laboratory-reared eggs, larvae, pupae, and adults (females and males) of *An. funestus* from the FUMOZ colony were used in this research. FUMOZ was established in 2000 using wild-caught *An. funestus* material from southern Mozambique (Hunt *et al*., 2005). The colony is housed in the Botha De Meillon Insectary (Vector Control Reference Laboratory (VCRL), National Institute of Communicable Diseases (NICD), Johannesburg), at 80% humidity and 25°C with a 12-hour light; 12-hour dark cycle and 45-minute dusk/ dawn simulation. Mosquito larvae were fed a powdered diet consisting of a mixture of Beeno® dog biscuits (Beeno® South Africa, http://www.beeno.co.za) and Brewer's yeast in a 3:1 ratio (Zengenene *et al*., 2021A).

2.2.2. Experimental setup to determine that the designed HSF primers efficiently target the *HSF* gene

2.2.2.1. Primer design

Primers targeting the *HSF* gene were designed by Dr. Yael Dahan-Moss using the Vector Base accession number AFUN004137 and manufactured by Macrogen, South Korea (Table 1; Figure 5). This set of primers was evaluated to ensure the correct gene target was amplified using *An. funestus* complementary DNA (cDNA) template for qPCR. A no-template control (excludes DNA template) and a negative control (includes only SYBR® Green Supermix and water, but no primers or cDNA) were included to ensure the reagents and primers were not contaminated.

Table 1: Primers sequences and amplicon length of the predicted product (Dahan, unpublished).

		Sequence 5'-3'	Primer Tm	Amplicon length
HSF	Forward	GCACCCGTAGTAGCAATGGT	60.11°C	206 bp
	Reverse	CCAAGGTTCCTTGATCGTGT	57.81°C	

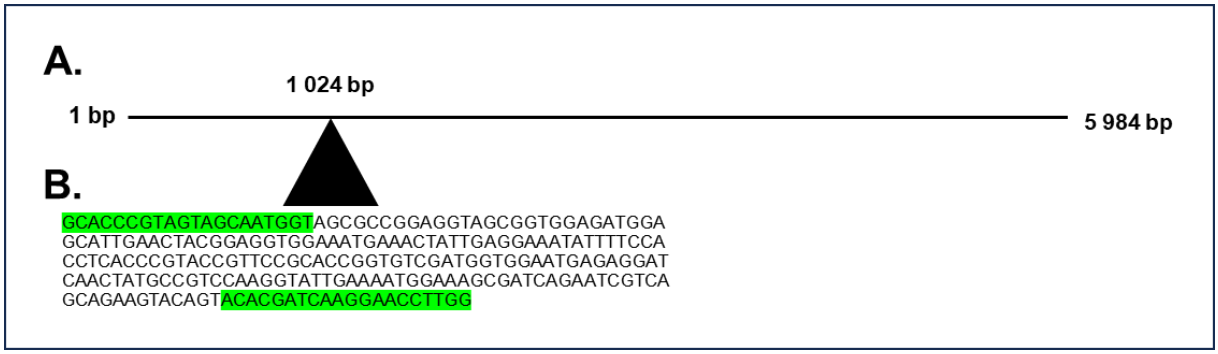


Figure 5: *HSF* gene and the position of the primers. A) the full length of the *HSF* gene B) a portion of the *HSF* sequence that was amplified and the position of the HSF primers (highlighted in green).

2.2.2.2. RNA extraction and cDNA synthesis

Ribonucleic acid (RNA) was extracted from newly emerged (less than 12 hours old) *An. funestus* adults (20 males and 20 females) in a 1:1 ratio to represent one biological replicate. A total of three biological replicates were conducted. The total RNA was extracted using the TRIzol extraction method (Invitrogen catalogue number 15596018). The quality and integrity of the RNA were evaluated using a NanoDrop™ spectrophotometer (Thermo Scientific catalogue number ND-2000) and RNA native gels, respectively (Winnebeck *et al*., 2010). RNA samples with values below 1.8 and considerably above 1.8 for both the 260/280 and 260/230 ratios were not used going forward as these samples had organic contaminants, such as (but not limited to): phenol, TRIzol, chaotropic salts and other aromatic compounds (Heidary and Kakhki, 2014).

RNA was extracted and quantified (in the range of 900- 1 400 ng/µl) and this RNA was used to synthesise cDNA (Figure 6) using the QuanitiNova Reverse Transcription Kit (Qiagen catalogue number 205411). RNA from males and females were combined so that there was no gender bias in the results. The quality of cDNA was confirmed using a NanoDrop™ spectrophotometer. Good quality cDNA had an A260/280 ratio of approximately 1.8, while a lower ratio was considered to have a significant number of contaminants, such as phenol and TRIzol. All cDNA samples were diluted to a concentration of 50 ng/µl (Appendix B) and were used for downstream qPCR analysis. The remaining undiluted cDNA was stored at -20°C.

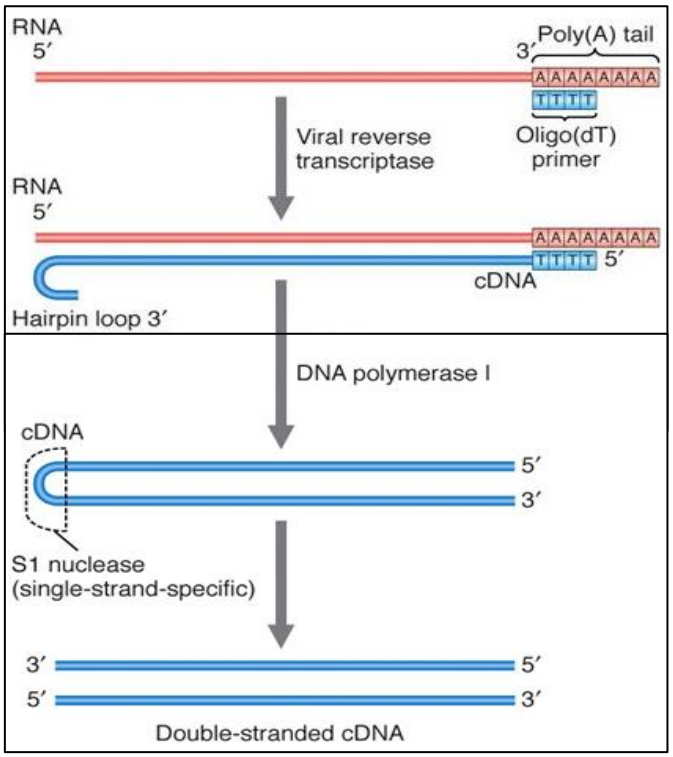


Figure 6: Complementary DNA (cDNA) synthesis. Single-stranded mRNA (ss mRNA) (red) uses the enzyme reverse transcriptase, which uses the ss mRNA as a template and a short 3' primer complementary to the strand to direct the synthesis of cDNA (blue). DNA polymerase makes a complimentary copy of the single cDNA strand and then nuclease cleaves the hairpin loop to form double-stranded cDNA, which was then used as a template for PCR (Permission obtained from Carr and Kasbekar, 2022; Appendix C).

2.2.2.3. Confirmation of HSF primers

Solutions to be used in qPCR were prepared using the cDNA, mentioned above, and HSF primers (Table 1) and were performed in triplicate, per each of the three biological replicates. *Anopheles funestus* cDNA (2 µl from a 100 ng/µl solution) was added to the 96-well plate and thereafter, a PCR reaction mix of 3 µM of HSF primers, nuclease-free water and SYBR® Green Supermix (dNTPs, iTaq™ DNA Polymerase, $MgCl_2$, fluorescein; BioRad catalogue number 1708882) was added making up a final volume of 25 µl. The qPCR cycling conditions for one cycle were as follows: 94°C for 2 minutes (one cycle) and then 94°C for 30 seconds, 55°C for 30 seconds and 72°C for 40 seconds for 42 cycles. A final auto extension cycling was included at 72°C for 10

minutes and the amplified mixtures were held at a 4°C hold. Thereafter, samples were then stored at 4°C.

Following the PCR reaction, 10 µl per technical replicate per sample were electrophoresed on a 2.5% agarose gel containing 12 µl ethidium bromide, from a 10 mg/ml solution, per 400 ml of gel. The gel was viewed using a Molecular Imager Gel Doc XR System (BioRad catalogue number 170-8170). The remaining PCR amplification products underwent Sanger sequencing (Macrogen, South Korea) to confirm the identity of the three amplicons (Figure 7). The BioEdit tool (version 7.7) (Hall, 1999) was used to construct a HSF consensus sequence, which was then analysed by the BLAST VectorBase tool (https://vectorbase.org/vectorbase/app/workspace/blast/new).

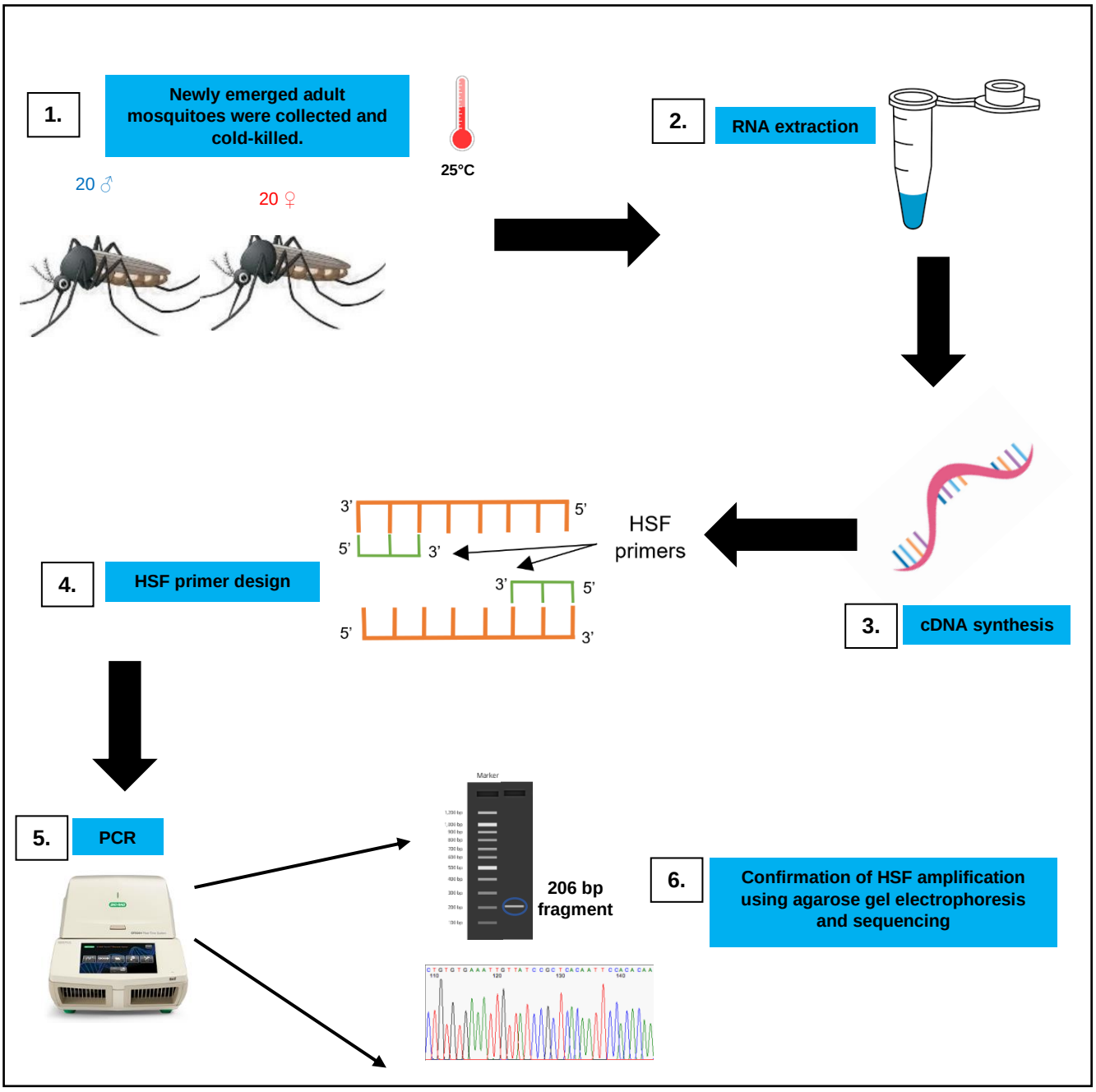


Figure 7: Flow diagram of the methods involved in determining if the HSF primers that were designed targeted the *HSF* gene. (1) Newly emerged adults were collected and cold-killed. (2) RNA was extracted from the mosquitoes. (3) cDNA was synthesised. (4) Primers complementary to the HSF sequence were synthesised. (5) Polymerase chain reaction (PCR) was performed. The PCR amplicon was divided and one half was electrophoresed on a gel and the rest of the amplicons were sent off for (6) Sanger sequencing to confirm the correct sequence was amplified.

2.2.3. Experimental setup for assessing *HSF* transcript abundance at different life stages

2.2.3.1. Obtaining study samples

Experimental setup involved obtaining samples from each stage of the *An. funestus* life cycle at 25°C. This temperature was selected as this is the standard insectary rearing temperature for all life stages. Newly emerged (less than 12 hours old) *An. funestus* female and male adults were placed in BugDorm® rearing cages (W32.5 X D32.5 X H32.5 cm; Megaview Science Co., Ltd, Taiwan) in the Botha De Meillon Insectary. The three cages, per each of the three biological replicates, contained 40 female and 40 male adults each to allow for mating for 10 days. During this time mosquitoes were allowed to feed *ad libitum* on 10% sucrose solution. At day 10 the males were removed and the females were used for downstream analysis.

2.2.3.2. Spermathecal capsule dissection

Ten females from each cage were removed after 10-day mating period, immobilised and spermathecal capsule dissections were performed to assess their insemination status, per each of the three biological replicates. This was important to ensure mating occurred and that females were ready for their reproductive cycle (blood feeding and egg production). Reproductive success was vital for the continuation of this study. The terminalia and last abdominal segment of the females were removed in order to expose the spermatheca which was subsequently observed via microscopy at 100X magnification to determine mating status (Methods in *Anopheles* Research Manual, 2015). The females were either scored “yes” for the presence of spermatozoa (mated) or “no” for the absence of spermatozoa (unmated). The proportion of females mated

was calculated as a percentage for each biological replicate. The presence of spermatozoa (above 60%) indicated successful mating and females could be blood fed (Zengenene *et al*., 2021B; Felamboahangy *et al.,* 2022). On days 11 and 13, the remaining female mosquitoes were allowed to blood feed. This was essential to ensure egg production to continue with the *HSF* transcript abundance study for all life stages.

2.2.3.3. Obtaining samples from each life stage

On day 13, blood fed females were removed from the cages and placed in separate oviposition cups, per each of the three biological replicates (Figure 8). The eggs laid in each oviposition cup were removed, counted and 300 eggs were used for RNA extraction and stored in the laboratory in a distilled water solution at 4°C until RNA extraction was completed later that day (Figure 9A). The remaining eggs were transferred into rectangular larval rearing bowls (120 mm width X 200 mm length X 70 mm height) filled with 750 ml of distilled water and left to further develop. Larvae were fed twice daily on a mixture described in section 2.2.1.

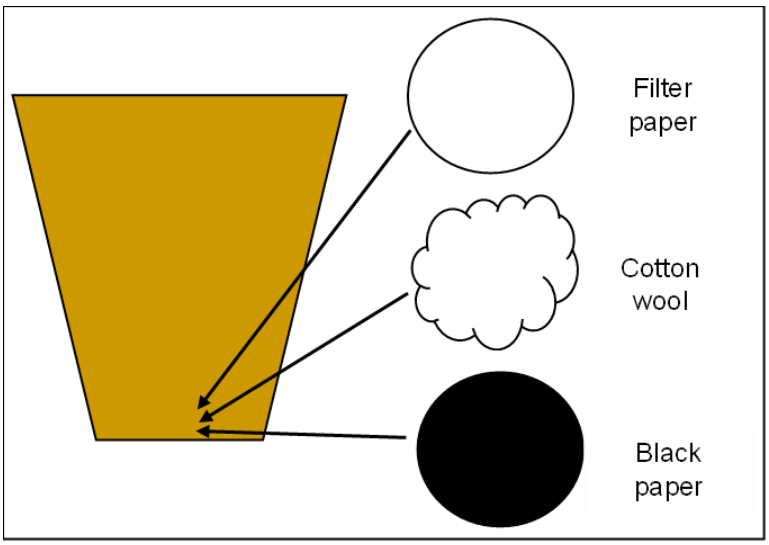


Figure 8: Illustration of the oviposition cup. There are three layers at the bottom for ovipositing. The black photocopy paper was placed down first, cotton wool was added and moistened with distilled water. The filter paper was then placed on top of the cotton wool and was securely placed so that it lay flush against the sides of the cup.

After 13 days, 30 fourth instar larvae (Figure 9B) were removed from each bowl and cold-killed at -20°C to be stored in the laboratory for RNA extraction. The remaining larvae were left to develop into pupae and once a larva had pupated (Figure 9C), 30 pupae (15 males and 15 females) were removed, cold-killed, and stored in the laboratory at 4°C for RNA extraction. The remaining pupae were monitored and once the adults underwent eclosion, male (Figure 9D) and female (Figure 9E) adults were removed in a 1:1 ratio from each bowl, cold-killed, and stored in the laboratory at 4°C for RNA extraction and cDNA synthesis, which was used for transcript abundance studies (Figure 10). The pupae being used for RNA extraction were viewed under a microscope to determine the gender of each pupa. It is difficult to sex individual eggs and larvae, although some laboratories use size separation on *Aedes* mosquitoes as a technique. Size separation is not possible for anophelines and therefore, it was assumed that the eggs and larvae were mixed with both males and females in equal ratios as no gender distortion has been reported for this colony (Zengenene *et al.,* 2021B). In order to allow for proper comparison, it was decided that the pupae and adults of both genders should be mixed in equal proportion as well.



Figure 9: Microscope images showing the four stages of *An. funestus* development. A: Rod-shaped singly laid *An. funestus* eggs; B: *An. funestus* fourth instar larvae; C: *An. funestus* male (above) and female (below) pupae distinguished by their distinctive terminalia; D: *An. funestus* adult male and E: female. Male and female adults differ by the unique differences in the antennae and mouthparts. Images at a scale of 100 µm at 10X magnification.

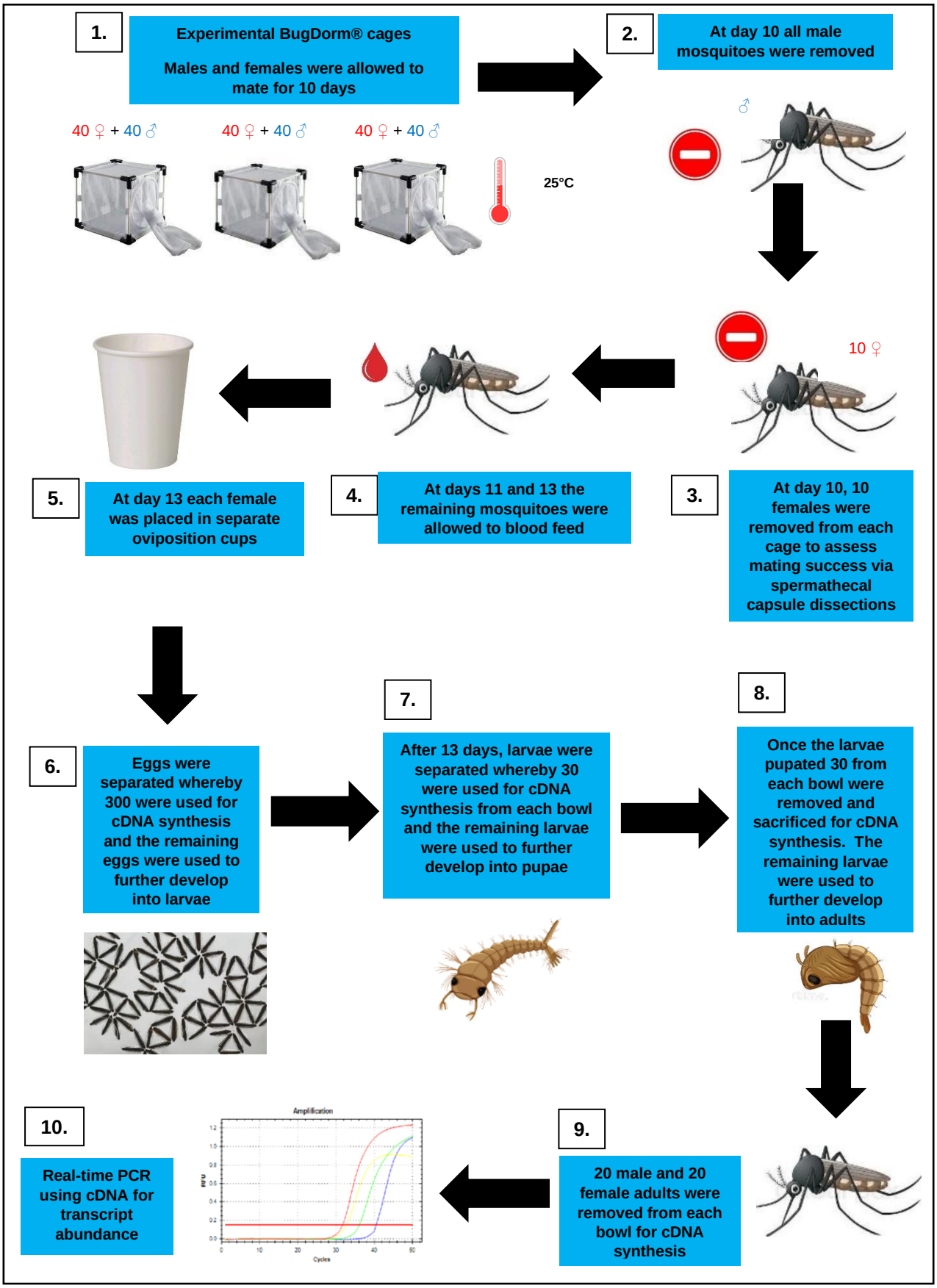


Figure 10: Flow diagram of the methods involved in assessing life stage transcript abundance. (1) Three cages were setup whereby these each contained 40 females and 40 males to allow for mating for 10 days. (2) Males were removed from the cages and (3) 10 female mosquitoes were dissected to determine mating success. (4)

Females were blood fed (days 11 and 13) and (5) individual blood fed females were placed in oviposition cups. (6) Eggs were collected and used for cDNA synthesis (n=300), while the remaining eggs were used for rearing. (7) After 13 days, a subset of larvae (n=30) was used for cDNA synthesis. (8) Once the larvae pupated, 30 pupae were used for cDNA synthesis, while the remaining pupae were allowed to develop into adults. (9) Samples from each life stage were used for cDNA synthesis and (10) transcript abundance was assessed using qPCR

2.2.3.4. RNA extraction and cDNA synthesis

RNA was extracted and cDNA was synthesised as described in section 2.2.2.2. The number of eggs, larvae, pupae, and adults required for RNA extraction differed. RNA was extracted from 300 eggs, 20 larvae, 16 mixed pupae and 16 mixed adults in a 1:1 gender ratio, per each of the three biological replicates. Due to the size difference between eggs and larvae compared to pupae and adults, more biological material (300 eggs and 20 larvae vs. 16 pupae and 16 adults) was required to ensure sufficient RNA was extracted. Three biological replicates were performed and a total of 900 eggs, 60 fourth instar larvae, 48 pupae and 48 newly emerged adults were required for RNA extraction and subsequent cDNA synthesis.

2.2.3.5. Reference gene selection

The identification of reference genes is crucial in producing reliable qPCR results (Bustin *et al*., 2009; Nardini *et al*., 2017). Five reference genes were evaluated namely, ribosomal protein S7 (*RPS7*), ribosomal protein L19 (*RPL19*), glyceraldehyde-3-phosphate dehydrogenase (*GAPDH)*, ribosomal protein S26 (*RPS26*) and *An. funestus* ribosomal protein 18S (*FUN18S)* (Spillings, 2012). Primers targeted to the reference genes were synthesised through Macrogen, South Korea (https://www.macrogen-europe.com/services/oligo-synthesis) (Table 2). All five

reference genes were evaluated using cDNA from two-day old *An. funestus* adults and were based on the Ct values (Silver *et al*., 2006) produced using qPCR (Appendix D).

Table 2: Primers sequences, melting temperatures and amplicon lengths for each reference gene that was evaluated in qPCR.

Primer	Sequence 5'→ 3'	Primer Tm	Amplicon length	Genbank Accession Number	Reference
RPL19 (forward)	GAAACACCAACTCCCGACA	60.2°C	223 bp	DQ910355.1	Spillings, 2012
RPL19 (reverse)	TCAACAGGCGACGCAACAC	62.3°C			
RPS7 (forward)	TTACTGCTGTGTACGATGCC	60.4°C	134 bp	EF450776.1	Amenya *et al*., 2008.
RPS7 (reverse)	GATGGTGGTCTGCTGGTTC	62.3°C			
GAPDH (forward)	GACTGCCACTCGTCCATC	62.2°C	139 bp		Spillings, 2012
GAPDH (reverse)	CCTTGGTCTGCATGTACTTG	60.4°C			
RPS26 (forward)	GATAAGGCAATCAAGAAGTTCG	59.0°C	160 bp	CD577850.1 /AF-NORA-contig_270	Spillings, 2012
RPS26 (reverse)	TACGGACAACCTTCGAGTGG	62.5°C			
FUN18S (forward)	GTGTACTTGGGCGTTACTCTGTG	64.6°C	116 bp	AF417780.1	Spillings, 2012
FUN18S (reverse)	CTTTGAGCACTCTAATTTGTTCAAG	59.7°C			

SYBR® green technology was used to quantify transcript abundance. SYBR® green is a dye that intercalates non-specifically into dsDNA and fluoresces, allowing measurement of the amount of PCR product. Hence, as amplification proceeds, the amount of DNA product increases. In real-time PCR, the results produced is the number of cycles required to reach a threshold level known as Ct. The changes in the transcript abundance of the target gene in treated subjects will be compared to that of the reference gene transcript abundance levels. The raw Ct values had to be transformed into relative quantities (RQ) using the formula $RQ = E^{-\Delta Ct}$, where E is qPCR efficiency. ΔCt was calculated using the formula $\Delta Ct = Ctmin - Ctsample$, with

Ctsample being the raw Ct value for each gene and Ctmin being the minimal raw Ct value (the sample with the highest relative quantity) over a range of samples.

2.2.3.6. Real-time PCR for quantitative analysis

Ct values were generated for each life stage. The same approach was used to obtain the Ct values for the selected two reference genes, *RPS7* and *GAPDH*. The values generated from both reference genes were averaged to give an average Ct value for all treatments going forward. Three biological replicates for each sample type were analysed to determine transcript abundance at each life stage.

2.2.3.7. Data analysis

The change in Ct (∆Ct) was calculated as ∆Ct = Ct (average Ct of the gene of interest) – Ct (average Ct of reference gene) (Livak and Schmittgen, 2001; Pfaffl, 2001). This normalises the gene of interest to a gene which is not affected by your experiment, hence the reference genes.

The ∆Ct was subsequently used to calculate the delta-delta Ct (∆∆Ct) value, which is the difference between the aforementioned ∆Ct values. The ∆∆Ct method, also known as the 2–∆∆Ct method, is a simple formula used in order to calculate the relative fold transcript abundance of samples when performing real-time PCR. This method gives an output of a relative fold change (FC) value which is an increase or decrease of the gene of interest normalised against a reference gene (Livak and Schmittgen, 2001). These values were evaluated for normality using the Shapiro-Wilks test and analysed using a one-way ANOVA (an alpha value of 0.05 was used for all tests). A Tukey *post-hoc* test (for multiple comparisons) using the tool GraphPad Prism (Version 9.0 for

Windows, GraphPad Software, USA, www.graphpad.com) to indicate statistical differences between comparisons or to allow for graphic representation on the graphs even if no statistical differences were present. The spermathecal dissections were scored as a percentage of success. These values were evaluated for normality using the Shapiro-Wilks test and analysed using a one-way ANOVA.

2.3. Results

2.3.1. HSF-designed primers successfully amplified the *HSF* gene

RNA was extracted and then cDNA was successfully synthesised. Using the cDNA. the PCR amplification of the *HSF* gene produced an amplicon at 206 bp, which corresponds to the region of the gene to which the *HSF* primers hybridised (Figure 11). The PCR amplicon was sequenced and European Molecular Biology Open Software Suite (EMBOSS) water alignment (Rice *et al.*, 2000) analysis of the sense and antisense sequences confirmed that there was a 98.4% and 100% sequence identity to the VectorBase sequence AFUN004137 respectively. AFUN004137 is the accession number for the sequence in VectorBase corresponding to the *HSF* gene sequence. The *HSF* consensus sequence had a 97.57% sequence identity to the VectorBase AFUN004137 sequence. Fewer mismatches in base pairs were observed in the sense strand at the 3' end, which can explain why the identity percentage was lower than 100%. This is not unusual and is due to sequence artefacts where mismatches are common at the 3'/5' ends. This gene is 206 bp and it is located on chromosome one at position CM012072.1:80651961:80668394:1 (Appendix E). This confirmed that the HSF primers designed successfully amplify the gene of interest and are suitable for subsequent experiments.

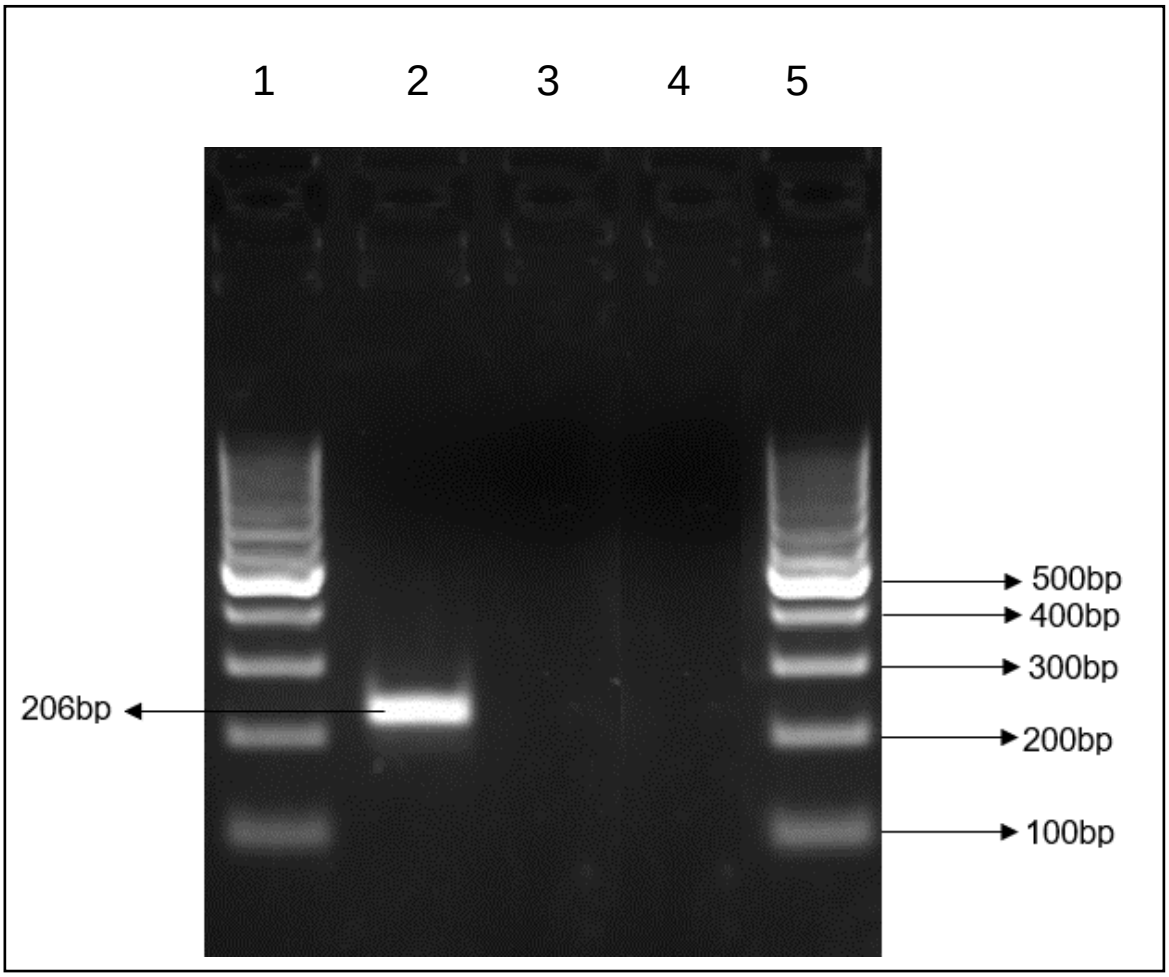


Figure 11: Gel image of PCR products using HSF primer pairs (206 bp). Lanes 1 and 5: GeneRuler 100bp DNA ladder (Life Technologies, USA); Lane 2: *An. funestus* cDNA; Lane 3: negative control; Lane 4: no template control (NTC)**.**

2.3.2. Reference gene selection

Two reference genes, *RPS7 and GAPDH*, with the lowest stability values (M) identified using NormFinder software (Andersen *et al*., 2004) analysis were selected to be used to normalise transcript abundance levels in qPCR. These genes had the lowest M-values of 0.656 (*RPS7*) and 0.916 (*GAPDH*) (Table 3) and are therefore the most stable.

Table 3: Stability values of each reference gene. *RPS7* (pink) and *GAPDH* (purple) were the two genes with the lowest M-values.

Gene name	M- value
RPS7	0.656
GAPDH	0.916
FUN18S	1.009
RPS26	1.457
RPL19	2.159

2.3.3. Sequencing confirming reference gene identity

GAPDH and *RPS7* amplicons were sequenced to confirm transcript identity. The EMBOSS water alignment analysis of the sense and the antisense sequences of *GAPDH* revealed a 99.1% and 99.5% sequence identity to accession number AFUN003850 on VectorBase. The BioEdit tool (version 7.7) was used to construct a *GAPDH* consensus sequence from both strands, which was then analysed by the BLAST VectorBase tool. There was a 97.12% sequence identity between the *GAPDH* consensus sequence and the gene glyceraldehyde 3-phosphate dehydrogenase (*GAPDH*).

The *RPS7* sequences were also analysed and the EMBOSS water alignment analysis of the sense and the antisense sequence revealed a 99.8% and 100% sequence identity to accession number AFUN007153, respectively. The software BioEdit was used to construct a *RPS7* consensus sequence from both strands, which was then analysed by the BLAST Vector Base tool. There was a 97.76% sequence identity

between the *RPS7* consensus sequence and the gene 40S ribosomal protein S7 (*RPS7*).

2.3.4. *HSF* transcript abundance across the different life stages

This experiment required biological material from all life stages. A cohort of adults was combined in a cage for mating and blood feeding and the female offspring were used for this part of the study.

i. Confirmation of mating

Spermathecal capsule dissections were performed on 10 females from each treatment cage on day 10. The insemination status (% insemination ± S.D.) between the three biological replicates varied from 78.67% ± 3.18, 83.34% ± 2.96 and 84.34% ± 2.33. There were no significant statistical differences between the biological replicates (one-way ANOVA: p= 0.3839, F= 1.128, DF= (2, 6)) (Figure 12). The remaining females were, therefore, used for blood feeding to obtain eggs, larvae, pupae, and adults for the life stages to be analysed. The biological material was collected from the same life cycle (from adult to adult) to allow a more controlled experiment and eliminate unknown biological variations.

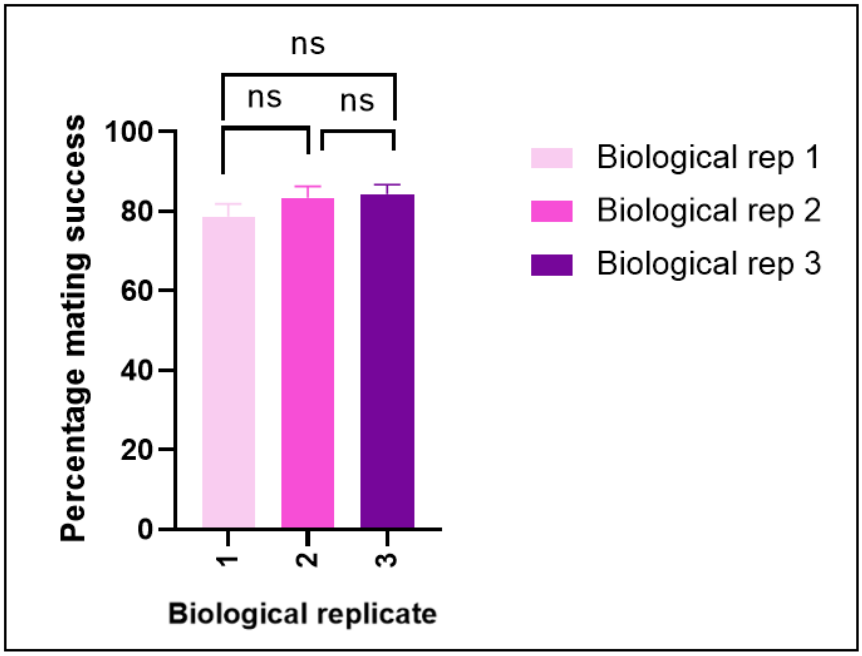


Figure 12: The percentage of mating success in females across three biological replicates. No significance (ns) between replicates was calculated using a Tukey *post-hoc* test. Error bars represent the standard deviation (S.D.).

ii. HSF transcript abundance

HSF was expressed in all the life stages, with the highest relative fold transcript abundance seen in *An. funestus* adults and the lowest in eggs. *HSF* transcript abundance was statistically significantly different across all life stages (one-way ANOVA: $p< 0.0001$, $F= 10.29$, DF (3, 8)). A Tukey-honestly significant difference (HSD) test showed significant transcript abundance differences between eggs and larvae ($p< 0.0001$), eggs and pupae ($p= 0.0080$), eggs and adults ($p< 0.0001$), adults and pupae ($p= 0.0002$) and larvae and pupae ($p= 0.0008$). Interestingly, there was no significant difference in transcript abundance between larvae and adults ($p= 0.3551$) (Figure 13) (raw Ct values found in Appendix F).

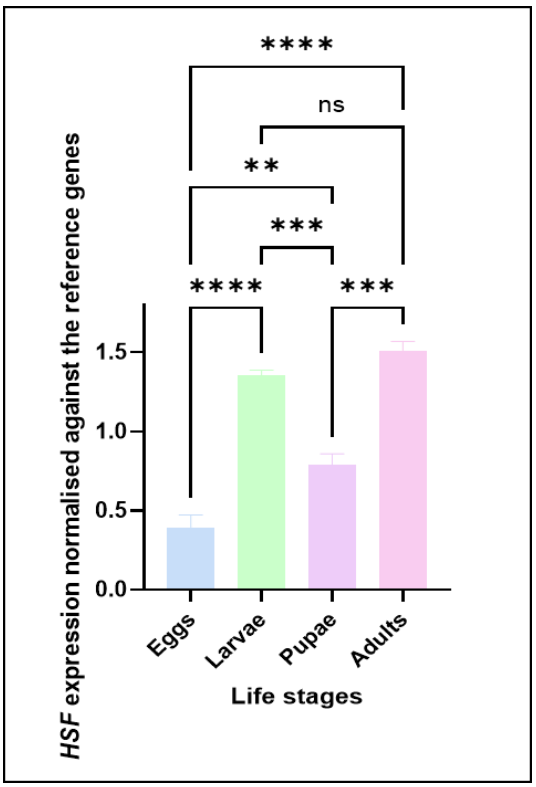


Figure 13: The relative *HSF* transcript abundance normalised against the reference genes, *RPS7* and *GAPDH*, across the four life stages of *An. funestus*. The asterisks indicate a Tukey *post-hoc* test (ns $p > 0.05$; * $p \leq 0.05$; ** $p \leq 0.01$; *** $p \leq 0.001$; **** $p \leq 0.0001$). Error bars represent standard error of the mean (SEM).

2.4. Discussion

This study is the first to investigate *HSF* transcript abundance at all life stages in the malaria vector *An. funestus.* HSF was expressed in all life stages and therefore is most likely to be a critical transcript in insect development and survival. Primers were specific to amplify the *HSF* gene. Samples used to evaluate transcript abundance were obtained by allowing male and female adults to mate and females were then subsequently blood fed. Mating were confirmed by spermathecal capsule dissections and insemination rates were not significantly different between the biological replicates ($p > 0.05$). Maharaj *et al.* (2022) who also worked on *An. funestus* found similar results. After blood feeding, the progeny were used to evaluate the *HSF* transcript abundance between eggs, larvae, pupae, and adults by using qPCR.

Results showed that eggs and pupae had a significantly lower *HSF* transcript abundance levels when compared to larvae and adults. *HSF* transcript abundance increased 3.25-fold from egg to larval stages. *HSF* decreased when larvae were compared to the resting pupal phase (0.5-fold decrease). An increase of 1.9-fold was observed in adults when compared to pupae.

Jedlicka *et al*. (1997) identified four mutant alleles of the *Drosophila HSF* gene in order to clarify the *in vivo* roles of HSF. The mutant alleles included a null and temperature-sensitive allele. Results showed that the hsf^4 mutant defined the role of *HSF* in early larval development and oogenesis. The *hsf* mutants were isolated in genetic screens for recessive lethal mutations under conditions of no external stress, revealing a requirement for HSF function under normal growth conditions in *Drosophila*. In *Chilo suppressalis*, a rice pest moth, it was shown that *HSF* transcript abundance was greatly increased during the adult stage (Dong *et al.*, 2023) and this was also observed in *An. funetsus*. These species-specific variations in the *HSF* transcript abundance profile highlights the imporatace to examine this in *An. funestus* (Figure 14). There are very few insect studies looking at *HSF* transcript abundance in the different life stages. This gap in the knowledge that has been identified should encourage researchers to do similar studies in other Diptera so that the knowledge on *HSF* transcript abundance can be expanded.

The complicated life cycle of mosquitoes comprises of both aquatic and terrestrial stages. Temperatures can have an impact on mosquito developmental time and certain life stages are more susceptible to environmental stress than others (Harada and Goto, 2017). Higher temperatures and stressors are combatted in insects using

the heat shock response whereby HSF initiates this. Therefore, *HSF* transcript abundance during periods of high stress and heat may be particularly crucial at certain stages of development (Sørensen and Loechcke, 2002).

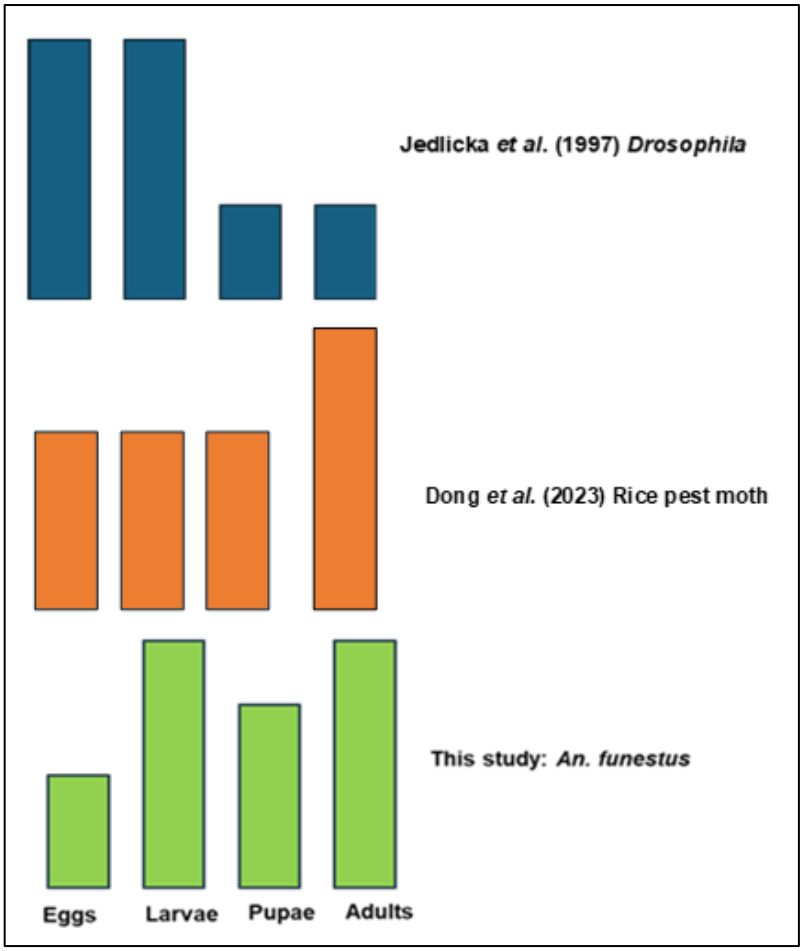


Figure 14: Graphical representation of the *HSF* transcript abundance profile in *Drosophila melanogaster* (Jedlicka *et al*., 1997) (blue), the rice pest moth (Dong *et al.,* 2023) (orange) and *An. funestus* (this study) (green). Not drawn to scale and is purely an illustrative proxy of HSF abundance per species.

Eggs, larvae and pupae of *An. funestus* are found in water, with larvae and pupae displaying a relative low *HSF* transcript abundance compared to the larvae. This may be due to the fact that eggs have three layers, the exochorion, endochorion and serosal cuticle, that allows the egg to be viable outside of the water (Farnesi *et al*., 2017). In this case HSF may not be required at such large quantities in this life stage due to

other mechanisms of protection. It is also worth considering that the egg and pupal stages are the developmental stages and it is possible that HSF does not play a big role during these stages. In other *An. gambiae* transcript studies (whole genome studies) the eggs have the fewest differentially expressed genes, hence during embryo development the insect might put resources into other transcripts that are important for development (Gokhale *et al*., 2013).

Larvae undergo four stages called instars and this stage is the longest of all four life stages. The fact that HSF expression was highest at this stage suggests a metamorphosis or moulting role and that HSF might be expressed to deal with environmental stress and larval-pupal transition. HSF may also be a critical protein to protect and enhance the survival of *An. funestus.* The eggs and pupae stages are short (two days) and the larvae stages are much longer (16 to 21 days) (Zengenene *et al*., 2021). Larvae are, therefore, exposed to environmental conditions for longer periods of time.

The adult stage is the only terrestrial stage and showed a high HSF transcript level compared to eggs and pupae. This suggests HSF plays a crucial role in terms of survival against environmental conditions and regulation of growth and aging. This may further extend to perhaps play a role in germline cell development such as oogenesis and spermatogenesis as seen in *Drosophila* species (Jagla *et al*., 2018) which suggests a reproductive role.

2.5. Conclusion

Transcript abundance of *HSF* was confirmed to be present at all life stages of *An. funestus*, however, the biological role of HSF in this species' life table parameters is still unknown. HSF knockdown by siRNA can provide vital information on the biological role of this gene. Therefore, sugar feeding as a siRNA delivery system for *An. funestus* was optimised and confirmed in the subsequent study.

CHAPTER 3

EXPLORING SUGAR WATER AS A DELIVERY MEDIUM FOR siRNA-MEDIATED GENE KNOCKDOWN AND VALIDATION THROUGH *RPL19* IN *ANOPHELES FUNESTUS*

3.1. Introduction

The biological role of HSF can be studied by inhibiting the gene transcript and evaluating the impact on *An. funestus* life table parameters. Ribonucleic acid interference (RNAi) can be used for this purpose. However, it will need to be delivered to the mosquito, absorbed into the mosquito body and only then can transcript inhibition be achieved. Most genes are transcribed into mRNA, which can be successfully translated into an amino acid chain. Cells employ several strategies to promote or inhibit the breakdown of these mRNA molecules (Bai *et al*., 2022). Employing siRNA to target endogenous mRNA enables RNAi gene manipulation in *An. funestus*. This chapter will investigate siRNA delivery through sugar water feeding. Developing an appropriate methodology for HSF knockdown was imperative before experimentation could be initiated for subsequent chapters.

3.1.1. Ribonucleic acid interference (RNAi)

Knockdown studies or reverse genetics enable a better understanding of genes and their functions (Joga *et al.,* 2016). RNAi is one technique used to study the biological function of a gene within an organism and was used in this study (Brown *et al*., 2003A; Mello and Conte Jr, 2004). RNAi works by knocking down a gene by interfering or silencing transcript abundance via double-stranded RNA (dsRNA) or siRNA. In

research, siRNA has often been used as a silencing trigger (Tomari and Zamore, 2000) and is a secondary molecule produced when dsRNA is introduced into an organism to produce a silencing effect.

Introducing dsRNA into the organism causes the dsRNA to bind to a nuclease called Dicer (Hutvágner and Simard, 2008). Dicer cleaves the dsRNA via adenosine triphosphate (ATP) into smaller double-stranded 21-25 nucleotide short siRNA fragments with 5'-phosphorylated and two hydroxyl group nucleotide 3' overhangs (Zamore *et al.,* 2000; Hutvágner and Zamore, 2002; Hannon, 2002; Meister and Tuschl, 2004; Siomi and Siomi, 2009; Perrimon *et al.,* 2010). Dicer activity varies between tissues, i.e., whole body, gut, and haemolymph (Peng *et al.*, 2018). Dicer contains five domains: a PAZ (Piwi-Argonaute-Zwille) domain, two RNase III domains, a helicase domain, and a dsDNA binding domain, which are all involved in protein-protein interactions (Hoa *et al.,* 2003).

The fragments of siRNA assemble onto the PAZ domain of the catalytic component argonaute (Echeverri and Perrimon, 2006; MacRae *et al*., 2006). Argonaute is a member of a large family of proteins with a PAZ and C-terminal Piwi domain (Cerutti, 2003). A single guide strand is incorporated into the RNA-induced silencing complex (RISC). The guide strand binds to complementary mRNAs and RISC mediates degradation or translational suppression of the endogenous transcript in the absence of ATP (Zamore, 2001; Agrawal *et al.*, 2003; Brown *et al*., 2003B; Sanchez-Vargus, 2004; Whitehead *et al*., 2009; Murphy *et al.*, 2016). The target mRNA is destroyed and no protein is synthesised, thus resulting in gene silencing (Fire, 2007) (Figure 15).

Although many researchers use long dsRNA (~300-400 bp) molecules in their anopheline mosquito studies, the direct use of siRNA molecules enables confirmation of phenotypes using multiple interfering RNAs. Purchased pre-synthesised siRNA targets different 21-25 bp sites in a single gene, which can alleviate concerns that the phenotype under analysis has arisen from off-site targeting that results from using dsRNA molecules (Mysore *et al*., 2017; Wiltshire and Duman-Scheel, 2020).

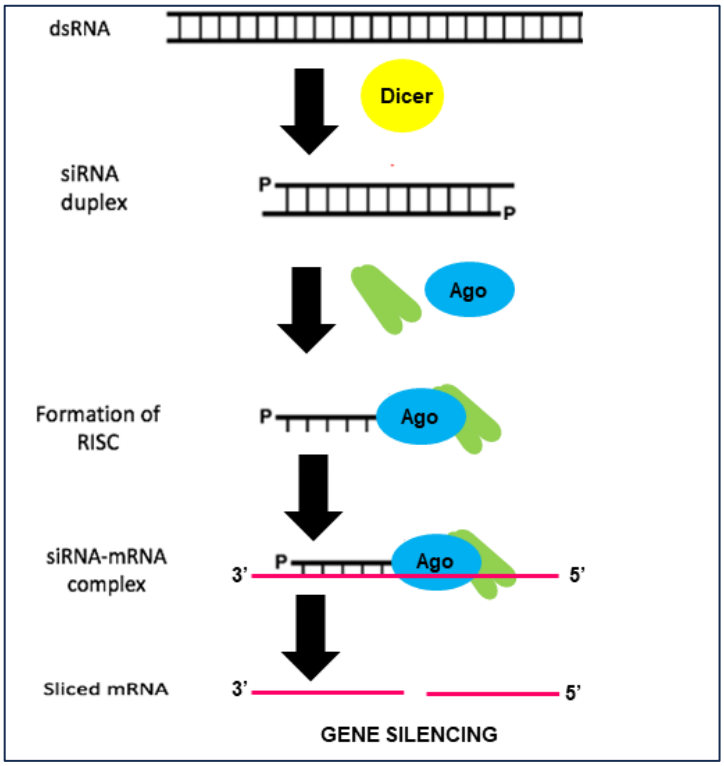


Figure 15: Mechanism of siRNA silencing. Double-stranded RNA is introduced into the cell and binds to an enzyme, Dicer (yellow). Dicer cleaves the dsRNA into siRNA. The siRNA attaches to RISC (green) and with the assistance of Ago proteins (blue), the guide strand binds to complementary mRNAs. It mediates the degradation of the endogenous transcript (pink), which results in gene silencing.

Regardless of whether dsRNA or siRNA are used, different mechanisms are in place that enable the molecules to enter the cells of insects, also called receptor-mediated endocytosis. Since this study's chosen method of siRNA delivery is sugar feeding, the siRNA molecules will be ingested into the mosquito midgut before entering cells.

3.1.2. Receptor-mediated endocytosis to assist in cell membrane crossing

Different cell membrane crossing mechanisms exist in organisms. For example, in nematodes (*Caenorhabditis elegans*), a transmembrane protein called the systemic RNA interference defective protein 1 (SID-1) exists. The SID-1 protein binds to the dsRNA molecules in order for them to cross the cell membrane by interacting with RISC (as discussed in section 3.1.1) (Zhang *et al*., 2010; Lu and Wan, 2011). Dipterans, such as mosquitoes, lack SID-1, which prevents the entry of dsRNA and RNA-dependent RNA polymerase (RdRP) across the cell membrane. The function of SID-1 is replaced by receptor-mediated endocytosis (Murphy *et al.,* 2016). Receptor-mediated endocytosis requires help from pattern recognition receptors (PRRs) (Joga *et al*., 2016). Two major classes of pattern recognition receptors are the Toll receptors and the scavenger receptors (Saleh *et al*., 2006; Tulvila *et al*., 2006).

Receptor-mediated endocytosis for this study will take place in the midgut. The insect midgut consists of a single layer of columnar cells with microvilli, endocrine cells, and stem cells at the base (Figure 16). The midgut has a large absorption surface area via the microvilli, with many channels and endocytosis apparatuses to absorb nutrients and the dsRNA (this study) from the gut lumen (Saleh *et al*., 2006; Huvenne and Smagghe, 2010).

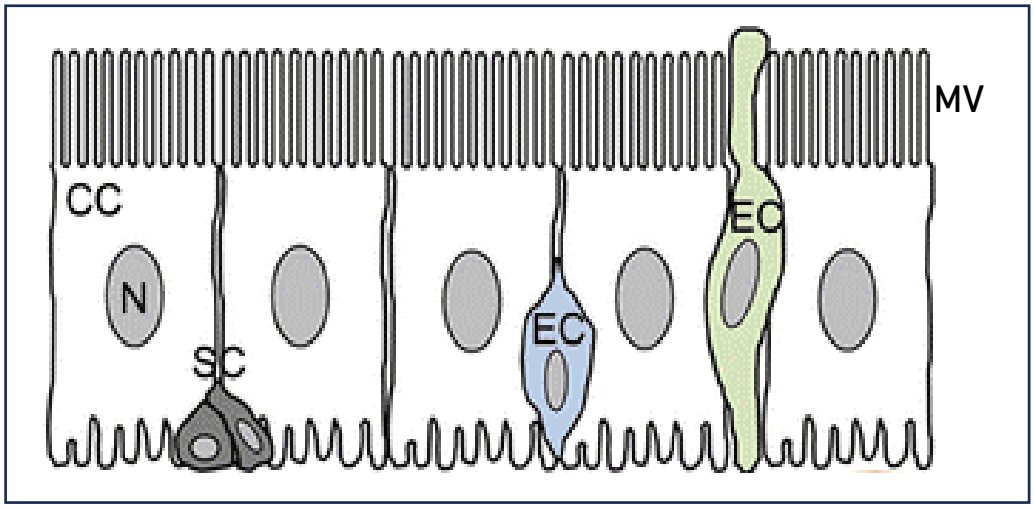


Figure 16: Schematic representation of cell types that form the insect midgut epithelium. Endocrine cells (EC) are intercalated to columnar cells (CC), with microvilli (MV) the major cell type. A closed EC and an open EC are shown in blue and green, respectively. Stem cells (SC) are located at the base of the epithelium, isolated or grouped depending on the insect (adapted from Caccia *et al*., 2019).

3.1.3. Delivery systems used to introduce dsRNA into an organism

There are multiple ways to deliver dsRNA or synthesised siRNA into a mosquito. Feeding methods include direct ingestion, larval soaking, nanoparticle-mediated uptake with chitosan or other nanoparticles and vector systems such as bacteria and yeast (Wiltshire and Duman-Scheel, 2020). Ingestion (Negri *et al*., 2019), microinjection (Debalke *et al*., 2029) and soaking (Pillai *et al.*, 2016) are the most utilised methods in *Anopheles* research, all with great success. Letinić (2021) compared the use of CRISPR-i and microinjection as a means of knockdown of the gene *akirin* in *An. arbiensis*. Results showed that knockdown results were similar between the two methods. The details of these RNAi delivery methods will be briefly discussed, along with their advantages and disadvantages.

Micro-injection involves the injection of dsRNA (including synthesised siRNA) into an organism's abdomen or thorax via a microinjection needle. According to some studies

(Pillai *et al*., 2017), microinjection is the most reliable and effective method as the exact concentration of injected dsRNA or siRNA is quantifiable. However, others claim that microinjection is not useful due to the trauma caused at the injection site, which might compromise the organism (Ghosh *et al*., 2017). Injection can stress the organism, which will complicate the phenotype characterisation study. Furthermore, conducting microinjections under field conditions is challenging because it requires expertise and specialised equipment (Wiltshire and Duman-Scheel, 2020). However, a study by Maharaj *et al*. (2022) showed no significant difference in life table parameters (fecundity, fertility, longevity and susceptibility to *P. falciparum* infection) between *An. funestus* dsRNA injected and uninjected control groups. It suggests that the injection procedures had no adverse side effects in *An. funestus*. Microinjection works well on adults but is more challenging when investigating other life stages (larvae or pupae). Microinjection is also challenging if the transcript knockdown effect is needed in experiments over extended periods that might need multiple injections (more than 10 days).

Soaking is a technique to deliver dsRNA or siRNA into mainly the aquatic stages (but adults can also be used). This method was developed when Lopez-Martinez *et al*. (2012) investigated how to induce RNAi of HSP90 in *Cx. pipiens* larvae. They dehydrated the larvae in a salt solution, followed by rehydration in water containing siRNA. They showed that this was an easy knockdown method and that the effect was also visible in adults. Like sugar feeding, soaking does not allow one to quantify the amount of siRNA absorbed. Even though soaking might not be ideal, it has the advantage that it is not life stage specific (Boisson *et al*., 2006; Yu *et al.,* 2013; Whyard *et al.*, 2015; Airs and Bartholomay, 2017; Pillai *et al*., 2017; Bally *et al*., 2018). Soaking can also be applied to adults in a technique called thorax spotting whereby a droplet

of solution is applied to the dorsal thorax using a dropper. Due to the hydrophobic properties of the thorax in insects, this technique requires that the droplet is absorbed (Pridgeon *et al.,* 2008). However, thorax spotting is labour-intensive taking a considerable amount of time.

Mixing the dsRNA or siRNA with a liquid, usually coloured dye (Bilgi *et al*., 2017) and/or sugar water (Mysore *et al*., 2022) allows the organism to ingest the dsRNA while feeding. This can be a more practical delivery system as the insects remain healthier due to no trauma from handling or injection (Ghosh *et al.,* 2017). Feeding is also beneficial for ease of use (fewer skills are required, it is less labour intensive, and it is faster to train people). However, the amount of solution ingested by the organism is unknown (Murphy *et al*., 2016). This method has been performed in *An. gambiae* (Taracena *et al*., 2022) mosquitoes before and was found to be very effective in silencing the intended genes. This method allows for feeding large numbers of adult mosquitoes over prolonged periods (days), making this technique the most viable option for this study. Another advantage of using sugar feeding as a delivery mechanism is that it will allow for field-based studies. Technology used for attractive toxic sugar baits (ATSBs), where insects are drawn to a baited sugar solution that causes mortality when consumed (Fiorenzano *et al*., 2017), will allow for dsRNA studies on wild *An. funestus* populations. Sugar is readily available for large-scale studies without stress to the organism. This method was therefore selected for this study.

3.1.4. Aim and objectives

The aim of the study described in this chapter was to determine if sugar water can be used as a delivery system for siRNA in *An. funestus* and to validate the methodology for future studies. The following objectives were formulated:

3.1.4.1. To optimise sugar feeding protocol for *An. funestus.*

3.1.4.2. To validate the siRNA sugar feeding protocol by evaluating transcript abundance for a known target gene *RPL19* before targeting *HSF.*

- It is hypothesised that there will be a decrease in *RPL19* transcript abundance due to the effective chosen method of siRNA introduction. The pre-ordered HSF-siRNA is costly and for this reason, the optimisation and validation of the technique was conducted on RPL19 using already available siRNA in the laboratory.

3.2. Materials and Methods

3.2.1. Best feeding proportions to maximise feeding success

Since the siRNA will be delivered to *An. funestus* adult mosquitoes using a sugar solution, it was important to ensure that a reliable method was developed to isolate females that fed on siRNA spiked sugar solution from those that did not ingest siRNA spiked sugar solution. Adding a food colouring dye to the sugar water would provide a visual detection method. However, it was unknown which food dye would be best to use. This method was, therefore, optimised prior to siRNA experimentation commencement. Four paper cups with a volume of 280 ml were used, each consisting

of 10 mixed gender newly emerged adult *An. funestus* mosquitoes. Each cup was covered by a 15 cm-by-15 cm piece of gauze secured by an elastic band (Figure 17).

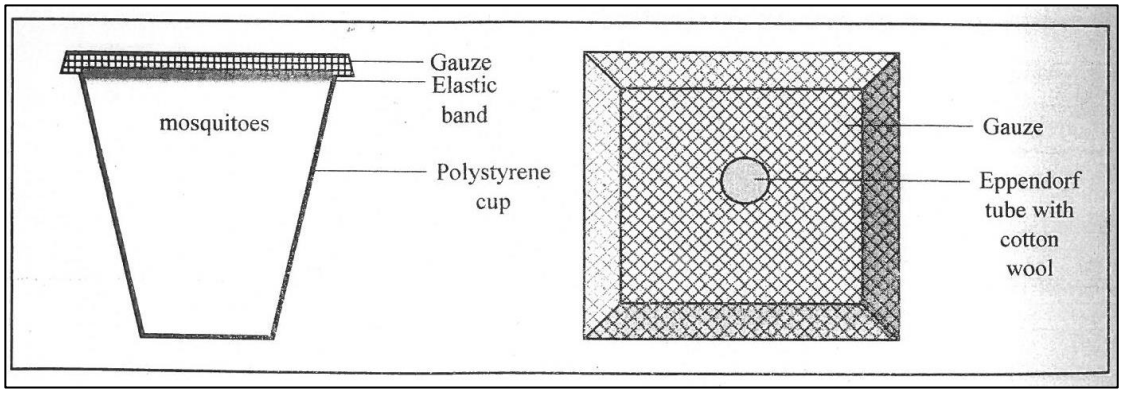


Figure 17: Illustration showing how the paper cups containing mosquitoes were covered to perform feeding optimisation experiments without siRNA treated sugar water. The gauze also contained a small hole to allow the insertion of a 1.5 ml microcentrifuge tube containing sugar water (Permission obtained from E Silva, 2017).

A 1 ml solution of 5% sugar water solution was added directly into each microcentrifuge tube that had the lid removed. The solution was made up of 50% (500 µl) RNA free water, 50% (500 µl) of a 10% sucrose solution and a drop of green or blue gel food colouring (Cake Flora Gel Food Colouring, Forest Green and Navy Blue, www.cakeflora.co.za). Sterilised cotton wool (0.1 g pieces) was placed into the opening of each microcentrifuge tube and saturated with sugar solution. A small hole was pierced at the bottom of each tube to minimise a vacuum effect and to allow complete saturation of the cotton wool. A small opening was made in the centre of the gauze covering the cup, and the 1.5 ml microcentrifuge tubes were placed upside down through the gauze (Figure 17). Twenty-four-hour old adult mosquitoes previously fed on a 10% sugar solution for 24 hours were placed into four cups and were fed on either blue (n=2 cups) or green solution (n=2 cups) for 24 hours (Figure 18).



Figure 18: Feeding cups. Two green paper cups had a solution consisting of green food colouring dye and two pink paper cups had solution with blue food colouring. The cotton wool in the microcentrifuge tubes can be seen to be completely saturated by each solution.

The cups were placed in the Botha De Meillon Insectary and the mosquitoes were allowed to feed on the solution *ad libitum* for 24 hours at 25°C. After 24 hours the mosquitoes were immobilised by being placed at -20°C for 10 minutes and were then viewed under a dissecting microscope. The coloured dye in the mosquitoes' abdomens would indicate uptake of the solution. Due to low feeding rate (results section 3.3.1), the mosquitoes (n=40) were starved for 16 hours prior to feeding in order to enhance the feeding efficiency.

Once feeding methods were optimised, the efficiency of the siRNA delivery system was evaluated using RPL19-siRNA and the reduction in *RPL19* transcript abundance was evaluated using real-time quantitative PCR (qPCR) to validate the protocol.

3.2.2. Short Interfering RNA (siRNA)

The siRNA was delivered to the mosquitoes via sugar water solution. Three controls were included in these experiments. A reference gene, *RPL19* was used as a positive control as this gene was uniformly expressed in *An. funestus* (Nardini *et al.,* 2017*)*. This gene was used to validate the siRNA ingestion method. An exogenous gene, mouse beta-2-microglobulin (*β2m*) was used as a non-specific negative control (Da costa *et al*., 2014). *β2m* is not present in *An. funestus* and therefore feeding this siRNA to mosquitoes should not alter the transcript abundance of *RPL19*. A no-siRNA control was included, which contains sugar water and food colouring dye, but no siRNA. This control will be referred to as the no-siRNA control. The siRNA was designed by Dr. Yael Dahan-Moss and synthesised by Ambion (Life Technologies, USA) (Table 4).

Table 4: Primers sequences and amplicon length of *RPL19*-siRNA and *β2m-siRNA*.

Primer	Sequence 5'→ 3'	Amplicon length	Gene sequence
RPL19 (forward)	ACAACGAUUCUCCACUUAA	21 bp	AFUN005878-RA (Vector Base)
RPL19 (reverse)	UUAAGUGGAGAAUCGUUGU		
β2m (forward)	GAGAAUGGGAAGCCGAACAUA	21 bp	AH001856.2 (GenBank)
β2m (reverse)	UAUGUUCGGCUUCCCAUUCUC		

3.2.3. Experimental setup to validate siRNA delivery system using *RPL19* transcript abundance

The efficacy of siRNA delivery through sugar water feeding was evaluated using the positive control, *RPL19*. Knockdown of this gene by RPL19-siRNA would confirm that

the sugar water delivery system used was adequate to result in gene knockdown and that the siRNA was effective. Newly emerged *An. funestus* females and males were separated based on gender and placed into six BugDorm® rearing cages. Three cages contained 20 females each and three cages contained 20 males each. These represent three technical replicates with a total of 120 adults (60 males and 60 females). Mosquitoes were starved for 16 hours (overnight) at 25°C before feeding on experimental sugar solution containing either 20 ng/µl RPL19-siRNA in dyed 10% sucrose solution (positive control), 20 ng/µl β2m-siRNA in a dyed 10% sucrose solution (negative control) and a dyed 10% sucrose solution (no-siRNA control). The siRNA sugar solution was mixed with green food colouring dye, as this is easier to visualise under the microscope, and ensures the uptake of the siRNA. Three biological replicates were performed with a total of 360 adults and these were used for subsequent qPCR.

3.2.4. RNA Extraction and cDNA Synthesis

After 24 hours of *ad libitum* feeding, the mosquitoes were visually inspected for dye-sugar uptake, and those with a dye-sugar solution in their abdomens were used. RNA was extracted and cDNA was synthesised as described in section 2.2.2.2. All cDNA samples were diluted to a 50 ng/µl concentration in a 100 µl distilled water solution (Appendix G).

3.2.5. *RPL19* sequence identity confirmation

One amplicon was generated by qPCR and the sense and antisense strands were sequenced in both directions (Macrogen) to confirm their identity, as described in section 2.3.1.

3.2.6. Data analysis

Data analysis was performed as described in section 2.2.3.7.

3.3. Results

3.3.1. Feeding optimisation

The feeding optimisation experiment showed that six mosquitoes fed on the blue dye whereas two mosquitoes fed on the green dye. Therefore, out of the 40 mosquitoes that were fed, five males and three females (20%) had coloured abdomens (Figure 19).



Figure 19: *Anopheles funestus* female adults viewed under a dissecting microscope. Abdomens were full of dyed sugar water after ingestion against a blue background. Blue dye (left) and green dye (right) were used. Images at a scale of 100 µm at 10X magnification.

The 16-hour (overnight) starvation prior to feeding, improved the feeding rate, with 17 out of 20 mosquitoes (12 males and five females) having fed on sugar water containing the blue dye. Similar results were achieved for adults fed on sugar solution containing green dye, where 15 out of 20 mosquitoes (nine males and six females) were fed. Therefore, out of the 40 mosquitoes fed on the sugar solution containing the two different dyes, 32 (80%) fed as indicated by the coloured abdomens. These feeding

conditions using green dye, which was visually easier to see under the microscope than the blue dye, were used going forward for siRNA treatment.

3.3.2. RPL19 sequence identity confirmation

The RPL19 PCR amplicon was Sanger sequenced and EMBOSS water alignment analysis of the sense and the antisense sequence confirmed a 99.4% and 98% sequence identity to the *AFUN005878* gene respectively. The BioEdit tool (version 7.7) was used to construct the RPL19 consensus sequence, which was analysed by the BLAST Vector Base tool. The RPL19 consensus sequence had a 98.761% sequence identity to the *AFUN005878* gene. This gene has 219 bp and is located on chromosome two at position AfunF3_2:52743479..52744793. This confirmed that the RPL19 primers were designed successfully, amplify the gene of interest and are suitable for subsequent experiments.

3.3.3. Experimental setup to validate siRNA delivery system using *RPL19*

Adult *An. funestus* females and males were fed with either 20 ng/µl RPL19-siRNA or β2m-siRNA spiked sugar water at 25°C. The *RPL19* transcript abundance was measured between the treatment and control groups (β2m-siRNA control and no-siRNA control). RPL19, the positive control, was analysed first to validate a new siRNA protocol by evaluating transcript abundance for the target gene *RPL19*.

Analysis of the *RPL19* transcript abundance of the males was reduced by 1.25-fold when compared to both the β2m-siRNA and no-siRNA treatments, but this change was not significant (one-way ANOVA: p= 0.445, F = 1.117, DF (2, 6)) (Figure 20A). In

contrast, the *RPL19* transcript abundance in the females decreased by 4-fold when compared to both the β2m-siRNA and no-siRNA treatments and this change was statistically significant (one-way ANOVA: p= 0.010, F= 2.386, DF (2, 6)) (Figure 20B) (Appendix H). To determine which treatments resulted in a significant difference, a Tukey HSD *post-hoc* test was used. Results showed a statistically significant difference between the values of the RPL19-siRNA and the negative control, β2m-siRNA (p= 0.0186) and no-siRNA control (p= 0.0138). As expected, there were no statistically significant differences between the negative control (β2m-siRNA) and the no-siRNA control (p= 0.9619), indicating that the siRNA ingestion does not impact the transcript abundance of the target gene.

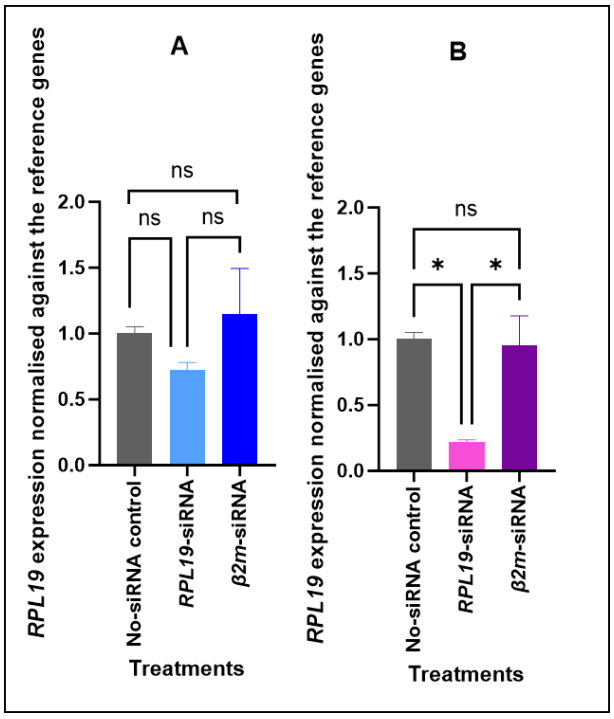


Figure 20: The normalised relative *RPL19* transcript abundance values against the reference genes, *RPS7* and *GAPDH,* in males (A) and females (B) after treatment with 20 ng/µl RPL19-siRNA and 20 ng/µl β2m-siRNA at 25°C. The asterisks indicate a Tukey *post-hoc* test (ns p > 0.05; * p ≤ 0.05; ** p ≤ 0.01; *** p ≤ 0.001; **** p ≤ 0.0001). Error bars represent the standard error of the mean (SEM).

3.4. Discussion

This research evaluates sugar feeding as a delivery system for siRNA in *An. funestus*. It also examined the application of siRNA for gene knockdown in the aforementioned malaria vector. Gene knockdown using dsRNA has been investigated before in *An. funestus* (Maharaj *et al*., 2022), but using siRNA in *An. funestus* as a knockdown method has never been explored. The aim of this study was to determine if gene knockdown via siRNA technology using sugar water as a delivery system in *An. funestus* adults was plausible.

The mosquitoes were starved for 16 hours prior to feeding, which is effective for the uptake of sugar water. This confirms other studies in which *An. farauti* feeding rates were examined in relation to various factors before and during direct membrane feeding, including the starvation circumstances and length of starvation prior to feeding (Timinao *et al*., 2021). In addition, overnight starvation (± 20 hours) in *An. funestus* yielded the highest feeding rates (Aswat *et al*., 2023).

The *RPL19* transcript abundance in *An. funestus* females was significantly reduced after being fed with RPL19-siRNA treated sugar water compared to females fed with either the β2m-siRNA or no-siRNA controls. However, males showed no significance in *RPL19* transcript change compared to controls. The uptake of siRNA may differ due to the volume of sugar water that can be ingested between males and females. This would result in a difference in transcript abundance. In a study by Olsen *et al*. (2020), male and female *Ae. aegypti* mosquitoes had total sugar contents of 0.27 g and 0.79 g, respectively, when the females were not blood-fed. Therefore, females can ingest almost 3-fold more than males. A lower volume intake by males would mean a lower

concentration of spiked sugar water and, thus, a lower impact on transcript abundance in siRNA studies.

This experiment, however, showed that the delivery system of adding siRNA directly to sugar water and allowing the adults to ingest the siRNA over a 24-hour period is working and suitable for further HSF-siRNA studies. One disadvantage is that the quantity of siRNA ingested can vary between individual mosquitoes. The advantage of oral delivery of siRNA as opposed to injection or soaking is that the mosquito's body is not compromised and the method is favourable when doing large-scale experiments simultaneously (Bilgi *et al.,* 2017).

3.5. Conclusion

The methodology optimised during this experiment confirmed that siRNA feeding via sugar water is a suitable delivery method of siRNA in *An. funestus.* This approach can be used for downstream experiments to evaluate the effect of HSF-siRNA on *HSF* transcript abundance and subsequent life table parameters in this species.

CHAPTER 4

ACHIEVING KNOCKDOWN OF HEAT SHOCK FACTOR (HSF) IN *ANOPHELES FUNESTUS* VIA SPECIFIC SHORT-INTERFERING RNA (siRNA)

4.1. Introduction

Insects employ a variety of survival tactics when exposed to high temperatures. The HSR is quickly produced by heat or other environmental and physiological stressors, as explained in Chapter 1. HSF would be translocated to the nucleus whereby there would be more HSF based transcription but this would not mean a higher *HSF* transcript abundance (Demirovic *et al*., 2014). The HSF itself acts as a transcription factor whereby it transcribes HSPs. Therefore, the transcript abundance of HSPs would increase but not of HSF itself regardless of the temperature.

There is a paucity of data pertaining to HSF in anophelines but the identified information will be discussed below. In *An. gambiae*, there are three different isoforms of the HSF coding sequence, namely, HSF1, HSF2, and HSF3. To the best of my knowledge, it is unknown whether *An. funestus* contains the same three isoforms and further work on this is required. However, what is known in other insect and mosquitoes is that the three isoforms are produced during HSF transcription (Neueder *et al*., 2014). The DNA binding domain is shared by all isoforms. HSF1 and HSF2 have a 90% sequence similarity, while HSF2 has an extra exon in its sequence. Heat shock factor 3 (HSF3) is a shorter splice variant isoform of HSF1 and HSF2 (Dottorini *et al*., 2013). Apart from the DNA binding domain on HSF discussed in Chapter 1, the authors also showed that HSF1 was found to have binding sites to male accessory gland genes.

This would imply that HSF has roles other than responding to stressors and impacts mosquito physiology.

4.1.1. Aim and objectives

The study described in this chapter aimed to evaluate the impact of *HSF transcript abundance* when adults were housed at different temperatures and fed on different siRNA concentrations. The following objectives were formulated:

4.1.1.1. To confirm if the optimised protocol (described in Chapter 3) could successfully be used to achieve HSF knockdown in *An. funestus*.

4.1.1.2. To determine the impact of treating *An. funestus* adults with different HSF-siRNA concentrations at different temperatures on *HSF transcript abundance*.

4.2. Materials and methods

4.2.1. Confirming that the optimised protocol (described in Chapter 3) could successfully be used to achieve HSF knockdown

4.2.1.1. Short interfering RNA

siRNA was delivered to the mosquitoes via a sugar water solution (as described in section 3.2.1). HSF-siRNA was designed by Dr. Yael Dahan-Moss and synthesised by Ambion (Life Technologies, USA). The details pertaining to the HSF-siRNA can be seen below in Table 5.

Table 5: Primers sequences and amplicon length for the HSF-siRNA

Primer	Sequence 5'→ 3'	Amplicon length	Gene sequence
HSF (forward)	GACGAUGAAGCAGGAGAAUGA	21 bp	AFUN004137 (Vector Base)
HSF (reverse)	UCAUUCUCCUGCUUCAUCGUC		

4.2.1.2. Experimental setup

A summary of the methods can be seen in Figure 21. Newly emerged *An. funestus* adults were separated based by gender. Sixty females were divided into three cages, of 20 females each, and the same was done for the males (one biological replicate). Three biological replicates were performed. These mosquitoes were starved for 16 hours and then allowed to feed *ad libitum* on 20 ng/µl siRNA while adults were housed under standard insectary conditions of 25°C. After 24 hours of feeding, the mosquitoes with visually dyed abdomens were cold-killed and their RNA was extracted as described in section 2.2.2.2. The cDNA was synthesised from the RNA (as described in section 2.2.2.2.). Thereafter, qPCR analysis was performed as per protocol described in section 2.2.2.3. to confirm the transcript abundance of *HSF.*

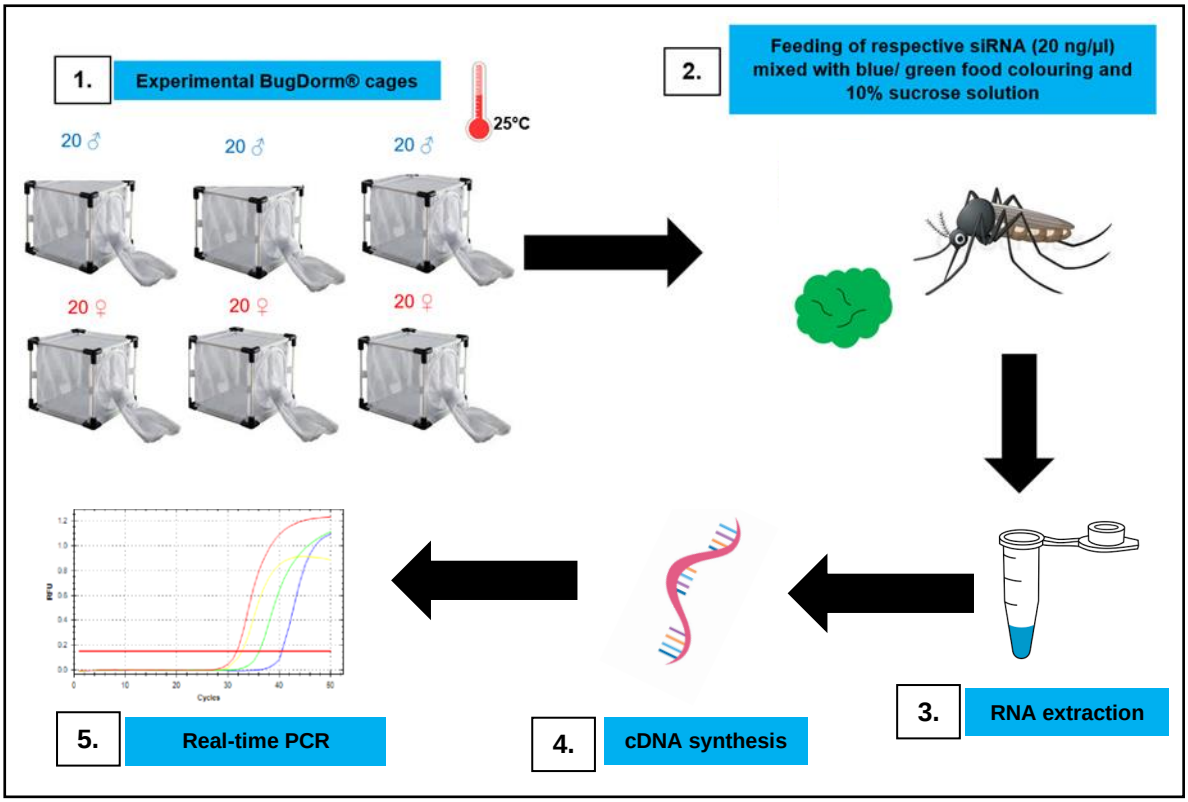


Figure 21: Flow diagram of the methods involved in determining if the protocol described in chapter 3 can achieve HSF knockdown. (1) Six cages were set up whereby three contained 20 female adults in each and the other three 20 male adults in each. (2) The adult mosquitoes were fed a mixture of 20 ng/µl siRNA in spiked sugar. (3) The fed mosquitoes were cold-killed and their RNA was extracted. (4) cDNA was synthesised from the extracted RNA. (5) Real-time PCR was performed to determine *HSF* transcript abundance.

4.2.2. Determining the effect of siRNA concentration and adult exposure temperatures on *HSF* transcript reduction

4.2.2.1. Experimental set up

Once it was confirmed that HSF knockdown was successful using the protocol established, 60 *An. funestus* males and 60 females were separated and were fed either 10 ng/µl, 20 ng/µl or 30 ng/µl β2m-siRNA and HSF-siRNA at either 20, 25 or 30°C as per the protocol mentioned in section 3.2.1 (one biological replicate). Three biological replicates were performed. Three rooms were used in the insectary whereby the three

temperatures were adjusted and maintained. The above-mentioned *An. funestus* adults were cold-killed, RNA was extracted and cDNA synthesised, as described in section 2.2.2.2. This cDNA was diluted (Appendix I) and was used for transcript abundance studies using qPCR (Figure 22). Analysis was conducted as described in section 2.2.3.7. However, even when the one-way ANOVA showed no statistical difference, a *post-hoc* test (Tukey-HSD) was performed to represent the results graphically in figures.

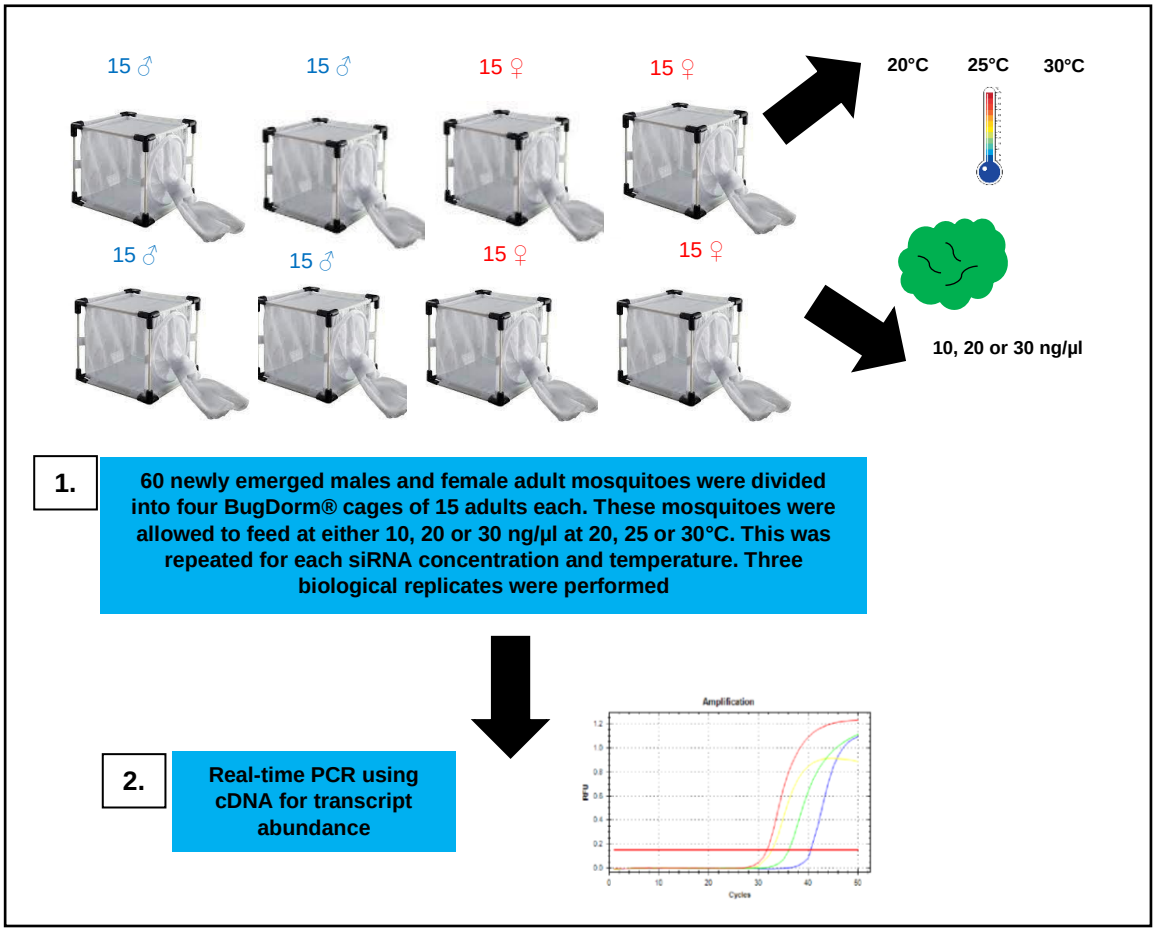


Figure 22: Flow diagram of the methods involved in determining the level of transcript abundance after siRNA ingestion. (1) 60 males and 60 female adult mosquitoes were divided into four BugDorm® cages of 15 adults each. These mosquitoes were allowed to feed on either 10, 20 or 30 ng/µl siRNA at 20, 25 or 30°C. Three biological replicates were performed. The mosquitoes were then cold-killed, RNA was extracted and then cDNA was synthesised (2) The cDNA was used in qPCR to determine transcript abundance against two reference genes.

4.3. Results

4.3.1. Real-time PCR for quantitative analysis for the optimised protocol (as described in Chapter 3) to assess success in HSF knockdown

The transcript abundance of *HSF* was examined in HSF-siRNA, β2m-siRNA and no-siRNA control treated males and females (as described in section 2.2.3.6). *Anopheles funestus* males fed at 25°C with HSF-siRNA (20 ng/µl) showed that the effect of HSF-siRNA feeding significantly decreased *HSF* transcript abundance by 2.5-fold when compared to the effect of β2m-siRNA and no-siRNA controls (one-way ANOVA: p= 0.0004, F= 37, DF (2, 6)). A Tukey-HSD test showed that *HSF* transcript abundance after HSF-siRNA treatment was significantly lower when compared to the effect of the β2m-siRNA control (p= 0.0007). This significant transcript abundance decrease was also observed between the no-siRNA control and HSF-siRNA treatments (p= 0.0007). However, there were no significant difference in transcript abundance between β2m-siRNA control or the no-siRNA control (p= 0.9989) (Figure 23A).

In females, HSF-siRNA feeding significantly decreased *HSF* transcript abundance by 2.5-fold when compared to the β2m-siRNA and no-siRNA controls (one-way ANOVA: p= 0.0024, F= 19, DF (2, 6)). A Tukey-HSD test showed that HSF-siRNA transcript abundance differed significantly when compared to the β2m-siRNA control (p= 0.0102), and to the no-siRNA control (p= 0.0023). The no-siRNA control was not significantly different when compared to the β2m-siRNA control (p= 0.3333) (Figure 23B). The fold reduction (2.5-fold) in *HSF* transcript abundance were equal between male and females. The siRNA downregulation was successful and therefore the study was continued to evaluate the impact of HSF-siRNA concentrations on the *HSF* transcript abundance when adults were housed at different temperatures.

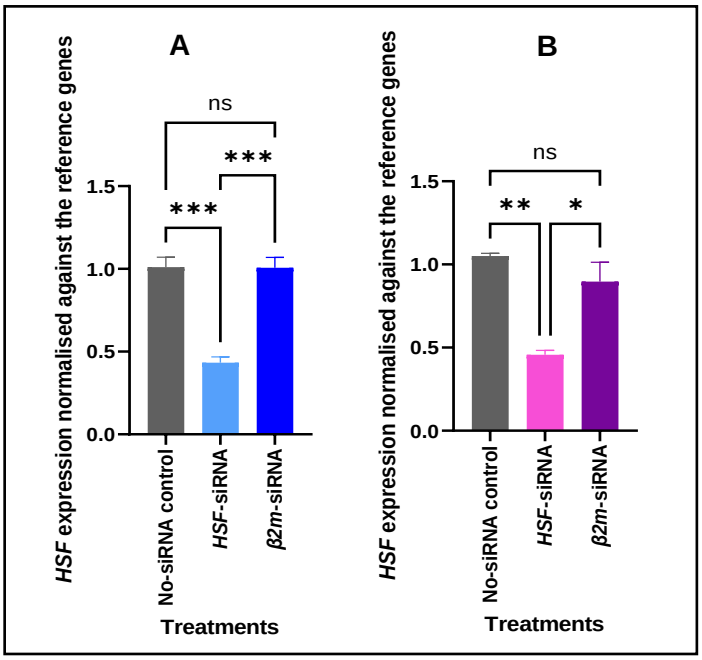


Figure 23: The relative *HSF* transcript abundance normalised against the reference genes, *RPS7* and *GAPDH*, in males (A) and females (B) at 25°C with treatment of 20 ng/µl siRNA. The asterisks indicate a Tukey *post-hoc* test (ns $p > 0.05$; * $p \leq 0.05$; ** $p \leq 0.01$; *** $p \leq 0.001$; **** $p \leq 0.0001$). Error bars represent standard error of the mean (SEM).

4.3.2. Determination of the impact of siRNA concentration and specific temperatures on HSF transcript abundance

Adult *An. funestus* females and males were treated with 10 ng/µl, 20 ng/µl and 30 ng/µl HSF-siRNA at 20°C, 25°C and 30°C and *HSF* transcript abundance was measured between the treatment and control groups. A Tukey *post-hoc* test was included to determine the effectiveness of the siRNA treatment at all concentrations and temperatures. These results will be provided per experimental set-up under specific temperature conditions (raw Ct values found in Appendix J). The below figures have also been simplified and tabulated and can be found in Appendix K.

i. Adults housed at 20°C

a. 10 ng/µl

The *HSF* transcript abundance in *An. funestus* males fed with HSF-siRNA (10 ng/µl) at 20°C was significantly reduced by 2.5-fold compared to males fed with no-siRNA or with β2m-siRNA (one-way ANOVA: p= 0.0005, F= 33.74, DF (2, 6)). A Tukey-HSD test showed that *HSF* transcript abundance after HSF-siRNA treatment differed significantly when compared to the effect of the β2m-siRNA (p= 0.0009) and no-siRNA control (p= 0.001) and not significant when the no-siRNA control was compared to the *β2m-siRNA* control (p= 0.996) (Figure 24A). *Anopheles funestus* females showed that the effect of HSF-siRNA feeding significantly reduced *HSF* transcript abundance by 3-fold (one-way ANOVA: p= 0.002, F= 20.76, DF (2, 6)). A Tukey-HSD test showed that *HSF* transcript abundance differed significantly when compared to the effect of β2m-siRNA (p= 0.0054) and no-siRNA (p= 0.0024) and not significant when the no-siRNA control was compared to β2m-siRNA (p= 0.6786) (Figure 24B).

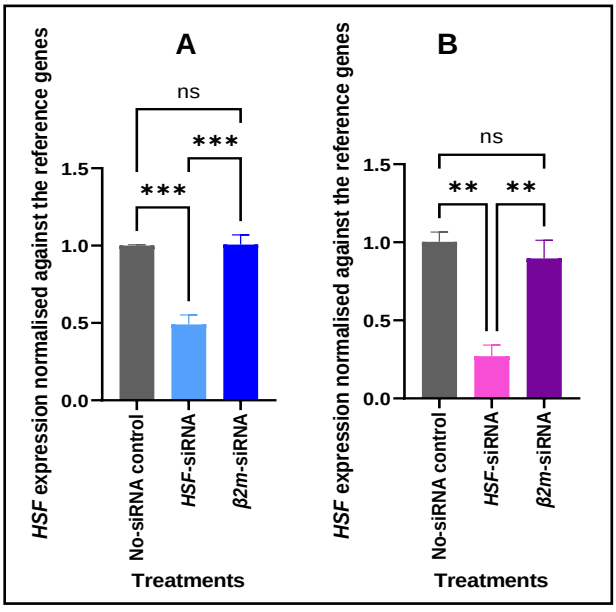


Figure 24: The relative *HSF* transcript abundance normalised against the reference genes, *RPS7* and *GAPDH*, in males (A) and females (B) at 20°C with treatment of 10 ng/µl siRNA. The asterisks indicate a Tukey *post-hoc* test (ns p > 0.05; * p ≤ 0.05; ** p ≤ 0.01; *** p ≤ 0.001; **** p ≤ 0.0001). Error bars represent standard error of the mean (SEM).

b. 20 ng/µl

The effect of 20 ng/µl siRNA at 20°C in *An. funestus* males showed a decrease of 3.3-fold in *HSF* transcript abundance, which was significant when compared to the controls (one-way ANOVA: *p*= 0.0006, F= 31.78, DF (2, 6)). A Tukey-HSD test showed HSF-siRNA feeding significantly decreased *HSF* transcript abundance when compared to the effect of β2m-siRNA (*p*= 0.0014), with the no-siRNA control also being significant when compared to HSF-siRNA (*p*= 0.0009). There was no significant difference in the no-siRNA control when compared to the β2m-siRNA control (*p*= 0.8776) (Figure 25A). The effect of HSF-siRNA feeding on *HSF* transcript abundance in females showed a significant decrease of 2.9-fold in *An. funestus* when compared to controls (one-way ANOVA: *p*= 0.00119, F= 10.13, DF (2, 6)). A Tukey-HSD test showed that *HSF* transcript abundance was significantly different when compared to β2m-siRNA transcript abundance (*p*= 0.0207), with the no-siRNA control also being significant when compared to HSF-siRNA (*p*= 0.0171). The no-siRNA control was not significant when compared to the β2m-siRNA control (*p*= 0.9846) (Figure 25B).

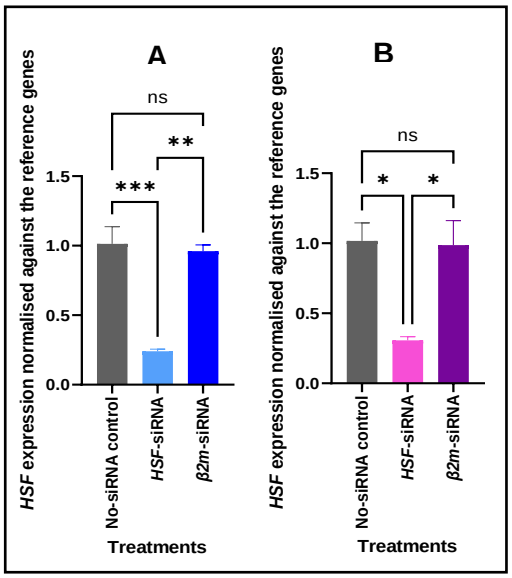


Figure 25: The relative *HSF* transcript abundance normalised against the reference genes, *RPS7* and *GAPDH*, in males (A) and females (B) at 20°C with treatment of 20 ng/µl siRNA. The asterisks indicate a Tukey *post-hoc* test (ns p > 0.05; * p ≤ 0.05; ** p ≤ 0.01; *** p ≤ 0.001; **** p ≤ 0.0001). Error bars represent standard error of the mean (SEM).

c. 30 ng/µl

At a temperature of 20°C and a siRNA concentration of 30 ng/µl it was shown that the effect of HSF-siRNA on *HSF* transcript abundance decreased by 2.5-fold in males, but this was not statistically significant when compared to controls (one-way ANOVA: p= 0.0974, F= 3.521, DF (2, 6)). To represent this graphically (Figure 26A), a Tukey-HSD test was also conducted and confirmed that HSF-siRNA feeding did not significantly decrease *HSF transcript abundance* when compared to the effect of β2m-siRNA (p= 0.1207) and the no-siRNA control (p= 0.1458). Between β2m-siRNA and no-siRNA control (p= 0.9880) transcript abundance did also not differ significantly (Figure 26A). However, *An. funestus* females showed that the effect of HSF-siRNA significantly influenced *HSF* transcript abundance with a 10-fold decrease in transcript abundance when compared to controls (one-way ANOVA: p= 0.0002, F= 53.02, DF (2, 6)). A Tukey-HSD test showed that HSF and β2m-siRNA differed significantly (p= 0.0004), with the no-siRNA control also being significant when compared to HSF-siRNA (p= 0.0002) and the no-siRNA control being not significant when compared to the β2m-siRNA control (p= 0.4641) (Figure 26B).

ii. Adults housed at 25°C

d. 10 ng/µl

It was observed that *An. funestus* males housed at 25°C and fed with 10 ng/µl HSF-siRNA, did not significantly influence *HSF* transcript abundance when compared to the controls (one-way ANOVA: *p*= 0.639, F= 5.711, DF (2, 6)) (Figure 27A). *Anopheles funestus* females showed that the effect of HSF-siRNA significantly influenced *HSF* transcript abundance with a 2.2-fold decrease when compared to controls (one-way ANOVA: *p*= 0.0226, F= 7.613, DF (2, 6)). A Tukey-HSD test showed that *HSF*

transcript abundance differed significantly when compared to β2m-siRNA (p= 0.0360), with the no-siRNA control also being significant when compared to HSF-siRNA (p= 0.0327) and the no-siRNA control being not significant when compared to β2m-siRNA control (p= 0.9964) (Figure 27B).

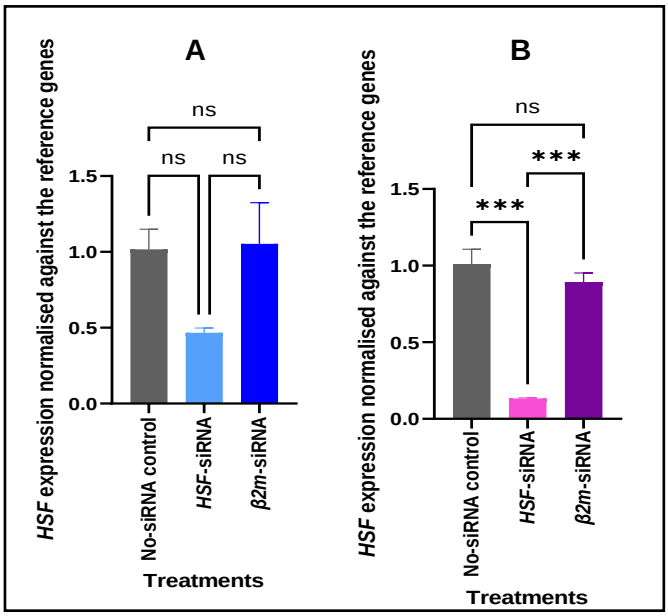


Figure 26: The relative *HSF* transcript abundance normalised against the reference genes, *RPS7* and *GAPDH*, in males (A) and females (B) at 20°C with treatment of 30 ng/µl siRNA. The asterisks indicate a Tukey *post-hoc* test (ns p > 0.05; * p ≤ 0.05; ** p ≤ 0.01; *** p ≤ 0.001; **** p ≤ 0.0001). Error bars represent the standard error of the mean (SEM).

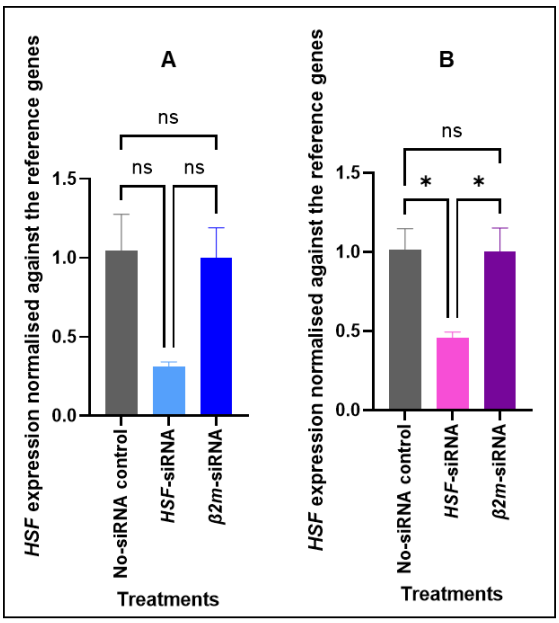


Figure 27: The relative *HSF* transcript abundance normalised against the reference genes, *RPS7* and *GAPDH*, in males (A) and females (B) at 25°C with treatment of 10 ng/µl siRNA. The asterisks indicate a Tukey *post-hoc* test (ns $p > 0.05$; * $p \leq 0.05$; ** $p \leq 0.01$; *** $p \leq 0.001$; **** $p \leq 0.0001$). Error bars represent standard error of the mean (SEM).

e. 20 ng/µl

This analysis of adults housed at 25°C and treated with 20ng/ul siRNA was previously performed in section 4.3.1. However, it was repeated for this study in order for all analyses to be done concurrently. *Anopheles funestus* males fed at 25°C on siRNA (20 ng/µl) showed that the effect of HSF-siRNA demonstrated a 1.6-fold decrease in *HSF* transcript abundance, but this did not differ significantly when compared to controls (one-way ANOVA: p= 0.0608, F= 5.711, DF= (2, 6)) (Figure 28A). *Anopheles funestus* females showed that the effect of HSF-siRNA also did not significantly influence *HSF* transcript abundance although there was a 2.5-fold decrease in transcript abundance when compared to controls (one-way ANOVA: p= 0.0627, F= 4.500, DF= (2, 6)) (Figure 28B).

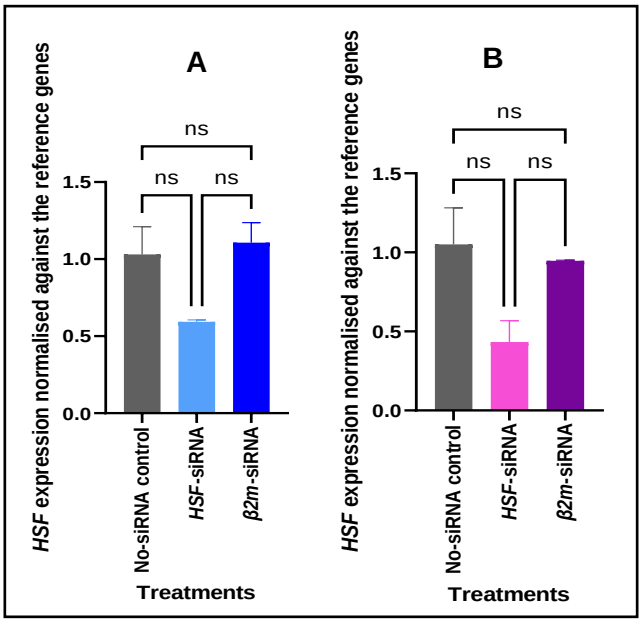


Figure 28: The relative *HSF* transcript abundance normalised against the reference genes, *RPS7* and *GAPDH*, in males (A) and females (B) at 25°C with treatment of 20 ng/µl siRNA. The asterisks indicate a Tukey *post-hoc* test (ns $p > 0.05$; * $p \leq 0.05$; ** $p \leq 0.01$; *** $p \leq 0.001$; **** $p \leq 0.0001$). Error bars represent standard error of the mean (SEM).

f. 30 ng/µl

The effect of 30 ng/µl siRNA at 25°C on *An. funestus* males showed a 1.6-fold decrease in *HSF* transcript abundance but this was not significant when compared to the controls (one-way ANOVA: p= 0.0739, F= 4.149, DF (2, 6)) (Figure 29A). *HSF* transcript abundance was not significantly influenced in *An. funestus* females when a 1.3-fold decrease of transcript abundance was reported (one-way ANOVA: p= 0.5229, F= 0.7237, DF (2, 6)) (Figure 29B).

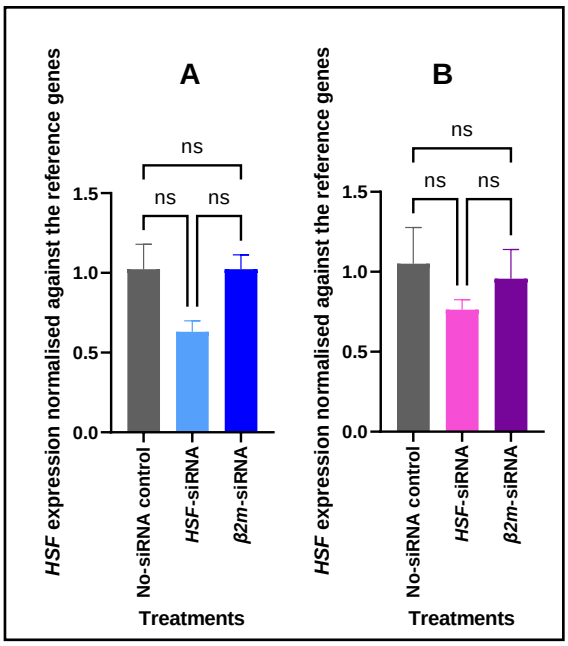


Figure 29: The relative *HSF* transcript abundance normalised against the reference genes, *RPS7* and *GAPDH*, in males (A) and females (B) at 25°C with treatment of 30 ng/µl siRNA. The asterisks indicate a Tukey *post-hoc* test (ns $p > 0.05$; * $p \leq 0.05$; ** $p \leq 0.01$; *** $p \leq 0.001$; **** $p \leq 0.0001$). Error bars represent standard error of the mean (SEM).

iii. Adults housed at 30°C

g. 10 ng/µl

Anopheles funestus males fed at 30°C on siRNA (10 ng/µl) showed that the effect of HSF-siRNA did not significantly influence *HSF* transcript abundance, yet transcript abundance was reduced 2-fold when compared to controls (one-way ANOVA: p= 0.2625, F= 1.685, DF (2, 6)) (Figure 30A). *HSF* transcript abundance in *An. funestus* females were reduced by 2.5-fold when fed 10 ng/µl, but this was not significantly influenced when compared to controls (one-way ANOVA: p= 0.0644, F= 4.485, DF (2, 6)).

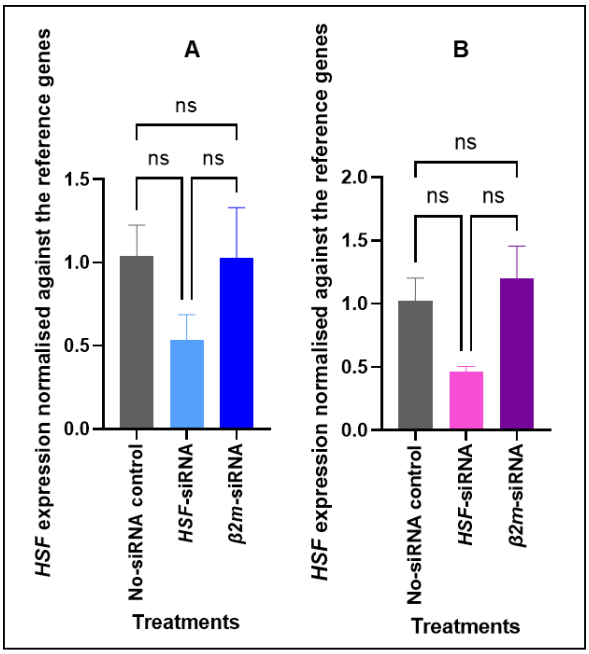


Figure 30: The relative *HSF* transcript abundance normalised against the reference genes, *RPS7* and *GAPDH*, in males (A) and females (B) at 30°C with treatment of 10 ng/µl siRNA. The asterisks indicate a Tukey *post-hoc* test (ns $p > 0.05$; * $p \leq 0.05$; ** $p \leq 0.01$; *** $p \leq 0.001$; **** $p \leq 0.0001$). Error bars represent standard error of the mean (SEM).

h. 20 ng/µl

It was observed at 30°C that when *An. funestus* males were fed 20 ng/µl siRNA, this 2-fold reduction in *HSF* transcript abundance was not significant when compared to the controls (one-way ANOVA: p= 0.539, F= 5.663, DF (2, 6)) (Figure 31A). *Anopheles funestus* females showed the effect of HSF-siRNA significantly reduced *HSF* transcript abundance by 2.9-fold when compared to controls (one-way ANOVA: p= 0.0141, F= 9.442, DF (2, 6)). A Tukey-HSD test showed that *HSF* transcript abundance when compared to the β2m-siRNA control differed significantly (p= 0.0230), with the no-siRNA control also being significant when compared to HSF-siRNA (p= 0.0210) and the no-siRNA control being not significant when compared to β2m-siRNA (p= 0.9967) (Figure 31B).

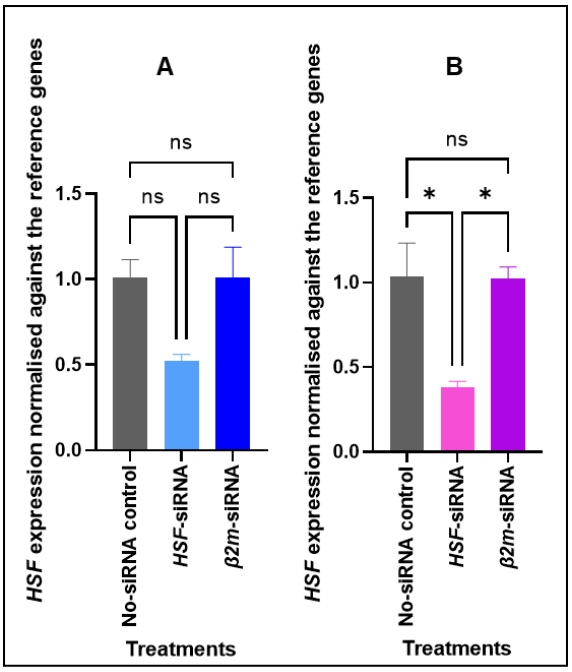


Figure 31: The relative *HSF* transcript abundance normalised against the reference genes, *RPS7* and *GAPDH*, in males (A) and females (B) at 30°C with treatment of 20 ng/µl siRNA. The asterisks indicate a Tukey *post-hoc* test (ns $p > 0.05$; * $p \leq 0.05$; ** $p \leq 0.01$; *** $p \leq 0.001$; **** $p \leq 0.0001$). Error bars represent standard error of the mean (SEM).

i. 30 ng/µl

Anopheles funestus males fed at 30°C on siRNA (30 ng/µl) showed that the effect of HSF-siRNA significantly reduced *HSF* transcript abundance by 3.3-fold when compared to controls (one-way ANOVA: p= 0.0117, F= 10.23, DF (2, 6)). A Tukey-HSD test showed that *HSF* transcript abundance differed significantly when compared to β2m-siRNA (p= 0.0188), with the no-siRNA control also being significant when compared to HSF-siRNA (p= 0.0179) and not significant when compared to β2m-siRNA (p= 0.9990) (Figure 32A). *Anopheles funestus* females showed the effect of HSF-siRNA significantly decreased *HSF* transcript abundance by 2.5-fold when compared to controls (one-way ANOVA: p= 0.0101, F= 10.88, DF (2, 6)). A Tukey-HSD test showed that *HSF* transcript abundance differed significantly when compared

to β2m-siRNA (*p*= 0.0106), with the no-siRNA control also being significant when compared to HSF-siRNA (*p*= 0.0296) and not significant when compared to β2m-siRNA (*p*= 0.6520) (Figure 32B).

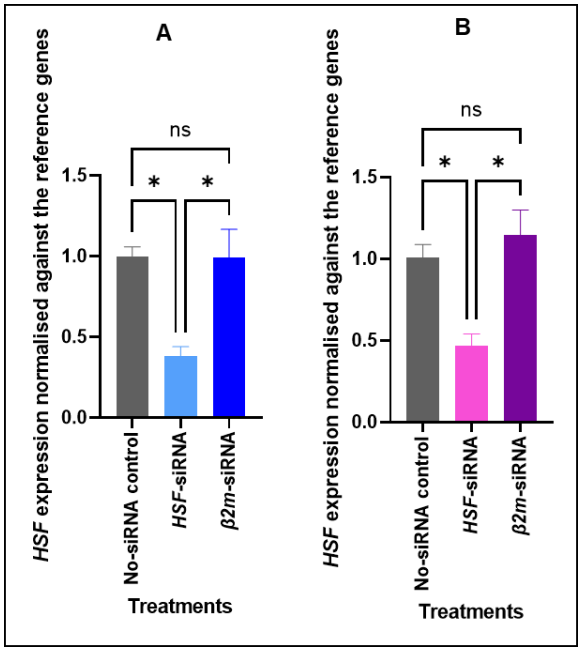


Figure 32: The relative *HSF* transcript abundance normalised against the reference genes, *RPS7* and *GAPDH*, in males (A) and females (B) at 30°C with treatment of 30 ng/µl siRNA. The asterisks indicate a Tukey *post-hoc* test (ns p > 0.05; * p ≤ 0.05; ** p ≤ 0.01; *** p ≤ 0.001; **** p ≤ 0.0001). Error bars represent standard error of the mean (SEM).

j. Effect of siRNA concentration on HSF transcript abundance at a set temperature

The transcript abundance of *HSF* after HSF-siRNA treatment at different concentrations and at a specific temperature was compared to the β2m-siRNA and no-siRNA controls. The 2-ΔΔCt values were normalised against the no-siRNA control which allowed comparison across the three concentrations at any one temperature. Since no statistically significant difference between the no-siRNA control and the negative control (β2m-siRNA) at all temperatures and concentrations was observed,

the β2m-siRNA control was not used. The 2-ΔΔCt values were evaluated for normality using the Shapiro-Wilks test and analysed using one-way ANOVA. Males across the three concentrations were analysed at each temperature separately from the females.

Results showed that there was no significant difference in *HSF* transcript abundance in males that were treated with different concentrations of HSF-siRNA regardless of the concentrations used within a temperature range e.g. 20°C (one-way ANOVA: p= 0.0649, F= 4.464, DF (2, 6)) (Figure 33A), 25°C (one-way ANOVA: p= 0.1340, F= 2.862, DF (2, 6)) (Figure 33B) and 30°C (one-way ANOVA: p= 0.2238, F= 1.941, DF (2, 6)) (Figure 33C). In addition, there was no significant difference in *HSF* transcript abundance in females treated with different concentrations of HSF-siRNA. At 20°C (one-way ANOVA: p= 0.1530, F= 2.689, DF (2, 6)) (Figure 34A), 25°C (one-way ANOVA: p= 0.2090, F= 2.005, DF (2, 6)) (Figure 34B) and 30°C (one-way ANOVA: p= 0.5721, F= 0.6139, DF (2, 6)) (Figure 34C).

k. The impact of adult exposure to varying temperature on *HSF* transcript abundance

Adult mosquitoes that were housed under different temperatures (but at the same HSF-siRNA concentrations) were compared and the *HSF* transcript abundance that was normalised against the no-siRNA control was investigated. The *HSF* transcript abundance was not statistically different in either *An. funestus* males (one-way ANOVA: p= 0.2037, F= 2.099, DF (2, 6)) (Figure 35) or females (one-way ANOVA: p= 0.3013, F= 1.431, DF (2, 6)) (Figure 36) that were fed with 10 ng/µl HSF-siRNA at different temperatures. This was also true when females were fed on 20 ng/µl siRNA concentration at all three temperatures (one-way ANOVA: p= 0.5896, F= 0.5776, DF

(2, 6)). However, males fed with (20 ng/µl) showed a significant decrease when exposed to 20°C and 25°C (p= 0.0078) as well as between 20°C and 30°C (p= 0.0239), but not for adults exposed to 25°C and 30°C (p= 0.5873).

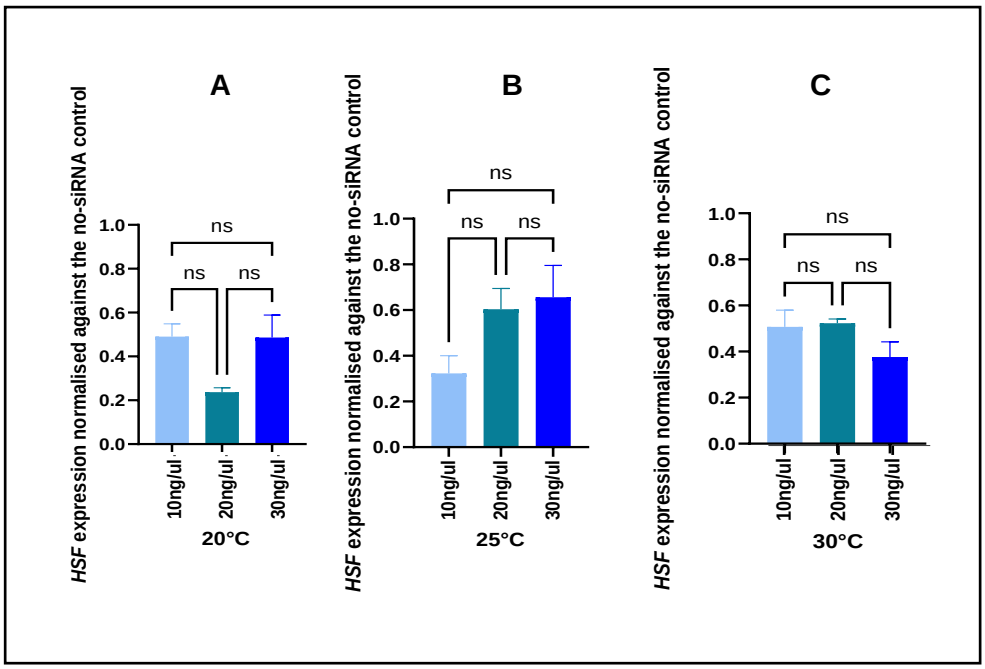


Figure 33: The relative *HSF* transcript abundance normalised against the no-siRNA control in males at 20°C (A), 25°C (B) and 30°C (C) after treatment with 10 ng/µl, 20 ng/µl and 30 ng/µl HSF-siRNA. The asterisks indicate a Tukey *post-hoc* test (ns p > 0.05; * p ≤ 0.05; ** p ≤ 0.01; *** p ≤ 0.001; **** p ≤ 0.0001). Error bars represent standard error of the mean (SEM**).**

There was no statistical difference in *HSF* transcript abundance in males when adults were fed with 30 ng/µl siRNA (one-way ANOVA: p= 0.2510, F= 0.1518, DF (2, 6)). Females fed at this concentration (30 ng/µl) showed a significant decrease in *HSF* transcript abundance when exposed to 20°C compared to those exposed to 25°C (p= 0.0247) but not when compared to adults exposed to and 30°C (p= 0.2532). There was no statistical difference in *HSF* transcript abundance between females exposed to 25°C and to 30°C fed at all concentrations of siRNA (p= 0.2259) (Figure 36).

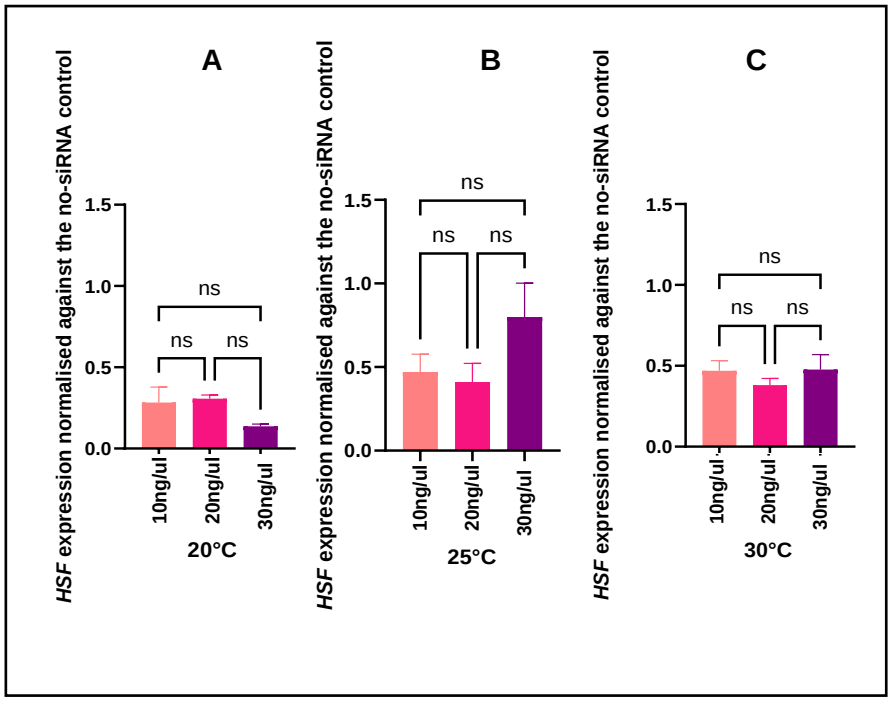


Figure 34: The relative *HSF* transcript abundance normalised against the no-siRNA control in females at 20°C (A), 25°C (B) and 30°C (C) after treatment with 10 ng/µl, 20 ng/µl and 30 ng/µl HSF-siRNA. The asterisks indicate a Tukey *post-hoc* test (ns $p > 0.05$; * $p \leq 0.05$; ** $p \leq 0.01$; *** $p \leq 0.001$; **** $p \leq 0.0001$). Error bars represent standard error of the mean (SEM).

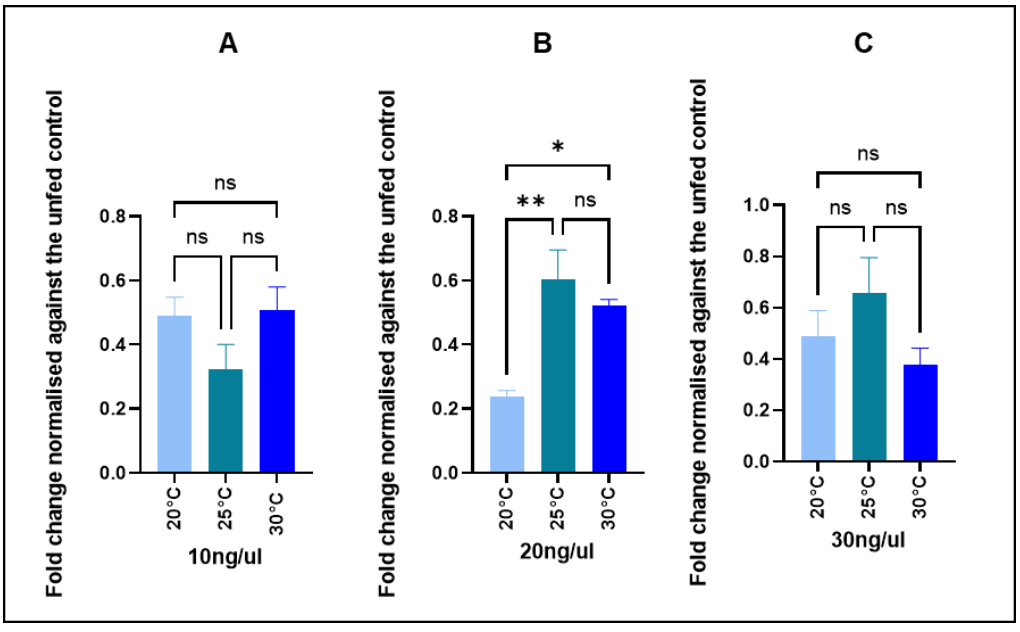


Figure 35: The relative *HSF* transcript abundance normalised against the no-siRNA control in males with an HSF-siRNA concentration of 10 ng/µl (A), 20 ng/µl (B) and 30 ng/µl (C) across all three temperatures. The asterisks indicate a Tukey *post-hoc* test (ns $p > 0.05$; * $p \leq 0.05$; ** $p \leq 0.01$; *** $p \leq 0.001$; **** $p \leq 0.0001$). Error bars represent standard error of the mean (SEM).

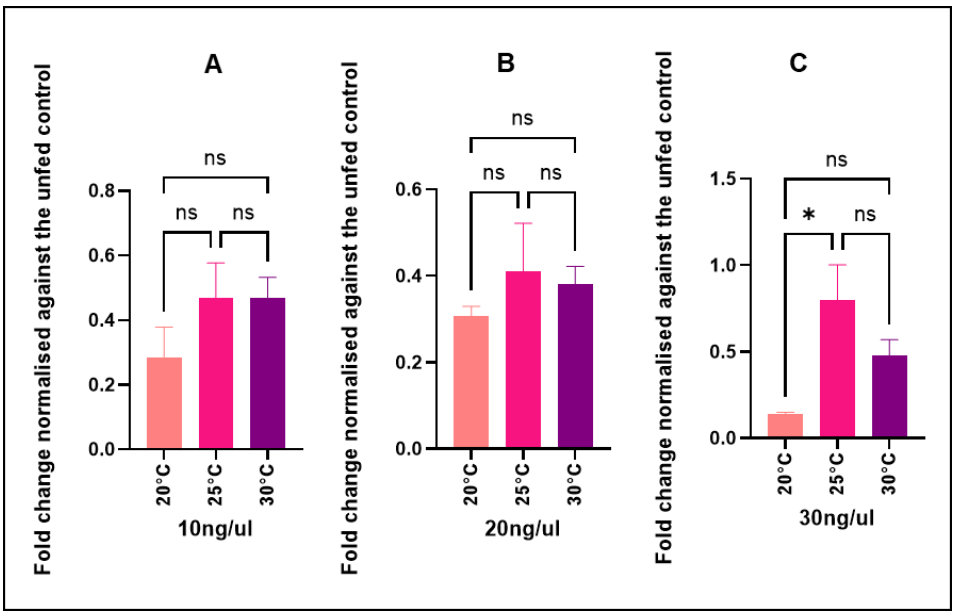


Figure 36: The relative *HSF* transcript abundance was normalised against the no-siRNA control in females with an HSF-siRNA concentration of 10 ng/µl (A), 20 ng/µl (B) and 30 ng/µl (C) across all three temperatures. The asterisks indicate a Tukey *post-hoc* test. (ns $p > 0.05$; * $p \leq 0.05$; ** $p \leq 0.01$; *** $p \leq 0.001$; **** $p \leq 0.0001$). Error bars represent standard error of the mean (SEM).

4.4. Discussion

There are few studies pertaining to HSF in mosquitoes and more importantly, to the best of my knowledge, none on the main African malaria vector, *An. funestus.* This study is the first study to investigate the plausibility of utilising siRNA in order to silence the *HSF* gene in *An. funestus*. In addition, this study chapter investigated the impact of HSF-siRNA concentrations and adult environmental housing temperatures on transcript reduction.

Both *An. funestus* males and females were used and to ensure siRNA uptake, food colouring was used to visualise the mosquitoes' abdomens. The previously described optimised protocol (Chapter 3) was followed, however the target gene was *HSF.* Knockdown of HSF was achieved in both *An. funestus* males and

females. In addition, there was no significant change in transcript abundance between adults fed with no-siRNA control or the β2m-siRNA control, indicating that the siRNA treatment method did not impact HSF transcription and that the decrease in HSF transcript observed is due to the HSF-siRNA treatment.

Once it was confirmed that the feeding of *An. funestus* adults with HSF-siRNA successfully achieved knockdown, different siRNA concentrations (10 ng/µl, 20 ng/µl and 30 ng/µl) were fed to male and female *An. funestus* adults, under three temperatures (20°C, 25°C and 30°C). Different concentrations and temperatures were tested to evaluate the impact of different concentrations or temperatures on the fold change after treatment. In all the experiments conducted, the knockdown of HSF in *An. funestus* males and females did not significantly differ between adults without siRNA (no-siRNA control) treatment or with β2m-siRNA treatment. There was statistically significantly lower *HSF* transcript abundance in adults fed on HSF-siRNA when compared to both controls (no-siRNA or β2m-siRNA) under specific experimental conditions.

Although *HSF* transcript abundance was significantly reduced in HSF-siRNA treated females when compared to the β2m-siRNA and no-siRNA treated controls at 20°C (10 ng/µl, 20 ng/µl and 30 ng/µl), 25°C (10 ng/µl) and 30°C (20 ng/µl), this phenomenon was less evident in males. Another reason for the discrepancies between males and females could be that the concentration of siRNA was not sufficient to observe a reduction in the male cohort, most likely due to a lower volume of sugar solution ingested hence a lower concentration of siRNA ingested. Females can ingest a larger volume of sugar solution compared to males due to the elasticity of their abdomens as

explained in Chapter 3. A study examined the sugar-feeding habits of *Cx. quinquefasciatus* and *Ae. aegypti*. The mean sugar volume in the bodies of female *Aedes* and *Culex* was higher than that of the males. *Culex quinquefasciatus* males had a mean total sugar uptake of 11.74 µg whereas females had 22.85 µg. *Aedes aegypti* males had 2.12 µg of sugar and females 11.56 µg. The authors assumed a higher sugar volume suggested a higher volume uptake of sugar bait in females when compared to males (Olson *et al.*, 2020). However, this hypothesis needs to be tested. This technique however, is a good possible addition to future studies.

In addition, during the protocol validation experiment where both males and females were fed on HSF-siRNA at 25°C (20 ng/µl siRNA), both males and females showed a significant reduction in *HSF* transcript abundance when compared to the controls. However, when the experiment was repeated at 25°C with a range of HSF-siRNA concentrations, the transcript abundance of HSF did not decrease significantly in *An. funestus* male or female adults treated with 20 ng/µl HSF-siRNA when compared to the control treatments. This discrepancy in results may be because the experiments were performed two weeks apart from each other and the humidity and temperatures may have been unstable due to electricity outages. Considering these factors, additional optimisation is required and when using males and siRNA feeding time should be longer to ensure consistency.

After normalising the transcript abundance of *HSF* against the no-siRNA control, it was evident that the *HSF* transcript abundance of adults exposed to a set temperature was not affected by the concentration of HSF-siRNA fed to these adults. The fact that there was no significant difference across each temperature and siRNA concentration when normalised against the no-siRNA control indicates that the 10 ng/µl-30 ng/µl siRNA

had no impact on the HS*F* transcription. This confirms that the feeding of siRNA via sugar water is not sensitive to the concentration of siRNA that was evaluated in this study. Future studies should look at higher concentrations of siRNA to confirm the trend observed here. Another alternative would be to evaluate knockdown using more than one siRNA molecule targeted to the same gene (Wang *et al*., 2006).

However, when adults were fed the same concentration of siRNA, but exposed to different temperatures, the *HSF* transcript abundance was affected significantly. Males appeared to show lower *HSF* transcript abundance at a lower temperature of 20°C when compared to 25°C and 30°C after treatment with HSF-siRNA. In contrast, females fed on HSF-siRNA, only showed a decrease in HSF abundance at 20°C when compared to 25°C, but not when adults were exposed to 30°C. One could speculate that at 30°C, the heat shock response would be activated, resulting in translocation of HSF but not necessarily a higher *HSF* transcript abundance as mentioned above in section 4.1. Between all experiments, the no-siRNA and β2m-siRNA controls behaved similarly meaning that temperature does not impact the relative fold transcript abundance of *HSF* as mentioned above.

These results are important as there was significant HSF knockdown regardless of a change in temperatures. One could utilise this knockdown approach in a gene editing tactic whereby HSF can be switched on and off under specific conditions and a complex CRISPR system would be needed. Thus, determining the biological role that HSF has in *An. funestus* will advance our knowledge of this understudied African vector.

4.5. Conclusion

Gene knockdown of *HSF* in *An. funestus* using an optimised sugar-feeding system was successful. *Anopheles funestus* treated with different temperatures and concentrations consistently reduced *HSF* transcript abundance. Thus, the results of this chapter made it possible to choose an optimal temperature and concentration at which to investigate life-table parameters on *An. funestus* after HSF is knocked down.

CHAPTER 5

THE EFFECT OF siRNA, TARGETING THE *HSF* GENE, ON LIFE TABLE PARAMETERS OF *ANOPHELES FUNESTUS*

5.1. Introduction

HSF has proven to play a role in survival, fecundity, and fertility and these will be discussed in more detail below. These life table parameters (amongst others) influence the success of a vector and interruptions of any of these will have an impact on the vectoral capacity.

5.1.1. Role of HSF on survival

The Kaplan-Meier curves are generally used to show the cumulative survival probabilities of organisms (Kaplan and Meier, 1958). This survival are also referred to as longevity. Longevity (the median lifespan of an organism), especially in female mosquitoes, is very important as 10-18 days are required for the parasite to mature inside the mosquito (Beck-Johnson *et al*., 2013). Before the parasite can be transmitted, the female mosquito will first have to survive long enough to acquire the parasite from the blood meal, undergo the incubation period and then transmit the parasite (Rajatileka *et al*., 2011; Beck-Johnson *et al*., 2013). Therefore, the expectancy or longevity of a vector female can impact the malaria transmission dynamics. The longer a female survives in nature, the higher the possibility that she will be able to transmit the parasite and the more time she will have to be able to feed on humans and reproduce. For example, *An. funestus* is known for having a longer lifespan when

compared to another African malaria vector species, *An. gambiae* (Osoro *et al*., 2022). Colonised FUMOZ strains have a median survival of 52 days in females and 49 days in males (Ngowo *et al*., 2021), whereas FANG, a colonised strain of *An. funestus* from southern Angola, had a median survival time of 28 days in females and 44 days in males (Zengene *et al*., 2021B). Adults (F1s) reared from wild-caught females in Tanzania (FUTAZ-F1's) showed similar median survival times between females and males (32 and 33, respectively). Even European species such as colonised *An. atroparvus* showed survival surpassing nine weeks in both males and females (Birnberg *et al*., 2020). *Anopheles gambiae* have a median survival time of 26 days (Barreaux *et al*., 2018), while *An. coluzzii* have a median survival time of 19 days (Krajacich *et al*., 2020). However, even within the same species variation in longevity has been reported due to colonisation effect or geographical differences. For example, in *An. arabiensis,* mean longevity of 29 days was reported in F1 males from Kruger National Park *versus* 45 days from a historical colony from the same site and 26 days and 31 days, respectively, for females (Munhenga *et al*., 2011). In contrast, another *An. arabiensis* strain showed a mean male survival of 13.5 days (Munhenga *et al.,* 2016), while a strain from KwaZulu Natal (KWAG) showed a mean survival of 23 days (Dandalo *et al*., 2017)

The studies above were conducted under laboratory conditions and longevity can be influenced in nature by temperature and predation. A study in south-western Cameroon showed that wild-caught *An. funestus* median longevity was 24.4 days in comparison to *An. gambiae* with a 16.5 days median longevity (Tanga *et al.*, 2010). This shows that in nature the longevity of mosquitoes can be shorter than when reared under laboratory conditions. Longevity can be affected by high temperatures in two ways. Firstly, higher temperatures cause the metabolic processes responsible for the

development and life-history traits such as fecundity and fertility to speed up. Secondly, the temperatures may increase damage caused by metabolic by-products such as reactive oxygen species causing mosquito weakness and high mortality (Keil *et al*., 2015). Faiman *et al.* (2017) found that *An. coluzzii* longevity increased by two days at temperatures of 22°C-23.5°C whereas at 27°C longevity decreased by two days.

High temperatures are a huge stress on insects and affect larvae weight and size which also has a continued effect on adult longevity (Chen *et al*., 2014; Agyekum *et al*., 2022B). In *An. gambiae* (Afrane *et al*. 2006; Barreaux *et al*., 2018), *An. superpictus* (Ayetkin *et al*. 2009) and *Cx. tarsalis* (Reisen *et al.* 1984), adults derived from heat stressed larval regimens were found to have lifespans reduced by several days. In addition to temperature, a study by Kurapati *et al*. (2000) showed that young adult *Drosophila* strains that were selected in the laboratory to have longer lifespans produced flies with higher transcript abundance of *HSF*, suggesting that higher *HSF* transcript abundance may promote longevity. This leads to the hypothesis that if *HSF* transcript abundance is decreased or knocked down then the longevity of the vector might be significantly reduced and directly reduce a female's ability to transmit malaria.

5.1.2. *Anopheles funestus* female reproductive fitness

Female reproduction in anophelines is complex, starting with mating. Accessory gland proteins (Acps) in mosquitoes are secreted from the male accessory glands to the female bursa within the reproductive tract when transferring sperm (Baldini *et al*, 2012). Silencing of HSF1 results in a large downregulation of genes encoding Acps, which would mean that HSF not only functions in the HSR but plays a role in reproduction. A

study by Dottorini *et al*. (2012; 2013) used RNAi against HSF in *An. gambiae*, which resulted in the suppression of 50% of seminal fluid proteins. The females that mated with these males produced significantly fewer offspring. They showed that the phenotypic effects observed after the silencing of HSF included decrease in mating success, egg production anomalies, decrease in the induction of oogenesis, ovulation, and oviposition and thus concluded there would be a significant reduction in mosquito populations in *An. gambiae* if HSF is silenced. Functional gene studies by Dottorini *et al.* (2013) revealed that the function of HSF is in controlling the transcription of the *Acp* genes and have shown how HSF silencing led to a notable drop in *Acp* transcripts. This was linked to a considerable reduction in oviposition (fecundity) and hatching rate, which was noticeable in the decreased number of offspring produced by those females. This proves that HSF does influence anopheline reproduction.

In order to evaluate the biological role of HSF, the same concentration of siRNA in both males and females will be used in order to make comparisons between males and females. The decision to use 20 ng/µl of siRNA was also dependent on the relatively high cost of the siRNA and this concentration at a set temperature did not affect *HSF* transcript abundance (Figures 33 and 34). It was also selected as the mean concentration between 10 and 30ng/ul (see Chapter 4 for details). Using the 20 ng/µl rather than 30 ng/µl solution is more economical since 40 additional reactions can be performed at the lower concentration when using commercial siRNA.

5.1.3. Aim and Objectives

The aim of the study described in this chapter was to determine the effects of HSF knockdown on the life table parameters in *An. funestus*. The following objectives were formulated:

5.1.3.1. To determine the effect of RNAi knockdown on *An. funestus* longevity.

- It is hypothesised that HSF knockdown will reduce the longevity (median survival) of adult *An. funestus.*

5.1.3.2. To confirm siRNA knockdown at days three and 10 to ensure it can be sustained throughout the experiment.

- It would be expected that knockdown will be sustained throughout the experiment due to continual daily siRNA feeding. This is important for future studies to confirm the role of HSF in fecundity and fertility.

5.1.3.3. To assess mating success in females to ensure that differences in reproduction are due to treatments and not differences in mating.

- It is hypothesised that females will be mated due to the optimal mating time for *An. funestus* being used and this will not affect fecundity, fertility and the time-to-hatch.

5.1.3.4. To determine if HSF RNAi affects fecundity in *An. funestus*.

5.1.3.5. To determine if HSF RNAi affects fertility in *An. funestus*.

5.1.3.6. To determine the time-to-hatch of the eggs in *An. funestus.*

- It is hypothesised that HSF knockdown will reduce fecundity, fertility, and time of egg hatching.

5.2. Materials and methods

5.2.1. Experimental setup for longevity studies

Survival analysis was conducted to determine whether HSF knockdown influenced *An. funestus* longevity. Three treatments were included as described in section 3.2.2. Longevity was evaluated at 25°C using a total of 40 newly emerged adult female and male mosquitoes per treatment, which were fed *ad libitum* on either HSF-siRNA, β2m-siRNA (20 ng/µl in sugar water) or 10% sucrose solution (as per section 3.2.1.). All solutions included food colouring dye in order to visualise solution uptake. These mosquitoes were provided with siRNA-treated sugar water daily in order to sustain knockdown. Three biological replicates were performed. Survival analysis was performed in BugDorm® rearing cages in the Botha De Meillon insectary.

The rate of survival was monitored until 100% mortality was reached for all three treatments and respective treatment solutions were maintained at the correct concentrations throughout the experiment. A Kaplan-Meier survival curve (Goel *et al.,* 2010) was constructed using the software GraphPad Prism (Version 9.0 for Windows, GraphPad Software, USA, www.graphpad.com) to assess the rate of *An. funestus* survival between the various treatments. The probability of survival for each treatment was displayed as horizontal lines on the survival curve, while the change in cumulative probability was displayed as vertical lines (Kaplan and Meier, 1958). The cumulative probability changed when a death occurred (Rich *et al.,* 2010). The Log-rank test (Bland and Altman, 2004) was used to determine whether there was a statistically significant difference in vector longevity between the various treatments (Log-rank: $p < 0.05$).

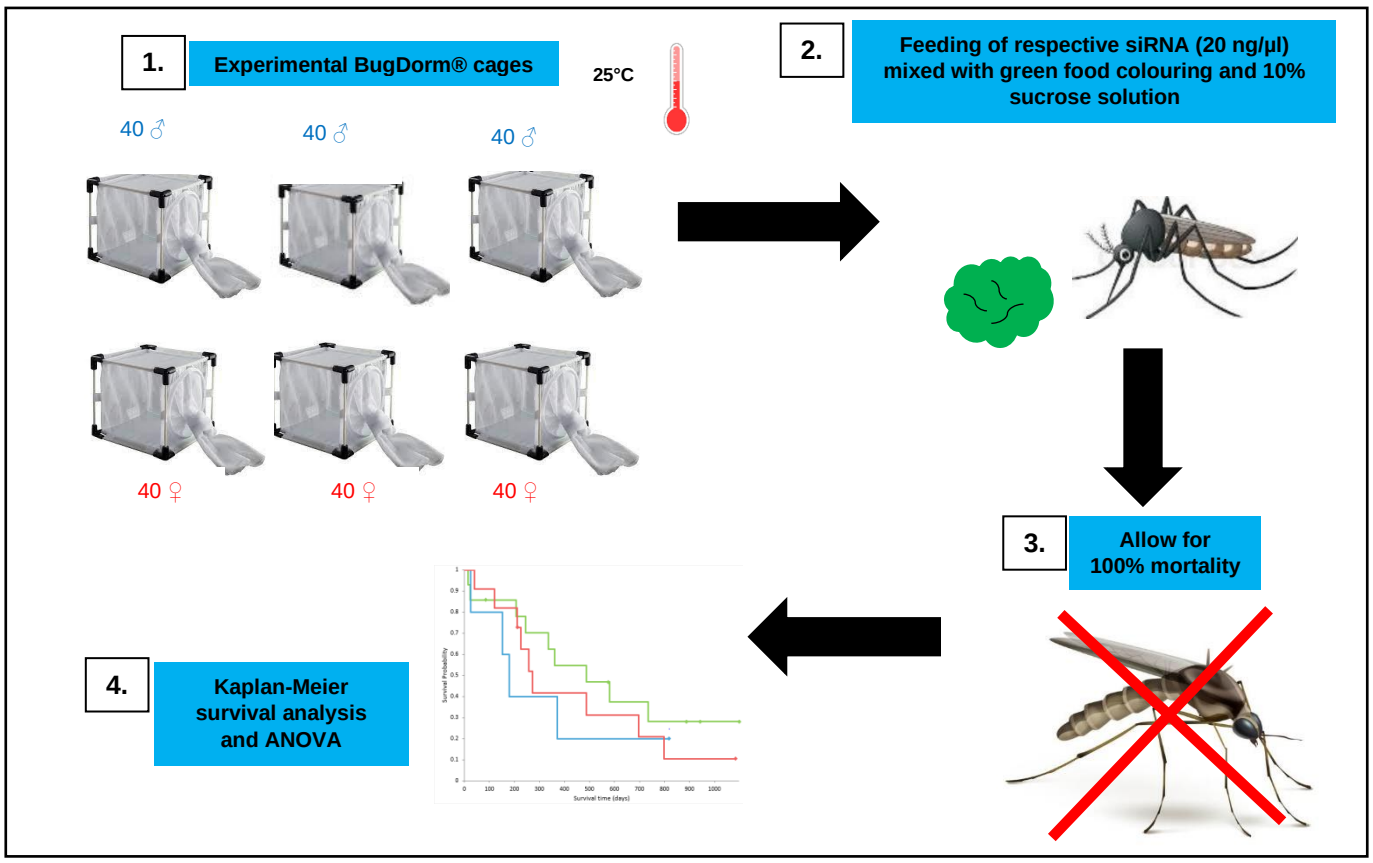


Figure 37: Flow diagram of the methods involved in assessing longevity. (1) Six cages were setup whereby three contain 40 female adults in each and the other three 40 male adults in each. (2) The adult mosquitoes were fed a mixture of either 20 ng/µl HSF-siRNA, green food colouring and 10% sucrose solution, 20 ng/µl β2m-siRNA, green food colouring and 10% sucrose solution or green food colouring and 10% sucrose solution only. This was performed at 25°C. (3) The mosquitoes were allowed to feed *ad libitum* until 100% mortality was reached. (4) Survivability between treatments was analysed using a Kaplan-Meier survival analysis (Log-rank: $p<0.05$). The variance between treatments were calculated using a one-way analysis of variance (ANOVA) and a Tukey *post-hoc* test.

5.2.2. Experimental setup for fecundity studies

Mosquito fecundity was analysed using a total of 40 newly emerged virgin female *An. funestus* adult mosquitoes per each treatment. Forty females were placed in a BugDorm® cage and were sustained *ad libitum* on 10% sucrose solution (no-siRNA control), 40 female adults were placed in a second cage and with *ad libitum* access to a 20 ng/µl β2m-siRNA treated sugar solution and the remaining 40 females were

placed in a third cage and were given *ad libitum* 20 ng/µl *HSF*-siRNA in a sugar solution. All solutions included green food colouring to ensure visualisation of solution uptake. Optimal mating time for *An. funestus* is 10 days (Maharaj *et al*., 2022) and two-day-old male mosquitoes were used as genital rotation of all males only reaches the final stage of rotation 36 hours post emergence (Dahan and Koekemoer, 2013). Forty untreated two-day-old males were introduced to each cage and were then removed after 10 days of mating to assess knockdown success (section 2.2.4.1.). Females were not used to assess knockdown success to ensure the maximum number of females could be used in the reproduction assay. At day 10, 15 females from each treatment were removed from each cage to assess mating success via spermathecal dissections. The remaining females were allowed to feed on distilled water *ad libitum* which replaced the 10% spiked sucrose solution to encourage blood feeding at day 11.

Two subsequent blood meals were offered to mated females at days 11 and 13 (Maharaj *et al*., 2022) and the females were provided with 10% sucrose solution to feed *ad libitum* throughout this period. After receiving the second blood meal at day 13, each female was transferred into a separate oviposition cup as described in section 2.2.3.3. Mosquitoes were maintained on their respective sucrose solutions by 0.1 g of sterilised cotton wool placed on top of the gauze throughout the experiment until oviposition had taken place. The number of eggs laid were counted by microscopy (Figure 38). The mean number of eggs laid per female (fecundity) was compared between the treatment and controls, using a one-way analysis of variance (ANOVA), and a Tukey *post-hoc* test. This was done to analyse the differences in means of each variable (Munhenga *et al*., 2016), and report on differences that were observed. Three biological replicates were performed.

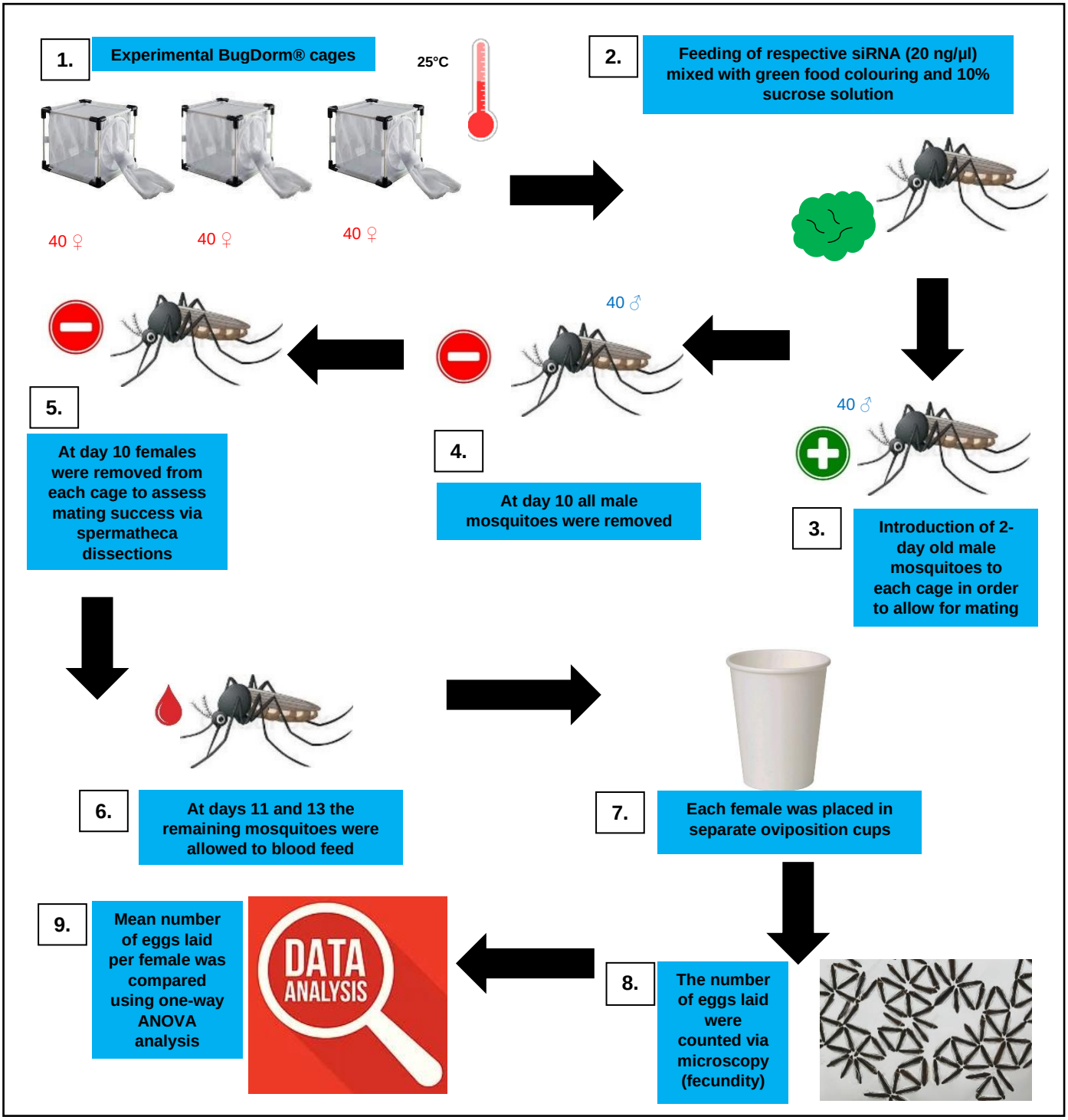


Figure 38: Flow diagram of the methods involved in assessing fecundity. (1) Three cages were setup. (2) The mosquitoes were fed either 20 ng/µl HSF-siRNA, green food colouring and 10% sucrose solution, 20 ng/µl β2m-siRNA, green food colouring and 10% sucrose solution or green food colouring and 10% sucrose solution only. (3) Male mosquitoes were added to each of the three cages to allow for mating. (4) At day 10 all male mosquitoes were removed. (5) At day 10, 10 female mosquitoes were removed from each cage to assess mating success. (6) Females were allowed to blood feed at days 11 and 13. (7) At day 13, each female was removed and placed in separate oviposition cups. (8) The number of eggs laid were counted using microscopy. (9) The mean number of eggs laid per female was calculated. Variance

between treatments was calculated using a one-way analysis of variance (ANOVA) and a Tukey *post-hoc* test.

5.2.3. Experimental setup to determine time-to-hatch and fertility studies

i. Fertility

Fertility was measured as the number of larvae hatched by the total number of eggs. Fertility was compared between the treatment and controls, using ANOVA, and a Tukey *post-hoc* test. This was done to analyse the differences in means of each variable (Munhenga *et al*., 2016), and report on differences that were observed in females across treatments.

ii. Time-to-hatch

Fertility experimental setup followed on from the fecundity study whereby the laid eggs were monitored to determine the time taken to hatch. Time-to-hatch was determined by monitoring the hatch time over ten days. Eggs that did not hatch ten days post-oviposition were considered infertile. Three biological replicates were performed. The Kaplan-Meier survival curve was used to analyse time-to-hatch. The Log-rank test was used to determine whether there was a statistically significant difference in vector time-to-hatch between the various treatments (Log-rank: $p<0.05$)

5.2.4. Confirmation of siRNA knockdown throughout the experiment

Fifteen female and 15 males for each treatment during the longevity study were placed in three separate BugDorm® cages at the beginning of the experiment (one biological replicate). Three biological replicates were performed. These adults were allowed to

feed *ad libitum* on 10% sucrose solution on the respective treatments for 48 hours. Males were removed after 48 hours to assess knockdown success for this experiment and future experiments. At day 10, males were removed to prevent ongoing mating and to allow females to blood feed and were used to assess knockdown success for this experiment. It was assumed that this will confirm that siRNA was ingested by adult mosquitoes for the full duration of the experiment.

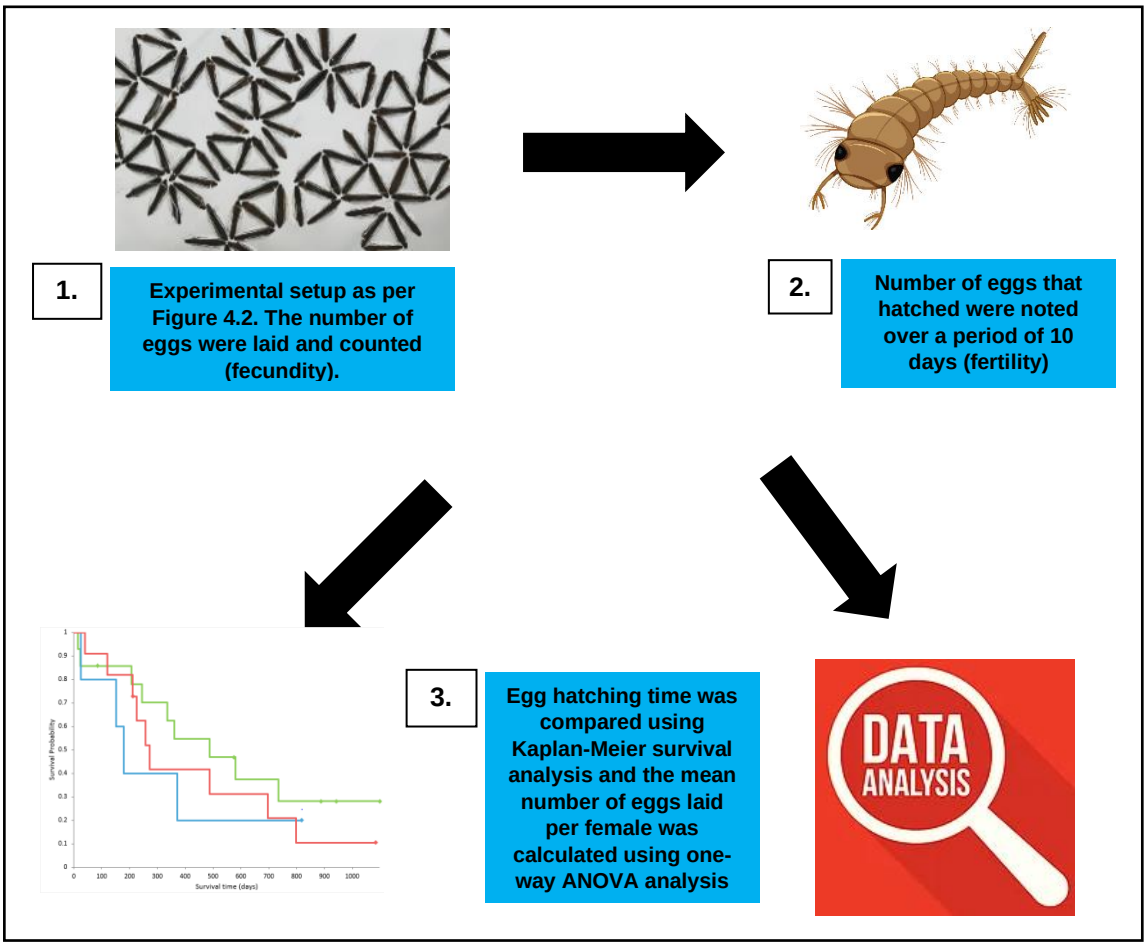


Figure 39: Flow diagram of the methods involved in assessing fertility. (1) The number of eggs laid were counted using microscopy. Previous steps follow that of Figure 38. (2) The number of eggs that hatched were noted for 10 days. (3) The mean percentage of eggs hatched per female was determined. The variance between treatments was calculated using a one-way ANOVA analysis. The egg hatching time between treatments was analysed using a Kaplan-Meier survival curve was used to analyse egg hatching time and the Log-Rank test was used to calculate statistical significance. The Log-rank test was used to determine whether there was a statistically significant difference in vector hatching time between the various treatments (Log-rank: $p<0.05$).

5.2.5. RNA Extraction and cDNA Synthesis

RNA was extracted and cDNA synthesised and then diluted (Appendix L) as described in section 2.2.2.2.

5.2.6. Real-time PCR for quantitative analysis

Data analysis was performed as described in section 2.2.3.7.

5.3. Results

5.3.1. Effect of HSF knockdown on *An. funestus* longevity

Longevity was assessed in both males and females to determine whether HSF knockdown affected *An. funestus* survival. The rate of survival was monitored until 100% mortality was reached for all treatments. HSF-siRNA treated males had a significant decrease in longevity when compared to the control treated males (Log-rank: $\chi 2= 7.381$, $p= 0.0066$, DF= 2). HSF-siRNA treated males had 100% mortality at 43 days post-emergence and both β2m-siRNA treated and no-siRNA control males had 100% mortality at 50 days post-feeding (Figure 40). Upon assessing the median longevity, *An. funestus* males treated with HSF-siRNA had a median survival time in days (IQR: Q1 - Q3) of 25 (23-26) days post feeding and *An. funestus* that were treated with β2m-siRNA and no-siRNA had a median survival time of 31 (30-33) days and 32 (31-33) days respectively. This translated to a 19.35% decrease in longevity, when the

median survival time was compared between the HSF knockdown samples and the control treatments.

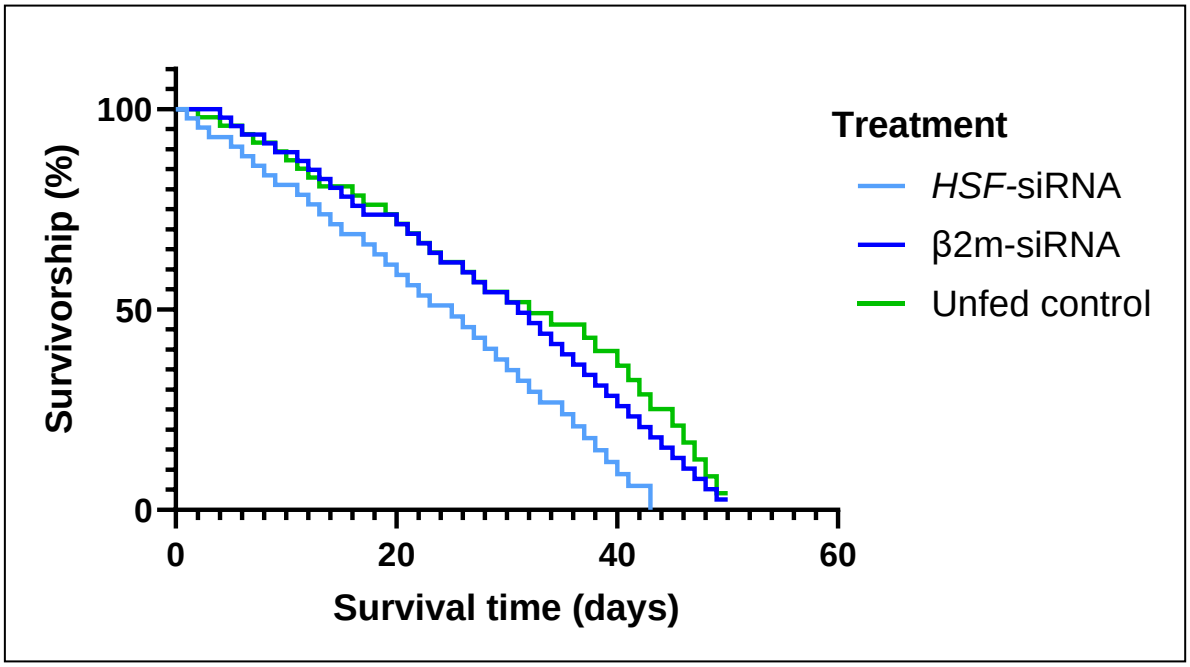


Figure 40: Kaplan-Meier survival analysis of male *An. funestus* assessed after treatment with siRNA. Samples treated with HSF-siRNA is indicated in light blue; samples treated with β2m-siRNA in dark blue and the no-siRNA control is indicated in green.

The overall vector longevity was significantly reduced in the HSF knockdown female *An. funestus* mosquitoes when compared to the control (β2m-siRNA knockdown and no-siRNA control) treated females (Log-rank: $\chi 2 = 7.956$, $p = 0.0048$, DF= 2). *Anopheles funestus* females treated with HSF-siRNA reached 100% mortality at day 57 post-emergence, while the females that were treated with β2m-siRNA had 100% mortality at 66 days post-feeding. The no-siRNA control *An. funestus* had 100% mortality at 65 days (Figure 41). *Anopheles funestus* females treated with HSF-siRNA had a median survival time median survival time in days (IQR: Q1 - Q3) of 32 (31-33) days post-feeding. The median survival time for *An. funestus* treated with β2m-siRNA and no-siRNA had a median survival time of 39 (37-40) days and 40 (39-42) days

respectively. This translated to a median 17.95% decrease in survival time when HSF knockdown females were compared to the females from the control treatments.

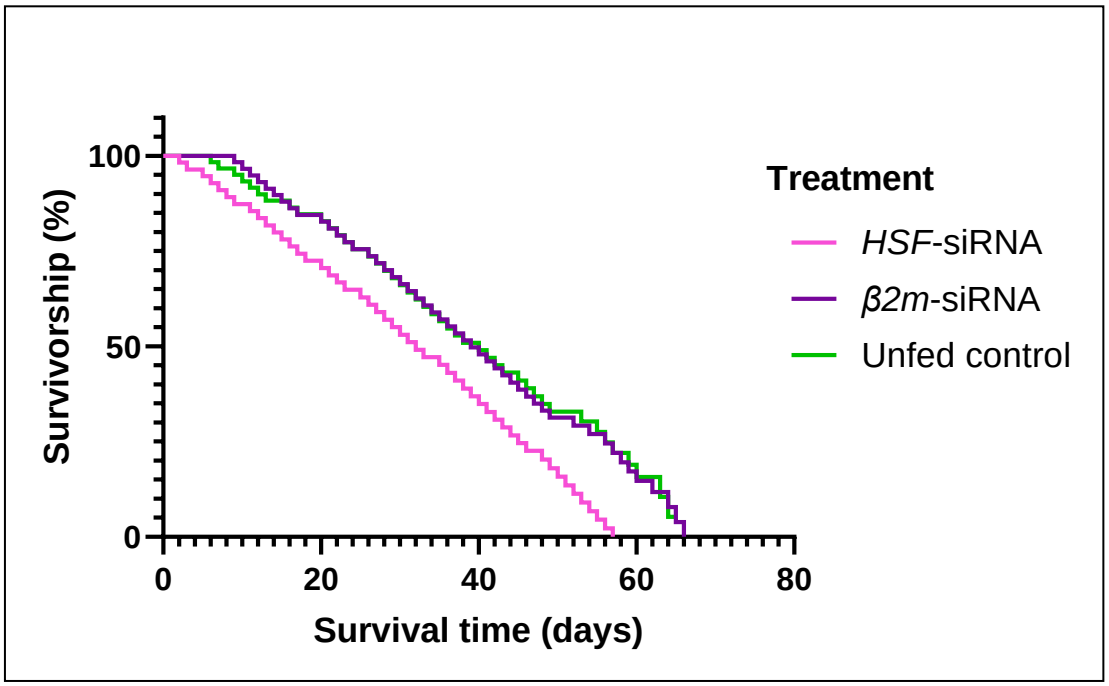


Figure 41: Kaplan-Meier survival analysis of female *An. funestus* assessed after treatment with siRNA. Samples treated with HSF-siRNA in pink; samples treated with β2m-siRNA in purple and the no-siRNA control in green.

Survivability between males and females was investigated and there was a significant decrease in longevity in males when compared to females (one-way ANOVA: $p< 0.0001$, F= 241.4, DF= 2). A log-rank test showed that HSF-siRNA males and females survivability differed significantly, with the β2m-siRNA males and females ($p< 0.0001$) and no-siRNA control males and females ($p< 0.0001$) respectively.

5.3.2. Spermathecal capsule dissection

Spermathecal capsule dissections were performed on ten females from each treatment cage at day 10 as described in section 2.2.3.2. Three biological replicates were performed. There was no significant difference in mating success between females

treated with HSF-siRNA, β2m-siRNA or without siRNA (one-way ANOVA: *p*= 0.3944, F= 0.3636, DF (2, 6)) (Figure 42). Females treated with HSF-siRNA had an insemination status (% insemination ± S.D.) of 86.67% ± 2.69, β2m-siRNA (80% ± 10.06) and no-siRNA control females (73.33% ± 3.09).

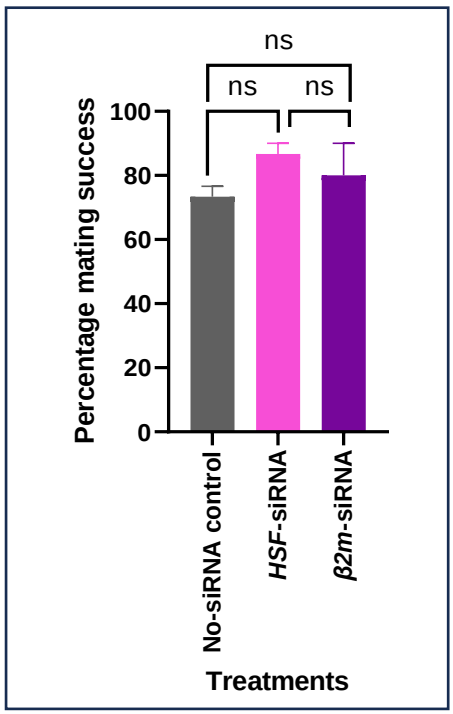


Figure 42: Mating success in females across three treatments. HSF knockdown (86.67%), *β2m* knockdown (80%) and no-siRNA control (73.33%). No significance (ns) between replicates was calculated using a Tukey *post-hoc* test. Error bars represent the standard deviation (S.D.).

5.3.3. Effect of HSF knockdown on *An. funestus* fecundity

The β2m-siRNA and no-siRNA control treatments had a mean fecundity of approximately 60 eggs laid per female mosquito, while those treated with HSF-siRNA had mean fecundity of approximately 38 eggs laid per female (Table 6). *Anopheles funestus* treated with HSF-siRNA had a 36.6% decrease in fecundity, when compared to the control treatments (one-way ANOVA: p<0.0001, F=3 100, DF (2, 6)).

Table 6: Mean fecundity values between the *An. funestus* mosquitoes which ingested three siRNA treatments (HSF, β2m and no-siRNA control). Results are shown for each treatment, with the average standard deviation (±S.D.) and total sample size (N).

Treatment	Total number of eggs laid	Mean number of eggs laid per female ±S.D. (% eggs laid); (95% CI); N
HSF-siRNA	922	38.42 ± 0.4452 (79.99% [a]); (38.89- 38.00); 30
β2m-siRNA	1, 608	61.85 ±0.3223 (86.67% [b]); (61.85- 61.26); 30
No-siRNA control	1, 600	59.26 ± 0.4120 (89.99% [b]); (59.88- 59.10); 30

Data was analysed using a one-way ANOVA test ($p< 0.001$). Letters that differ are statistically significant as determined by a *post-hoc* Tukey test

5.3.4. Effect of HSF knockdown on *An. funestus* fertility and time-to-hatch

i. Fertility

The overall vector fertility was significantly reduced in the HSF knockdown *An. funestus* mosquitoes when compared to the two control treatments. *Anopheles funestus* females treated with HSF-siRNA had a 9.2% decrease in fertility, when compared to the mean of the β2m-siRNA and no-siRNA control treatments, and this was statistically significant (one-way ANOVA: $p= 0.003$, F= 17.55, DF (2, 6)). The control treatments had a mean hatch rate of 76%, while those treated with HSF-siRNA had a mean hatch rate of 69% (Table 7).

ii. Time-to-hatch

All eggs that were oviposited by *An. funestus* females were allowed to hatch over a period of 10 days and the median time-to-hatch values were then compared. When assessing the median time-to-hatch in days (IQR: Q1 - Q3), the eggs laid by *An. funestus* females treated with HSF-siRNA had a hatch time of 8 (6.5-8.5) days post-oviposition. Eggs that were oviposited by *An. funestus* females that were treated with β2m-siRNA had a median time-to-hatch of 5.5 (3.5-5) days post-oviposition and the no-siRNA control had a median time-to-hatch of 6 (5.5-7) days post-oviposition. The median time-to-hatch values were compared between the HSF knockdown samples and the control treatments (Log-rank: $\chi 2 = 2.895$, $p = 0.235$, DF= 2) (Figure 43). This translated to a 21.4% decrease when compared to the average median time-to-hatch of the controls, but did not differ statistically significantly.

Table 7: Mean fertility values between the *An. funestus* mosquitoes which ingested one of three siRNA treatments (HSF, β2m or no-siRNA control). Results are shown for each treatment, with the average standard deviation (±S.D.) and total sample size (N)

Treatment	Total number of eggs hatched	Mean % of eggs hatched ±S.D.; (95% CI); N	Median time-to-hatch (days) (Inter-quartile range)
HSF-siRNA	630	63 ±0.443; (62.3-64.5); 30[a]	8 (6.5-8.5)
β2m-siRNA	1, 203	75 ±0.567; (75.3-76.7); 30[b]	5.5 (3.5-5)
No-siRNA control	1, 237	77 ±0.496; (77.9-78.1); 30[b]	6 (5.5-7)

Data was analysed using a one-way ANOVA test ($p < 0.001$). Letters that differ are statistically significant as determined by a *post-hoc* Tukey test

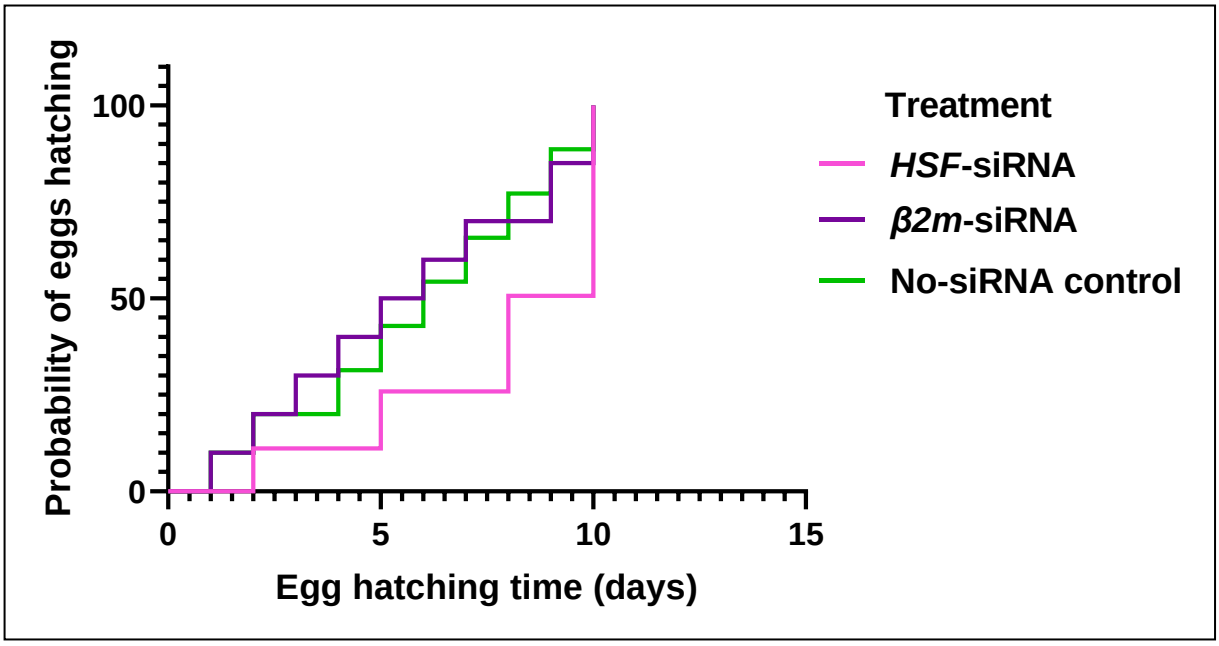


Figure 43: Kaplan-Meier time-to-event of *An. funestus* fertility (time-to-hatch) assessed after treatment with siRNA. Samples treated with HSF-siRNA in pink; β2m-siRNA in purple and the no-siRNA control in green.

5.3.5. Confirmation of siRNA knockdown throughout the experiment

Adult *An. funestus* females and males that underwent three treatments (20 ng/µl HSF-siRNA, 20 ng/µl β2m-siRNA and no-siRNA control) were cold-killed and their RNA extracted and cDNA synthesised in order to continue with qPCR. Males and females at two days post-treatment were analysed separately from the males at day 10 post-treatment to assess whether the siRNA knockdown was sustained throughout the experiment. *HSF* transcript abundance was measured between the treatment and control groups (negative β2m control and no-siRNA control).

Analysis of the day two post-treatment males showed a statistically significant 1.2-fold reduction of *HSF* transcript abundance versus control treatments (one-way ANOVA*: p*= 0.0027, F = 18.55, DF (2, 6)). In addition, analysis of the two-day post-treatment adult females showed a statistically significant decrease of transcript abundance between treatments (one-way ANOVA: *p*= 0.0009, F= 28.19, DF (2, 6)).

In order to determine which treatments result in a significant difference a Tukey-HSD test was performed. In the males, results showed a statistically significant reduction between the *HSF* transcript abundance and the negative control (β2m*)* (*p*= 0.0026) and no-siRNA control (*p*= 0.0117) (Figure 44A). As expected, there were no statistically significant differences between the negative control (β2m*)* and the no-siRNA control (*p* = 0.3343), indicating that the siRNA ingestion does not impact on transcript abundance of the target gene in this experiment. In females, the same is true, whereby there was a statistically significant 3.3-fold decrease between the *HSF* transcript abundance values and the negative control (β2m*)* (*p*= 0.0008) and no-siRNA control (*p*= 0.0061) in females treated with 20 ng/µl siRNA (Figure 44B).

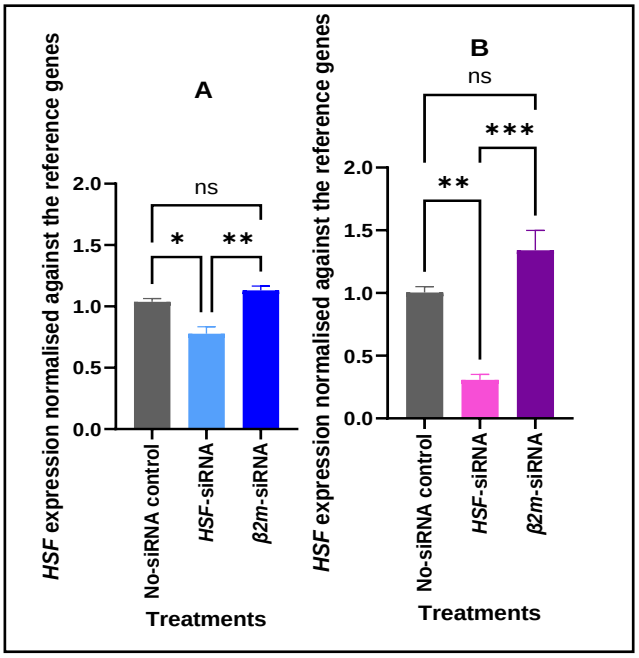


Figure 44: The normalised relative *HSF* transcript abundance values against the reference genes, *RPS7* and *GAPDH,* in males (A) and females (B) two days post treatment with 20 ng/µl HSF-siRNA and β2m-siRNA at 25°C. The asterisks indicate a *post-hoc* test (ns p > 0.05; * p ≤ 0.05; ** p ≤ 0.01; *** p ≤ 0.001; **** p ≤ 0.0001). Error bars represent standard error of the mean (SEM).

At day 10 post-treatment, males were removed from the fecundity and fertility study cages, which were analysed to determine knockdown efficiency later during the experiment. There was found to be a statistically significant 1.3-fold decrease in *HSF* transcript abundance between treatments (one-way ANOVA: *p*= 0.0019, F= 21.32, DF (2, 6)). In order to determine which treatments resulted in a significant difference, a Tukey-HSD analysis was performed. In the males, results showed a statistically significant decrease between the *HSF* transcript abundance and the negative control (*β2m*) (*p*= 0.0232) and no-siRNA control (*p*= 0.0015). As expected, there were no statistically significant differences between the negative control (β2m) and the no-siRNA control (*p*= 0.0703) (Figure 45). However, the statistical significance between the HSF-siRNA and controls suggests that at day 10, knockdown was still sustained and it was assumed to also be reflected in the females that were used to determine fecundity.

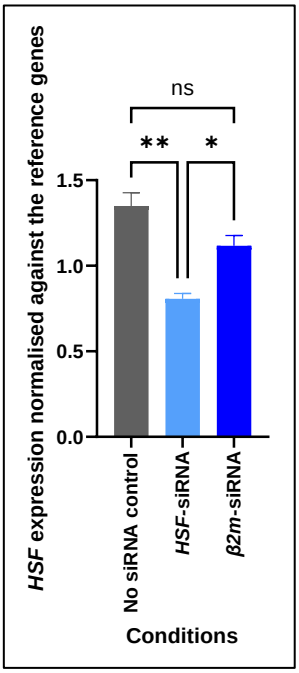


Figure 45: The normalised relative *HSF* transcript abundance values at day 10 against the reference genes, *RPS7* and *GAPDH,* in males after treatment with 20 ng/µl HSF-siRNA and β2m-siRNA at 25°C. The asterisks indicate a *post-hoc* test (ns p > 0.05; * p ≤ 0.05; ** p ≤ 0.01; *** p ≤ 0.001; **** p ≤ 0.0001). Error bars represent the standard error of the mean (SEM).

5.4. Discussion

There have been no studies that have examined HSF knockdown in *An. funestus.* Thus, the aim of this study was to determine the biological role of the *HSF* gene on specific life table parameters (longevity, mating success, fecundity, fertility, and time-to-hatch) on *An. funestus*. This was achieved through the knockdown of the gene via targeted siRNA delivery through feeding.

Results showed that male and female longevity was significantly affected after HSF knockdown. Males and females had a 18.65% decrease in longevity when compared to the negative β2m control and the no-siRNA control. Females and males experienced 100% mortality nine and seven days earlier than the negative β2m-siRNA and no-siRNA controls, respectively. The no-siRNA female control reached 100% mortality at 65 days whereas the no-siRNA control males reached 100% mortality at day 50. The difference in longevity between males and females was investigated to determine if there was a significant difference across treatments which there was. Males lived significantly shorter than females. This is consistent with what is known in the literature (Kalonji, 2021; De *et al*., 2022; Lambert *et al*., 2022). The disparity between males and females may be because females generally survive longer since they require time to mate, feed primarily on blood, digest that meal, make eggs, and then lay those eggs in a favourable area (Lambert *et al.,* 2022). Males, however, mate and perish soon after (Barredo and DeGennaro, 2020).

Additionally, several different species of mosquitoes' adult females can endure hostile situations, yet when males are faced with such brutal circumstances, they only occasionally persist (Kirby and Lindsay, 2009). The same pattern is seen in this study

whereby HSF-siRNA females had a median survival of 39 days and males 25 days. This was an important discovery since *Anopheles* mosquitoes can spread malaria parasites 14 days after gametocyte infection (Bray and Garnham, 1982). Given that the female mosquito must remain alive for at least 14 days after gametocyte infection in order to transmit the parasite, eliminating the vector population, by utilising information regarding HSF knockdown, before the end of the extrinsic incubation period would have a small impact on malaria transmission.

Mating success was assessed in a few females via spermathecal capsule dissections to ensure that if a difference in fecundity, fertility and time-to-hatch seen, was not due to differences in mating success. HSF knockdown females had 86.67% mating success, β2m knockdown had 80% mating success, and no-siRNA control had 73.33% mating success, which was sufficient in order to continue the experiment. Mating success was not significantly different, so differences in life table parameters were not due to differences in mating success. HSF knockdown in *An. funestus* resulted in a 36.6% decrease in vector fecundity, a 9.2% decrease in vector fertility and a 21.4% decrease in time-to-hatch.

To determine if the siRNA knockdown was sustained throughout the experiment, *HSF transcript abundance* was measured on day 2 and day 10. There was a significant knockdown of HSF on both days, suggesting knockdown achieved during this experimental period. It is important to note that the HSF-siRNA was fed to the mosquitoes throughout the duration of the experiment to sustain HSF knockdown. This further supports the fact that sugar water combined with siRNA feeding is a suitable mechanism to achieve RNAi knockdown. A potential future study will need to determine the duration of HSF-siRNA knockdown after a single initial feeding. If the

impact is long-lasting, then it would not be necessary to keep the mosquitoes on siRNA throughout the experiment.

This study showed that three (longevity, fecundity and fertility) of the four parameters were negatively affected. The impact on *An. funestus* populations, when the combined effect of the 20% decrease in longevity, almost 40% decrease in fecundity and almost 10% reduction in fertility are at play, will need to be determined. In addition, the impact might be increased if multiple siRNA molecules are used or if more than one gene is targeted. However, this will need to be investigated.

Because reproduction was affected, it is possible that HSF-siRNA impacted midgut homeostasis which may lessen the availability of nutrients following a blood meal in addition to shortening the mosquito's lifespan (Taracena-Agarwal *et al.*, 2024). Re-absorption of the growing follicles due to HSF knockdown during the gonotrophic cycle might limit vector oviposition in *An. funestus*. These observations are seen by Lea *et al*. (1972) in *Ae. aegypti* whereby the hypothesis that the size of an egg batch is matched by the re-absorption of developing follicles was postulated. In addition, eggs hatched two days later in HSF-siRNA treated females than in controls. Eggs that remain in the water for longer are more vulnerable and exposed to ovicides such as dinitrophenol compounds and petroleum oils (Smith and Salkeld, 1966). This would ultimately mean the eggs would be targeted and the life cycle would not continue. However, one could argue that ovicides in the water pose a deleterious effect on human health (Agrawal *et al*., 2010). Eco-friendly tools have been recently implemented against mosquito vectors, including botanical insecticides (Benelli, 2015).

The results of this study thus demonstrate that *HSF* transcript abundance in *An. funestus* can be suppressed and sustained via RNAi. Additionally, it demonstrates that *An. funestus* vector survival, fecundity, and fertility can all significantly decline when *HSF* transcript abundance is reduced. If a gene editing approach is to be used, this could represent what is seen in classical sterile insect technique programs (Alphey *et al*., 2010; Peccerillo *et al*., 2023; Dumont and Yatat-Djeumen, 2024). However, there would be huge challenges in maintaining a colony of such high numbers for operational research. Thus, understanding the biological side, rather than the control aspect must be the focus.

CHAPTER 6

CONCLUSION

Vector-borne diseases, which include the Black Death (also known as the plague), yellow fever, and malaria, have a well-known negative influence on humankind. The development of vector control treatments and research has greatly lowered the spread of disease. Despite these efforts, infectious vector-borne diseases, particularly diseases spread by mosquitoes, continue to cause over 700,000 fatalities and leave more than 80% of the world's population in danger (WHO, 2017).

Every year, the World Health Organization publishes the "World Malaria Report," which offers a comprehensive and current assessment of advancements made in the global fight against malaria. Regretfully, 249 million cases of malaria were reported worldwide in 2022, five million more than in 2021 (WHO, 2022; WHO, 2023A). Following years of attempts to eradicate malaria, which included the development of two recent vaccines (RTS,S/AS01 and R21/Matrix-M) (WHO, 2023D), it is clear that further measures are required to break through the lull in malaria reduction.

The continued malaria transmission is due to confounding challenges, including the lack of knowledge of dynamic vector biology, their biological systems and how they adapt to environmental changes. These knowledge gaps reduce the developmental speed and implementation of new malaria vector control strategies. New categories of malaria vector tools will be expected to become available and receive approval from WHO’s Vector Control Advisory Group during the next five years. Regardless, most of these methods are likely to remain insecticide-based methods. Traditional control measures, such as insecticide-treated bed nets and indoor residual spraying, are

increasingly facing resistance and ecological concerns. A paradigm shift towards targeted approaches is imperative to overcome these challenges. By deciphering the molecular mechanisms in vectors will allow for novel appraoches for vector control to be explored. This study investigated the molecular transcriptomic profile of HSF in an understudied African malaria vector, *An. funestus* and tried to understand its pleiotropic function in this species. In addition, this adds to the body of knowledge available of molecular mechanisms in *An. funestus*.

It was uncovered in this study that the *HSF* transcript abundance in *An. funestus* showed a dynamic flexibility (up and down) as the eggs develop through to the adult. This is not unique to *An. funestus*, and differences in *HSF* transcript abundance have also been observed in *Chilo suppressalis,* a rice pest moth (Dong *et al*., 2023) and *Cotesia chilonis, a* parasitoid wasp (He *et al*., 2021). Results from this study and other aforementioned studies suggest that *HSF* expression differs between life stages due to its potential role in insect species during developmental and physiological stages and might be species-specific.

In order to understand the biological role HSF has in *An. funestus*, various avenues can be investigated. This study continued by focusing specifically on adults and using siRNA as a method to inhibit HSF transcripts. However, it was important to optimise the methodologies in a step-by-step manner. Since adult males and females depend on sugar for their survival, a protocol was developed to ensure knockdown can be achieved successfully. Once the protocol was established and the transcription of a “housekeeping” gene was successfully reduced, the system was evaluated for HSF-

transcript inhibition. This study also showed that *HSF* transcript inhibition can be achieved by a wide concentration range of the siRNA target molecule. In addition, this study confirmed that the adult holding temperatures were not a major factor impacting siRNA transcript inhibition for *HSF.*

During the last part of this thesis, the biological role of HSF in adults was investigated by evaluating the impact of *HSF* transcript inhibition on specific life table parameters in *An. funestus*. These include evaluations on longevity, fecundity and fertility. HSF knockdown was achieved via siRNA and the adults could ingest the molecules as part of their sugar diet. It was observed that longevity (both males and females), fecundity and fertility were significantly reduced. However, additional research will be needed to understand the molecular pathway of HSF involvement in longevity, fecundity and fertility and to ensure phenotypic observations are not due to off-site targeting of other regions in the genome by HSF-siRNA. Future studies should evaluate differences between HSF-siRNA-treated and untreated adults at transcriptomic and proteomic levels. This can potentially identify additional pathways where HSF may be involved.

It is true that the almost 20% reduction in longevity observed in the HSF-siRNA-treated females will still enable these females to feed and transmit malaria. The additional reduction in fecundity (just under 40%) and fertility (almost 10%) might reduce population numbers, but will most likely not eliminate the vector. However, it is possible to use RNAi approaches and combine different target genes in a "*super sugar bomb*" tactic to have the desired impact. To expand on this idea, dsRNA is extremely stable and past studies have shown that dsRNA can last at least 7+ days under insectary conditions (Bennett and Koekemoer, unpublished), hence making this an attractive

idea to supplement current sugar toxic baited approaches. In theory, adding multiple dsRNA molecules targeting different genes into one sugar bait to create a "*super sugar bomb*" is possible. Other target genes that have been targeted by RNAi and shown to result in reduced reproductive success include the G protein-coupled receptors (GPCRs) (Keyes-Scott *et al.*, 2023), reproductive genes (*GAP005958, AGAP011377* and *AGAP007280*) (Hammond *et al.,* 2016), ribosomal proteins (RPS6 and RPL26) (Estep *et al.,* 2016), Krüppel homologue 1 (*Kr-h1*) (Ojani *et al*., 2018), etc. The "*super sugar bomb*" approach can easily be evaluated under laboratory and semi-field conditions as a proof of principle. Spraying vegetation and bait stations are two common implementation strategies for attractive toxic sugar bait (ATSB) (Kumar *et al*., 2023). The ATSB approach has proven to be quite effective in suppressing the mosquito vector population in sub-Saharan Africa, Israel, and the United States of America, among other regions (Müller *et al*., 2010; Revay *et al*., 2015; Fiorenzano *et al*., 2017). For example, ATSB used against *Anopheles* mosquitoes in Mali drastically reduced the density of mosquitoes, the number of older females and sporozoite prevalence, demonstrating how ATSB significantly reduces malaria parasite transmission (Traore *et al*., 2020).

Although mosquitoes' food sources in nature are still understudied, some plants have been identified already (Hawks and Hopkins, 2022). As our knowledge expands on the main plant food sources used by vector mosquitoes, it is interesting to imagine alternative vector control method where these plants are genetically modified so that the nectar will contain hairpin RNAs that operate similarly to the siRNA to target specific genes. However, the regulation of genetically modified organisms is complicated and the environmental impact studies will have to be done (Tromans, 2001). The transfer of dsRNA in transgenic plants have already been utilised to reduce gene transcript

abundance in a number of insect species (Baum *et al*., 2007; Zha *et al*., 2011). Baum *et al*. (2007) developed dsRNA targeting three genes (the hexose transporter gene *NlHT1*, the carboxypeptidase gene Nlcar and the trypsin-like serine protease gene *Nltry*) that are highly expressed in the brown planthopper midgut. Zha *et al*. (2011) designed dsRNA targeted to the genes α-tubulin and V-ATPase in the western corn rootworm. Unfortunately, this application has not been tested in culicidae yet, so more research is required.

As with any study, this study has its limitations. Although this study included a large sample size for the three biological replicates, perhaps five biological replicates with more samples per replicate could have been included to ensure accurate results. It was also not possible in this study to quantify the amount of siRNA that was ingested by the mosquitoes. The results therefore cannot accurately draw a conclusion as to how much siRNA elicited a knockdown effect and it was purely determined by just the ingestion of any amount of siRNA alone. Therefore, future studies are encouraged.

REFERENCES

Abaza, S. M. (2015) Heat shock proteins: Part III. Arthropods. Parasitologists United Journal, 8, pp.95-100.

Accrombessi, M., Cook, J., Dangbenon, E., Yovogan, B., Akpovi, H., Sovi, A., Adoha, C., Assongba, L., Sidick, A., Akinro, B., Ossè, R., Tokponnon, F., Aïkpon, R., Ogouyemi-Hounto, A., Padonou, G. G., Kleinschmidt, I., Messenger, L. A., Rowland, M., Ngufor, C., Protopopoff, N. and Akogbeto, M. C. (2023) Efficacy of pyriproxyfen-pyrethroid long-lasting insecticidal nets (LLINs) and chlorfenapyr-pyrethroid LLINs compared with pyrethroid-only LLINs for malaria control in Benin: a cluster-randomised, superiority trial. Lancet, 11(401), pp.435-446.

Adams, K. L., Selland, E. K., Willett, B. C., Carew, J. W. and Vidoudez, C. (2023) Selection for insecticide resistance can promote *Plasmodium falciparum* infection in Anopheles. PLOS Pathogens, 19(6): pp.e1011448.

Afrane, Y. A., Zhou, G., Lawson, B. W., Githeko, A.K. and Yan, G. (2006) Effects of microclimatic changes caused by deforestation on the survivorship and reproductive fitness of *Anopheles gambiae* in western Kenya highlands. American Journal of Tropical Medicine Hygiene, 74 (5), pp.772-778.

Agrawal, N., Dasaradhi, P. V. N., Mohmmed, A., Malhotra, P., Bhatnagar, R. K. and Mukherjee, S. K. (2003) RNA interference: biology, mechanism, and applications. Microbiology and Molecular Biology Reviews, 67 (4), pp.657–685.

Agrawal, A., Pandey, R. and Sharma, B. (2010) Water pollution with special reference to pesticide contamination in India. Journal of Water Resource and Protection, 2(5), pp.432-448.

Agyekum, T. P., Botwe, P. K., Arko-Mensah, J., Issah, I., Acquah, A. A., Hogarh, J. N., Dwomoh, D., Robins, T. G. and Fobil, J. N. (2021) A systematic review of the effects of temperature on *Anopheles* mosquito development and survival: implications for malaria control in a future warmer climate. International Journal of Environmental Research and Public Health, 18, pp.7255-7279.

Agyekum, T. P., Arko-Mensah, J., Botwe, P. K., Hogarh, J. N., Issah, I., Dadzie, S. K., Dwomoh, D., Billah, M. K., Robins, T. and Fobil, J.N. (2022A) Relationship between temperature and *Anopheles gambiae* sensu lato mosquitoes' susceptibility to pyrethroids and transcript abundance of metabolic enzymes. Parasites & Vectors, 15(1), pp.1-11.

Agyekum, T. P., Arko-Mensah, J., Botwe, P.K., Hogarh, J. N., Issah, I., Dwomoh, D., Billah, M. K., Dadzie, S. K., Robins, T. G. and Fobil, J. N. (2022B) Effects of elevated temperatures on the development of immature stages of *Anopheles gambiae* (s.l.) mosquitoes. Tropical Medicine and International Health, 27(4), pp.338-346.

Ahmed, A., Abubakr, M., Ali, Y., Siddig, E. E. and Mohamed, N. S. (2022) Vector control strategy for *Anopheles stephensi* in Africa. The Lancet, 3(6), pp.e403.

Aikpon, R., Osse, R., Padonou, G., Anagonou, R., Salako, A., Ahogni, I. and Akogbeto, M. (2017) Involvement of both *Anopheles gambiae* and *Anopheles funestus* (Diptera: Culicidae) in the perennial malaria transmission through a seasonal abondance in savannah area in Benin. International Journal of Mosquito Research, 4(3), pp.107-112.

Airs, P. M. and Bartholomay, L. C. (2017) RNA Interference for mosquito and mosquito-borne disease control. Insects, 8 (4), pp.190-195.

Åkerfelt, M., Morimoto, R. I. and Sistonen, L. (2010) Heat shock factors: integrators of cell stress, development, and lifespan. Nature Reviews Molecular and Cell Biology, 11(8), pp. 545–555.

Alphey, L., Benedict, M., Bellini, R., Clark, G. G., Dame, D. A., Service, M. W. and Dobson, S. L. (2010) Sterile-insect methods for control of mosquito-borne diseases: an analysis. Vector Borne Zoonotic Diseases, 10(3), pp.295-311.

Alto, B. W. and Juliano, S. A. (2001) Precipitation and temperature effects on populations of *Aedes albopictus* (Diptera: Culicidae): implications for range expansion. Journal of Medical Entomology, 38(5), pp.646-656.

Aly, A. S., Vaughan, A. M. and Kappe, S. H. (2009) Malaria parasite development in the mosquito and infection of the mammalian host. Annual Reviews in Microbiology, 63, pp.195-221.

Amenya, D. A., Naguran, R., Lo, T. C. M., Ranson, H., Spillings, B. L., Wood, O. R., Brooke, B. D., Coetzee, M. and Koekemoer, L. L. (2008) Over transcript abundance of a Cytochrome P450 (CYP6P9) in a major African malaria vector, *Anopheles funestus*, resistant to pyrethroids. Insect Molecular Biology, 17(1), pp.19-25.

Andersen, C. L., Jensen, J. L. and Ørntoft, T. F. (2004) Normalization of real-time quantitative reverse transcription-PCR data: a model-based variance estimation approach to identify genes suited for normalization, applied to bladder and colon cancer data sets. Cancer Research, 64(15), pp.5245-5250.

Anee, H. K., Khandaker, A. M., Begum, R. A., and Shahjahan, R. (2021). Transcript abundance of heat shock protein genes *Aaehsp26*, *Aaehsp83* and *Aaehsc70* in response to thermal stress in *Aedes aegypti* larvae. Dhaka University Journal of Biological Sciences, 30(2), pp.233–241.

Ansari, M., Moraiet, M. and Ahmad, S. (2014) Insecticides: impact on the environment and human health. In: Malik, A., Grohmann, E. and Akhtar, R. (eds) Environmental Deterioration and Human Health. Springer, Dordrecht.

Ashu, F. A., Fouet, C., Ambadiang, M. M., Penlap-Beng, V. and Kamdem, C. (2023) Enhancing the efficacy of neonicotinoids against mosquitoes and overcoming resistance issues. bioRxiv [Preprint].

Aswat, A. S., Christian, R. and Koekemoer, L. L. (2023) Optimisation of adult *Anopheles funestus* blood-feeding on an artificial membrane feeding system. African Entomology, 31(1), pp. e16314.

Awasthi, A., Wu, C. and Hwang, J. (2012). Diving as an anti-predator behaviour in mosquito pupae. Zoological Studies, 51, pp.1225-1234.

Aytekin, S., Aytekin, M. and Alten, B. (2009) Effect of different larval rearing temperatures on the productivity (R_o) and morphology of the malaria vector *Anopheles superpictus Grassi* (Diptera: Culicidae) using geometric morphometrics. Journal of Vector Ecology, 34(1), pp.32-42.

Bai, J., Liu, Y., Wei, R., Wang, Y., Gong, W. and Du, Y. (2022) Knockdown of heat shock transcription factor 1 decreases temperature stress tolerance in *Bemisia tabaci* MED. Scientific Reports, 12(1), pp.16059-16070.

Baldini, F., Gabrieli, P., Rogers, D. W. and Catteruccia, F. (2012) Function and composition of male accessory gland secretions in *Anopheles gambiae*: a comparison with other insect vectors of infectious diseases. Pathogy Global Health, 106(2), pp.82-93.

Bally, J., Fishilevich, E., Bowling, A. J., Pence, H. E., Narva, K. E. and Waterhouse, P. M. (2018) Improved insect-proofing: expressing double-stranded RNA in chloroplasts. Pest Management Science, 13(2), pp.45-49.

Barna, J., Csermely, P. and Vellai, T. (2018) Roles of heat shock factor 1 beyond the heat shock response. Cellular and Molecular Life Sciences, 17(1), pp.67-72.

Barreaux, A. M. G., Stone, C. M., Barreaux, P. and Koella, J. C. (2018) The relationship between size and longevity of the malaria vector *Anopheles gambiae* (s.s.) depends on the larval environment. Parasites & Vectors, 11, pp.1-9.

Barredo, E. and DeGennaro, M. (2020) Not just from blood: mosquito nutrient acquisition from nectar sources. Trends in Parasitology, 36(5), pp. 473-484.

Baum, J. A., Bogaert, T., Clinton, W., Heck, G. R., Feldmann, P., Ilagan, O., Johnson, S., Plaetinck, G., Munyikwa, T., Pleau, M., Vaughn, T. and Roberts, J. (2007) Control of coleopteran insect pests through RNA interference. Nature Biotechnology, 25(11), pp.1322-1326.

Bayoh, M. N. and Lindsay, S. W. (2003) Effect of temperature on the development of the aquatic stages of *Anopheles gambiae* sensu stricto (Diptera: Culicidae). Bulletin of Entomological Research, 93, pp.375- 381.

Beck-Johnson, L. M., Nelson, W. A., Paaijmans, K. P., Read, A. F., Thomas, M. B. and Bjørnstad, O. (2013) The effect of temperature on *Anopheles* mosquito population dynamics and the potential for malaria transmission. PLoS ONE, 8(11), e79276.

Beier, J. C., Perkins, P. V., Wirtz, R. A., Whitmore, R. E., Mugambi, M. and Hockmeyer, W. T. (1987) Field evaluation of an enzyme-linked immunosorbent assay (ELISA) for

Plasmodium falciparum sporozoite detection in *Anopheline* mosquitoes from Kenya. American Journal of Tropical Medicine Hygiene, 36(3), pp.459-468.

Benedict, M. Q, Cockburn, A. F. and Seawright, J. A. (1993) The Hsp70 heat-shock gene family of the mosquito *Anopheles albimanus.* Insect Molecular Biology, 2(2), pp.93-102.

Benelli G. (2015) Plant-borne ovicides in the fight against mosquito vectors of medical and veterinary importance: a systematic review. Parasitology Research, 114(9), pp.3201-3212.

Benoit, J. B., Lopez-Martinez, G., Phillips, Z. P., Patrick, K. R. and Denlinger, D. L. (2010) Heat shock proteins contribute to mosquito dehydration tolerance. Journal of Insect Physiology, 56(2), pp.151-156.

Benoit, J. B., Lopez-Martineza, G., Patricka, K. R., Phillipsa, Z. P., Krausea, T. B. and Denlingera, D. L. (2011) Drinking a hot blood meal elicits a protective heat shock response in mosquitoes. Proceedings of the National Academy of Sciences, 108(19), pp.8026-8029.

Bilgi, V., Fosu-Nyarko, J. and Jones, M. G. K. (2017) Using vital dyes to trace uptake of dsRNA by green peach aphid allows effective assessment of target gene knockdown. International Journal of Molecular Sciences, 18, pp.80-88.

Birnberg, L., Aranda, C. and Talavera, S. (2020) Laboratory colonization and maintenance of *Anopheles atroparvus* from the Ebro Delta, Spain. Parasites & Vectors, 13(394), pp.1-12.

Bland, J.M. and Altman, D.G. (2004) The logrank test. British Medical Journal, 328(7447), p.1073.

Boisson, B., Jacques, J. C., Choumet, V., Martin, E., Xu, J., Vernick, K. and Bourgouin, C. (2006) Gene silencing in mosquito salivary glands by RNAi. FEBS Letters, 580(8), pp.1988-1992.

Bouwman, H., van den Berg, H. and Kylin, H. (2011) DDT and malaria prevention: addressing the paradox. Environmental Health Perspectives, 199(6), pp.744-747.

Bowler, K. (2005) Acclimation, heat shock and hardening. Journal of Thermal Biology, 30, pp.125-130.

Bowler, K. and Terblanche, J. S. (2008) Insect thermal tolerance: what is the role of ontogeny, ageing and senescence? Biological Reviews, 83, pp.339–355.

Bray, R. S. and Garnham, P. C. C. (1982) The life cycle of primate malaria parasites. British Medical Bulletin, 38(2), pp.117-122.

Brooke, B., Koekemoer, L. L., Kruger, P., Urbach, J., Misiani, E. and Coetzee, M. (2013) Malaria vector control in South Africa. South African Medical Journal, 103(10), pp.784-788.

Brown, A. E., Bugeon, L., Crisanti, A. and Catteruccia, F. (2003A) Stable and heritable gene silencing in the malaria vector *Anopheles stephensi*. Nucleic Acids Research, 31(15), pp.1-6.

Brown, A. E., Crisanti, A. and Catteruccia, F. (2003B) Comparative analysis of DNA vectors at mediating RNAi in *Anopheles* mosquito cells and larvae. The Journal of Experimental Biology, 206, pp.1817-1823.

Bustin, S. A., Benes, V., Garson, J. A., Hellemans, J., Huggett, J., Kubista, M., Mueller, R., Nolan, T., Pfaffl, M. W., Shipley, G. L., Vandesompele, J. and Wittwer, C. T. (2009) The MIQE Guidelines: Minimum Information for Publication of Quantitative Real-Time PCR Experiments. Clinical Chemistry, 55(4), pp.611-622.

Caccia, S., Casartelli, M and Tettamanti, G. (2019) The amazing complexity of insect midgut cells: types, peculiarities, and functions. Cell and Tissue Research, 23(4), pp.33-56.

Carrasco-Escobar, G., Fornace, K. and Benmarhnia, T. (2021) Mapping socioeconomic inequalities in malaria in Sub-Sahara African countries. Scientific Reports, 11(15121), pp.1-8.

Carlson, C. J., Bannon, E., Mendenhall, E., Newfield, T. and Bansal, S. (2023) Rapid range shifts in African *Anopheles* mosquitoes over the last century. Biology Letters, 19, pp. 1-5.

Carr, S. and Kasbekar, P. (2022) Why do so many Indian men have hairy ears? Rediscovering School Science, pp. 63-68.

Cerutti, H. D. (2003) RNA interference: traveling in the cell and gaining functions? Trends in Genetics, 19(1), pp.39-46.

Chandra, G. and Mukherjee, D. (2022) Chapter 35 - effect of climate change on mosquito population and changing pattern of some diseases transmitted by them. Advances in Animal Experimentation and Modeling, Academic Press, pp.455-460.

Chang, Y. W., Zhang, X. X., Chen, J. Y., Lu, M. X., Gong, W. R. and Du, Y. Z. (2018) Characterization of three heat shock protein 70 genes from *Liriomyza trifolii* and transcript abundance during thermal stress and insect development. Bulletin of Entomological Research, 109(2), pp.150-159.

Charlwood, J.D. (2017) Some like it hot: a differential response to changing temperatures by the malaria vectors *Anopheles funestus* and *An. gambiae* s.l. PeerJ, 5:e3099.

Charlwood, J.D., Thompson, R. and Madsen, H. (2003) Observations on the swarming and mating behaviour of *Anopheles funestus* from southern Mozambique. Malaria Journal, 2 (2), pp.1-10.

Charlwood, J.D. and Braganca, M. (2012) The effect of rainstorms on adult *Anopheles funestus* behavior and survival. Journal of Vector Ecology, 37 (1), pp.252-256.

Chen, H., Zheng, X., Luo, M., Guo, J., Luo, Y., Zhou, Z. and Wan, F. (2014) Effects of high temperature on body size and weight of *Ophraella communa*, Biocontrol Science and Technology, 24(8), pp. 882-890.

Chen, B., Feder, M. E. and Kang, L. (2018A) Evolution of heat-shock protein transcript abundance underlying adaptive responses to environmental stress. Molecular Ecology, 27(15), pp.3040-3054.

Chen, W., Geng, S., Song, Z., Li, Y., Wang, H. and Cao, J. (2018B) Alternative splicing and expression analysis of HSF1 in diapause pupal brains in the cotton bollworm, Helicoverpa armigera. Pest Management Science, 75(5), pp.1258-1269.

Childs, L. M., Cai, F. Y., Kakani, E. G., Mitchell, S. N., Paton, D., Gabrieli, P., Buckee, C. O. and Catteruccia, F. (2016) Disrupting mosquito reproduction and parasite development for malaria control. PLoS Pathogens, 2(12), pp.e1006060.

Chou, S. D., Prince, T., Gong, J. and Calderwood, S. K. (2012) mTOR Is Essential for the Proteotoxic Stress Response, *HSF1* Activation and Heat Shock Protein Synthesis. Public Library of Science ONE, 7(6), e39679.

Christiansen-Jucht, C., Parham, P. E., Saddler, A., Koella, J. C. and Basáñez, M. (2014) Temperature during larval development and adult maintenance influences the survival of *Anopheles gambiae* s.s. Parasites & Vectors, 7(489), pp.1-10.

Ciechanover, A. and Kwon, Y. T. (2017) Protein quality control by molecular chaperones in neurodegeneration. Frontiers in Neuroscience, 11, pp.110- 118.

Clements, A. N. (2000) The Biology of Mosquitoes. Sensory Reception and Behavior, Vol. 1. CAB International Publication, London.

Coetzee, M. and Fontenille, D. (2004) Advances in the study of *Anopheles funestus*, a major vector of malaria in Africa. Insect Biochemistry and Molecular Biology, 34(7), pp.599-605.

Coetzee, M. and Koekemoer, L. L. (2013) Molecular systematics and insecticide resistance in the major African malaria vector *Anopheles funestus.* Review of Entomology, 58, pp.393-412.

Coetzee, M., Kruger, P., Hunt, R.H., Durrheim, D.N., Urbach, J. and Hansford, C.F. (2013) Malaria in South Africa: 110 years of learning to control the disease. South African Medical Journal, 103(10), pp.770-778.

Cohuet, A., Simard, F., Toto, J. C., Kengne, P., Coetzee, M. and Fontenille, D. (2003) Species identification within the *Anopheles funestus* group of malaria vectors in Cameroon and evidence for a new species. The American Journal of Tropical Medicine and Hygiene, 69(2), pp.200-205.

Colinet, H., Siaussat, D., Bozzolan, F. and Bowler, K. (2013) Rapid decline of cold tolerance at young age is associated with transcript abundance of stress genes in *Drosophila melanogaster*. The Journal of Experimental Biology, 216, pp.253-259.

Da Costa, M., Pinheiro-Silva, R., Antunes, S., Moreno-Cid, J. A., Custódio, A., Villar, M., Silveira, H., de la Fuente, J. and Domingos, A. (2014) Mosquito *Akirin* as a potential antigen for malaria control. Malaria Journal, 13 (470), pp.207-215.

Dahan, Y. L. and Koekemoer, L. L. (2013) Analysis of the genitalia rotation in the male *Anopheles funestus* (Diptera: Culicidae). Acta Tropica, 132, Suppl:S20-5.

Dandalo, L. C., Munhenga, G., Kaiser, M. L., and Koekemoer, L. L. (2017). Development of a genetic sexing strain of *Anopheles arabiensis* for KwaZulu-Natal, South Africa. Medical and Veterinary Entomology, 32(1), pp. 61–69.

Dasgupta, S. (2018) Burden of climate change on malaria mortality. Journal of Hygienic Environmental Health, 221(5), pp.782-791.

Davies, C., Coetzee, M. and Lyons, C. L. (2016) Effect of stable and fluctuating temperatures on the life history traits of *Anopheles arabiensis* and *An. quadriannulatus* under conditions of inter- and intra-specific competition. Parasites & Vectors, 9, pp.1-9.

De, S., Sharma, G., Bhattacherjee, R., Mandal, U., Banerjee D. and Suman, D. S. (2022) Life table, survival and fecundity parameters of *Aedes albopictus* (Diptera: Culicidae) strains from desert and coastal regions of India. Acta Tropica, 235, pp. 106625-106639.

Debalke, S., Habtewold, T. and Duchateau, L. (2019) The effect of silencing immunity related genes on longevity in a naturally occurring Anopheles arabiensis mosquito population from southwest Ethiopia. Parasites & Vectors 12(174), pp.1-15.

Demirovic, D., de Toda, I. M., Nizard, C. and Rattan, S. I. (2014) Differential translocation of heat shock factor-1 after mild and severe stress to human skin fibroblasts undergoing aging in vitro. Journal of Cellular Communication Signal, 8(4), pp.333-339.

Dia, I., Guelbeogo, M.W. and Ayala, D. (2013) Chapter 7: Advances and perspectives in the study of the malaria mosquito *Anopheles funestus*. InTechOpen, pp.197-218.

Djouka, R., Akoton, R., Tchigossou, G. M., Atoyebi, S. M., Irving, H., Kusimo, M. O., Djegbe, I., Riveron, J. M., Tossou, E., Yessoufou, A. and Wondji, C. S. (2017) Mapping the distribution of *Anopheles funestus* across Benin highlights a sharp contrast of susceptibility to insecticides and infection rate to *Plasmodium* between southern and northern populations. Wellcome Open Research, 1, 28.

Dodson, B. L., Kramer, L. D. and Ragson, J. L. (2012) Effects of larval rearing temperature on immature development and West Nile virus vector competence of *Culex tarsalis.* Parasites & Vectors, 5, pp.1-6.

Dong, C. L., Feng, Z., Lu, M. X., and Du, Y. Z. (2023). *Chilo suppressalis* heat shock proteins are regulated by heat shock factor 1 during heat stress. Insect Molecular Biology, 32(1), pp.69-78.

Dottorini, T., Persampieri, T., Palladino, P., Spaccapelo, R. and Crisanti, A. (2012) Silencing of the *HSF* gene, the transcriptional regulator of *An. gambiae* male accessory glands, inhibits the formation of the mating plug in mated females and disrupts their monogamous behaviour. Pathogens and Global Health, 106(7), pp.405-412.

Dottorini, T., Persampieri, T., Palladino, P., Baker, D. A., Spaccapelo, R., Senin, N. and Crisanti, A. (2013) Regulation of *Anopheles gambiae* male accessory gland genes influences postmating response in female. The FASEB Journal, 27, pp.86 –97.

Dumont, Y. and Yatat-Djeumen, I. V. (2024) About contamination by sterile females and residual male fertility on the effectiveness of the sterile insect technique. Impact on disease vector control and disease control, Mathematical Biosciences, 370, pp.25-33.

E Silva, B. (2017) Examining the role of heat shock factor in *Anopheles funestus* male genitalia rotation (Masters dissertation), University of the Witwatersrand.

Estep, A. S., Sanscrainte, N. D. and Becnel, J. J. (2016) DsRNA-mediated targeting of ribosomal transcripts RPS6 and RPL26 induces long-lasting and significant reductions in fecundity of the vector *Aedes aegypti*. Journal of Insect Physiology, 90, pp.17-26.

Echeverri, C. J. and Perrimon, N. (2006) High-throughput RNAi screening in cultured cells: a user's guide. Nature Reviews in Genetics, 7(5), 373-384.

Ezeakacha, N. F. and Yee, D. A. (2019) The role of temperature in affecting carry-over effects and larval competition in the globally invasive mosquito *Aedes albopictus.* Parasites & Vectors, 12, pp.1-11.

Faiman, G., Solon-Biet, S., Sullivan, M., Huestis, D. L. and Lehmann, T. (2017) The contribution of dietary restriction to extended longevity in the malaria vector *Anopheles coluzzii.* Parasites & Vectors, 10, pp.1-13.

Farnesi, L. C., Vargas, H. C. M., Valle, D. and Rezende, G. L. (2017) Darker eggs of mosquitoes resist more to dry conditions: Melanin enhances serosal cuticle contribution in egg resistance to desiccation in Aedes, Anopheles and Culex vectors. PLoS Neglected Tropical Diseases, 11(10), pp.e0006063.

Feder, M. E. and Hofmann, G. E. (1999) Heat-shock proteins, molecular chaperones, and the stress response: evolutionary and ecological physiology. Annual Reviews in Physiology, 61, pp.243–282.

Felamboahangy, L. N., Kaiser, M. L., Zengenene, M. P., Okumu, F., Munhenga, G. and Koekemoer, L. L. (2023) Optimisation of laboratory-rearing parameters for *Anopheles funestus* larvae and adults. Acta Tropica, 238, pp.106784-106792.

Ferguson, H. M., John, B., Ng'habi, K. and Knols, B. G. J. (2005) Redressing the sex imbalance in knowledge of vector biology. Trends in Ecology and Evolution, 20(4), pp.87-95.

Fiorenzano, J.M., Koehler, P.G., Xue, R.D. (2017) Attractive toxic sugar bait (ATSB) for control of mosquitoes and its impact on non-target organisms: a review. International Journal of Environmental Research Public Health, 14(398), pp.345-360.

Fire, A. Z. (2007) Gene silencing by double-stranded RNA (Nobel lecture). Angewandte Chemie International Edition, 46(37), pp. 6966-6984.

Foster, W. A. (1995) Mosquito sugar feeding and reproductive energetics. Annual Review of Entomology, 40(1), pp.443-474.

Gabriel, S., Czerny, T. and Riegel, E. (2023) Repression motif in HSF1 regulated by phosphorylation. Cellular Signalling, 110, pp.169-179.

Gakhar, S. K. and Shandilya, H. (1999) Heat shock response during development of the malaria vector *Anopheles stephensi* (Culicidae: Diptera). Cytobios, 99(392), pp.173-182.

Gallo, G. J., Prentice, H. and Kingston, R. E. (1993) Heat shock factor is required for growth at normal temperatures in the fission yeast *Schizosaccharomyces pombe*. Molecular Cellular Biology, 13, pp.749-761.

Garbuz, D., Evgenev, B. D., Feder, M. E. and Zatsepina, O. G. (2003) Evolution of thermotolerance and the heat-shock response: evidence from inter/intraspecific comparison and interspecific hybridization in the virilis species group of *Drosophila*. I Thermal phenotype. Journal of Experimental Biology, 206(14), pp.2399–2408.

Ghosh, S. K. B., Hunter, W. B., Park, A. L. and Gundersen-Rinda, D. E. (2017) Double strand RNA delivery system for plant sap-feeding insects. PLOS ONE, 12(2), e0171861.

Gillies, M. T. and De Mellion, B. (1968) The Anophelinae of Africa south of the Sahara (Ethiopian Zoogeographical Region). Johannesburg: Publications of the South African Institute for Medical Research, 54, pp.1-343.

Gillies, M.T. and Coetzee, M. (1987) A supplement to the Anophelinae of Africa South of the Sahara (Afrotropical Region). Johannesburg: Publications of the South African Institute for Medical Research, 55, pp.1-143.

Glunt, K. D., Oliver, S. V., Hunt, R. H. and Paaijmans, K. P. (2018) The impact of temperature on insecticide toxicity against the malaria vectors *Anopheles arabiensis* and *Anopheles funestus*. Malaria Journal, 17, pp.1-8.

Goel, M. K., Khanna, P. and Kishore, J. (2010) Understanding survival analysis: Kaplan-Meier estimate. International Journal of Ayurveda Research, 1(4), pp.212-220.

Gokhale, K., Patil, D. P. and Dhotre, D. P. (2013) Transcriptome analysis of *Anopheles stephensi* embryo using expressed sequence tags. Journal of Bioscience, 38, pp.301–309.

Gomez-Pastor, R., Burchfel, E. T. and Thiele, D. J. (2018) Regulation of heat shock transcription factors and their roles in physiology and disease. Nature Reviews Molecular and Cell Biology 19(1), pp.4–19.

Gonçalvez de Carvalho, S. C., de Jesus Martins Junior, A., Pereira Lima, J. B. and Valle, D. (2002) Temperature Influence on Embryonic Development of *Anopheles albitarsis* and *Anopheles aquasalis.* Memórias do Instituto Oswaldo Cruz, 97(8), pp.1117-1120.

Govoetchan, R., Fongnikin, A., Syme, T., Small, G., Gbego, M., Todjinou, D., Rowland, M., Nimmo, D., Padanou, G. G. and Ngufor, C. (2022) VECTRON™ T500, a new broflanilide insecticide for indoor residual spraying, provides prolonged control of pyrethroid-resistant malaria vectors. Malaria Journal, 21, pp.1-14.

Gross, T. L., Myles, K. M. And Adelman, Z. N. (2009) Identification and characterization of Heat Shock 70 Genes in *Aedes aegypti* (Diptera: Culicidae). Journal of Medical Entomology, 46(3), pp.496-504.

Hahn, J., Hu, H., Thiele, D. J. and Iyer, V. R. (2004) Genome-wide analysis of the biology of stress responses through heat shock transcription factor. Molecular and Cell Biology, 24(12), pp.5249–5256.

Hall, T. A. (1999) BioEdit: A User-Friendly Biological Sequence Alignment Editor and Analysis Program for Windows 95/98/NT. Nucleic Acids Symposium Series, 41, pp.95-98.

Hammond, A., Galizi, R. and Kyrou, K. (2016) A CRISPR-Cas9 gene drive system targeting female reproduction in the malaria mosquito vector *Anopheles gambiae*. Nature Biotechnology, 34, pp.78-83.

Hannon, G. R. (2002) RNA interference. Nature, 418, pp.244-251.

Harada, E. and Goto, S. G. (2017) Upregulation of heat-shock proteins in larvae, but not adults, of the flesh fly during hot summer days. Cell Stress Chaperones, 22(6), pp. 823-831.

Hargreaves, K., Koekemoer, L. L., Brooke, B. D., Hunt, R. H., Mthembu, J. and Coetzee, M. (2000) *Anopheles funestus* resistant to pyrethroid insecticides in South Africa. Medical and Veterinary Entomology, 14(2), pp.181-189.

Hartl, F. U. (1996) Molecular chaperones in cellular protein folding. Nature, 381, pp.312-320.

Hawkes, F. M. and Hopkins, R. J. (2022) The mosquito: An introduction. In: Hall, M. and Tamïr, D., editors. Mosquitopia: The Place of Pests in a Healthy World [Internet]. New York: Routledge.

He, F., Zhu, F., Lu, M. and Du, Y. (2021) Comparison of morphology, development and transcript abundance patterns of *HSF* and hsp11.0 of *Cotesia chilonis* under normal and high temperature. PeerJ, 9, pp.e11353.

Heidary, M. and Kakhki, P. (2014) TRIzol-based RNA Extraction: A Reliable Method for Gene Expression Studies. Journal of Sciences, 25(1), pp.13-17.

Hightower, L. E. (1991) Heat shock, stress proteins, chaperones, and proteotoxicity. Cell, 66, pp.191-197.

Hoa, N. T., Keene, K. M, Olson, K. E. and Zheng, L. (2003) Characterization of RNA interference in an *Anopheles gambiae* cell line. Insect Biochemistry and Molecular Biology, 33, pp.949-957.

Hu, C., Yang, J., Qi, Z., Wu, H., Wang, B., Zou, F., Mei, H., Liu, J., Wang, W. and Liu, Q. (2022) Heat shock proteins: biological functions, pathological roles, and therapeutic opportunities. MedComm, 3(3), pp.e161.

Hunt, R. H., Brooke, B. D., Pillay, C., Koekemoer, L. L. and Coetzee, M. (2005) Laboratory selection for and characteristics of pyrethroid resistance in the malaria vector *Anopheles funestus*. Medical and Veterinary Entomology, 19(3), pp.271-275.

Hutvágner, G. and Zamore, P. D. (2002) A microRNA in a multiple-turnover RNAi enzyme complex. Science, 297(5589), pp.2056-2060.

Hutvágner, G. and Simard, M. J. (2008) Argonaute proteins: key players in RNA silencing. Nature, 9, pp.12-21.

Huvenne, H. and Smagghe, G. (2010) Mechanisms of dsRNA uptake in insects and potential of RNAi for pest control: A review. Journal of Insect Physiology, 56, pp.227-235.

Ikemoto, T. (2008) Tropical malaria does not mean hot environments. Journal of Medical Entomology, 45(6), pp.963-969.

Intergovernmental Panel on Climate Change (IPCC) (2022) Climate Change: Impacts, Adaptation and Vulnerability. Contribution of Working Group II to the Sixth Assessment Report of the Intergovernmental Panel on Climate Change, pp. 433–467. Parry, M. L., Canziani, O. F., Palutikof, J. P., van der Linden, P. J. and Hanson, C. E. (eds.), Cambridge University Press, Cambridge, United Kingdom.

Jagla, T., Dubińska-Magiera, M., Poovathumkadavil, P., Daczewska, M. and Jagla, K. (2018) Developmental expression and functions of the small heat shock proteins in Drosophila. International Journal of Molecular Science, 19(11), pp.3441-3450.

Jedlicka, P., Mortin, M. A. and Wu, C. (1997) Multiple functions of *Drosophila* heat shock transcription factor in vivo. EMBO Journal, 16, pp.2452–2462.

Joga, M. R., Zotti, M. J., Smagghe, G. and Christiaens, O. (2016) RNAi efficiency, systemic properties, and novel delivery methods for pest insect control: what we know so far. Frontiers in Physiology, 7, pp.553-560.

Kahamba, N. F., Finda, M., Ngowo, H. S., Msugupakulya, B. J., Baldini, F., Koekemoer, L. L., Ferguson, H. M. and Okumu, F. O. (2022) Using ecological observations to improve malaria control in areas where *Anopheles funestus* is the dominant vector. Malaria Journal, 21(158), pp.1-15.

Käfer, H., Kovac, H., Simov, N., Battisti, A., Erregger, B., Schmidt, A. K. D. and Stabentheiner, A. (2020) Temperature tolerance and thermal environment of European seed bugs. Insects, 11(3), pp.197-206.

Kalonji, M. N. (2021) The biology of *Anopheles funestus* (Diptera: Culicidae): effects of the sugar diet – advances towards SIT (Masters thesis), University of the Witwatersrand.

Kaplan, E. L. and Meier, P. (1958) Nonparametric estimation from incomplete observations. Journal of the American Statistical Association, 53(282), pp.457-481.

Keil, G., Cummings, E. and de Magalhaes, J. P. (2015) Being cool: how body temperature influences ageing and longevity. Biogerontology, 16, pp.383–397.

Keyes-Scott, N. I., Swade, K. R., Allen, L. R. and Vogel, K. J. (2023) RNAi-mediated knockdown of two orphan G protein coupled receptors reduces fecundity in the yellow fever mosquito *Aedes aegypti*. Frontiers in Insect Science, 3, pp.70-79.

Killeen, G. F., Masalu, J. P., Chinula, D., Fotakis, E. A., Kavishe, D. R., Malone, D and Okumu, F. (2017) Control of malaria vector mosquitoes by insecticide-treated combinations of window screens and eave baffles. Emerging Infectious Diseases, 23(5), pp.782-789.

King, A. M. and MacRae, T. H. (2015) Insect heat shock proteins during stress and diapause. Annual Review of Entomology, 60, pp.59–75.

Kirby, M. J. and Lindsay, S. W. (2009) Effect of temperature and inter-specific competition on the development and survival of *Anopheles gambiae* sensu stricto and *An. arabiensis* larvae. Acta Tropica, 109, pp.118-123.

Koekemoer, L. L., Kamau, L., Hunt, R. H. and Coetzee, M. (2002) A cocktail polymerase chain reaction assay to identify members of the *Anopheles funestus*

(Diptera: Culicidae) group. American Journal of Tropical Medicine Hygiene, 6(6), pp.804–811.

Krajacich, B. J., Sullivan, M., Faiman, R., Veru, L., Graber, L. and Lehmann, T. (2020) Induction of long-lived potential aestivation states in laboratory *An. gambiae* mosquitoes. Parasites & Vectors, 13(1), pp.1-14.

Kregel, K. C. (2002) Heat shock proteins: modifying factors in physiological stress responses and acquired thermotolerance. Journal of Applied Physiology, 92, pp.2177-2186.

Kulkarni, M. A., Duguay, C. and Ost, K. (2022) Charting the evidence for climate change impacts on the global spread of malaria and dengue and adaptive responses: a scoping review of reviews. Global Health, 18(1), pp.78-82.

Kumar, G., Gupta, S. K. and Pasi, S. (2023) Attractive toxic sugar baits: a magic bullet for control of malaria and dengue in urban settings of India?. Journal of Vector Borne Diseases 60(3), pp.340-341.

Kurapati, R., Passananti, H. B., Rose, M. R. and Tower, J. (2000) Increased hsp22 RNA levels in *Drosophila* lines genetically selected for increased longevity. Journals of Gerontology. Series A, Biological Sciences and Medical Sciences, 55, pp.B552–559.

Kurashova, N. A., Madaeva, I.M. and Kolesnikova, L. I. (2020) Expression of HSP70 heat-shock proteins under oxidative stress. Advances in Gerontology, 10, pp.20-25.

Lambert, B., North, A., Charles, H. and Godfray, J. (2022) A Meta-analysis of Longevity Estimates of Mosquito Vectors of Disease. bioRxiv, Cold Spring Harbor Laboratory.

Lea, A.O. (1972) Regulation of egg maturation in the mosquito by the neurosecretory system: the role of the corpus cardiacum. General and Comparative Endocrinology, Supplement 3, pp.602-608.

Le Sueur, D. and Sharp, B. L. (1991) Temperature-dependent variation in *Anopheles merus* larval head capsule width and adult wing length: implications for Anopheline taxonomy. Medical and Veterinary Entomology, 5, pp.55-62.

Letinić, B. D., Dahan-Moss, Y. and Koekemoer, L. L. (2020) Characterising the effect of *Akirin* knockdown on *Anopheles arabiensis* (Diptera: Culicidae) reproduction and survival, using RNA-mediated interference. PloS One, 15(2), pp.e0228576.

Li, C. and Managi, S. (2022) Global malaria infection risk from climate change. Environmental Research, 214(3), pp.125-171.

Lim, A. Y., Cheong, H.K. and Chung, Y. (2021) Mosquito abundance in relation to extremely high temperatures in urban and rural areas of Incheon Metropolitan City, South Korea from 2015 to 2020: an observational study. Parasites & Vectors 14(559), pp. 1-14.

Lindquist, S. and Craig, E. A. (1988) The heat-shock proteins. Annual Review Genetics, 22, pp.631–677.

Liu, N. (2015) Insecticide resistance in mosquitoes: impact, mechanisms, and research directions. Annual Review of Entomology, 60, pp.537–559.

Livak, K. J. and Schmittgen, T. D. (2001) Analysis of relative gene transcript abundance data using real- time quantitative PCR and the $2^{-\Delta\Delta ct}$ method. Methods, 25, pp.402–408.

Lopez-Martinez, G., Meuti, M. and Denlinger, D. L. (2012) Rehydration driven RNAi: a novel approach for effectively delivering dsRNA to mosquito larvae. Journal of Medical Entomology, 49(1), pp.215-218.

Lu, Z. and Wan, F. (2011) Using double-stranded RNA to explore the role of heat shock protein genes in heat tolerance in *Bemisia tabaci* (Gennadius). The Journal of Experimental Biology, 214, pp.764-769.

Lyimo, E. O., Takken, W. and Koella, J. C. (1992) Effect of rearing temperature and larval density on larval survival, age at pupation and adult size of *Anopheles gambiae.* Entomologia Experimentalis et Applicata, 63, pp.265-271.

Lyons, C. L., Coetzee, M., Terblanche, J. S. and Chown, S. L. (2012) Thermal limits of wild and laboratory strains of two African malaria vector species, *Anopheles arabiensis* and *Anopheles funestus*. Malaria Journal, 11, pp.1-14.

Lyons, C. L., Coetzee, M. and Chown, S. L. (2013) Stable and fluctuating temperature effects on the development rate and survival of two malaria vectors, *Anopheles arabiensis* and *Anopheles funestus*. Parasites & Vectors, 6(1), pp.1-9.

Lyons, C. L., Oliver, S. V., Hunt, R. H. and Coetzee, M. (2016) The influence of insecticide resistance, age, sex, and blood feeding frequency on thermal tolerance of wild and laboratory phenotypes of *Anopheles funestus* (Diptera: Culicidae). Journal of Medical Entomology, 53(2), pp.394–400.

MacRae, I. J., Zhou, K., Repic, A., Brooks, A. N., Cande, W. Z., Adams, P. D. and Doudna, J. A. (2006) Structural basis for double-stranded RNA processing by Dicer. Science, 311, pp.195-198.

Maharaj, S., Ekoka, E., Erlank, E., Nardini, L., Reader, J., Birkholtz, L. and Koekemoer, L. L. (2022) The ecdysone receptor regulates several key physiological factors in *Anopheles funestus*. Malaria Journal, 21, pp1-13.

Mapua, S. A., Hape, E. E., Kihonda, J., Bwanary, H., Kifungo, K., Kilalangongono, M., Kaindoa, E. W., Ngowo, H. S. and Okumu, F. O. (2022) Persistently high proportions of plasmodium-infected *Anopheles funestus* mosquitoes in two villages in the Kilombero valley, South-Eastern Tanzania. Parasite Epidemiology and Control, 18, pp. 214-220.

Mayer, M. P., Bukau, B. (2005) Hsp70 chaperones: Cellular functions and molecular mechanism. Cellular Molecular Life Sciences, 62, pp.670–684.

Meister, G. and Tuschl, T. (2004) Mechanisms of gene silencing by double-stranded RNA. Nature, 431(7006), pp.343-349.

Mello, C. C. and Conte Jr, D. (2004) Revealing the world of RNA interference. Nature, 431, pp.338-342.

Methods in Anopheles Research - MR4 (2015) Available at: https://www.yumpu.com/en/document/view/49409322/methods-in-anopheles-research-mr4. [Accessed 10 July 2023].

Morano, K. A. and Thiele, D. J. (1999) Heat shock factor function and regulation in response to cellular stress, growth, and differentiation signals. Gene Expression, 7(4-6), pp.271-282.

Moreno, R., Banerjee, S., Jackson, A. W. and Quinn, J. (2021) The stress-responsive kinase DYRK2 activates heat shock factor 1 promoting resistance to proteotoxic stress. Cell Death and Differentiation 28, pp.1563-1578.

Müller, G.C., Beier, J.C., Traore, S.F. *et al*. Successful field trial of attractive toxic sugar bait (ATSB) plant-spraying methods against malaria vectors in the *Anopheles gambiae* complex in Mali, West Africa. Malar J 9, 210 (2010).

Mungezi, L. M. J., Akosah-Brempong, G., Tchouakui, M., Menze, B. D., Tekoh, T. A., Tchoupo, M., Nkemngo, F. N., Wondji, M. J., Nwaefuna, E. K., Osae, M. and Wondji, C. S. (2022) Escalating pyrethroid resistance in two major malaria vectors *Anopheles*

funestus and *Anopheles gambiae* (s.l.) in Atatam, Southern Ghana. BMC Infectious Diseases, 22(799), pp.145-152.

Munhenga, G., Brooke, B. D., Chirwa, T. F., Hunt, R. H., Coetzee, M., Govender, D. and Koekemoer, L. L. (2011) Evaluating the potential of the sterile insect technique for malaria control: relative fitness and mating compatibility between laboratory colonized and a wild population of *Anopheles arabiensis* from the Kruger National Park, South Africa. Parasites & Vectors, 4, pp.1-12.

Munhenga, G., Brooke, B. D., Gilles, J. R., Slabbert, K., Kemp, A., Dandalo, L. C., Wood, O. R., Lobb, L. N., Govender, D., Renke, M. and Koekemoer, L. L. (2016) Mating competitiveness of sterile genetic sexing strain males (GAMA) under laboratory and semi-field conditions: steps towards the use of the Sterile Insect Technique to control the major malaria vector *Anopheles arabiensis* in South Africa. Parasites & Vectors, 9, pp.1-12.

Murphy, K. A., Tabuloc, C. A., Cervantes, K. R. and Chiu, J. C. (2016) Ingestion of genetically modified yeast symbiont reduces fitness of an insect pest via RNA interference. Scientific Reports, 6, pp.22587-22598.

Mysore, K., Hapairai, L. K. and Sun, L. (2017) Yeast interfering RNA larvicides targeting neural genes induce high rates of Anopheles larval mortality. Malaria Journal 16(461), pp.1-10.

Mysore, K., Hapairai, L. K., Realey, J. S., Sun, L., Roethele, J. B. and Duman-Scheel, M. (2022) Sugar-baited delivery of small interfering RNA for gene silencing in adult mosquitoes. Cold Spring Harbor Protocols, 8, pp.76-85.

Nagao, R. T., Kimpel, J. A. and Key, J. L. (1990) Molecular and cellular biology of the heat-shock response. Advances in Genetics, 28, pp.235-268.

Nardini, L., Hunt, R. H., Dahan-Moss, Y. L., Christie, N., Christian, R. N., Coetzee, M. and Koekemoer, L. K. (2017) Malaria vectors in the Democratic Republic of the Congo: the mechanisms that confer insecticide resistance in *Anopheles gambiae* and *Anopheles funestus.* Malaria Journal, 16, pp.1-15.

Negri, A., Ferrari, M. and Nodari, R. (2019) Gene silencing through RNAi and antisense Vivo-Morpholino increases the efficacy of pyrethroids on larvae of *Anopheles stephensi.* Malaria Journal, 18(294), pp.1-7.

Nepomichene, T. N., Andrianaivolambo, L., Boyer, S. and Bourgouin, C. (2017) Efficient method for establishing F1 progeny from wild populations of *Anopheles* mosquitoes. Malaria Journal, 16(21), pp.1-8.

Neueder, A., Achilli, F., Moussaoui, S. and Bates, G. P. (2014) Novel isoforms of heat shock transcription factor 1, HSF1γα and HSF1γβ, regulate chaperone protein gene transcription. Journal of Biological Chemistry, 18(29), pp.289-298.

Neven, G. (2000) Physiological responses of insects to heat. Postharvest Biology and Technology, 21(1), pp.103-111.

Ngongang-Yipmo, E. S., Tchouakui, M., Menze, B. D., Mungezi, L. M. J., Njiokou, F. and Wondji, C. S. (2022) Reduced performance of community bed nets against pyrethroid-resistant *Anopheles funestus* and *Anopheles gambiae*, major malaria vectors in Cameroon. Parasites & Vectors, 15(230), pp.1-15.

Ngowo, H. S., Hape, E. E., Matthiopoulos, J., Ferguson, H. M. and Okumu, F. O. (2021) Fitness characteristics of the malaria vector *Anopheles funestus* during an attempted laboratory colonization. Malaria Journal, 20, pp.1-13.

Nielsen, M., Overgaard, J., Sørensen, J., Holmstrup, M., Justesen, J. and Loeschcke, V. (2006) Role of HSF activation for resistance to heat, cold and high-temperature knock-down. Journal of Insect Physiology, 51, pp.1320-1329.

Njoroge, T.M., Hamid-Adiamoh, M. and Duman-Scheel, M. (2023) Maximizing the Potential of attractive targeted sugar baits (ATSBs) for integrated vector management. Insects,14(7), pp.585-599.

Nkya, T. E., Fillinger, U., Sangoro, O. P., Marubu, R., Chanda, E. and Mutero, C. M. (2022) Six decades of malaria vector control in southern Africa: a review of the entomological evidence-base. Malaria Journal, 21, pp.1-16.

Ojani, R., Fu, X., Ahmed, T., Liu, P. and Zhu, J. (2018), Krüppel homologue 1 acts as a repressor and an activator in the transcriptional response to juvenile hormone in adult mosquitoes. Insect Molecular Biology, 27, pp.268-278.

Okal, M. N., Lindh, J. M., Torr, S. J., Masinde, E., Orindi, B., Lindsay, S. W. and Fillinger, U. (2015) Analysing the oviposition behaviour of malaria mosquitoes: design considerations for improving two-choice egg count experiments. Malaria Journal, 14, pp.1-17.

Oliver, S. V. and Brooke, B. D. (2017) The effect of elevated temperatures on the life history and insecticide resistance phenotype of the major malaria vector *Anopheles arabiensis* (Diptera: Culicidae). Malaria Journal, 16, pp.1-13.

Olivier, L. J. G. (1950) Organised Malaria Control-Northern Transvaal. Pub: Health., 14(12), pp.375-379.

Olson, M. F., Garcia-Luna, S., Juarez, J. G., Martin, E., Harrington, L. C., Eubanks, M. D., Badillo-Vargas, I. E. and Hamer, G. L. (2020) Sugar Feeding Patterns for *Aedes aegypti* and *Culex quinquefasciatus* (Diptera: Culicidae) Mosquitoes in South Texas. Journal of Medical Entomology, 57(4), pp.1111-1119.

Omondi, S., Kosgei, J. and Agumba, S. (2022) Natural sugar feeding rates of *Anopheles* mosquitoes collected by different methods in western Kenya. Scientific Reports, 12, pp.568-577.

Osoro, J. K., Machani, M. G. and Ochomo, E. (2022) Insecticide resistant *Anopheles gambiae* have enhanced longevity but reduced reproductive fitness and a longer first gonotrophic cycle. Scientific Reports, 12(8646), pp.1-7.

Pampana, E. (1969) A textbook of malaria eradication. 2nd edition. London: Oxford University Press, pp.1-593.

Parsell, D. A. and Lindquist, S. (1993). The function of heat-shock proteins in stress tolerance: degradation and reactivation of damaged proteins. Annual Review of Genetics, 27, pp.437–496.

Peccerillo, C., Mainardi, C. E., Nieri, R., Fouani, J. M., Cemmi, A., Cristofaro, M., Anfora, G. and Mazzoni, V. (2023) The effect of the sterile insect technique on vibrational communication: the case of *Bagrada hilaris* (Hemiptera: Pentatomidae). Insects, 14, pp.353-360.

Peng, Y., Wang, K., Fu, W., Sheng, C. and Han, Z. (2018) Biochemical comparison of dsRNA degrading nucleases in four different insects. Frontiers in Physiology, 9(624), pp.806-814.

Pereira, M. H., & Paim, R. M. M., Lahondère, C. and Lazzari, C. (2017). Heat shock proteins and blood-feeding in arthropods. Heat Shock Proteins in Veterinary Medicine and Sciences, pp.349-359.

Perrimon, N., Ni, J. and Perkins, L. (2010) In vivo RNAi: Today and Tomorrow. Cold Spring Harbor Perspectives in Biology, 2, pp.a003640.

Pfaffl, M. W. (2001) A new mathematical model for relative quantification in real-time RT–PCR. Nucleic Acids Research, 29(9), pp.e45.

Phasomkusolsil, S., Lerdthusnee, K., Khuntirat, B., Kongtak, W., Pantuwatana, K. and Murphy, J. R. (2011) Effect of temperature on laboratory reared *Anopheles dirus* Peyton and Harrison and *Anopheles sawadwongporni* Rattanarithikul and Green. The Southeast Asian Journal of Tropical Medicine and Public Health, 42(11), pp.63-70.

Pillai, A. B., Nagaranjan, U., Mitra, A., Krishnan, U., Rajendran, S., Hoti, S. L. and Mishra, R. K. (2017) RNA interference in mosquito: understanding immune responses, double-stranded RNA delivery systems and potential applications in vector control. Insect Molecular Biology, 26(2), pp.127-139.

Pondeville E, David J. P., Guittard, E., Maria, A., Jacques, J. C., Ranson, H., Bourgouin, C. and Dauphin-Villemant, C. (2013) Microarray and RNAi analysis of P450s in *Anopheles gambiae* male and female steroidogenic tissues: CYP307A1 is required for ecdysteroid synthesis. PLoS One, 8(12), pp.e79861.

Pörtner, H., Bock C. and Mark, F. C. (2017) Oxygen- and capacity-limited thermal tolerance: bridging ecology and physiology. Journal of Experimental Biology, 220, pp.2685-2696.

Pridgeon, J. W., Pereira, R. M., Becnel, J. J., Allam, S. A. Clark, G. G. and Linthicum, K. J. (2008) Susceptibility of *Aedes aegypti*, *Culex quinquefasciatus* Say, and *Anopheles quadrimaculatus* Say to 19 pesticides with different modes of action, Journal of Medical Entomology, 45(1), pp.82–87.

Pryce, J., Medley, N. and Choi, L. (2022) Indoor residual spraying for preventing malaria in communities using insecticide-treated nets. Cochrane Database Systematic Reviews, 17(1) pp.CD012688.

Qu, J., Schinkel, M., Chiggiato, L., Machado, S. R., Overheul, G. J., Miesen, P. and van Rij, R. P. (2023) The *HSF1*-sHsp cascade has pan-antiviral activity in mosquitoes. bioRxiv, Cold Spring harbor Laboratory.

Qualls, W. A., Müller, G. C., Revay, E. E., Allan, S. A., Arheart, K. L., Beier, J. C., Smith, M. L., Scott, J. M., Kravchenko, V. D., Hausmann, A. and Yefremova, Z. A. (2014) Evaluation of attractive toxic sugar bait (ATSB)—barrier for control of vector and nuisance mosquitoes and its effect on non-target organisms in sub-tropical environments in Florida. Acta Tropica, 131, pp.104-110.

Rajatileka, S., Burhani, J. and Ranson, H. (2011) Mosquito age and susceptibility to insecticides. Transactions of the Royal Society of Tropical Medicine and Hygiene, 105, pp.247-253.

Reisen, W. K., Milby, M. M. and Bock, M. E. (1984) The effects of immature stress on selected events in the life history of *Culex tarsalis*. Mosquito News, 44(3), pp.385-395.

Revay, E. E., Schlein, Y., Tsabari, O., Kravchenko, V., Qualls, W., De-Xue, R., Beier, J. C., Traore, S. F., Doumbia, S., Hausmann, A. and Müller, G. C. (2015) Formulation of attractive toxic sugar bait (ATSB) with safe EPA-exempt substance significantly diminishes the *Anopheles sergentii* population in a desert oasis. Acta Tropica, 150, pp.29-34.

Ricci, F. (2012) Social implications of malaria and their relationships with poverty. Mediterrian Journal of Hematological Infectious Diseases, 4(1), pp.e2012048.

Rice, P., Longden, I. and Bleasby, A. (2000) EMBOSS: The European Molecular Biology Open Software Suite. Trends in Genetics, 16(6), pp.276-277.

Rich, J. T., Neely, J. G., Paniello, R. C., Voelker, C. C., Nussenbaum, B. and Wang, E. W. (2010) A practical guide to understanding Kaplan-Meier curves. Otolaryngology-Head and Neck Surgery, 143(3), pp.331-336.

Richards, S. L., Byrd, B. D., Reiskind, M. H. and White, A. V. (2020) Assessing insecticide resistance in adult mosquitoes: perspectives on current methods. Environmental Health Insights, 14, pp.1-7.

Richter, K., Haslbeck, M. and Buchner, J. (2010) The heat shock response: life on the verge of death. Molecular Cell, 40(2), pp.253-266.

Ritossa, F. (1962) A new puffing pattern induced by temperature shock and DNP in *Drosophila*. Experientia, 18, pp.571–573.

Rogers, D. J. and Randolph, S. E. (2000) The global spread of malaria in a future, warmer world. Science, 289, pp.1763-1766.

Rozendaal, J. A. (1997) Mosquitoes and other biting Diptera. In: Vector Control: Methods for Use by individuals and communities. Geneva, World Health Organization, pp.6-28.

Saleh, M. C., van Rij, R. P., Hekele, A., Gillis, A., Foley, E., O' Farrell, P. H. and Andino, R. (2006) The endocytic pathway mediates cell entry of dsRNA to induce RNAi silencing. Nature Cell Biology, 8(8), pp.793-802.

Sanchez-Vargas, I., Travanty, E. A., Keene, K. M., Franz, A. W. E., Beaty, B. J., Blair, C. D. and Olson, K. E. (2004) RNA interference, arthropod-borne viruses, and mosquitoes. Virus Research, 102, pp.65–74.

Sato, S. (2021) Plasmodium - a brief introduction to the parasites causing human malaria and their basic biology. Journal of Physiological Anthropology, 40(1), pp.1-13.

Schaper, S. and Hernandez-Charvarria, F. (2006), Scanning electron microscopy of the four larval instars of the Dengue fever vector *Aedes aegypti* (Diptera: Culicidae), Revista de Biología Tropical, 54, pp.847-852.

Semenza, J. C., Rocklöv, J. and Ebi, K. L. (2022) Climate change and cascading risks from infectious disease. Infectious Disease Therapy, 11, pp.1371–1390.

Sharp, B. L. and Le Sueur, D. (1996) Malaria in South Africa the past, the present and selected implications for the future. South African Medical Journal, 86(1), pp. 83-89.

Shi, Y., Mosser, D. D. and Morimoto, R. I. (1998) Molecular chaperones as *HSF*1-specific transcriptional repressors. Genes & Development, 12, pp.654–666.

Si, F., Qiao, L., He, Q., Zhou, Y., Yan, Z. and Chen, B. (2019) HSP superfamily of genes in the malaria vector Anopheles sinensis: diversity, phylogenetics and association with pyrethroid resistance. Malaria Journal, 18, pp.1-15.

Silver, N., Best, S., Jiang, J. and Thein, S. L. (2006) Selection of housekeeping genes for gene transcript abundance studies in human reticulocytes using real-time PCR. BMC Molecular Biology, 7(33), pp.89-99.

Sinka, M. E., Bangs, M. J., Manguin, S., Coetzee, M., Mbogo, C. M., Hemingway, J., Patil, A. P., Temperley, W. H., Gething, P. W., Kabaria, C. W. and Okara, R. M. (2010) The dominant *Anopheles* vectors of human malaria in Africa, Europe and the Middle East: occurrence data, distribution maps and bionomic précis. Parasites & Vectors, 3, p.1-34.

Siomi, H. and Siomi, M. C. (2009) On the road to reading the RNA-interference code. Nature, 457(7228), pp.396-404.

Sivan, A., Shriram, A. N., Muruganandam, N. and Thamizhmani, R. (2017) Transcript abundance of heat shock proteins (HSPs) in *Aedes aegypti* (L) and *Aedes albopictus* (Skuse) (Diptera: Culicidae) larvae in response to thermal stress. Acta Tropica, 167, pp.121-127.

Smith, E H. and Salkeld, E. H. (1966) The use and action of ovicides. Annual Review of Entomology, 11(1), pp.331-368.

Sørensen, J. G. and Loeschcke, V. (2002) Decreased heat-shock resistance and down-regulation of Hsp70 transcript abundance with increasing age in adult *Drosophila melanogaster.* Functional Ecology,16, pp.379–384.

Spillings, B. L. (2012) Insecticide resistance and Bionomics in laboratory reared and field caught *Anopheles funestus* Giles (Diptera: Culicidae) (Doctoral thesis), University of the Witwatersrand.

Stephanou, A. and Latchman, D. S. (2011) Transcriptional modulation of heat-shock protein gene transcript abundance. Biochemistry Research International, 11, pp.769-777.

Suh, P. F., Elanga-Ndille, E., Tchouakui, M., Sandeu, M. M., Tagne, D., Wondji, C. and Ndo, C. (2023) Impact of insecticide resistance on malaria vector competence: a literature review. Malaria Journal, 22(19), pp.1-11.

Syme, T., N'dombidjé, B. and Gbegbo, M. (2023) PermaNet Dual, a new deltamethrin-chlorfenapyr mixture net, shows improved efficacy against pyrethroid-resistant *Anopheles gambiae* sensu lato in southern Benin. Scientific Reports, 13, pp.12232-12240.

Tanga, M. C., Ngunduc, W. I., Juditha, N, Mbuha, J., Tendongfor, N., Simarde, F. and Wanji, S. (2010) Climate change and altitudinal structuring of malaria vectors in south-western Cameroon: their relation to malaria transmission. Transactions of the Royal Society of Tropical Medicine and Hygiene, 6(10), pp.78-86.

Taracena, M., Hunt, C., Pennington, P., Andrew, D., Jacobs-Lorena, M., Dotson, E. and Wells, M. (2022) Effective oral RNA interference (RNAi) administration to adult Anopheles gambiae mosquitoes. Journal of Visualised Experiments, 1(181), pp.10-18.

Thuy, T. (2015) Effects of DDT on environment and human health. Journal of Education and Social Sciences, 2, pp.203-210.

Timinao, L., Vinit, R., Katusele, M., Schofield, L., Burkot, T.R. and Karl, S. (2021) Optimization of the feeding rate of *Anopheles farauti* s.s. colony mosquitoes in direct membrane feeding assays. Parasites & Vectors, 14(1), pp.1-9.

Tintó-Font, E. and Cortés, A. (2022) Malaria parasites do respond to heat. Trends in Parasitology, 38(6), pp.435-439.

Tissieres, A., Mitchell, H. K. and Tracy, U. M. (1974) Protein synthesis in salivary glands of *Drosophila melanogaster*: relation to chromosome puffs. Journal of Molecular Biology, 84, pp.389-398.

Tomari, Y. and Zamore, P. D. (2005) Perspective: machines for RNAi. Genes & Development, 19, pp.517-529.

Traore, M. M., Junnila, A. and Traore, S. F. (2020) Large-scale field trial of attractive toxic sugar baits (ATSB) for the control of malaria vector mosquitoes in Mali, West Africa. Malaria Journal, 19(72), pp.1-14.

Tromans, S. (2001). Promise, Peril, Precaution: The Environmental Regulation of Genetically Modified Organisms. Indiana Journal of Global Legal Studies, 9(1), pp.187-205.

Tulvila, J., Parikka, M., Kleino, A., Sormunen, R., Ezekowitz, R. A., Kocks, C. and Rämet, M. (2006). Double-stranded RNA is internalized by scavenger receptor-mediated endocytosis in *Drosophila* S2 cells. Journal of Biological Chemistry, 281, pp.14370-14375.

Ugwu, F. S. O. (2023) Why the World Health Organization should reconsider long lasting insecticide nets (LLIN) and indoor residual spraying (IRS) in primary mosquito/malaria control in favour of house screening. Bio-Research, 21(1), pp.234-239.

Upshur, I.F., Bose, E.A., Hart, C. and Lahondère, C. (2019) Temperature and sugar feeding effects on the activity of a laboratory strain of Aedes aegypti. Insects, 10(10), pp.347-360.

Vihervaara, A. and Sistonen, L. (2014) *HSF*1 at a glance. Journal of Cell Science, 127(2), pp.261-266.

Voellmy, R. and Boellmann, F. (2007) Chaperone regulation of the heat shock protein response. Advances in Experimental Medicine and Biology, 594, pp.89-99.

Waite, J. L., Suh, E., Lynch P. A. and Thomas M. B. (2019) Exploring the lower thermal limits for development of the human malaria parasite, Plasmodium falciparum. Biology Letters, 15, pp.20190275.

Wang, S., Shi, Z., Liu, W., Jules, J. and Feng, X. (2006) Development and validation of vectors containing multiple siRNA expression cassettes for maximizing the efficiency of gene silencing. BMC Biotechnology, 6(2), pp.50-56.

Wang, G. H., Gamez, S., Raban, R. R., Marshall, J. M., Alphey, L., Li, M., Rasgan, J. L. and Akbari, O. S. (2021) Combating mosquito-borne diseases using genetic control technologies. Nature Communications, 12(4388), pp.1-12.

Wat'senga, F., Manzambi, E. Z., Lunkula, A., Mulumbu, R., Mampangulu, T., Lobo, N., Hendershot, A., Fornadel, C., Jacob, D., Niang, M., Ntoya, F., Muyembe, T., Likwela, J., Irish, S. R. and Oxborough, R. M. (2018) Nationwide insecticide resistance status

and biting behaviour of malaria vector species in the Democratic Republic of Congo. Malaria Journal, 17, pp.1-13.

Westbrook, C. J., Reiskind, M. H., Pesko, K. N., Greene, K. E., & Lounibos, L. P. (2010). Larval environmental temperature and the susceptibility of *Aedes albopictus* Skuse (Diptera: Culicidae) to Chikungunya virus. Vector Borne and Zoonotic Diseases (Larchmont, N.Y.), 10(3), pp.241-247.

Westerheide, S., Kawahara, T., Orton, K. and Morimoto, R. (2006). Triptolide, an Inhibitor of the human heat shock response that enhances stress-induced cell death. The Journal of Biological Chemistry, 281, pp.9616-9622.

Whitehead, K. A., Langer, R. and Anderson, D. G. (2009) Knocking down barriers: advances in siRNA delivery. Nature Reviews, 8, pp.129-138.

Whiten, S. R. and Peterson, R. K. (2015) The influence of ambient temperature on the susceptibility of *Aedes aegypti* (Diptera: Culicidae) to the pyrethroid insecticide permethrin. Journal of Medical Entomology, 53, pp.139-143.

Whyard, S., Singh, A. D. and Wong, S. (2015) Ingested double-stranded RNAs can act as species-specific insecticides. Insect Biochemistry and Molecular Biology, 39, pp.824-832.

Williams, J. and Pinto, J. (2012) Training manual on malaria entomology for entomology and vector control technicians (basic level). Pan American Health Organization, pp.1-78.

Wiltshire, R. M. and Duman-Scheel, M. (2020) Advances in oral RNAi for disease vector mosquito research and control. Current Opinion in Insect Science, 20, pp.38-52.

Winnebeck, E.C., Millar, C.D. and Warman, G.R. (2010) Why does insect RNA look degraded? Journal of Insect Science, 10(1), pp.1-7.

World Health Organization (1997) Chemical methods for the control of vectors and pests of public health importance (Edited by Chavasse, D. C., and Yap, H. H.). Geneva. Available at: https://www.who.int/whopes/resources/who_ctd_whopes_97.2/en/. [Accessed on 12 December 2022].

World Health Organization (2015) Indoor residual spraying: an operational manual for indoor residual spraying (IRS) for malaria transmission control and elimination. Available at: https://www.who.int/publications/i/item/9789241508940 [Accessed 7 May 2023].

World Health Organization (2017) Achieving and maintaining universal coverage with long-lasting insecticidal nets for malaria control. Available at: http://apps.who.int/iris/bitstream/10665/259478/1/WHO-HTM-GMP-2017.20eng.pdf [Accessed 11 April 2022].

World Health Organization (2020) Global Vector Control Response. Available at: https://www.who.int/teams/controlofneglectedtropicaldiseases/interventions/strategies/vector-control. [Accessed 15 August 2023].

World Health Organization (2022A) World Malaria Report. Geneva. Available at: https://www.who.int/teams/global-malaria-programme/reports/world-malaria-report-2022. [Accessed on 7 May 2023].

World Health Organization (2022B) Manual for monitoring insecticide resistance in mosquito vectors and selecting appropriate interventions. Available at: https://www.who.int/publications/i/item/9789240051089. [Accessed on 18 April 2023].

World Health Organization (2023A) World Malaria Report 2023. Available at: https://www.who.int/publications/i/item/9789240086173. [Accessed on 30 November 2023].

World Health Organization (2023B) WHO publishes recommendations on two new types of insecticide-treated nets. Available at: https://www.who.int/news/item/14-03-2023-who-publishes-recommendations-on-two-new-types-of-insecticide-treated-nets. [Accessed on 7 May 2023].

World Health Organization (2023C) Map production: Global Malaria Programme. Available at:

https://apps.who.int/malaria/maps/threats/#/maps?theme=prevention&mapType=prevention%3A0&bounds=%5B%5B-194.066994834237%2C-41.589230350971924%5D%2C%5B197.68075864902193%2C71.3595537299567%5D%5D&insecticideClass=NEONICOTINOIDS&insecticideTypes=&assayTypes=MOLECulAR_ASSAY%2CBIOCHEMICAL_ASSAY%2CSYNERGIST-INSECTICIDE_BIOASSAY&synergistTypes=&species=&vectorSpecies=&surveyTypes=&mmType=1&excludeLowerPatients=false&excludeLowerSamples=false&endemicity=false&storyMode=false&storyModeStep=0&years=2010%2C2023. [Accessed 8 May 2023].

WHO recommends R21/Matrix-M vaccine for malaria prevention in updated advice on immunization (2023D) Available at: https://www.who.int/news/item/02-10-2023-who-recommends-r21-matrix-m-vaccine-for-malaria-prevention-in-updated-advice-on-immunization [Accessed 6 May 2024]

Wrońska, A. K. and Boguś, M. I. (2020) Heat shock proteins (HSP90, 70, 60, and 27) in *Galleria mellonella* (Lepidoptera) hemolymph are affected by infection with *Conidiobolus coronatus* (Entomophthorales). PLoS One, 5(2), pp.e0228556.

Xu, Y., Yang, X. and Sun, X. (2020) Transcription factor FTZ-F1 regulates mosquito cuticular protein CPLCG5 conferring resistance to pyrethroids in *Culex pipiens pallens*. Parasites & Vectors 13(514), pp.1-13.

Yu, N., Christiaens, O., Liu, J., Niu, J., Cappelle, K., Caccia, S., Huvenne, H. and Smagghe, G. (2013) Delivery of dsRNA for RNAi in insects: an overview and future directions. Insect Science, 20, pp.4-14.

Zamore, P. D., Tuschl, T., Sharp, P. A. and Bartel, D. P. (2000) RNAi: Double-Stranded RNA Directs the ATP-Dependent Cleavage of mRNA at 21 to 23 Nucleotide Intervals. Cell, 101, pp.25-33.

Zamore, P.D. (2001) RNA interference: listening to the sound of silence. Nature Structural Biology, 8(9), pp.746-750.

Zengenene, M. P., Munhenga, G., Okumu, F. and Koekemoer, L. L. (2021A) Effect of larval density and additional anchoring surface on the life-history traits of a laboratory colonized *Anopheles funestus* strain. Medical and Veterinary Entomology, 36(2), pp.451-459.

Zengenene, M.P., Munhenga, G., Chidumwa, G. and Koekemoer, L. L. (2021B) Characterization of life-history parameters of an *Anopheles funestus* (Diptera: Culicidae) laboratory strain. Journal of Vector Ecology, 46(1), pp.24-29.

Zha, W., Peng, X., Chen, R., Du, B., Zhu, L. and He, G. (2011) Knockdown of midgut genes by dsRNA-transgenic plant-mediated RNA interference in the hemipteran insect *Nilaparvata lugens*. PloS one, 6(5), pp.e20504.

Zhang, X., Zhang, J. and Zhu, K. Y. (2010) Chitosan/double-stranded RNA nanoparticle-mediated RNA interference to silence chitin synthase genes through larval feeding in the African malaria mosquito (Anopheles gambiae). Insect Molecular Biology, 19(5), pp.683-693.

Zhang, M., Zhao, A., Guo, C. and Guo, L. (2021) A combined modelling and experimental study of heat shock factor SUMOylation in response to heat shock. Journal of Theoretical Biology, 530, pp.201-211.

Zhao, L. and Jones, W. A. (2012) Transcript abundance of heat shock protein genes in insect stress response. Invertebrate Survival Journal, 9(1), pp.93-101.

Zhu, L., Marshall, J. M., Qualls, W. A., Schlein, Y., McManus, J. W., Arheart, K. L., Hlaing, W. M., Traore, S. F., Doumbia, S., Müller, G. C. and Beier, J. C. (2015) Modelling optimum use of attractive toxic sugar bait stations for effective malaria vector control in Africa. Malaria Journal, 14, pp.1-12.

Zinszer, K. and Talisuna, A. O. (2022) Fighting insecticide resistance in malaria control. The Lancet, 23(2), pp.138-139.

Zoh, M. G., Bonneville, J. M., Tutagata, J. and Laporte, F. (2021) Experimental evolution supports the potential of neonicotinoid-pyrethroid combination for managing insecticide resistance in malaria vectors. Scientific Reports, 11(19501), pp.1-16.

APPENDICES

APPENDIX A: Permission obtained to use Figure 3

Gmail — Nerissa Bloch <nerissa.wendy@gmail.com>

Figure Permission
3 messages

Nerissa Bloch <nerissa.wendy@gmail.com> Thu, Feb 29, 2024 at 9:14 AM
To: r-morimoto@northwestern.edu

Dear Dr. Morimoto,

I hope this email finds you well.

I am a PhD candidate at the University of the Witwatersrand in South Africa. I am writing up my thesis titled "HEAT SHOCK FACTOR (*HSF*) TRANSCRIPT ABUNDANCE AND ITS EFFECT ON LIFE TABLE PARAMETERS IN THE MAIN AFRICAN MALARIA VECTOR *ANOPHELES FUNESTUS*".

I would like to please ask your permission to use Figure 6 from your paper titled "Triptolide, an Inhibitor of the Human Heat Shock Response That Enhances Stress-induced Cell Death".

Your response in this regard would be greatly appreciated!

Kind regards,

Nerissa Bloch, MSc(Med)
PhD Candidate

Vector Reference Laboratory
Centre for Emerging, Zoonotic and Parasitic Diseases,
National Institute for Communicable Diseases and
WITS Research Institute for Malaria (WRIM)
Email: nerissa.wendy@gmail.com / nerissab@nicd.ac.za

Richard I Morimoto <r-morimoto@northwestern.edu> Thu, Feb 29, 2024 at 11:57 AM
To: Nerissa Bloch <nerissa.wendy@gmail.com>
Cc: Rebecca Phend <rebecca.phend@northwestern.edu>

dear nerissa,

it is a pleasure to provide permission for you to use figure 6 in the westerheide paper on triptolide published in jbc.

best wishes on your thesis.

rick morimoto

APPENDIX B: CDNA Dilutions for Determining *HSF* Transcript Abundance in All Four *An. funestus* Life Stages

Technical replicate 1

FUMOZ Eggs 1 = $C_1V_1=C_2V_2$
(50 ng/µl)(100 µl)= (2191 ng/µl)(V_2)
5000/ 2191= V_2
V_2= 2 µl + 98 µl H_20

FUMOZ larvae 1 = $C_1V_1=C_2V_2$
(50 ng/µl)(100 µl)= (4843.8 ng/µl)(V_2)
5000/ 4843.8= V_2
V_2= 1µl + 99µl H_20

FUMOZ male pupae 1 = $C_1V_1=C_2V_2$
(50 ng/µl)(100 µl)= (2451.6 ng/µl)(V_2)
5000/ 2451.6= V_2
V_2= 2 µl + 98 µl H_20

FUMOZ female pupae 1 = $C_1V_1=C_2V_2$
(50 ng/µl)(100 µl)= (2627.8 ng/µl)(V_2)
5000/ 2627.8= V_2
V_2= 2 µl + 98 µl H_20

FUMOZ male adult 1 = $C_1V_1=C_2V_2$
(50 ng/µl)(100 µl)= (2981.2 ng/µl)(V_2)
5000/ 2981.2= V_2
V_2= 1.8 µl + 98.2 µl H_20

FUMOZ female adult 1 = $C_1V_1=C_2V_2$
(50 ng/µl)(100 µl)= (2863.3 ng/µl)(V_2)
5000/ 2863.3= V_2
V_2= 1.8 µl + 98.2 µl H_20

Technical replicate 2

FUMOZ Eggs 2 = $C_1V_1=C_2V_2$

(50ng/µl)(100 µl)= (2529.4ng/µl)(V_2)

5000/ 2529.4= V_2

V_2= 2 µl + 98 µl H_20

FUMOZ larvae 2 = $C_1V_1=C_2V_2$

(50 ng/µl)(100 µl)= (2694.2 ng/µl)(V_2)

5000/ 2694.2= V_2

V_2= 1.9 µl + 98.1 µl H_20

FUMOZ male pupae 2 = $C_1V_1=C_2V_2$

(50 ng/µl)(100 µl)= (1838 ng/µl)(V_2)

5000/ 1838= V_2

V_2= 2.5 µl + 97.5 µl H_20

FUMOZ female pupae 2 = $C_1V_1=C_2V_2$

(50 ng/µl)(100 µl)= (2790.1 ng/µl)(V_2)

5000/ 2790.1= V_2

V_2= 1.8 µl + 98.2 µl H_20

FUMOZ male adult 2 = $C_1V_1=C_2V_2$

(50 ng/µl)(100 µl)= (2744.6 ng/µl)(V_2)

5000/ 2744.6= V_2

V_2= 1.9 µl + 98.1 µl H_20

FUMOZ female adult 2 = $C_1V_1=C_2V_2$

(50 ng/µl)(100 µl)= (2783.4 ng/µl)(V_2)

5000/ 2783.4= V_2

V_2= 1.8 µl + 98.2 µl H_20

Technical replicate 3

FUMOZ Eggs 3 RNA = $C_1V_1=C_2V_2$

(50 ng/µl)(100 µl)= (2364.8 ng/µl)(V_2)

5000/ 2364.8= V_2

V_2= 2 µl + 98 µl H_20

FUMOZ larvae 3 = $C_1V_1=C_2V_2$

(50 ng/µl)(100 µl)= (2783.8 ng/µl)(V_2)

5000/ 2783.8= V_2

V_2= 1.8 ul + 98.2 µl H_20

FUMOZ male pupae 3 = $C_1V_1=C_2V_2$

(50 ng/µl)(100 µl)= 4946.3 ng/µl)(V_2)

5000/ 4946.3= V_2

V_2= 1 µl + 99µl H_20

FUMOZ female pupae 3 = $C_1V_1=C_2V_2$

(50 ng/µl)(100 µl)= (2617.7 ng/µl)(V_2)

5000/ 2617.7= V_2

V_2= 2 µl + 98 µl H_20

FUMOZ male adult 3 = $C_1V_1=C_2V_2$

(50 ng/µl)(100 µl)= (2847.4 ng/µl)(V_2)

5000/ 2847.4= V_2

V_2= 1.9 µl + 98.1 µl H_20

FUMOZ female adult 3 = $C_1V_1=C_2V_2$

(50 ng/µl)(100 µl)= (3609.6 ng/µl)(V_2)

5000/ 3609.6= V_2

V_2= 1.5 µl + 98.5 µl H_20

APPENDIX C: Permission obtained to use Figure 6

Gmail — Nerissa Bloch <nerissa.wendy@gmail.com>

Figure Permission
2 messages

Nerissa Bloch <nerissa.wendy@gmail.com> Thu, Feb 29, 2024 at 9:36 AM
To: "scarr@mun.ca" <scarr@mun.ca>

Dear Dr. Carr,

I hope this email finds you well.

I am a PhD candidate at the University of the Witwatersrand in South Africa. I am writing up my thesis titled "HEAT SHOCK FACTOR (*HSF*) TRANSCRIPT ABUNDANCE AND ITS EFFECT ON LIFE TABLE PARAMETERS IN THE MAIN AFRICAN MALARIA VECTOR *ANOPHELES FUNESTUS*".

I would like to please ask your permission to use your Figure titled "Synthesis of complementary DNA (cDNA) from mRNA by reverse transcription ".

Your response in this regard would be greatly appreciated!

Kind regards,

Nerissa Bloch, MSc(Med)
PhD Candidate

Vector Reference Laboratory
Centre for Emerging, Zoonotic and Parasitic Diseases,
National Institute for Communicable Diseases and
WITS Research Institute for Malaria (WRIM)
Email: nerissa.wendy@gmail.com / nerissab@nicd.ac.za

Carr, Steven <scarr@mun.ca> Thu, Feb 29, 2024 at 1:53 PM
To: Nerissa Bloch <nerissa.wendy@gmail.com>

Dear Nerissa

Thank you for writing. I hope you are well.

Please feel free to use the figure for your thesis. It's modified from a very old genetics text that was the first to try teaching "DNA First, Peas Later", same way I do it.

Good luck with your thesis!

Steve

APPENDIX D: Reference Gene Selection CT Values

Table S.1A: Ct values produced using qPCR of two-day-old male and female adults. N/A indicates no amplification. Three technical replicates were performed.

Primer	Ct Value	Mean Ct Value
HSF 1	33.25	33.15
HSF 2	33.08	
HSF 3	33.12	
HSF NTC		N/A
RPL19 1	34.26	33.6
RPL19 2	34.14	
RPL19 3	32.42	
RPL19 NTC		N/A
RPS7 1	33.16	32.38
RPS7 2	33.10	
RPS7 3	30.87	
RPS7 NTC		N/A
GAPDH 1	31.98	31.36
GAPDH 2	30.94	
GAPDH 3	31.17	
GAPDH NTC		N/A
RPS26 1	34.39	33.43
RPS26 2	N/A	
RPS26 3	32.47	
RPS26 NTC		N/A
FUN18S 1	18.16	18.06
FUN18S 2	18.46	
FUN18S 3	17.56	
FUN18S NTC		N/A

Table S.1B: Ct values produced using qPCR of two-day old male and female adults. The values for the gene of interest (*HSF*) have been omitted.

NormFinder	Two-day old 1	Two-day old 2	Two-day old 3
RPL19	34.26	34.25	32.42
RPS7	33.16	31.40	30.87
GAPDH	31.98	31.07	31.17
RPS26	34.39	34.04	32.47
FUN18S	18.16	20.20	17.56

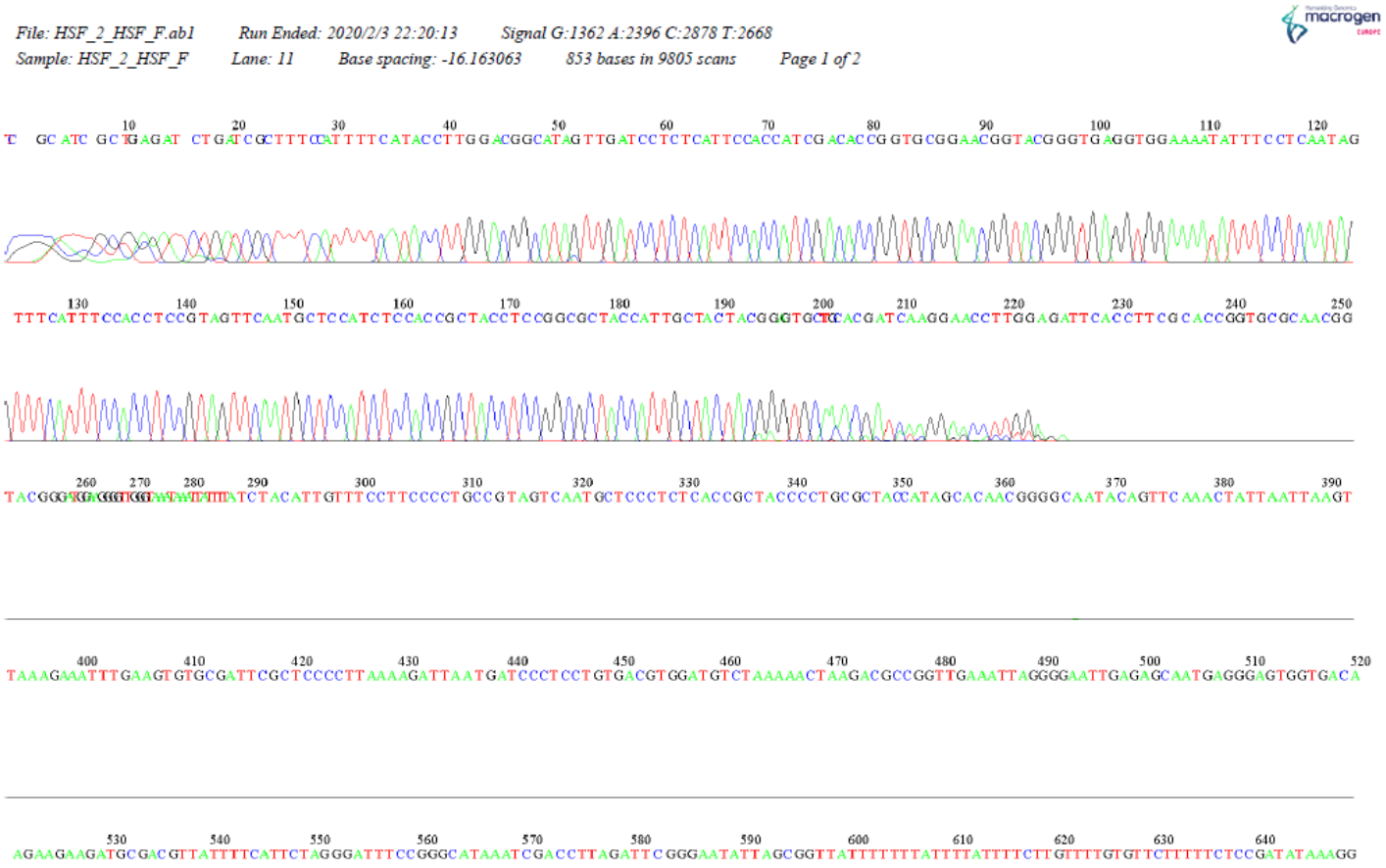
Table S.1C: Stability values generated by the software NormFinder for each reference gene tested. *RPS7* and *GAPDH* were selected as reference genes as they had the lowest stability values.

Gene name	Stability value
RPS7	0.656
GAPDH	0.916
FUN18S	1.009
RPS26	1.457
RPL19	2.159

APPENDIX E*:* HSF Sequencing Results

Sense Sequence

Chromatogram



Sequence

CATACTGGACGCTTTCCATTTTCAATACCTTGGACGGCATAGTTGATCCTCTCAT

TCCACCATCGACACCGGTGCGGAACGGTACGGGTGAGGTGGAAAATATTTCCT

CAATAGTTTCATTTCCACCTCCGTAGTTCAATGCTCCATCTCCACCGCTACCTCC

GGCGCTACCATTGCTACTACGGGTGC

EMBOSS Water Alignment

```
#=======================================
#
# Aligned_sequences: 2
# 1: EMBOSS_001
# 2: EMBOSS_001
# Matrix: EBLOSUM62
# Gap_penalty: 10.0
# Extend_penalty: 0.5
#
# Length: 188
# Identity:     185/188 (98.4%)
# Similarity:   185/188 (98.4%)
# Gaps:           0/188 ( 0.0%)
# Score: 1076.0
#
#
#=======================================

EMBOSS_001         1 GCACCCGTAGTAGCAATGGTAGCGCCGGAGGTAGCGGTGGAGATGGAGCA     50
                     ||||||||||||||||||||||||||||||||||||||||||||||||||
EMBOSS_001      1025 GCACCCGTAGTAGCAATGGTAGCGCCGGAGGTAGCGGTGGAGATGGAGCA   1074

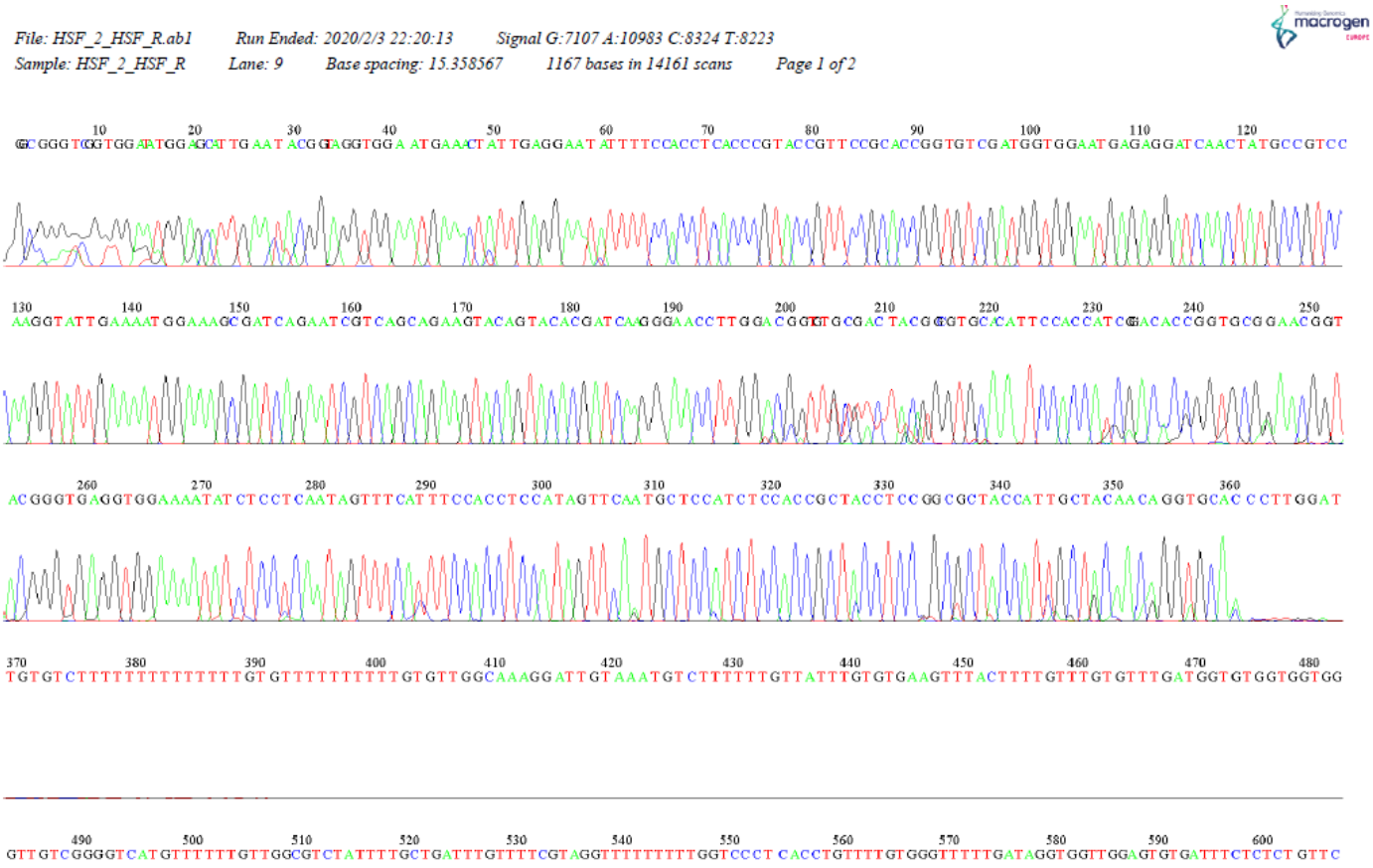
EMBOSS_001        51 TTGAACTACGGAGGTGGAAATGAAACTATTGAGGAAATATTTTCCACCTC    100
                     ||||||||||||||||||||||||||||||||||||||||||||||||||
EMBOSS_001      1075 TTGAACTACGGAGGTGGAAATGAAACTATTGAGGAAATATTTTCCACCTC   1124

EMBOSS_001       101 ACCCGTACCGTTCCGCACCGGTGTCGATGGTGGAATGAGAGGATCAACTA    150
                     ||||||||||||||||||||||||||||||||||||||||||||||||||
EMBOSS_001      1125 ACCCGTACCGTTCCGCACCGGTGTCGATGGTGGAATGAGAGGATCAACTA   1174

EMBOSS_001       151 TGCCGTCCAAGGTATTGAAAATGGAAAGCGTCCAGTAT    188
                     ||||||||||||||||||||||||||||..|||.||
EMBOSS_001      1175 TGCCGTCCAAGGTATTGAAAATGGAAAGCGATCAGAAT   1212
```

Antisense Sequence

Chromatogram



Sequence

CCGTAGTAGCAATGGTAGCGCCGGAGGTAGCGGTGGAGATGGAGCATTGAACT

ACGGAGGTGGAAATGAAACTATTGAGGAAATATTTTCCACCTCACCCGTACCGT

TCCGCACCGGTGTCGATGGTGGAATGAGAGGATCAACTATGCCGTCCAAGGTA

TTGAAAATGGAAAGCGATCAGAATCGTCAGCAGAAGTACAGT

EMBOSS Water Alignment

```
#=======================================
#
# Aligned_sequences: 2
# 1: EMBOSS_001
# 2: EMBOSS_001
# Matrix: EBLOSUM62
# Gap_penalty: 10.0
# Extend_penalty: 0.5
#
# Length: 202
# Identity:     202/202 (100.0%)
# Similarity:   202/202 (100.0%)
# Gaps:           0/202 ( 0.0%)
# Score: 1167.0
#
#
#=======================================

EMBOSS_001         1 CCGTAGTAGCAATGGTAGCGCCGGAGGTAGCGGTGGAGATGGAGCATTGA     50
                     ||||||||||||||||||||||||||||||||||||||||||||||||||
EMBOSS_001      1029 CCGTAGTAGCAATGGTAGCGCCGGAGGTAGCGGTGGAGATGGAGCATTGA   1078

EMBOSS_001        51 ACTACGGAGGTGGAAATGAAACTATTGAGGAAATATTTTCCACCTCACCC    100
                     ||||||||||||||||||||||||||||||||||||||||||||||||||
EMBOSS_001      1079 ACTACGGAGGTGGAAATGAAACTATTGAGGAAATATTTTCCACCTCACCC   1128

EMBOSS_001       101 GTACCGTTCCGCACCGGTGTCGATGGTGGAATGAGAGGATCAACTATGCC    150
                     ||||||||||||||||||||||||||||||||||||||||||||||||||
EMBOSS_001      1129 GTACCGTTCCGCACCGGTGTCGATGGTGGAATGAGAGGATCAACTATGCC   1178

EMBOSS_001       151 GTCCAAGGTATTGAAAATGGAAAGCGATCAGAATCGTCAGCAGAAGTACA    200
                     ||||||||||||||||||||||||||||||||||||||||||||||||||
EMBOSS_001      1179 GTCCAAGGTATTGAAAATGGAAAGCGATCAGAATCGTCAGCAGAAGTACA   1228

EMBOSS_001       201 GT    202
                     ||
EMBOSS_001      1229 GT   1230
```

Consensus Sequence (BioEdit)

GCACCCGTAGTAGCAATGGTAGCGCCGGAGGTAGCGGTGGAGATGGAGCATT

GAACTACGGAGGTGGAAATGAAACTATTGAGGAAATATTTTCCACCTCACCCGT

ACCGTTCCGCACCGGTGTCGATGGTGGAATGAGAGGATCAACTATGCCGTCCA

AGGTATTGAAAATGGAAAGCGCAGATGTCAGCAGAAGTACAGT

BLAST Results From VectorBase

> AFUN004137 protein_coding|CM012072.1:80651961:80668394:1|gene:AFUN004137

Length = 5984

Score = 380

Expect = 2e-94

Identity = 97.5728%

Strand = Plus/Plus

Aln Length = 206

Frame: 1 / 1 isTagged: . hitName: AFUN004137-RA

1 GCACCCGTAGTAGCAATGGTAGCGCCGGAGGTAGCGGTGGAGATGGAGCA TTGAACTACG 60

||||||||||||||||||||||||||||||||||||||||||||||||||||||||||||

Sbjct 102 5 GCACCCGTAGTAGCAATGGTAGCGCCGGAGGTAGCGGTGGAGATGGAGCA TTGAACTACG 108 4

Quer y 61 GAGGTGGAAATGAAACTATTGAGGAAATATTTTCCACCTCACCCGTACCGTT CCGCACCG 120

||||||||||||||||||||||||||||||||||||||||||||||||||||||||||||

Sbjct 108 5 GAGGTGGAAATGAAACTATTGAGGAAATATTTTCCACCTCACCCGTACCGTT CCGCACCG 114 4

Quer y 121 GTGTCGATGGTGGAATGAGAGGATCAACTATGCCGTCCAAGGTATTGAAAAT GGAAAGCG 180

||||||||||||||||||||||||||||||||||||||||||||||||||||||||||||

Sbjct	1145	GTGTCGATGGTGGAATGAGAGGATCAACTATGCCGTCCAAGGTATTGAAAATGGAAAGCG	1204

Query	181	--CAGA--TGTCAGCAGAAGTACAGT	202
		|||| |||||||||||||	
Sbjct	1205	ATCAGAATCGTCAGCAGAAGTACAGT	1230

APPENDIX F: HSF Transcript Abundance In All Life Stages (Fig 13)

i. *HSF* transcript abundance in eggs

Table S.2 shows cycle threshold (Ct) values produced during a QPCR for reference genes *RPS7* and *GAPDH* (A) as well as the gene of interest, *HSF* (B**)**

Table S.2A

	RPS7			*GAPDH*			
Sample	**Ct 1**	**Ct 2**	**Ct 3**	**Ct 1**	**Ct 2**	**Ct 3**	**Average Ct of both *RPS7* and *GAPDH* technical replicates**
No-siRNA Control 1	30.07	32.09	31.42	29.34	32.34	31.65	30.91
No-siRNA Control 2	30.11	32.14	31.61	30.99	32.74	32.33	31.65
No-siRNA Control 3	30.44	32.08	31.11	31.12	32.65	32.99	31.73
Eggs 1	31.82	32.09	32.08	30.05	30.96	30.08	31.18
Eggs 2	32.11	32.14	32.08	30.61	30.07	30.59	31.27
Eggs 3	32.81	32.06	32.08	30.49	N/A	30.36	31.56

Numerical value (1,2,3) in rows and columns: indicate biological replicates and technical replicates respectively. N/A indicates no Ct.

Table S.2B

	HSF						
Sample	**Ct 1**	**Ct 2**	**Ct 3**	**Average Ct**	**∆Ct**	**∆∆Ct**	**2^-∆∆Ct**
No-siRNA Control 1	30.45	31.99	29.99	29.22	-1.69	-0.52	1.43
No-siRNA Control 2	30.22	31.00	29.95	30.39	-1.26	-0.09	1.07
No-siRNA Control 3	30.55	31.96	31.00	31.17	-0.56	0.61	0.66
Eggs 1	29.10	29.02	29.55	29.22	-1.96	1.18	0.55
Eggs 2	29.06	29.27	29.53	29.29	-1.98	-0.81	0.38
Eggs 3	29.99	29.82	29.75	29.85	-1.71	-0.53	0.37

Numerical value (1,2,3) in rows and columns: indicate biological replicates and technical replicates respectively. N/A indicates no Ct.

Table S.3 shows the average 2^-ΔΔCt, standard deviation (SD) and standard error of the mean (SEM) values of the *HSF* egg transcript abundance and the no-siRNA control

Average 2^-ΔΔCt	Average	SD	SEM
No-siRNA control	**1.05**	0.39	0.22
Eggs	**0.43**	0.10	0.06

Table S.4 shows the *HSF* egg transcript abundance normalised against the no-siRNA control for each biological replicate

	Eggs/ control
Biological rep 1	0.38
Biological rep 2	0.36
Biological rep 3	0.56

ii. *HSF* transcript abundance in larvae

Table S.5 shows cycle threshold (Ct) values produced during a QPCR for reference genes RPS7 and GAPDH (A) as well as the gene of interest, *HSF* (B)

Table S.5A

	RPS7			*GAPDH*			
Sample	**Ct 1**	**Ct 2**	**Ct 3**	**Ct 1**	**Ct 2**	**Ct 3**	**Average Ct of both *RPS7* and *GAPDH* technical replicates**
No-siRNA Control 1	34.07	33.89	34.55	33.09	32.34	34.99	34.12
No-siRNA Control 2	34.65	33.99	34.07	34.14	32.74	34.30	33.98
No-siRNA Control 3	34.11	33.98	34.11	34.17	32.65	34.01	33.84
Larvae 1	35.99	35.91	35.75	34.09	34.87	35.56	35.36
Larvae 2	35.87	35.11	35.06	34.06	34.08	35.97	35.03
Larvae 3	35.99	35.91	35.44	34.26	34.88	35.55	35.34

Numerical value (1,2,3) in rows and columns: indicate biological replicates and technical replicates respectively.

Table S.5B

	HSF						
Sample	**Ct 1**	**Ct 2**	**Ct 3**	**Average Ct**	**ΔCt**	**ΔΔCt**	**2^-ΔΔCt**
No-siRNA Control 1	35.60	35.50	35.60	36.43	2.31	0.65	0.64
No-siRNA Control 2	35.00	35.42	35.78	35.40	1.42	-0.24	1.18
No-siRNA Control 3	35.03	34.22	35.99	35.08	1.24	-0.41	1.33
Larvae 1	36.18	36.52	36.58	36.43	1.32	0.09	1.42
Larvae 2	36.11	36.55	36.02	36.23	1.20	-0.45	1.37
Larvae 3	36.19	36.97	36.36	36.51	1.17	-0.49	1.40

Numerical value (1,2,3) in rows and columns: indicate biological replicates and technical replicates respectively.

Table S.6 shows the average 2^-ΔΔCt, standard deviation (SD) and standard error of the mean (SEM) values of the *HSF* larval transcript abundance and the no-siRNA control

	Average 2^-ΔΔCt	**SD**	**SEM**
No-siRNA control	**1.05**	0.37	0.21
Larvae	**1.40**	0.03	0.01

Table S.7 shows the *HSF* larvae transcript abundance normalised against the no-siRNA control for each biological replicate

	Larvae/ control
Biological rep 1	2.23
Biological rep 2	1.16
Biological rep 3	1.05

iii. *HSF* transcript abundance in pupae

Table S.8 shows cycle threshold (Ct) values produced during a QPCR for reference genes *RPS7* and *GAPDH* (A) as well as the gene of interest, *HSF* (B)

Table S.8A

	RPS7			*GAPDH*			
Sample	**Ct 1**	**Ct 2**	**Ct 3**	**Ct 1**	**Ct 2**	**Ct 3**	**Average Ct of both *RPS7* and *GAPDH* technical replicates**
No-siRNA control 1	33.62	33.89	33.98	33.09	32.34	34.99	33.91
No-siRNA control 2	33.78	33.99	33.00	33.17	32.74	34.30	33.50
No-siRNA control 3	33.82	33.98	33.09	33.17	32.65	34.01	33.45
Pupae 1	34.09	34.09	34.65	34.56	34.44	34.08	34.32
Pupae 2	34.00	34.12	34.87	34.55	34.65	34.36	34.43
Pupae 3	34.51	34.02	34.87	34.39	34.69	34.23	34.45

Numerical value (1,2,3) in rows and columns: indicate biological replicates and technical replicates respectively.

Table S.8B

	HSF						
Sample	**Ct 1**	**Ct 2**	**Ct 3**	**Average Ct**	**ΔCt**	**ΔΔCt**	**2^-ΔΔCt**
No-siRNA control 1	31.79	31.89	31.99	33.25	-0.66	0.62	0.65
No-siRNA control 2	31.99	32.07	32.00	32.02	-1.48	-0.19	1.14
No-siRNA control 3	31.55	31.69	31.99	31.74	-1.71	-0.43	1.34
Pupae 1	32.89	33.95	32.91	33.25	-0.18	-0.86	0.76
Pupae 2	32.01	33.79	33.92	33.24	-1.19	0.10	0.93
Pupae 3	32.00	33.77	32.38	32.72	-1.74	-0.45	0.70

Numerical value (1,2,3) in rows and columns: indicate biological replicates and technical replicates respectively.

Table S.9 shows the average 2^-ΔΔCt, standard deviation (SD) and standard error of the mean (SEM) values of the *HSF* pupal transcript abundance and the no-siRNA control

Average 2^-ΔΔCt	**Average**	**SD**	**SEM**
No-siRNA control	**1.05**	0.36	0.21
Pupae	**0.80**	0.12	0.07

Table S.10 shows the *HSF* larvae transcript abundance normalised against the no-siRNA control for each biological replicate

	Pupae/ control
Biological rep 1	1.17
Biological rep 2	0.82
Biological rep 3	0.52

iv. *HSF* transcript abundance in adults

Table S.11 shows cycle threshold (Ct) values produced during a QPCR for reference genes *RPS7* and *GAPDH* (A) as well as the gene of interest, *HSF* (B)

Table S.11A

	RPS7			***GAPDH***			
Sample	**Ct 1**	**Ct 2**	**Ct 3**	**Ct 1**	**Ct 2**	**Ct 3**	**Average Ct of both *RPS7* and *GAPDH* technical replicates**
No-siRNA control 1	33.62	33.89	34.55	33.09	32.34	34.99	34.03
No-siRNA control 2	33.78	33.99	34.07	33.17	32.74	34.30	33.68
No-siRNA control 3	33.82	33.98	34.11	33.17	32.65	34.01	33.62
Adults 1	36.88	35.03	36.37	34.00	34.25	34.88	35.24
Adults 2	36.77	35.20	36.82	34.67	34.71	34.00	35.36
Adults 3	36.82	35.02	36.96	34.21	34.24	34.18	35.24

Numerical value (1,2,3) in rows and columns: indicate biological replicates and technical replicates respectively.

Table S.11B

	HSF						
Sample	**Ct 1**	**Ct 2**	**Ct 3**	**Average Ct**	**ΔCt**	**ΔΔCt**	**2^-ΔΔCt**
No-siRNA control 1	34.98	34.38	34.72	35.52	1.49	0.43	0.74
No-siRNA control 2	35.01	34.07	34.88	34.65	0.98	-0.08	1.06
No-siRNA control 3	34.52	N/A	34.15	34.34	0.71	-0.35	1.27
Adults 1	36.31	35.24	35.00	35.52	0.02	-0.96	1.40
Adults 2	35.34	35.36	35.88	35.53	0.17	-0.89	1.54
Adults 3	35.29	35.69	36.08	35.69	0.45	-0.61	1.53

Numerical value (1,2,3) in rows and columns: indicate biological replicates and technical replicates respectively.

Table S.12 shows the average 2^-ΔΔCt, standard deviation (SD) and standard error of the mean (SEM) values of the *HSF* adult transcript abundance and the no-siRNA control

Average 2^-ΔΔCt	Average	SD	SEM
No-siRNA control	**1.02**	0.27	0.15
Adults	**1.49**	0.08	0.04

Table S.13 shows the *HSF* adult transcript abundance normalised against the no-siRNA control for each biological replicate

	Adults/ control
Biological rep 1	1.88
Biological rep 2	1.46
Biological rep 3	1.20

APPENDIX G: cDNA Calculations To Validate SiRNA Delivery System Using *RPL19*

Technical replicate 1

Males 20 ng/µl *RPL19*-siRNA = $C_1V_1=C_2V_2$
(50 ng/µl)(100 µl)= (2684 ng/µl)(V_2)
5000/ 2684= V_2
V_2= 1.9 ul + 98.1 ul H_20

Females 20 ng/µl *RPL19*-siRNA = $C_1V_1=C_2V_2$
(50 ng/µl)(100 µl)= (2263.3 ng/µl)(V_2)
5000/ 2263.3= V_2
V_2= 2.2 µl + 97.8 µl H_20

Males 20 ng/µl *β2m-siRNA* = $C_1V_1=C_2V_2$
(50 ng/µl)(100 µl)= (2400.1 ng/µl)(V_2)
5000/ 2400.1= V_2
V_2= 2.1 µl + 97.9 µl H_20

Females 20 ng/µl *β2m-siRNA*= $C_1V_1=C_2V_2$
(50n g/µl)(100 µl)= (1463.7 ng/µl)(V_2)
5000/ 1463.7= V_2
V_2= 3.4 µl + 96.6 µl H_20

Males no-siRNA control = $C_1V_1=C_2V_2$
(50 ng/µl)(100 µl)= (2859.2 ng/µl)(V_2)
5000/ 2859.2= V_2
V_2= 1.7 µl + 98.3 µl H_20

Females no-siRNA control= $C_1V_1=C_2V_2$
(50 ng/µl)(100 µl)= (2577 ng/µl)(V_2)
5000/ 2577= V_2
V_2= 1.9 µl + 98.1 µl H_20

Technical replicate 2

Males 20 ng/µl *RPL19*-siRNA = $C_1V_1=C_2V_2$
(50 ng/µl)(100 µl)= (2008.7 ng/µl)(V_2)
5000/ 2008.7= V_2
V_2= 2.5 µl + 97.5 µl H_20

Females 20 ng/µl *RPL19*-siRNA = $C_1V_1=C_2V_2$
(50 ng/µl)(100 µl)= (2199.6 ng/µl)(V_2)
5000/ 2199.6= V_2

V_2= 2.3 µl + 97.7 µl H_20
Males 20 ng/µl *B2m-siRNA* = $C_1V_1=C_2V_2$
(50 ng/µl)(100 µl)= (3087.6 ng/µl)(V_2)
5000/ 3087.6= V_2
V_2= 1.6 µl + 98.4 µl H_20

Females 20 ng/µl *B2m-siRNA*= $C_1V_1=C_2V_2$
(50 ng/µl)(100 µl)= (3306.5 ng/µl)(V_2)
5000/ 3306.5= V_2
V_2= 1.5 µl + 98.5 µl H_20

Males no-siRNA control = $C_1V_1=C_2V_2$
(50 ng/µl)(100 µl)= (2808.8 ng/µl)(V_2)
5000/ 2808.8= V_2
V_2= 1.8 µl + 98.2 µl H_20

Females no-siRNA control= $C_1V_1=C_2V_2$
(50 ng/µl)(100 µl)= (2370.6 ng/µl)(V_2)
5000/ 2370.6= V_2
V_2= 2.1 µl + 97.9 µl H_20

Technical replicate 3

Males 20 ng/µl *RPL19*-siRNA = $C_1V_1=C_2V_2$
(50 ng/µl)(100 µl)= (3046 ng/µl)(V_2)
5000/ 3046= V_2
V_2= 1.6 µl + 98.4 µl H_20

Females 20 ng/µl *RPL19*-siRNA = $C_1V_1=C_2V_2$
(50 ng/µl)(100 µl)= (1980.9 ng/µl)(V_2)
5000/ 1980.9= V_2
V_2= 2.5 µl + 97.5 µl H_20

Males 20 ng/µl *β2m-siRNA* = $C_1V_1=C_2V_2$
(50 ng/µl)(100 µl)= (2150.4 ng/µl)(V_2)
5000/ 2150.4= V_2
V_2= 2.3 µl + 97.7 µl H_20

Females 20 ng/µl *β2m-siRNA*= $C_1V_1=C_2V_2$
(50 ng/µl)(100 µl)= (2368.8 ng/µl)(V_2)
5000/ 2368.8= V_2
V_2= 2.1 µl + 97.9 µl H_20

Males no-siRNA control = $C_1V_1=C_2V_2$
(50 ng/µl)(100 µl)= (1618 ng/µl)(V_2)
5000/ 1618= V_2
V_2= 3 µl + 97 µl H_20

Females no-siRNA control= $C_1V_1=C_2V_2$
(50 ng/µl)(100 µl)= (2813.1 ng/µl)(V_2)
5000/ 2813.1= V_2
V_2= 1.8 µl + 98.2 µl H_20

APPENDIX H: *RPL19* Transcript Abundance

i. *RPL19* transcript abundance in males *(*Fig 20A*)*

Table S.14 shows cycle threshold (Ct) values produced during a QPCR for reference genes *RPS7* and *GAPDH* (A) as well as the gene of interest, *HSF* (B)

Table S.14A

	RPS7			***GAPDH***			
Sample	**Ct 1**	**Ct 2**	**Ct 3**	**Ct 1**	**Ct 2**	**Ct 3**	**Average Ct of both *RPS7* and *GAPDH* technical replicates**
No-siRNA control 1	28.51	28.45	28.10	28.64	28.90	28.84	28.57
No-siRNA control 2	28.59	28.89	28.14	27.55	27.66	27.01	27.97
No-siRNA control 3	28.36	28.14	28.15	28.07	28.41	28.05	28.20
***RPL19*-siRNA 1**	27.39	27.13	28.01	28.17	27.55	28.12	27.73
***RPL19*-siRNA 2**	27.05	27.87	27.65	26.56	26.81	27.04	27.16
***RPL19*-siRNA 3**	27.80	27.04	27.64	27.43	28.30	27.78	27.67
***β2m-siRNA* 1**	29.40	29.40	29.47	29.18	29.44	29.70	29.43
***β2m-siRNA* 2**	29.44	29.60	29.11	29.45	29.55	29.41	29.43
***β2m-siRNA* 3**	28.36	28.14	28.15	28.50	28.44	28.61	28.37

Numerical value (1,2,3) in rows and columns: indicate biological replicates and technical replicates respectively.

Table S.14B

	RPL19						
Sample	**Ct 1**	**Ct 2**	**Ct 3**	**Average Ct**	**ΔCt**	**ΔΔCt**	**2^-ΔΔCt**
No-siRNA control 1	28.07	28.18	29.18	28.48	-0.10	-0.48	1.39
No-siRNA control 2	28.45	28.76	28.56	28.59	0.62	0.24	0.85
No-siRNA control 3	28.70	28.76	28.99	28.82	0.62	0.24	0.85
***RPL19*-siRNA 1**	28.54	28.41	28.84	28.60	0.87	0.49	0.71
***RPL19*-siRNA 2**	28.09	28.51	28.11	28.24	1.07	0.69	0.62
***RPL19*-siRNA 3**	28.24	28.22	28.47	28.31	0.64	0.26	0.83
***β2m-siRNA* 1**	29.03	29.07	29.00	29.03	-0.40	-0.78	1.72
***β2m-siRNA* 2**	28.90	29.96	29.78	29.55	0.12	-0.26	1.20
***β2m-siRNA* 3**	29.88	29.62	29.54	29.68	1.31	0.93	0.52

Numerical value (1,2,3) in rows and columns: indicate biological replicates and technical replicates respectively.

Table S.15 shows the average 2^-ΔΔCt, standard deviation (SD) and standard error of the mean (SEM) values of the *RPL19* transcript abundance and the no-siRNA control

Average 2^-ΔΔCt	Average	SD	SEM
No-siRNA control	**1.02**	0.31	0.18
***RPL19*-siRNA**	**0.72**	0.10	0.06
β2m-siRNA	**1.15**	0.60	0.34

Table S.16 shows the *RPL19* transcript abundance normalised against the no-siRNA control for each biological replicate

	***RPL19*l control**
Biological rep 1	0.98
Biological rep 2	0.73
Biological rep 3	0.51

ii. *RPL19* transcript abundance in females (Fig 20B)

Table S.17 shows cycle threshold (Ct) values produced during a QPCR for reference genes *RPS7* and *GAPDH* (A) as well as the gene of interest, *RPL19* (B)

Table S.17A

	RPS7			***GAPDH***			
Sample	**Ct 1**	**Ct 2**	**Ct 3**	**Ct 1**	**Ct 2**	**Ct 3**	**Average Ct of both *RPS7* and *GAPDH* technical replicates**
No-siRNA control 1	27.01	27.16	27.11	29.22	29.08	29.40	28.16
No-siRNA control 2	27.08	27.02	27.17	29.45	29.30	29.32	28.22
No-siRNA control 3	27.11	27.35	27.54	29.15	29.45	29.10	28.28
***RPL19*-siRNA 1**	25.63	25.36	25.88	28.94	28.65	28.77	27.21
***RPL19*-siRNA 2**	26.21	25.93	26.00	28.15	28.25	28.95	27.25
***RPL19*-siRNA 3**	25.81	25.45	25.58	28.29	28.70	28.13	26.99
***β2m-siRNA* 1**	26.48	26.43	26.41	26.79	26.65	26.30	26.51
***β2m-siRNA* 2**	26.89	26.33	26.59	26.87	26.56	26.30	26.59
***β2m-siRNA* 3**	26.82	26.34	26.97	26.67	26.99	26.75	26.76

Numerical value (1,2,3) in rows and columns: indicate biological replicates and technical replicates respectively.

Table S.17B

	RPL19						
Sample	**Ct 1**	**Ct 2**	**Ct 3**	**Average Ct**	**ΔCt**	**ΔΔCt**	**2^-ΔΔCt**
No-siRNA control 1	27.44	27.23	27.93	27.53	-0.63	0.14	0.91
No-siRNA control 2	27.10	27.91	27.10	27.37	-0.85	-0.08	1.06
No-siRNA control 3	27.60	27.70	27.07	27.46	-0.83	-0.06	1.04
***RPL19*-siRNA 1**	28.31	28.88	28.40	28.53	1.33	2.10	0.23
***RPL19*-siRNA 2**	28.51	28.41	28.65	28.52	1.28	2.05	0.24
***RPL19*-siRNA 3**	28.67	28.82	28.40	28.63	1.64	2.41	0.19
***β2m-siRNA* 1**	26.29	26.32	26.85	26.49	-0.02	0.75	0.60
***β2m-siRNA* 2**	25.50	26.10	26.36	25.99	-0.60	0.17	0.89
***β2m-siRNA* 3**	25.50	25.10	25.99	25.53	-1.23	-0.46	1.37

Numerical value (1,2,3) in rows and columns: indicate biological replicates and technical replicates respectively.

Table S.18 shows the average 2^-ΔΔCt, standard deviation (SD) and standard error of the mean (SEM) values of the *RPL19* transcript abundance and the no-siRNA control

Average 2^-ΔΔCt	**Average**	**SD**	**SEM**
No-siRNA control	**1.00**	0.08	0.05
***RPL19*-siRNA**	**0.22**	0.03	0.02
β2m-siRNA	**0.51**	0.46	0.27

Table S.19 shows the *RPL19* transcript abundance normalised against the no-siRNA control for each biological replicate

	***RPL19*/ control**
Biological rep 1	0.21
Biological rep 2	0.23
Biological rep 3	0.22

APPENDIX I: cDNA Dilutions To Determine The Effect of Concentration and Temperature On HSF Knockdown

Technical replicate 1

Males 10 ng/µl *HSF*-siRNA = $C_1V_1=C_2V_2$
(50 ng/µl)(100 µl)= (2456.6 ng/µl)(V_2)
5000/ 2456.6= V_2
V_2= 2 µl + 98 µl H_20

Females 10 ng/µl *HSF*-siRNA = $C_1V_1=C_2V_2$
(50 ng/µl)(100 µl)= (2239.2 ng/µl)(V_2)
5000/ 2239.2= V_2
V_2= 2.2 µl + 97.8 µl H_20

Males 20 ng/µl *HSF*-siRNA = $C_1V_1=C_2V_2$
(50 ng/µl)(100 µl)= (2761.5ng/µl)(V_2)
5000/ 2761.5= V_2
V_2= 1.8 µl + 98.2 µl H_20

Females 20 ng/µl *HSF*-siRNA RNA = $C_1V_1=C_2V_2$
(50 ng/µl)(100 µl)= (2514.5 ng/µl)(V_2)
5000/ 2514.5= V_2
V_2= 2 µl + 98 µl H_20

Males 30 ng/µl *HSF*-siRNA = $C_1V_1=C_2V_2$
(50 ng/µl)(100 µl)= (2769.7 ng/µl)(V_2)
5000/ 2769.7= V_2
V_2= 1.8 µl + 98.2 µl H_20

Females 30 ng/µl *HSF-siRNA* = $C_1V_1=C_2V_2$
(50 ng/µl)(100 µl)= (1713.3 ng/µl)(V_2)
5000/ 1713.3= V_2
V_2= 2.9 µl + 97.1 µl H_20

Males 20 ng/µl *β2m-siRNA* = $C_1V_1=C_2V_2$
(50 ng/µl)(100 µl)= (4843.8 ng/µl)(V_2)
5000/ 4843.8= V_2
V_2= 1µl + 99µl H_20

Females 20 ng/µl *β2m-siRNA* = $C_1V_1=C_2V_2$
(50 ng/µl)(100 µl)= (2790.1 ng/µl)(V_2)
5000/ 2790.1= V_2
V_2= 1.8 µl + 98.2 µl H_20

Males no-siRNA control = $C_1V_1=C_2V_2$
(50 ng/µl)(100 µl)= (2859.2 ng/µl)(V_2)
5000/ 2859.2= V_2
V_2= 1.7 µl + 98.3 µl H_20

Females no-siRNA control= $C_1V_1=C_2V_2$
(50 ng/µl)(100 µl)= (2577 ng/µl)(V_2)
5000/ 2577= V_2
V_2= 1.9 µl + 98.1 µl H_20

Technical replicate 2

Males 10 ng/µl *HSF-siRNA* = $C_1V_1=C_2V_2$
(50 ng/µl)(100 µl)= (2615.4 ng/µl)(V_2)
5000/ 2615.4= V_2
V_2= 1.9 µl + 98.1 µl H_20

Females 10 ng/µl *HSF-siRNA* = $C_1V_1=C_2V_2$
(50 ng/µl)(100 µl)= (2235.1 ng/µl)(V_2)
5000/ 2235.1= V_2
V_2= 2.2 µl + 97.8 µl H_20

Males 20 ng/µl *HSF-siRNA* = $C_1V_1=C_2V_2$
(50 ng/µl)(100 µl)= (2178.5 ng/µl)(V_2)
5000/ 2178.5= V_2
V_2= 2.3 µl + 97.7 µl H_20

Females 20 ng/µl *HSF-siRNA* RNA = $C_1V_1=C_2V_2$
(50 ng/µl)(100 µl)= (3506.1ng/µl)(V_2)
5000/ 3506.1= V_2
V_2= 1.4 µl + 98.6 µl H_20

Males 30 ng/µl *HSF-siRNA* = $C_1V_1=C_2V_2$
(50 ng/µl)(100 µl)= (2592.5 ng/µl)(V_2)
5000/ 2592.5= V_2
V_2= 1.9 µl + 98.1 µl H_20

Females 30 ng/µl *HSF-siRNA* = $C_1V_1=C_2V_2$
(50 ng/µl)(100 µl)= (2762.1 ng/µl)(V_2)
5000/ 2762.1= V_2
V_2= 1.8 µl + 98.2 µl H_20

Males 20 ng/µl *β2m-siRNA* = $C_1V_1=C_2V_2$
(50 ng/µl)(100 µl)= (2627.8 ng/µl)(V_2)
5000/ 2627.8= V_2
V_2= 2 µl + 98 µl H_20

Females 20 ng/µl *β2m-siRNA* = $C_1V_1=C_2V_2$
(50 ng/µl)(100 µl)= (2744.6 ng/µl)(V_2)
5000/ 2744.6= V_2
V_2= 1.9 µl + 98.1 µl H_20

Males no-siRNA control = $C_1V_1=C_2V_2$
(50 ng/µl)(100 µl)= (1618 ng/µl)(V_2)
5000/ 1618= V_2
V_2= 3 µl + 97 µl H_20

Females no-siRNA control= $C_1V_1=C_2V_2$
(50 ng/µl)(100 µl)= (2813.1 ng/µl)(V_2)
5000/ 2813.1= V_2
V_2= 1.8 µl + 98.2 µl H_20

Technical replicate 3

Males 10 ng/µl *HSF-siRNA* = $C_1V_1=C_2V_2$
(50 ng/µl)(100 µl)= (2667.3 ng/µl)(V_2)
5000/ 2667.3= V_2
V_2= 1.9 µl + 98.1 µl H_20

Females 10 ng/µl *HSF-siRNA* = $C_1V_1=C_2V_2$
(50 ng/µl)(100 µl)= (2445.9 ng/µl)(V_2)
5000/ 2445.9= V_2
V_2= 2 µl + 98 µl H_20

Males 20 ng/µl *HSF-siRNA* = $C_1V_1=C_2V_2$
(50 ng/µl)(100 µl)= (2889.7 ng/µl)(V_2)
5000/ 2505.7= V_2
V_2= 1.7 µl + 98.3 µl H_20

Females 20 ng/µl *HSF-siRNA* RNA = $C_1V_1=C_2V_2$
(50 ng/µl)(100 µl)= (2193.9 ng/µl)(V_2)
5000/ 2193.9= V_2
V_2= 2.3 µl + 97.7 µl H_20

Males 30 ng/µl *HSF-siRNA* = $C_1V_1=C_2V_2$
(50 ng/µl)(100 µl)= (2631.1 ng/µl)(V_2)
5000/ 2631.1= V_2
V_2= 1.9 µl + 98.1 µl H_20

Females 30 ng/µl *HSF-siRNA* = $C_1V_1=C_2V_2$
(50 ng/µl)(100 µl)= (2447.9 ng/µl)(V_2)
5000/ 2447.9= V_2
V_2= 2 µl + 98 µl H_20

Males 20 ng/µl *β2m-siRNA* = $C_1V_1=C_2V_2$
(50ng/µl)(100 µl)= (2529.4ng/µl)(V_2)
5000/ 2529.4= V_2
V_2= 2 µl + 98 µl H_20

Females 20 ng/µl *β2m-siRNA* = $C_1V_1=C_2V_2$
(50 ng/µl)(100 µl)= (2783.8 ng/µl)(V_2)
5000/ 2783.8= V_2
V_2= 1.8 ul + 98.2 µl H_20

Males no-siRNA control = $C_1V_1=C_2V_2$
(50 ng/µl)(100 µl)= 4946.3 ng/µl)(V_2)
5000/ 4946.3= V_2
V_2= 1 µl + 99µl H_20

Females no-siRNA control = $C_1V_1=C_2V_2$
(50 ng/µl)(100 µl)= (1980.9 ng/µl)(V_2)
5000/ 1980.9= V_2
V_2= 2.5 µl + 97.5 µl H_20

APPENDIX J*: An. funestus* Treated With HSF-SiRNA

i. *An. funestus* males treated with HSF-siRNA (10 ng/µl) at 20°C (Fig 24A)

Table S.20 shows cycle threshold (Ct) values produced during a qPCR for reference genes *RPS7* and *GAPDH* (A) as well as the gene of interest, *HSF* (B)

Table S.20A

	RPS7			*GAPDH*			
Sample	**Ct 1**	**Ct 2**	**Ct 3**	**Ct 1**	**Ct 2**	**Ct 3**	**Average Ct of both *RPS7* and *GAPDH* technical replicates**
No-siRNA control 1	36.33	36.12	36.68	36.29	36.54	36.99	36.49
No-siRNA control 2	36.81	36.65	36.95	36.98	36.11	36.23	36.62
No-siRNA control 3	36.20	36.60	36.83	36.87	36.92	36.95	36.73
***HSF*-siRNA 1**	27.40	27.55	28.10	29.89	29.50	29.86	28.72
***HSF*-siRNA 2**	27.39	28.03	28.07	29.33	29.30	29.17	28.55
***HSF*-siRNA 3**	27.61	28.82	27.42	28.94	29.17	29.48	28.57
***β2m-siRNA* 1**	33.45	33.96	33.89	33.56	33.09	33.67	33.60
***β2m-siRNA* 2**	33.23	33.02	33.71	33.97	33.12	33.18	33.37
***β2m-siRNA* 3**	33.45	33.28	33.65	33.97	33.41	33.29	33.51

Numerical value (1,2,3) in rows and columns: indicate biological replicates and technical replicates respectively.

Table S.20B

	HSF						
Sample	**Ct 1**	**Ct 2**	**Ct 3**	**Average Ct**	**ΔCt**	**ΔΔCt**	**2^-ΔΔCt**
No-siRNA control 1	37.00	37.27	37.49	37.25	0.76	0.00	1.00
No-siRNA control 2	37.77	37.15	37.28	37.40	0.78	0.02	0.99
No-siRNA control 3	37.31	37.21	37.88	37.47	0.74	-0.02	1.01
***HSF*-siRNA 1**	29.95	30.21	30.62	30.26	1.54	0.78	0.58
***HSF*-siRNA 2**	30.59	31.59	30.00	30.73	2.18	1.42	0.37
***HSF*-siRNA 3**	30.50	30.04	30.27	30.27	1.70	0.94	0.52
***β2m-siRNA* 1**	34.24	34.33	33.99	34.19	0.58	-0.18	1.13
***β2m-siRNA* 2**	34.08	34.13	34.38	34.20	0.82	0.07	0.96
***β2m-siRNA* 3**	34.04	35.04	34.05	34.38	0.87	0.11	0.93

Numerical value (1,2,3) in rows and columns: indicate biological replicates and technical replicates respectively.

Table S.21 shows the average 2^-ΔΔCt, standard deviation (SD) and standard error of the mean (SEM) values of the *HSF* transcript abundance and the no-siRNA control

Average 2^-ΔΔCt	Average	SD	SEM
No-siRNA control	**1.00**	0.01	0.01
***RPL19*-siRNA**	**0.49**	0.11	0.06
β2m-siRNA	**1.00**	0.11	0.06

Table S.22 shows the *HSF* transcript abundance normalised against the no-siRNA control for each biological replicate

	***HSF*/ control**
Biological rep 1	0.58
Biological rep 2	0.38
Biological rep 3	0.51

ii. *An. funestus* females treated with *HSF*-siRNA (10 ng/µl) at 20°C (Fig 24B)

Table S.23 shows cycle threshold (Ct) values produced during a QPCR for reference genes *RPS7* and *GAPDH* (A) as well as the gene of interest, *HSF* (B)

Table S.23A

	RPS7			GAPDH			
Sample	**Ct 1**	**Ct 2**	**Ct 3**	**Ct 1**	**Ct 2**	**Ct 3**	**Average Ct of both *RPS7* and *GAPDH* technical replicates**
No-siRNA control 1	28.17	29.74	28.00	31.57	31.68	31.07	30.04
No-siRNA control 2	28.64	28.74	28.78	30.95	31.43	31.84	30.06
No-siRNA control 3	28.32	28.54	N/A	31.31	32.88	31.27	30.46
***HSF*-siRNA 1**	25.43	25.93	26.02	29.88	29.10	30.04	27.73
***HSF*-siRNA 2**	25.74	25.04	25.08	28.54	29.08	29.33	27.14
***HSF*-siRNA 3**	26.31	25.68	25.86	29.05	29.18	N/A	27.22
***β2m-siRNA* 1**	25.64	25.49	N/A	28.16	28.68	28.68	27.33
***β2m-siRNA* 2**	25.49	24.98	25.35	27.78	28.20	28.17	26.66
***β2m-siRNA* 3**	25.19	25.12	25.86	29.35	28.70	28.81	27.17

Numerical value (1,2,3) in rows and columns: indicate biological replicates and technical replicates respectively. N/A indicates no Ct value.

Table S.23B

	HSF						
Sample	**Ct 1**	**Ct 2**	**Ct 3**	**Average Ct**	**ΔCt**	**ΔΔCt**	**2^-ΔΔCt**
No-siRNA control 1	32.19	32.36	32.40	32.32	2.28	0.18	0.88
No-siRNA control 2	32.01	32.03	32.23	32.09	2.03	-0.07	1.05
No-siRNA control 3	32.03	32.42	32.89	32.45	1.98	-0.11	1.08
***HSF*-siRNA 1**	30.88	31.47	30.95	31.10	3.37	1.27	0.41
***HSF*-siRNA 2**	31.43	30.82	31.75	31.33	4.20	2.10	0.23
***HSF*-siRNA 3**	32.16	31.72	31.71	31.86	4.65	2.55	0.17
***β2m-siRNA* 1**	29.49	29.35	29.10	29.31	1.98	-0.11	1.08
***β2m-siRNA* 2**	29.05	29.71	29.17	29.31	2.65	0.55	0.68
***β2m-siRNA* 3**	29.62	29.25	29.25	29.37	2.20	0.11	0.93

Numerical value (1,2,3) in rows and columns: indicate biological replicates and technical replicates respectively. N/A indicates no Ct value.

Table S.24 shows the average 2^-ΔΔCt, standard deviation (SD) and standard error of the mean (SEM) values of the *HSF* transcript abundance and the no-siRNA control

Average 2^-ΔΔCt	**Average**	**SD**	**SEM**
No-siRNA control	**1.00**	0.11	0.06
***RPL19*-siRNA**	**0.27**	0.13	0.07
β2m-siRNA	**0.90**	0.20	0.12

Table S.25 shows the *HSF* transcript abundance normalised against the no-siRNA control for each biological replicate

	***HSF*/ control**
Biological rep 1	0.47
Biological rep 2	0.22
Biological rep 3	0.16

iii. *An. funestus* males treated with *HSF*-siRNA (20 ng/µl) at 20°C (Fig 25A)

Table S.26 shows cycle threshold (Ct) values produced during a QPCR for reference genes *RPS7* and *GAPDH* (A) as well as the gene of interest, *HSF* (B)

Table S.26A

	RPS7			GAPDH			
Sample	**Ct 1**	**Ct 2**	**Ct 3**	**Ct 1**	**Ct 2**	**Ct 3**	**Average Ct of both *RPS7* and *GAPDH* technical replicates**
No-siRNA control 1	36.51	36.52	36.38	35.21	35.23	35.41	35.88
No-siRNA control 2	37.39	36.02	36.06	35.33	35.62	35.71	36.02
No-siRNA control 3	36.72	36.54	N/A	35.22	35.29	35.62	35.88
***HSF*-siRNA 1**	34.03	34.60	34.36	35.29	N/A	35.22	34.70
***HSF*-siRNA 2**	34.68	34.62	34.05	35.79	35.56	35.05	34.96
***HSF*-siRNA 3**	34.30	34.60	34.73	35.24	35.51	34.32	34.78
***β2m-siRNA* 1**	32.63	32.97	32.81	32.85	32.19	32.54	32.67
***β2m-siRNA* 2**	32.32	32.28	32.97	32.61	32.73	34.99	32.99
***β2m-siRNA* 3**	33.12	33.01	32.90	32.56	32.63	32.99	32.87

Numerical value (1,2,3) in rows and columns: indicate biological replicates and technical replicates respectively. N/A indicates no Ct value.

Table S.26B

	HSF						
Sample	**Ct 1**	**Ct 2**	**Ct 3**	**Average Ct**	**ΔCt**	**ΔΔCt**	**2^-ΔΔCt**
No-siRNA control 1	39.35	38.76	37.58	38.56	2.69	0.19	0.87
No-siRNA control 2	38.30	38.22	38.04	38.19	2.17	-0.33	1.26
No-siRNA control 3	38.22	N/A	38.79	38.51	2.63	0.13	0.91
***HSF*-siRNA 1**	39.60	39.26	39.54	39.47	4.77	2.27	0.21
***HSF*-siRNA 2**	N/A	39.59	39.25	39.42	4.46	1.97	0.26
***HSF*-siRNA 3**	39.26	N/A	39.31	39.29	4.50	2.01	0.25
***β2m-siRNA* 1**	35.13	35.19	N/A	35.16	2.50	0.00	1.00
***β2m-siRNA* 2**	35.93	N/A	35.01	35.47	2.48	-0.01	1.01
***β2m-siRNA* 3**	35.55	35.88	35.24	35.56	2.69	0.20	0.87

Numerical value (1,2,3) in rows and columns: indicate biological replicates and technical replicates respectively. N/A indicates no Ct value.

Table S.27 shows the average 2^-ΔΔCt, standard deviation (SD) and standard error of the mean (SEM) values of the *HSF* transcript abundance and the no-siRNA control

Average 2^-ΔΔCt	Average	SD	SEM
No-siRNA control	**1.01**	0.21	0.12
***RPL19*-siRNA**	**0.24**	0.03	0.02
β2m-siRNA	**0.96**	0.07	0.04

Table S.28 shows the *HSF* transcript abundance normalised against the no-siRNA control for each biological replicate

	***HSFl* control**
Biological rep 1	0.24
Biological rep 2	0.20
Biological rep 3	0.27

iv. *An. funestus* females treated with HSF-siRNA (20 ng/µl) at 20°C (Fig 25B)

Table S.29 shows cycle threshold (Ct) values produced during a QPCR for reference genes *RPS7* and *GAPDH* (A) as well as the gene of interest, *HSF* (B)

Table S.29A

	RPS7			***GAPDH***			
Sample	**Ct 1**	**Ct 2**	**Ct 3**	**Ct 1**	**Ct 2**	**Ct 3**	**Average Ct of both *RPS7* and *GAPDH* technical replicates**
No-siRNA control 1	31.87	31.49	31.52	32.16	31.56	31.84	31.74
No-siRNA control 2	31.25	31.11	31.84	31.43	30.74	31.02	31.23
No-siRNA control 3	31.33	31.28	31.55	31.58	31.59	31.89	31.54
***HSF*-siRNA 1**	27.88	28.20	28.12	29.49	29.98	30.30	29.00
***HSF*-siRNA 2**	28.22	29.25	28.23	30.83	30.49	30.72	29.62
***HSF*-siRNA 3**	28.56	27.90	27.93	30.00	30.87	30.88	29.36
***β2m-siRNA* 1**	27.35	27.17	28.12	27.77	27.59	28.11	27.69
***β2m-siRNA* 2**	27.14	29.99	27.52	26.94	27.67	27.32	27.46
***β2m-siRNA* 3**	27.11	26.57	26.51	27.31	27.54	27.94	27.16

Numerical value (1,2,3) in rows and columns: indicate biological replicates and technical replicates respectively.

Table S.29B

	HSF						
Sample	**Ct 1**	**Ct 2**	**Ct 3**	**Average Ct**	**ΔCt**	**ΔΔCt**	**2^-ΔΔCt**
No-siRNA control 1	32.94	32.96	33.24	33.05	1.31	-0.21	1.15
No-siRNA control 2	33.00	32.32	32.35	32.56	1.33	-0.19	1.14
No-siRNA control 3	33.34	33.10	33.90	33.45	1.91	0.40	0.76
***HSF*-siRNA 1**	31.51	32.11	32.43	32.02	3.02	1.51	0.35
***HSF*-siRNA 2**	33.06	32.90	32.55	32.84	3.21	1.70	0.31
***HSF*-siRNA 3**	32.36	33.09	32.94	32.80	3.44	1.93	0.26
***β2m-siRNA* 1**	28.79	28.87	29.15	28.94	1.25	-0.26	1.20
***β2m-siRNA* 2**	27.96	29.28	29.19	28.81	1.35	-0.17	1.12
***β2m-siRNA* 3**	29.13	29.55	29.29	29.32	2.16	0.65	0.64

Numerical value (1,2,3) in rows and columns: indicate biological replicates and technical replicates respectively.

Table S.30 shows the average 2^-ΔΔCt, standard deviation (SD) and standard error of the mean (SEM) values of the *HSF* transcript abundance and the no-siRNA control

Average 2^-ΔΔCt	**Average**	**SD**	**SEM**
No-siRNA control	**1.02**	0.22	0.13
***RPL19*-siRNA**	**0.31**	0.04	0.03
β2m-siRNA	**0.99**	0.30	0.18

Table S.31 shows the *HSF* transcript abundance normalised against the no-siRNA control for each biological replicate

	***HSF*/ control**
Biological rep 1	0.30
Biological rep 2	0.27
Biological rep 3	0.35

v. *An. funestus* males treated with HSF-siRNA (30 ng/µl) at 20°C (Fig 26A)

Table S.32 shows cycle threshold (Ct) values produced during a QPCR for reference genes *RPS7* and *GAPDH* (A) as well as the gene of interest, *HSF* (B)

Table S.32A

	RPS7			*GAPDH*			
Sample	**Ct 1**	**Ct 2**	**Ct 3**	**Ct 1**	**Ct 2**	**Ct 3**	**Average Ct of both *RPS7* and *GAPDH* technical replicates**
No-siRNA control 1	35.48	35.78	34.87	36.54	36.85	37.03	36.09
No-siRNA control 2	35.91	35.27	N/A	36.71	N/A	36.55	36.11
No-siRNA control 3	36.54	35.22	35.95	36.07	36.12	N/A	35.98
***HSF*-siRNA 1**	35.36	34.60	34.61	36.78	N/A	36.64	35.60
***HSF*-siRNA 2**	35.79	N/A	35.19	37.08	N/A	36.95	36.25
***HSF*-siRNA 3**	35.12	35.79	N/A	36.33	36.51	36.45	36.04
***β2m-siRNA* 1**	35.48	35.26	36.22	35.84	35.22	35.19	35.54
***β2m-siRNA* 2**	34.65	35.50	35.29	35.61	35.28	35.74	35.43
***β2m-siRNA* 3**	35.00	35.48	35.12	35.94	35.67	35.84	35.51

Numerical value (1,2,3) in rows and columns: indicate biological replicates and technical replicates respectively. N/A indicates no Ct value.

Table S.32B

	HSF						
Sample	**Ct 1**	**Ct 2**	**Ct 3**	**Average Ct**	**ΔCt**	**ΔΔCt**	**2^-ΔΔCt**
No-siRNA control 1	35.84	36.04	36.89	36.26	0.17	-0.26	1.20
No-siRNA control 2	37.02	37.00	36.75	36.92	0.81	0.39	0.76
No-siRNA control 3	35.37	36.29	37.16	36.27	0.29	-0.13	1.09
***HSF*-siRNA 1**	37.11	36.99	37.24	37.11	1.52	1.09	0.47
***HSF*-siRNA 2**	37.89	37.61	37.33	37.61	1.36	0.93	0.52
***HSF*-siRNA 3**	37.51	37.89	37.82	37.74	1.70	1.28	0.41
***β2m-siRNA* 1**	35.04	35.07	37.25	35.79	0.25	-0.17	1.13
***β2m-siRNA* 2**	34.26	35.68	35.92	35.29	-0.14	-0.56	1.48
***β2m-siRNA* 3**	35.77	37.11	37.47	36.78	1.28	0.85	0.55

Numerical value (1,2,3) in rows and columns: indicate biological replicates and technical replicates respectively. N/A indicates no Ct value.

Table S.33 shows the average 2^-ΔΔCt, standard deviation (SD) and standard error of the mean (SEM) values of the *HSF* transcript abundance and the no-siRNA control

Average 2^-ΔΔCt	Average	SD	SEM
No-siRNA control	**1.02**	0.23	0.13
***RPL19*-siRNA**	**0.47**	0.06	0.03
β2m-siRNA	**0.70**	0.35	0.20

Table S.34 shows the *HSF* transcript abundance normalised against the no-siRNA control for each biological replicate

	***HSF*/ control**
Biological rep 1	0.39
Biological rep 2	0.69
Biological rep 3	0.38

vi. *An. funestus* females treated with HSF-siRNA (30 ng/µl) at 20°C (Fig 26B)

Table S.35 shows cycle threshold (Ct) values produced during a QPCR for reference genes *RPS7* and *GAPDH* (A) as well as the gene of interest, *HSF* (B)

Table S.35A

	RPS7			***GAPDH***			
Sample	**Ct 1**	**Ct 2**	**Ct 3**	**Ct 1**	**Ct 2**	**Ct 3**	**Average Ct of both *RPS7* and *GAPDH* technical replicates**
No-siRNA control 1	31.09	31.14	31.16	33.08	33.29	33.52	32.21
No-siRNA control 2	31.78	31.87	31.45	33.30	33.33	33.03	32.46
No-siRNA control 3	31.22	N/A	31.18	33.43	33.34	33.37	32.51
***HSF*-siRNA 1**	27.08	27.02	26.19	31.03	30.01	31.26	28.77
***HSF*-siRNA 2**	26.86	27.09	26.61	30.28	30.06	29.95	28.48
***HSF*-siRNA 3**	26.26	26.80	26.88	29.95	29.93	29.96	28.30
***β2m-siRNA* 1**	33.01	32.02	32.60	33.42	33.26	33.38	32.95
***β2m-siRNA* 2**	32.70	32.80	33.27	33.17	33.14	33.46	33.17
***β2m-siRNA* 3**	32.59	32.25	33.09	35.12	33.50	33.00	33.26

Numerical value (1,2,3) in rows and columns: indicate biological replicates and technical replicates respectively. N/A indicates no Ct value.

Table S.35B

	HSF						
Sample	**Ct 1**	**Ct 2**	**Ct 3**	**Average Ct**	**ΔCt**	**ΔΔCt**	**2^-ΔΔCt**
No-siRNA control 1	33.30	33.16	33.48	33.31	1.10	0.07	0.95
No-siRNA control 2	33.22	33.41	33.04	33.22	0.76	-0.26	1.20
No-siRNA control 3	34.27	32.49	34.40	33.72	1.21	0.19	0.88
***HSF*-siRNA 1**	33.24	32.82	32.03	32.70	3.93	2.91	0.13
***HSF*-siRNA 2**	32.61	32.73	32.06	32.47	3.99	2.97	0.13
***HSF*-siRNA 3**	33.13	31.94	31.44	32.17	3.87	2.85	0.14
***β2m-siRNA* 1**	34.23	34.61	34.03	34.29	1.34	0.32	0.80
***β2m-siRNA* 2**	34.25	34.23	34.65	34.38	1.20	0.18	0.88
***β2m-siRNA* 3**	34.20	34.12	34.55	34.29	1.03	0.01	1.00

Numerical value (1,2,3) in rows and columns: indicate biological replicates and technical replicates respectively. N/A indicates no Ct value.

Table S.36 shows the average 2^-ΔΔCt, standard deviation (SD) and standard error of the mean (SEM) values of the *HSF* transcript abundance and the no-siRNA control

Average 2^-ΔΔCt	**Average**	**SD**	**SEM**
No-siRNA control	**1.01**	0.17	0.10
***RPL19*-siRNA**	**0.13**	0.01	0.003
β2m-siRNA	**0.89**	0.10	0.06

Table S.37 shows the *HSF* transcript abundance normalised against the no-siRNA control for each biological replicate

	***HSF*/ control**
Biological rep 1	0.14
Biological rep 2	0.11
Biological rep 3	0.16

vii. *An. funestus* males treated with HSF-siRNA (10 ng/µl) at 25°C (Fig 27A)

Table S.38 shows cycle threshold (Ct) values produced during a QPCR for reference genes *RPS7* and *GAPDH* (A) as well as the gene of interest, *HSF* (B)

Table S.38A

	RPS7			*GAPDH*			
Sample	**Ct 1**	**Ct 2**	**Ct 3**	**Ct 1**	**Ct 2**	**Ct 3**	**Average Ct of both *RPS7* and *GAPDH* technical replicates**
No-siRNA control 1	29.25	29.49	29.79	32.23	31.88	32.05	30.78
No-siRNA control 2	29.85	30.11	30.69	31.12	31.10	30.79	30.61
No-siRNA control 3	30.24	30.57	N/A	31.00	31.34	30.53	30.74
***HSF*-siRNA 1**	28.44	28.24	28.22	30.83	31.14	31.30	29.70
***HSF*-siRNA 2**	29.65	29.28	28.48	30.05	30.81	N/A	29.65
***HSF*-siRNA 3**	29.28	29.06	29.41	29.25	30.12	30.20	29.55
***β2m-siRNA* 1**	28.52	28.81	28.62	28.49	28.12	28.61	28.53
***β2m-siRNA* 2**	27.95	27.89	28.01	28.54	28.90	28.67	28.33
***β2m-siRNA* 3**	27.58	27.89	27.77	28.33	28.12	28.69	28.06

Numerical value (1,2,3) in rows and columns: indicate biological replicates and technical replicates respectively.

Table S.38B

	HSF						
Sample	**Ct 1**	**Ct 2**	**Ct 3**	**Average Ct**	**ΔCt**	**ΔΔCt**	**2^-ΔΔCt**
No-siRNA control 1	32.15	32.52	32.98	32.34	1.55	-0.59	1.50
No-siRNA control 2	33.23	33.16	33.02	33.14	2.53	0.39	0.77
No-siRNA control 3	33.09	33.00	33.15	33.08	2.34	0.20	0.87
***HSF*-siRNA 1**	33.26	33.54	33.61	33.47	3.78	1.63	0.32
***HSF*-siRNA 2**	33.21	33.25	33.33	33.26	3.61	1.47	0.36
***HSF*-siRNA 3**	33.62	33.51	33.98	33.70	4.15	2.01	0.25
***β2m-siRNA* 1**	30.07	30.51	30.03	30.20	1.68	-0.47	1.38
***β2m-siRNA* 2**	30.93	30.58	30.73	30.75	2.42	0.28	0.82
***β2m-siRNA* 3**	30.91	30.55	30.10	30.52	2.46	0.32	0.80

Numerical value (1,2,3) in rows and columns: indicate biological replicates and technical replicates respectively.

Table S.39 shows the average 2^-ΔΔCt, standard deviation (SD) and standard error of the mean (SEM) values of the *HSF* transcript abundance and the no-siRNA control

Average 2^-ΔΔCt	Average	SD	SEM
No-siRNA control	**1.05**	0.40	0.23
***RPL19*-siRNA**	**0.31**	0.06	0.03
β2m-siRNA	**1.00**	0.33	0.19

Table S.40 shows the *HSF* transcript abundance normalised against the no-siRNA control for each biological replicate

	***HSFl* control**
Biological rep 1	0.21
Biological rep 2	0.47
Biological rep 3	0.29

viii. *An. funestus* females treated with HSF-siRNA (10 ng/µl) at 25°C (Fig 27B)

Table S.41 shows cycle threshold (Ct) values produced during a QPCR for reference genes *RPS7* and *GAPDH* (A) as well as the gene of interest, *HSF* (B)

Table S.41A

	RPS7			***GAPDH***			
Sample	**Ct 1**	**Ct 2**	**Ct 3**	**Ct 1**	**Ct 2**	**Ct 3**	**Average Ct of both *RPS7* and *GAPDH* technical replicates**
No-siRNA control 1	26.58	26.21	26.38	30.25	30.08	29.59	28.18
No-siRNA control 2	26.40	26.55	26.02	28.80	28.98	28.07	27.47
No-siRNA control 3	26.35	25.74	26.37	28.27	28.83	N/A	27.11
***HSF*-siRNA 1**	27.08	27.42	26.44	32.68	33.08	32.87	29.93
***HSF*-siRNA 2**	26.97	27.54	26.77	32.36	32.34	32.59	29.76
***HSF*-siRNA 3**	27.39	26.65	27.72	32.33	32.51	32.68	29.88
***β2m-siRNA* 1**	25.47	25.20	25.69	28.06	28.10	28.17	26.78
***β2m-siRNA* 2**	26.05	25.31	26.02	28.06	28.14	28.34	27.12
***β2m-siRNA* 3**	25.83	25.75	26.26	28.41	28.61	28.71	27.26

Numerical value (1,2,3) in rows and columns: indicate biological replicates and technical replicates respectively. N/A indicates no Ct value.

Table S.41B

	HSF						
Sample	**Ct 1**	**Ct 2**	**Ct 3**	**Average Ct**	**ΔCt**	**ΔΔCt**	**2^-ΔΔCt**
No-siRNA control 1	31.15	31.52	30.98	31.22	3.04	-0.28	1.21
No-siRNA control 2	30.56	30.48	31.03	30.69	3.22	-0.10	1.07
No-siRNA control 3	30.74	30.74	30.93	30.80	3.69	0.38	0.77
***HSF*-siRNA 1**	34.68	34.08	34.87	34.54	4.62	1.30	0.41
***HSF*-siRNA 2**	34.36	34.24	34.29	34.30	4.53	1.22	0.43
***HSF*-siRNA 3**	34.20	34.11	34.05	34.12	4.24	0.92	0.53
***β2m-siRNA* 1**	30.76	30.22	30.66	30.55	3.77	0.45	0.73
***β2m-siRNA* 2**	30.29	30.74	30.10	30.38	3.25	-0.06	1.04
***β2m-siRNA* 3**	30.14	30.22	30.45	30.27	3.01	-0.31	1.24

Numerical value (1,2,3) in rows and columns: indicate biological replicates and technical replicates respectively. N/A indicates no Ct value.

Table S.42 shows the average 2^-ΔΔCt, standard deviation (SD) and standard error of the mean (SEM) values of the *HSF* transcript abundance and the no-siRNA control

Average 2^-ΔΔCt	**Average**	**SD**	**SEM**
No-siRNA control	**1.02**	0.23	0.13
***RPL19*-siRNA**	**0.45**	0.06	0.04
β2m-siRNA	**1.00**	0.25	0.15

Table S.43 shows the *HSF* transcript abundance normalised against the no-siRNA control for each biological replicate

	***HSF*/ control**
Biological rep 1	0.33
Biological rep 2	0.40
Biological rep 3	0.68

ix. *An. funestus* males treated with HSF-siRNA (20 ng/µl) at 25°C (Fig 28A)

Table S.44 shows cycle threshold (Ct) values produced during a QPCR for reference genes *RPS7* and *GAPDH* (A) as well as the gene of interest, *HSF* (B)

Table S.44A

	RPS7			*GAPDH*			
Sample	**Ct 1**	**Ct 2**	**Ct 3**	**Ct 1**	**Ct 2**	**Ct 3**	**Average Ct of both *RPS7* and *GAPDH* technical replicates**
No-siRNA control 1	30.13	30.52	29.74	30.90	30.43	30.51	30.37
No-siRNA control 2	29.19	29.88	30.27	30.61	31.06	30.05	30.18
No-siRNA control 3	30.16	30.71	30.45	31.41	31.48	31.25	30.91
***HSF*-siRNA 1**	33.58	33.69	33.57	33.16	33.02	32.96	33.33
***HSF*-siRNA 2**	33.51	33.97	33.54	33.44	33.61	N/A	33.61
***HSF*-siRNA 3**	33.98	33.41	33.87	34.02	N/A	33.55	33.77
***β2m-siRNA* 1**	29.17	29.48	28.53	29.22	29.60	29.41	29.24
***β2m-siRNA* 2**	28.98	28.58	N/A	28.51	28.34	28.75	29.12
***β2m-siRNA* 3**	29.25	29.41	28.98	30.22	30.18	N/A	29.61

Numerical value (1,2,3) in rows and columns: indicate biological replicates and technical replicates respectively. N/A indicates no Ct value.

Table S.44B

	HSF						
Sample	**Ct 1**	**Ct 2**	**Ct 3**	**Average Ct**	**ΔCt**	**ΔΔCt**	**2^-ΔΔCt**
No-siRNA control 1	34.67	34.03	33.72	34.14	3.77	0.29	0.82
No-siRNA control 2	33.43	34.24	33.84	33.84	3.66	0.18	0.88
No-siRNA control 3	33.92	33.67	34.14	33.91	3.00	-0.48	1.39
***HSF*-siRNA 1**	37.46	N/A	37.59	37.53	4.20	0.72	0.61
***HSF*-siRNA 2**	37.43	37.84	38.46	37.91	4.30	0.82	0.57
***HSF*-siRNA 3**	38.20	N/A	37.76	37.98	4.21	0.74	0.60
***β2m-siRNA* 1**	32.96	32.85	32.97	32.93	3.69	0.22	0.86
***β2m-siRNA* 2**	32.33	32.19	32.61	32.38	3.26	-0.22	1.16
***β2m-siRNA* 3**	32.61	32.58	32.94	32.71	3.10	-0.37	1.30

Numerical value (1,2,3) in rows and columns: indicate biological replicates and technical replicates respectively. N/A indicates no Ct value.

Table S.45 shows the average 2^-ΔΔCt, standard deviation (SD) and standard error of the mean (SEM) values of the *HSF* transcript abundance and the no-siRNA control

Average 2^-ΔΔCt	Average	SD	SEM
No-siRNA control	**1.03**	0.31	0.18
***RPL19*-siRNA**	**0.59**	0.02	0.01
β2m-siRNA	**1.11**	0.22	0.13

Table S.46 shows the *HSF* transcript abundance normalised against the no-siRNA control for each biological replicate

	***HSF*/ control**
Biological rep 1	0.74
Biological rep 2	0.64
Biological rep 3	0.43

x. *An. funestus* females treated with HSF-siRNA (20 ng/µl) at 25°C (Fig 28B)

Table S.47 shows cycle threshold (Ct) values produced during a QPCR for reference genes *RPS7* and *GAPDH* (A) as well as the gene of interest, *HSF* (B)

Table S.47A

	RPS7			***GAPDH***			
Sample	**Ct 1**	**Ct 2**	**Ct 3**	**Ct 1**	**Ct 2**	**Ct 3**	**Average Ct of both *RPS7* and *GAPDH* technical replicates**
No-siRNA control 1	27.84	27.61	27.59	28.64	28.57	27.87	28.02
No-siRNA control 2	27.31	27.92	27.62	28.95	28.96	28.65	28.24
No-siRNA control 3	27.31	27.69	27.33	28.80	29.51	29.70	28.39
***HSF*-siRNA 1**	28.27	28.86	28.09	28.95	28.96	28.65	28.63
***HSF*-siRNA 2**	28.24	28.33	28.25	28.94	28.61	28.35	28.45
***HSF*-siRNA 3**	29.71	29.76	29.81	28.99	28.87	28.95	29.35
***β2m-siRNA* 1**	27.88	28.06	27.54	27.45	27.96	27.81	27.72
***β2m-siRNA* 2**	27.43	28.03	27.97	27.51	27.51	27.51	27.66
***β2m-siRNA* 3**	27.81	27.79	27.43	27.65	27.98	27.32	27.66

Numerical value (1,2,3) in rows and columns: indicate biological replicates and technical replicates respectively. N/A indicates no Ct value.

Table S.47B

	HSF						
Sample	**Ct 1**	**Ct 2**	**Ct 3**	**Average Ct**	**ΔCt**	**ΔΔCt**	**2^-ΔΔCt**
No-siRNA control 1	30.22	30.93	31.40	30.85	2.83	-0.02	1.01
No-siRNA control 2	30.19	30.87	N/A	30.53	2.30	-0.56	1.47
No-siRNA control 3	31.44	31.95	32.06	31.82	3.43	0.58	0.67
***HSF*-siRNA 1**	32.25	31.24	32.91	32.13	3.50	0.65	0.64
***HSF*-siRNA 2**	31.71	32.49	32.88	32.36	3.91	1.06	0.48
***HSF*-siRNA 3**	34.68	34.52	34.83	34.68	5.33	2.48	0.18
***β2m-siRNA* 1**	31.03	30.40	30.52	30.65	2.93	0.08	0.95
***β2m-siRNA* 2**	30.69	30.32	30.73	30.58	2.92	0.07	0.95
***β2m-siRNA* 3**	30.91	30.16	30.75	30.61	2.94	0.09	0.94

Numerical value (1,2,3) in rows and columns: indicate biological replicates and technical replicates respectively. N/A indicates no Ct value.

Table S.48 shows the average 2^-ΔΔCt, standard deviation (SD) and standard error of the mean (SEM) values of the *HSF* transcript abundance and the no-siRNA control

Average 2^-ΔΔCt	**Average**	**SD**	**SEM**
No-siRNA control	**1.05**	0.40	0.23
***RPL19*-siRNA**	**0.43**	0.23	0.13
β2m-siRNA	**0.95**	0.01	0.004

Table S.49 shows the *HSF* transcript abundance normalised against the no-siRNA control for each biological replicate

	***HSF*/ control**
Biological rep 1	0.63
Biological rep 2	0.33
Biological rep 3	0.27

xi. *An. funestus* males treated with HSF-siRNA (30 ng/µl) at 25°C (Fig 29A)

Table S.50 shows cycle threshold (Ct) values produced during a QPCR for reference genes *RPS7* and *GAPDH* (A) as well as the gene of interest, *HSF* (B)

Table S.50A

	RPS7			*GAPDH*			
Sample	**Ct 1**	**Ct 2**	**Ct 3**	**Ct 1**	**Ct 2**	**Ct 3**	**Average Ct of both *RPS7* and *GAPDH* technical replicates**
No-siRNA control 1	31.47	31.16	30.89	31.20	31.02	31.05	31.13
No-siRNA control 2	30.01	30.54	29.65	30.50	30.54	30.68	30.32
No-siRNA control 3	31.36	31.38	30.85	30.13	30.05	30.11	30.65
***HSF*-siRNA 1**	32.59	32.54	31.94	31.38	31.97	32.71	32.19
***HSF*-siRNA 2**	32.05	32.12	32.54	32.01	32.47	32.22	32.24
***HSF*-siRNA 3**	33.02	33.19	32.67	31.70	31.84	32.50	32.49
***β2m-siRNA* 1**	29.60	29.60	29.21	29.50	29.51	29.60	29.19
***β2m-siRNA* 2**	28.49	28.26	28.04	29.65	29.41	29.35	28.87
***β2m-siRNA* 3**	29.58	29.48	29.60	29.31	29.01	29.02	29.33

Numerical value (1,2,3) in rows and columns: indicate biological replicates and technical replicates respectively. N/A indictaes no Ct value.

Table S.50B

	HSF						
Sample	**Ct 1**	**Ct 2**	**Ct 3**	**Average Ct**	**ΔCt**	**ΔΔCt**	**2^-ΔΔCt**
No-siRNA control 1	35.53	35.43	35.04	35.33	4.20	-0.42	1.33
No-siRNA control 2	35.17	35.29	N/A	35.23	4.91	0.29	0.82
No-siRNA control 3	35.29	35.08	35.79	35.39	4.74	0.12	0.92
***HSF*-siRNA 1**	37.87	38.01	37.49	37.79	5.60	0.98	0.51
***HSF*-siRNA 2**	37.29	37.62	37.68	37.53	5.30	0.68	0.63
***HSF*-siRNA 3**	37.50	37.44	37.61	37.52	5.03	0.41	0.75
***β2m-siRNA* 1**	33.50	33.54	33.60	33.55	4.36	-0.26	1.19
***β2m-siRNA* 2**	33.25	33.58	33.62	33.48	4.62	0.00	1.00
***β2m-siRNA* 3**	34.21	34.02	34.15	34.13	4.79	0.18	0.88

Numerical value (1,2,3) in rows and columns: indicate biological replicates and technical replicates respectively. N/A indictaes no Ct value.

Table S.51 shows the average 2^-ΔΔCt, standard deviation (SD) and standard error of the mean (SEM) values of the *HSF* transcript abundance and the no-siRNA control

Average 2^-ΔΔCt	Average	SD	SEM
No-siRNA control	**1.02**	0.27	0.16
***RPL19*-siRNA**	**0.63**	0.12	0.07
β2m-siRNA	**1.03**	0.16	0.09

Table S.52 shows the *HSF* transcript abundance normalised against the no-siRNA control for each biological replicate

	***HSFl* control**
Biological rep 1	0.38
Biological rep 2	0.77
Biological rep 3	0.82

xii. *An. funestus* females treated with HSF-siRNA (30 ng/µl) at 25°C (Fig 29B)

Table S.53 shows cycle threshold (Ct) values produced during a QPCR for reference genes *RPS7* and *GAPDH* (A) as well as the gene of interest, *HSF* (B)

Table S.53A

	RPS7			*GAPDH*			
Sample	**Ct 1**	**Ct 2**	**Ct 3**	**Ct 1**	**Ct 2**	**Ct 3**	**Average Ct of both *RPS7* and *GAPDH* technical replicates**
No-siRNA control 1	26.52	26.76	26.50	28.83	28.24	28.03	27.48
No-siRNA control 2	26.41	26.45	26.24	29.37	29.18	N/A	27.53
No-siRNA control 3	27.80	27.66	27.84	29.25	29.42	29.46	28.57
***HSF*-siRNA 1**	25.99	26.10	26.02	28.99	28.99	29.16	27.54
***HSF*-siRNA 2**	26.18	26.04	25.73	28.35	28.97	28.33	27.27
***HSF*-siRNA 3**	26.07	26.58	26.64	28.53	28.57	28.51	27.48
***β2m-siRNA* 1**	27.18	27.04	27.35	28.60	28.53	28.47	27.74
***β2m-siRNA* 2**	26.13	26.17	26.78	28.97	28.88	28.79	27.62
***β2m-siRNA* 3**	27.15	27.13	27.25	28.70	28.59	28.62	27.91

Numerical value (1,2,3) in rows and columns: indicate biological replicates and technical replicates respectively. N/A indicates no Ct value.

Table S.53B

	HSF						
Sample	**Ct 1**	**Ct 2**	**Ct 3**	**Average Ct**	**ΔCt**	**ΔΔCt**	**2^-ΔΔCt**
No-siRNA control 1	31.93	32.73	32.64	32.43	4.95	0.53	0.69
No-siRNA control 2	31.24	31.69	32.98	31.97	4.44	0.02	0.99
No-siRNA control 3	32.35	32.33	32.64	32.44	3.87	-0.55	1.47
***HSF*-siRNA 1**	32.05	32.14	32.51	32.23	4.69	0.27	0.83
***HSF*-siRNA 2**	32.55	32.14	32.33	32.34	5.07	0.65	0.64
***HSF*-siRNA 3**	32.22	32.20	32.16	32.19	4.71	0.29	0.82
***β2m-siRNA* 1**	32.04	32.94	32.45	32.48	4.74	0.32	0.80
***β2m-siRNA* 2**	32.33	32.31	32.73	32.46	4.84	0.42	0.75
***β2m-siRNA* 3**	32.02	32.19	31.56	31.92	4.02	-0.40	1.32

Numerical value (1,2,3) in rows and columns: indicate biological replicates and technical replicates respectively. N/A indicates no Ct value.

Table S.54 shows the average 2^-ΔΔCt, standard deviation (SD) and standard error of the mean (SEM) values of the *HSF* transcript abundance and the no-siRNA control

Average 2^-ΔΔCt	Average	SD	SEM
No-siRNA control	**1.05**	0.39	0.23
***RPL19*-siRNA**	**0.76**	0.11	0.06
β2m-siRNA	**0.96**	0.32	0.18

Table S.55 shows the *HSF* transcript abundance normalised against the no-siRNA control for each biological replicate

	***HSFl* control**
Biological rep 1	1.20
Biological rep 2	0.64
Biological rep 3	0.56

xiii. *An. funestus* males treated with HSF-siRNA (10 ng/µl) at 30°C (Fig 30A)

Table S.56 shows cycle threshold (Ct) values produced during a QPCR for reference genes *RPS7* and *GAPDH* (A) as well as the gene of interest, *HSF* (B)

Table S.56A

	RPS7			***GAPDH***			
Sample	**Ct 1**	**Ct 2**	**Ct 3**	**Ct 1**	**Ct 2**	**Ct 3**	**Average Ct of both *RPS7* and *GAPDH* technical replicates**
No-siRNA control 1	28.57	28.54	28.77	28.05	28.32	28.22	28.41
No-siRNA control 2	29.18	29.18	29.10	28.92	28.07	N/A	28.89
No-siRNA control 3	29.07	29.18	29.23	28.45	28.62	28.65	28.87
***HSF*-siRNA 1**	27.97	27.98	28.09	28.06	28.48	28.49	28.18
***HSF*-siRNA 2**	28.46	28.03	28.65	29.13	29.12	29.31	28.78
***HSF*-siRNA 3**	29.33	29.56	29.19	29.34	29.66	29.96	29.51
***β2m-siRNA* 1**	30.12	30.60	31.12	30.75	30.78	30.82	31.10
***β2m-siRNA* 2**	32.00	32.59	32.00	30.88	30.69	30.87	31.51
***β2m-siRNA* 3**	31.86	31.87	32.59	30.99	30.96	30.89	31.53

Numerical value (1,2,3) in rows and columns: indicate biological replicates and technical replicates respectively. N/A indicates no Ct value.

Table S.56B

	HSF						
Sample	**Ct 1**	**Ct 2**	**Ct 3**	**Average Ct**	**ΔCt**	**ΔΔCt**	**2^-ΔΔCt**
No-siRNA control 1	33.15	33.89	32.65	33.23	4.82	0.58	0.67
No-siRNA control 2	32.52	33.13	33.00	32.88	3.99	-0.25	1.19
No-siRNA control 3	33.00	33.15	32.19	32.78	3.91	-0.33	1.26
***HSF*-siRNA 1**	34.52	34.92	32.94	34.13	5.95	1.71	0.31
***HSF*-siRNA 2**	34.25	34.10	33.87	34.07	5.29	1.05	0.48
***HSF*-siRNA 3**	33.98	34.02	34.10	34.03	4.53	0.28	0.82
***β2m-siRNA* 1**	36.22	36.51	36.99	36.57	5.47	1.23	0.43
***β2m-siRNA* 2**	35.22	35.78	35.11	35.37	3.87	-0.38	1.30
***β2m-siRNA* 3**	35.22	35.26	35.50	35.33	3.80	-0.44	1.36

Numerical value (1,2,3) in rows and columns: indicate biological replicates and technical replicates respectively. N/A indicates no Ct value.

Table S.57 shows the average 2^-ΔΔCt, standard deviation (SD) and standard error of the mean (SEM) values of the *HSF* transcript abundance and the no-siRNA control

Average 2^-ΔΔCt	**Average**	**SD**	**SEM**
No-siRNA control	**1.04**	0.32	0.18
***RPL19*-siRNA**	**0.54**	0.26	0.15
β2m-siRNA	**1.03**	0.52	0.30

Table S.58 shows the *HSF* transcript abundance normalised against the no-siRNA control for each biological replicate

	***HSF*/ control**
Biological rep 1	0.46
Biological rep 2	0.41
Biological rep 3	0.65

xiv. *An. funestus* females treated with HSF-siRNA (10 ng/µl) at 30°C (Fig 30B)

Table S.59 shows cycle threshold (Ct) values produced during a qPCR for reference genes *RPS7* and *GAPDH* (A) as well as the gene of interest, *HSF* (B)

Table S.59A

	RPS7			*GAPDH*			
Sample	**Ct 1**	**Ct 2**	**Ct 3**	**Ct 1**	**Ct 2**	**Ct 3**	**Average Ct of both *RPS7* and *GAPDH* technical replicates**
No-siRNA control 1	26.96	26.16	26.82	28.65	28.74	28.56	27.65
No-siRNA control 2	26.80	26.89	26.66	28.68	28.83	28.24	27.68
No-siRNA control 3	26.61	26.27	26.64	28.22	28.24	28.12	27.35
***HSF*-siRNA 1**	26.07	26.21	26.59	29.32	29.15	29.42	27.79
***HSF*-siRNA 2**	27.41	27.32	26.61	29.40	29.34	29.64	28.29
***HSF*-siRNA 3**	26.83	26.88	26.97	29.00	29.29	29.92	28.15
***β2m-siRNA* 1**	25.03	25.20	25.00	27.66	27.31	27.04	26.93
***β2m-siRNA* 2**	27.19	27.87	27.75	27.63	27.54	27.98	27.66
***β2m-siRNA* 3**	27.03	27.15	27.09	27.95	27.84	27.61	27.45

Numerical value (1,2,3) in rows and columns: indicate biological replicates and technical replicates respectively.

Table S.59B

	HSF						
Sample	**Ct 1**	**Ct 2**	**Ct 3**	**Average Ct**	**ΔCt**	**ΔΔCt**	**2^-ΔΔCt**
No-siRNA control 1	32.94	32.96	32.35	32.75	5.10	0.18	0.88
No-siRNA control 2	32.22	32.13	32.08	32.14	4.46	-0.46	1.38
No-siRNA control 3	32.90	32.76	32.00	32.55	5.20	0.28	0.82
***HSF*-siRNA 1**	34.12	34.06	34.04	34.07	6.28	1.36	0.39
***HSF*-siRNA 2**	34.19	34.10	34.14	34.14	5.86	0.93	0.52
***HSF*-siRNA 3**	34.00	34.09	34.24	34.11	5.96	1.04	0.49
***β2m-siRNA* 1**	31.48	31.49	30.73	31.23	4.30	-0.62	1.54
***β2m-siRNA* 2**	33.16	33.51	32.61	33.09	5.43	0.51	0.70
***β2m-siRNA* 3**	32.26	32.33	31.19	31.93	4.48	-0.44	1.36

Numerical value (1,2,3) in rows and columns: indicate biological replicates and technical replicates respectively.

Table S.60 shows the average 2^-ΔΔCt, standard deviation (SD) and standard error of the mean (SEM) values of the *HSF* transcript abundance and the no-siRNA control

Average 2^-ΔΔCt	Average	SD	SEM
No-siRNA control	**1.03**	0.30	0.18
***RPL19*-siRNA**	**0.47**	0.07	0.04
β2m-siRNA	**1.20**	0.44	0.25

Table S.61 shows the *HSF* transcript abundance normalised against the no-siRNA control for each biological replicate

	***HSFl* control**
Biological rep 1	0.44
Biological rep 2	0.38
Biological rep 3	0.59

xv. *An. funestus* males treated with HSF-siRNA (20 ng/µl) at 30°C (Fig 31A)

Table S.62 shows cycle threshold (Ct) values produced during a QPCR for reference genes *RPS7* and *GAPDH* (A) as well as the gene of interest, *HSF* (B)

Table S.62A

	RPS7			***GAPDH***			
Sample	**Ct 1**	**Ct 2**	**Ct 3**	**Ct 1**	**Ct 2**	**Ct 3**	**Average Ct of both *RPS7* and *GAPDH* technical replicates**
No-siRNA control 1	28.47	28.65	28.84	28.33	28.44	28.68	28.57
No-siRNA control 2	28.25	28.39	28.41	28.99	28.95	28.23	28.54
No-siRNA control 3	28.67	28.37	28.56	28.59	28.93	28.94	28.68
***HSF*-siRNA 1**	26.47	26.55	27.57	27.33	27.85	27.91	27.28
***HSF*-siRNA 2**	26.66	26.87	26.78	27.55	27.53	27.49	27.15
***HSF*-siRNA 3**	26.82	26.59	26.93	27.52	27.41	27.20	27.08
***β2m-siRNA* 1**	31.39	31.34	31.16	32.13	32.39	31.61	31.38
***β2m-siRNA* 2**	30.16	30.12	30.32	31.84	31.92	32.13	31.08
***β2m-siRNA* 3**	30.86	30.00	30.29	30.70	30.00	30.79	30.44

Numerical value (1,2,3) in rows and columns: indicate biological replicates and technical replicates respectively.

Table S.62B

	HSF						
Sample	**Ct 1**	**Ct 2**	**Ct 3**	**Average Ct**	**ΔCt**	**ΔΔCt**	**2^-ΔΔCt**
No-siRNA control 1	32.45	32.26	33.20	32.64	4.07	-0.07	1.05
No-siRNA control 2	32.51	32.71	32.13	32.45	3.91	-0.22	1.17
No-siRNA control 3	32.98	33.09	33.24	33.10	4.43	0.29	0.82
***HSF*-siRNA 1**	32.05	32.32	32.44	32.27	4.99	0.85	0.55
***HSF*-siRNA 2**	32.01	32.05	32.19	32.08	4.94	0.80	0.57
***HSF*-siRNA 3**	32.11	32.34	32.68	32.38	5.30	1.16	0.45
***β2m-siRNA* 1**	35.21	35.26	35.14	35.20	3.83	-0.31	1.24
***β2m-siRNA* 2**	35.00	35.11	35.02	35.04	3.96	-0.17	1.13
***β2m-siRNA* 3**	35.22	35.03	35.18	35.14	4.70	0.57	0.67

Numerical value (1,2,3) in rows and columns: indicate biological replicates and technical replicates respectively.

Table S.63 shows the average 2^-ΔΔCt, standard deviation (SD) and standard error of the mean (SEM) values of the *HSF* transcript abundance and the no-siRNA control

Average 2^-ΔΔCt	**Average**	**SD**	**SEM**
No-siRNA control	**1.01**	0.18	0.10
***RPL19*-siRNA**	**0.52**	0.07	0.03
β2m-siRNA	**1.01**	0.30	0.17

Table S.64 shows the *HSF* transcript abundance normalised against the no-siRNA control for each biological replicate

	***HSF*/ control**
Biological rep 1	0.53
Biological rep 2	0.49
Biological rep 3	0.55

xvi. *An. funestus* females treated with HSF-siRNA (20 ng/µl) at 30°C (Fig 31B)

Table S.65 shows cycle threshold (Ct) values produced during a QPCR for reference genes *RPS7* and *GAPDH* (A) as well as the gene of interest, *HSF* (B)

Table S.65A

	RPS7			*GAPDH*			
Sample	**Ct 1**	**Ct 2**	**Ct 3**	**Ct 1**	**Ct 2**	**Ct 3**	**Average Ct of both *RPS7* and *GAPDH* technical replicates**
No-siRNA control 1	27.55	27.15	26.87	28.32	28.20	28.66	27.79
No-siRNA control 2	26.23	26.13	26.84	28.29	29.75	29.07	27.72
No-siRNA control 3	26.06	26.85	26.77	28.71	28.54	28.97	27.65
***HSF*-siRNA 1**	25.18	25.11	24.77	27.35	27.21	27.00	26.10
***HSF*-siRNA 2**	24.53	24.10	24.24	27.45	27.23	27.61	25.86
***HSF*-siRNA 3**	24.59	24.73	24.66	27.59	27.44	27.78	26.13
***β2m-siRNA* 1**	28.31	28.63	28.10	30.67	30.44	30.85	29.51
***β2m-siRNA* 2**	28.21	28.36	28.85	30.96	30.25	30.50	29.52
***β2m-siRNA* 3**	28.02	28.00	28.44	30.04	30.07	30.14	29.12

Numerical value (1,2,3) in rows and columns: indicate biological replicates and technical replicates respectively.

Table S.65B

	HSF						
Sample	**Ct 1**	**Ct 2**	**Ct 3**	**Average Ct**	**ΔCt**	**ΔΔCt**	**2^-ΔΔCt**
No-siRNA control 1	31.22	31.43	32.08	31.58	3.79	-0.50	1.41
No-siRNA control 2	31.22	32.54	32.42	32.06	4.34	0.06	0.96
No-siRNA control 3	32.07	32.71	32.34	32.37	4.72	0.44	0.74
***HSF*-siRNA 1**	31.33	31.36	31.88	31.52	5.42	1.14	0.45
***HSF*-siRNA 2**	31.90	31.29	31.84	31.68	5.82	1.53	0.35
***HSF*-siRNA 3**	31.64	31.76	32.50	31.97	5.84	1.55	0.34
***β2m-siRNA* 1**	33.98	33.82	33.87	33.89	4.38	0.10	0.94
***β2m-siRNA* 2**	33.45	33.60	33.73	33.59	4.07	-0.21	1.16
***β2m-siRNA* 3**	33.60	33.58	33.15	33.44	4.33	0.04	0.97

Numerical value (1,2,3) in rows and columns: indicate biological replicates and technical replicates respectively.

Table S.66 shows the average 2^-ΔΔCt, standard deviation (SD) and standard error of the mean (SEM) values of the *HSF* transcript abundance and the no-siRNA control

Average 2^-ΔΔCt	Average	SD	SEM
No-siRNA control	**1.04**	0.34	0.20
***RPL19*-siRNA**	**0.38**	0.06	0.04
β2m-siRNA	**1.02**	0.12	0.07

Table S.67 shows the *HSF* transcript abundance normalised against the no-siRNA control for each biological replicate

	***HSFl* control**
Biological rep 1	0.32
Biological rep 2	0.36
Biological rep 3	0.46

xvii. *An. funestus* males treated with HSF-siRNA (30 ng/µl) at 30°C (Fig 32A)

Table S.68 shows cycle threshold (Ct) values produced during a QPCR for reference genes *RPS7* and *GAPDH* (A) as well as the gene of interest, *HSF* (B)

Table S.68A

	RPS7			*GAPDH*			
Sample	**Ct 1**	**Ct 2**	**Ct 3**	**Ct 1**	**Ct 2**	**Ct 3**	**Average Ct of both *RPS7* and *GAPDH* technical replicates**
No-siRNA control 1	29.75	29.71	29.81	29.57	29.60	29.07	29.59
No-siRNA control 2	29.92	29.35	29.50	29.24	29.41	29.43	29.48
No-siRNA control 3	29.59	29.62	29.86	29.26	29.16	29.51	29.50
***HSF*-siRNA 1**	27.35	27.27	27.56	27.01	27.00	27.15	27.22
***HSF*-siRNA 2**	27.33	27.28	27.42	27.98	27.56	27.81	27.56
***HSF*-siRNA 3**	27.53	27.40	27.54	27.12	27.14	27.05	27.30
***β2m-siRNA* 1**	31.56	31.29	31.00	31.52	31.95	31.25	31.38
***β2m-siRNA* 2**	31.33	31.50	31.54	31.12	31.22	31.25	31.33
***β2m-siRNA* 3**	31.69	31.77	31.79	31.40	31.40	31.56	31.60

Numerical value (1,2,3) in rows and columns: indicate biological replicates and technical replicates respectively. N/A indicates no Ct value.

Table S.68B

	HSF						
Sample	**Ct 1**	**Ct 2**	**Ct 3**	**Average Ct**	**ΔCt**	**ΔΔCt**	**2^-ΔΔCt**
No-siRNA control 1	34.35	34.83	34.53	34.57	4.99	0.15	0.90
No-siRNA control 2	34.00	34.11	34.41	34.17	4.70	-0.14	1.10
No-siRNA control 3	33.93	34.24	34.84	34.34	4.84	0.00	1.00
***HSF*-siRNA 1**	33.24	33.03	33.61	33.29	6.07	1.23	0.43
***HSF*-siRNA 2**	33.31	33.56	33.79	33.55	5.99	1.15	0.45
***HSF*-siRNA 3**	34.09	34.23	34.00	34.11	6.81	1.97	0.26
***β2m-siRNA* 1**	36.97	35.00	35.45	35.81	4.43	-0.41	1.33
***β2m-siRNA* 2**	36.56	36.64	36.56	36.59	5.26	0.42	0.75
***β2m-siRNA* 3**	36.56	36.64	36.56	36.59	4.99	0.14	0.90

Numerical value (1,2,3) in rows and columns: indicate biological replicates and technical replicates respectively. N/A indicates no Ct value.

Table S.69 shows the average 2^-ΔΔCt, standard deviation (SD) and standard error of the mean (SEM) values of the *HSF* transcript abundance and the no-siRNA control

Average 2^-ΔΔCt	Average	SD	SEM
No-siRNA control	**1.00**	0.10	0.06
***RPL19*-siRNA**	**0.38**	0.11	0.06
β2m-siRNA	**0.99**	0.30	0.17

Table S.70 shows the *HSF* transcript abundance normalised against the no-siRNA control for each biological replicate

	***HSF*/ control**
Biological rep 1	0.47
Biological rep 2	0.41
Biological rep 3	0.25

xviii. *An. funestus* females treated with HSF-siRNA (30 ng/µl) at 30°C (Fig 32B)

Table S.71 shows cycle threshold (Ct) values produced during a QPCR for reference genes RPS7 and GAPDH (A) as well as the gene of interest, *HSF* (B)

Table S.71A

	RPS7			***GAPDH***			
Sample	**Ct 1**	**Ct 2**	**Ct 3**	**Ct 1**	**Ct 2**	**Ct 3**	**Average Ct of both *RPS7* and *GAPDH* technical replicates**
No-siRNA control 1	26.06	26.06	26.22	28.95	28.89	28.77	27.49
No-siRNA control 2	26.98	26.88	27.06	28.83	28.06	28.03	27.64
No-siRNA control 3	26.77	27.13	27.10	28.70	28.52	28.76	27.83
HSF-siRNA 1	26.39	26.47	26.68	29.69	29.90	30.06	28.20
HSF-siRNA 2	26.98	26.88	27.06	30.27	30.10	30.06	28.56
HSF-siRNA 3	26.45	26.97	26.73	30.32	30.25	29.61	28.39
***β2m-siRNA* 1**	30.15	30.05	30.40	29.83	29.84	29.72	29.90
***β2m-siRNA* 2**	29.77	29.79	29.62	29.95	29.81	29.85	29.80
***β2m-siRNA* 3**	29.95	30.02	30.14	30.25	30.16	30.84	30.23

Numerical value (1,2,3) in rows and columns: indicate biological replicates and technical replicates respectively.

Table S.71B

	HSF						
Sample	**Ct 1**	**Ct 2**	**Ct 3**	**Average Ct**	**ΔCt**	**ΔΔCt**	**2^-ΔΔCt**
No-siRNA control 1	32.10	32.40	32.30	32.27	4.78	0.11	0.93
No-siRNA control 2	32.07	32.26	32.93	32.42	4.78	0.11	0.92
No-siRNA control 3	32.21	32.24	32.37	32.27	4.44	-0.22	1.17
***HSF*-siRNA 1**	34.30	34.45	34.08	34.28	6.08	1.41	0.38
***HSF*-siRNA 2**	34.22	34.09	33.52	33.94	5.39	0.72	0.61
***HSF*-siRNA 3**	34.04	34.30	34.61	34.32	5.93	1.26	0.42
***β2m-siRNA* 1**	34.56	34.77	34.89	34.74	4.84	0.18	0.89
***β2m-siRNA* 2**	34.10	34.08	34.70	34.29	4.50	-0.17	1.13
***β2m-siRNA* 3**	34.50	34.65	34.00	34.38	4.16	-0.51	1.42

Numerical value (1,2,3) in rows and columns: indicate biological replicates and technical replicates respectively.

Table S.72 shows the average 2^-ΔΔCt, standard deviation (SD) and standard error of the mean (SEM) values of the *HSF* transcript abundance and the no-siRNA control

Average 2^-ΔΔCt	**Average**	**SD**	**SEM**
No-siRNA control	**1.01**	0.14	0.08
***RPL19*-siRNA**	**0.82**	0.41	0.23
β2m-siRNA	**1.14**	0.27	0.16

Table S.73 shows the *HSF* transcript abundance normalised against the no-siRNA control for each biological replicate

	***HSF*/ control**
Biological rep 1	0.41
Biological rep 2	0.66
Biological rep 3	0.36

APPENDIX K: HSF normalised against the control mean values for each treatment

Table S.74: HSF normalised against the control mean values of adult *An. funestus* males and females after being housed at one of three temperatures (20, 25 or 30°C) and being fed one of three siRNA treatments (HSF-siRNA, *β2m-siRNA* or no-siRNA control). Results are shown for each treatment.

Conditions		Males: HSF normalised against reference gene (SEM)	Females: HSF normalised against reference gene (SEM)
20°C 10ng/µl	No-siRNA control	1.000 (0.006)	1.003 (0,062)
	HSF-siRNA	0.490 (0.062) *	0.270 (0,072) *
	β2m-siRNA	1.007 (0.062)	0.897 (0,117)
20°C 20ng/µl	No-siRNA control	1,013 (0,124)	1,017 (0,128)
	HSF-siRNA	0,240 (0,015) *	0,307 (0,026) *
	β2m-siRNA	0,960 (0,045)	0,987 (0,175)
20°C 30ng/µl	No-siRNA control	1,017 (0,132)	1,01 (0,097)
	HSF-siRNA	0,467 (0,031)	0,133 (0,003) *
	β2m-siRNA	1,053 (0,271)	0,893 (0,058)
25°C 10ng/µl	No-siRNA control	1,047 (0,229)	1,017 (0,129)
	HSF-siRNA	0,310 (0,032)	0,457 (0,037) *
	β2m-siRNA	1.000 (0,190)	1,003 (0,149)
25°C 20ng/µl	No-siRNA control	1,030 (0,181)	1,050 (0,232)
	HSF-siRNA	0,593 (0,012)	0,433 (0,135)
	β2m-siRNA	1,107 (0,129)	0,947 (0,003)
25°C 30ng/µl	No-siRNA control	1,023 (0,156)	1,050 (0,227)
	HSF-siRNA	0,630 (0,069)	0,763 (0,062)
	β2m-siRNA	1,023 (0,090)	0,957 (0,182)
30°C 10ng/µl	No-siRNA control	1,040 (0,186)	1,027 (0,178)
	HSF-siRNA	0,537 (0,150)	0,467 (0,040)
	β2m-siRNA	1,030 (0,301)	1,200 (0,256)
30°C 20ng/µl	No-siRNA control	1,013 (0,103)	1,037 (0,198)
	HSF-siRNA	0,523 (0,037)	0,380 (0,035) *
	β2m-siRNA	1,013 (0,175)	1,023 (0,069)
30°C 30ng/µl	No-siRNA control	1.000 (0,058)	1,007 (0,082)
	HSF-siRNA	0,380 (0,060) *	0,470 (0,071) *
	β2m-siRNA	0,993 (0,174)	1,147 (0,153)

Asterisks indicate a statistically significant difference between treatments and controls when conducting the Tukey-HSD test

APPENDIX L: cDNA Dilutions To Confirm SiRNA Knockdown Throughout The Life Table Parameter Experiment

Day two

Males 20 ng/µl *HSF*-siRNA = $C_1V_1=C_2V_2$
(50 ng/µl)(100 µl)= (2456.6 ng/µl)(V_2)
5000/ 2456.6= V_2
V_2= 2 µl + 98 µl H_20

Females 20 ng/µl *HSF*-siRNA = $C_1V_1=C_2V_2$
(50 ng/µl)(100 µl)= (2239.2 ng/µl)(V_2)
5000/ 2239.2= V_2
V_2= 2.2 µl + 97.8 µl H_20

Males 20 ng/µl *β2m-siRNA* = $C_1V_1=C_2V_2$
(50 ng/µl)(100 µl)= (3087.6 ng/µl)(V_2)
5000/ 3087.6= V_2
V_2= 1.6 µl + 98.4 µl H_20

Females 20 ng/µl *β2m-siRNA* = $C_1V_1=C_2V_2$
(50 ng/µl)(100 µl)= (3306.5 ng/µl)(V_2)
5000/ 3306.5= V_2
V_2= 1.5 µl + 98.5 µl H_20

Males no-siRNA control = $C_1V_1=C_2V_2$
(50 ng/µl)(100 µl)= (2808.8 ng/µl)(V_2)
5000/ 2808.8= V_2
V_2= 1.8 µl + 98.2 µl H_20

Females no-siRNA control= $C_1V_1=C_2V_2$
(50 ng/µl)(100 µl)= (2370.6 ng/µl)(V_2)
5000/ 2370.6= V_2
V_2= 2.1 µl + 97.9 µl H_20

Day 10

Males 20 ng/µl *HSF*-siRNA = $C_1V_1=C_2V_2$
(50ng/µl)(100 µl)= (2529.4ng/µl)(V_2)
5000/ 2529.4= V_2
V_2= 2 µl + 98 µl H_20

Males 20 ng/µl *β2m-siRNA* = $C_1V_1=C_2V_2$

(50 ng/µl)(100 µl)= (2761.5ng/µl)(V_2)
5000/ 2761.5= V_2
V_2= 1.8 µl + 98.2 µl H_20

Males no-siRNA control = $C_1V_1=C_2V_2$
(50 ng/µl)(100 µl)= (2783.8 ng/µl)(V_2)
5000/ 2783.8= V_2
V_2= 1.8 ul + 98.2 µl H_20

APPENDIX M: Change Of Title Of Research

UNIVERSITY OF THE
WITWATERSRAND,
JOHANNESBURG

Private Bag 3 Wits, 2050
Fax: 027117172119
Tel: 02711 7172076

Reference: Mrs Sandra Benn
E-mail: sandra.benn@wits.ac.za

12 February 2023
Person No: 456102
TAA

Miss NW Bloch
Po Box 782139
Sandton
2146
South Africa

Dear Miss Nerissa Bloch

Doctor of Philosophy: Change of title of research

I am pleased to inform you that the following change in the title of your Thesis for the degree of **Doctor of Philosophy** has been approved:

From:	**The role of a sex-limited esterase (EZ976679) on anopheles funestus males**
To:	**HEAT SHOCK FACTOR (HSF) EXPRESSION AND ITS EFFECT ON LIFE TABLE PARAMETERS IN THE MAIN MALARIA VECTOR ANOPHELES FUNESTUS**

Yours sincerely

Mrs Sandra Benn
Faculty Registrar
Faculty of Health Sciences

APPENDIX N: Ethics Clearance Certificate

ANIMAL RESEARCH ETHICS COMMITTEE

Registration number: AREC-101210-002

Date: July 1, 2019

Certificate reference: 20190701-7O
Category: O
Re: Waiver from the Animal Research Ethics Committee of the University of the Witwatersran

Reference : Animal Ethics to complete
Re: Waiver from the Animal Research Ethics Committee of the University of the Witwatersrand
HoD applicant : Lizette Koekemoer
Staff number : 09700304
Degree : PhD/Msc Candidates
Study Title : "Studies on malaria vectors".
Department: Wits Research Institute for Malaria;
laboratory
Supervisor: Lizette Koekemoer, Givemore Munhenga, Yael Dahan-Moss, Shune Oliver, Basil Brooke and Maria Kaiser
Email: lizette.koekemoer@wits.ac.za
Address: 7 York Road, Parktown, Johannesburg, 2001
Tel: + 011-717 2486;
Full clearance certificate from the AREC of the University of the Witwatersrand is NOT required.
Reason: This study uses mosquitoes (invertebrates).
Comment/Notes :

1) This is a General Waiver for the PI and listed Supervisors.
2) Individual researchers and MSc & PhD candidates may require Ethics Clearance in the own name according to applicable rules of the Post-Graduate and other Committees.
3) Feeding of the mosquitos should be specified.

Please contact me should you require further information.

GP Candy

Geoffrey Candy PhD
Chair : Animal Research Ethics Committee

Geoffrey P Candy PhD
Professor, Department of Surgery, Faculty of Health Sciences, University of the Witwatersrand, 7 York Road Parktown 2193, Johannesburg; Tel: 27-11-717-2574; Email: geoffrey.candy@wits.ac.za

APPENDIX O: Plagiarism Declaration And Turnitin Report



PLAGIARISM DECLARATION TO BE SIGNED BY ALL HIGHER DEGREE STUDENTS

SENATE PLAGIARISM POLICY:

I, Nerissa Wendy Bloch (Student number: 456102) am a student registered for the degree of Doctor of Philosophy in the academic year 2023.

I hereby declare the following:

- I am aware that plagiarism (the use of someone else's work without their permission and/or without acknowledging the original source) is wrong.
- I confirm that the work submitted for assessment for the above degree is my own unaided work except where I have explicitly indicated otherwise.
- I have followed the required conventions in referencing the thoughts and ideas of others.
- I understand that the University of the Witwatersrand may take disciplinary action against me if there is a belief that this is not my own unaided work or that I have failed to acknowledge the source of the ideas or words in my writing.
- I have included as an appendix N report from "Turnitin" (or other approved plagiarism detection) software indicating the level of plagiarism in my research document.

Signature:  Date: 11 May 2024

Final_Nerissa Bloch_v5_Turnitin-1.docx

10 May 2023

ORIGINALITY REPORT

9%	8%	4%	2%
SIMILARITY INDEX	INTERNET SOURCES	PUBLICATIONS	STUDENT PAPERS

PRIMARY SOURCES

1	www.ncbi.nlm.nih.gov Internet Source	1%
2	wiredspace.wits.ac.za Internet Source	1%
3	Submitted to University of Witwatersrand Student Paper	<1%
4	www.science.gov Internet Source	<1%
5	Paul Jedlicka, Mark A. Mortin, Carl Wu. " Multiple functions of heat shock transcription factor ", The EMBO Journal, 1997 Publication	<1%
6	repositories.lib.utexas.edu Internet Source	<1%
7	www.coursehero.com Internet Source	<1%
8	Lalasoa Niain'ny Felamboahangy, Maria L. Kaiser, Munyaradzi Prince Zengenene, Fredros Okumu et al. "Optimisation of laboratory-	<1%

APPENDIX P : Publication Draft (awaiting comments from co-authors)

HEAT SHOCK FACTOR (*HSF*) EXPRESSION AND ITS EFFECT ON LIFE TABLE PARAMETERS IN THE MAIN AFRICAN MALARIA VECTOR *ANOPHELES FUNESTUS*

Bloch, N. W.[1,2], Koekemoer, L. L.[1,2] and Dahan-Moss, Y. L.[1,2]

[1] Wits Research Institute for Malaria, Faculty of Health Sciences, University of the Witwatersrand, Johannesburg, South Africa

[2] Centre for Emerging Zoonotic & Parasitic Diseases, National Institute for Communicable Diseases, a Division of the National Health Laboratory Service, Johannesburg, South Africa

ABSTRACT

Anopheles funestus is a major malaria vector in southern Africa and therefore it is essential to control this species. This necessitates studying the underlying factors that influence the biology of this species. In mosquitoes, the transcription factor, heat shock factor (HSF), is a key component in physiological and behavioral processes. However, there is limited information regarding HSF and its role in *An. funestus*. The aim of this study is to investigate the *HSF* transcript expression in the different life stages of *An. funestus*, and its biological role on the life table parameters in this species. The baseline transcript expression of *HSF* in all life stages of *An. funestus* were investigated using real-time quantitative PCR (qPCR). *Anopheles funestus* adults were fed with sugar water containing an optimised concentration of short interfering RNA that targets the *HSF* gene (HSF-siRNA). The transcript expression of *HSF* in HSF-siRNA treated *An. funestus* adults was confirmed via qPCR. The phenotypic effect of HSF-siRNA on longevity and reproduction in *An. funestus* was examined. *HSF* transcript expression analysis on the four life stages in *An. funestus*, showed that it was significantly lower at the egg and pupal stages compared to the larval and adult stages. The HSF-siRNA knockdown reduced both longevity and reproduction in *An.*

funestus. In conclusion, HSF is expressed at varying levels in all life stages, and might play a role in developmental processes. Heat shock factor plays a role in survival and reproduction, indicating the pleiotropic effect of HSF in *An. funestus*.

INTRODUCTION

Malaria is a devastating disease and according to the latest world malaria report, there has been an approximate 249 million cases and 608 000 malaria related death worldwide, with 94% of cases and 95% of death being in Africa (World Health Organization, 2023). Malaria is caused by the transmission of the protozoan, mainly *Plasmodium falciparum,* to humans by female *Anopheles* (Rogers and Randolph, 2000; Sinka *et al*., 2010). *Anopheles funestus* is a major malaria vector in Africa and therefore targeting this vector is crucial to reduce incidences of malaria. The use of insecticides is commonly used to control *An. funestus* such as pyrethroids, organophosphates, pyrroles, neonicotinoids, broflanilide, and carbamates (WHO, 1997; Govoetchan *et al.,* 2022; Ashu *et al.,* 2023). However, the rise of insecticide resistance in *An. funestus* populations from several locations in Africa such as, but not limited to, Sudan, Benin, Côte d'Ivoire and Tanzania, pose a problem for sustainable malaria control efforts (Sinka *et al*., 2010; World Health Organization, 2020; Akoton *et al*., 2023; Ibrahim *et al*., 2023; N'dri *et al*., 2023; Tungu *et al*., 2023). Therefore, other control interventions are necessary to reduce this species' population.

Heat shock factor is a transcription factor that exists mainly in a sequestrated and inactive state as a monomer which is inhibited by its association with heat shock proteins (HSPs) (Hightower, 1991). Cellular stresses can cause proteins in the cell to misfold and aggregate (Zhao and Jones, 2012; Chang *et al*., 2021) and once there is a cell stress such as heat, HSPs break away from HSF and bind to the misfolded proteins (Gross *et al.,* 2009). Once the HSPs have dissociated from HSF monomers, HSF trimerises and translocates to the cell nucleus where the HSF trimer binds to with heat shock elements (HSE) to activate the transcription of heat shock genes (Hightower, 1991; Gomez-Pastor *et al*., 2018).

Several studied have investigated insects under heat stress. Bai *et al*. (2022) investigated the gene *Bthsf1,* which encodes *HSF,* in the insect *Bemisia tabaci,* silverleaf whitefly. Analysis revealed that *Bthsf1* was up-regulated in *B. tabaci* adults and pupae. Additionally, after exposing *B. tabaci* to dsBthsf1 at -6°C and 41°C for one day, the expression of Bthsf1 was considerably downregulated, and mortality rose in comparison to the control (Bai et al., 2022). Similarly, heat stress dramatically raised the expression levels of *AhHsf* in *Agasicles hygrophila*. Double-stranded *AhHsf* RNA injection dramatically decreased egg production, shortened adult survival, and eventually decreased fertility in newly emerging adult *A. hygrophila* (Jin *et al*., 2020), while in *Liriomyza trifolii* high temperatures were generally accompanied by a decrease in *HSF1* expression. These opposing transcription patterns are indicative of the temporal nature of gene expression in response to heat stress (Chang *et al.*, 2021).

Heat shock factor is therefore necessary for temperature induced transcription, but pertinent to this study, it is also important for normal physiological roles such as development, under no stress, in several insect species (Ware-Gilmore *et al*., 2023). Jedlicka *et al.* (1997) identified four mutant alleles of the *Drosophila HSF* gene in order to clarify the *in vivo* roles of HSF. In Drosophila the reduced expression of *HSF* at a temperature of 25°C defined the role of *HSF* in early larval development and a *HSF* allele mutant that was sensitive to temperature was necessary for fertility while in *Chilo suppressalis* Walker, a rice pest moth, it was shown that *HSF* transcript expression was greatly increased during the male adult stage suggesting a role in adult development (Dong *et al.,* 2023). In *Anopheles gambiae*, there are three different isoforms of the HSF coding sequence, namely, HSF1, HSF2, and HSF3. These isoforms are produced during transcription. The DNA binding domain is shared by all isoforms. HSF1 and HSF2 have a 90% sequence similarity while HSF2 has an extra exon in its sequence. Heat shock factor 3 (HSF3) is a shorter splice variant isoform of HSF1 and HSF2 (Dottorini *et al*., 2013). The authors also showed that HSF1 have binding sites to male accessory gland genes suggesting a reproductive role. Therefore, it is important to investigate the reproductive and lifespan role that HSF plays in order to better understand the main malaria vector, *An. funestus*.

Since there is a need to understand *An. funestus* biology, for its control, and the fact that HSF is associated with physiological function in other anopheline and mosquito species, this study examined the importance of HSF in physiological roles such as longevity and reproduction in *An. funestus.*

RESULTS

The basal *HSF* gene transcript expression in the life stages of *An. funestus*

Heat shock factor transcript expression was significantly different across all the different life stages of *An. funestus* (one-way ANOVA: *p*= 0.0044, F= 9.98, DF (3, 8)). The HSF transcript expression was significantly lower in *An. funestus* eggs and pupae than larvae and adults, with adults having the highest HSF expression and eggs having a significantly lower expression of *HSF* than the other stages. The HSF transcript expression was 3.25-fold higher in larval versus egg stages (*p*< 0.0001), and 0.5-fold lower in the pupal versus the larval stage (*p*= 0.0008). The transcript expression of HSF was 1.9-fold higher in adults versus the pupal stage (p= 0.0002). The *HSF* transcript expression in *An. funestus* larvae versus adults was not significantly different (p= 0.3551) (Figure 1).

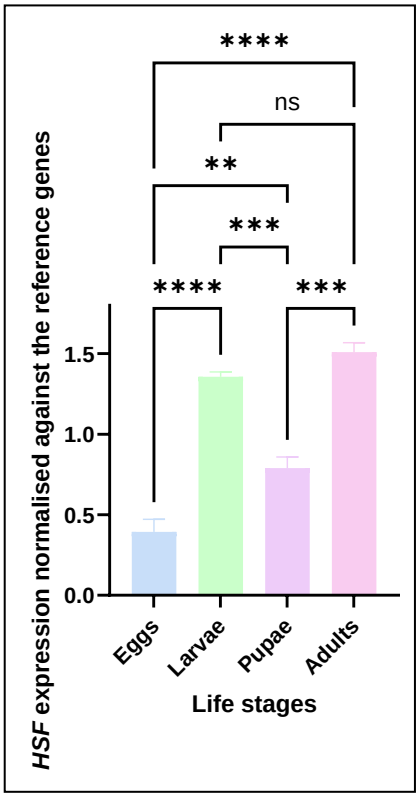


Figure 1: HSF transcript expression normalized against the reference genes, RPS7 and GAPDH, across the four life stages. The asterisks indicate a post-hoc test (ns p > 0.05; * p ≤ 0.05; ** p ≤ 0.01; *** p ≤ 0.001; **** p ≤ 0.0001). Error bars represent standard error of the mean (SEM)

Real-time quantitative PCR for quantitative analysis to assess success in HSF *knockdown*

The expression of *HSF* was examined in *An. funestus* males and females fed with 10% sugar water containing either HSF-siRNA, *β2m*-siRNA negative control or without siRNA (no-siRNA control), at 25°C. The HSF transcript expression was significantly lower in *An. funestus* males fed with HSF-siRNA versus males that fed with *β2m*-siRNA (p= 0.0007) or the no-siRNA control (p= 0.0007). However, HSF expression was not significantly different between males fed with *β2m*-siRNA control or the no-siRNA control (p= 0.9989) (Figure 2A).

The HSF expression was significantly lower in *An. funestus* females that were fed HSF-siRNA versus females fed with *β2m*-siRNA control (p= 0.0102), or the no-siRNA control (p= 0.0023). The HSF expression was similar in *An. funestus* females fed with *β2m*-siRNA control or no-siRNA (p= 0.3333) (Figure 2B). The feeding of *An. funestus* males and females with HSF-siRNA successfully reduced *HSF* expression and therefore HSF-siRNA was suitable to use in downstream experiments to examine the role of HSF in longevity and reproduction in *An. funestus*.

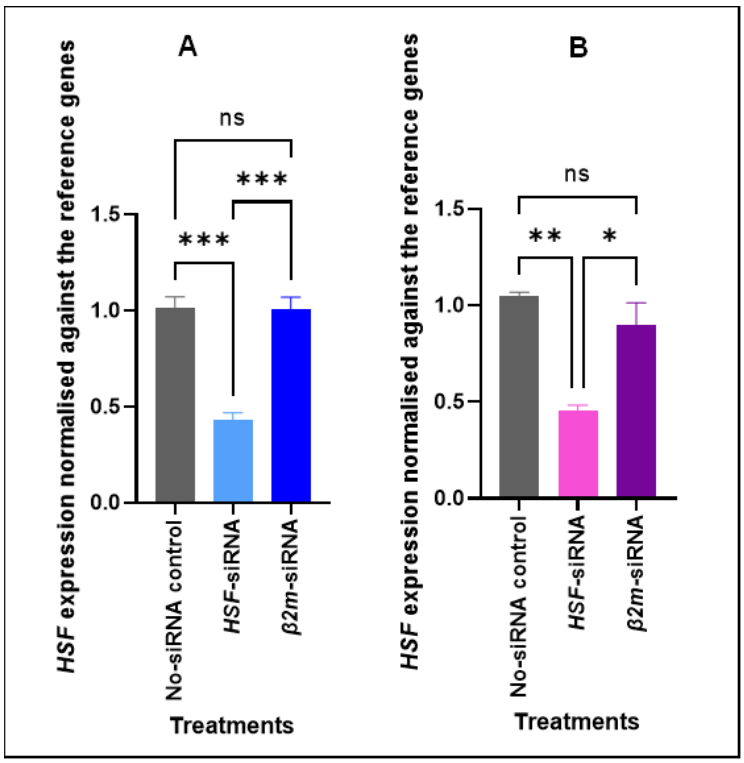


Figure 2: The relative HSF transcript expression normalised against the reference genes, RPS7 and GAPDH, in males (A) and females (B) at 25°C with treatment of 20 ng/µl siRNA. The asterisks indicate a post-hoc test (ns p > 0.05; * p ≤ 0.05; ** p ≤ 0.01; *** p ≤ 0.001; **** p ≤ 0.0001). Error bars represent standard error of the mean (SEM).

Determining the role of *HSF* in key life table parameters

i. Longevity

The feeding of *An. funestus* males and female adults with HSF-siRNA significantly reduced their longevity. HSF-siRNA treated males had a significant decrease in longevity when compared to the control males treated with *β2m*-siRNA (Log-rank: $\chi 2$= 7.381, *p*= 0.0066, DF= 2). Upon assessing the median longevity, *An. funestus* males fed with HSF-siRNA had a median survival time in days (IQR: Q1 – Q3) of 25 (23-26) days post feeding, while *An. funestus* that were treated with *β2m*-siRNA or no-siRNA had a median survival time of 31 (30-33) days and 32 (31-33) days respectively. This

translated to a 43% decrease in median survival time between the HSF knockdown samples and the control treatments (Figure 3A).

The overall vector longevity was significantly reduced in the HSF knockdown *An. funestus* female when compared to the females fed with *β2m*-siRNA or no-siRNA control (Log-rank: χ2= 7.956, p= 0.0048, DF= 2). *Anopheles funestus* females treated with HSF-siRNA had a median survival time of 32 (31-33) days post-feeding. The median survival time for *An. funestus* treated with *β2m*-siRNA and no-siRNA had a median survival time of 39 (37-40) days and 40 (39-42) days respectively. This translated to a 40.5% decrease in survival time in HSF knockdown females compared to the females from the control treatments (Figure 3B).

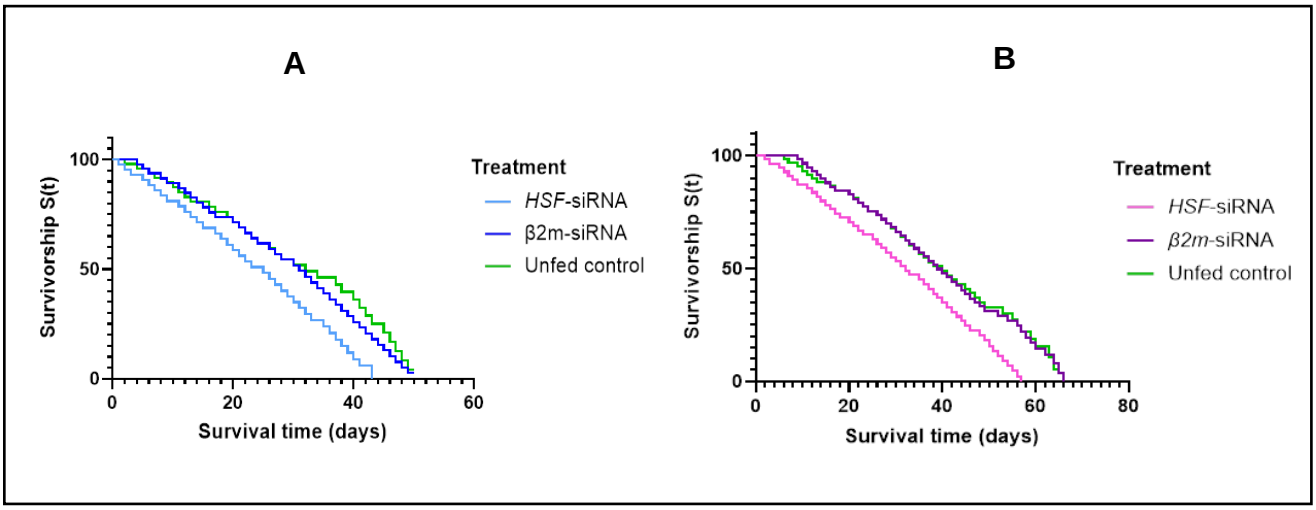


Figure 3: Kaplan-Meier survival analysis of male (A) and female (B) An. funestus assessed after treatment with siRNA. The different colours indicate the different treatments.

ii. Fecundity

Mating success of *An. funestus* females fed with HSF-siRNA, *β2m*-siRNA and no-siRNA control was assessed via spermathecal capsule dissections. The mating success was similar between *An. funestus* females treated with HSF-siRNA, *β2m*-siRNA or no-siRNA control (one-way ANOVA: *p*= 0.3944, F= 0.3636, DF (2, 6)) (Figure 4).

There was a statistically significant difference between the mean number of eggs laid per female and the control treatments. The *β2m*-siRNA and no-siRNA control treatments had a mean fecundity of approximately 60 eggs laid per female mosquito, while those treated with HSF-siRNA had mean fecundity of 38 eggs laid per female (Table 1). *Anopheles funestus* treated with HSF-siRNA had a 36.6% decrease in fecundity, when compared to the control treatments (one-way ANOVA: $p<0.0001$, F=3 100, DF (2, 6)).

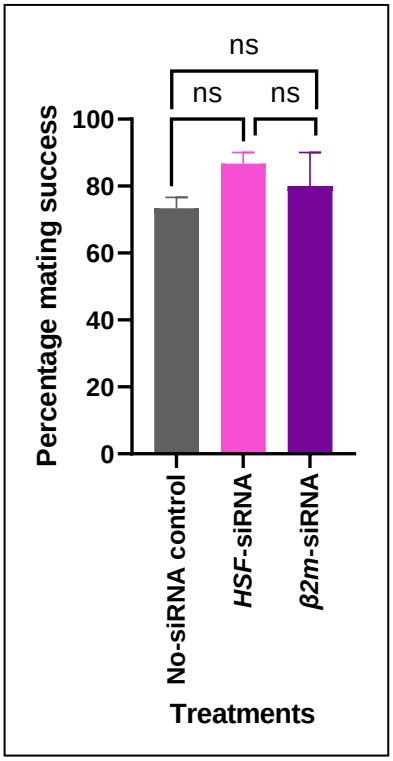


Figure 4: Percentage mating success in females across three treatments (HSF-siRNA knockdown (86.67%), β2m-siRNA knockdown (80%) and no-siRNA control (73.33%)). No significance (ns) between treatments was calculated. Error bars represent the standard deviation (S.D.).

Table 1: Mean fecundity values between the An. funestus mosquitoes which ingested three siRNA treatments (HSF-siRNA, β2m-siRNA and no-siRNA control). Results are shown for each treatment, with the average standard deviation (±S.D.) and total sample size (N).

Treatment	Total number of eggs laid	Mean number of eggs laid per female ±S.D. (% eggs laid); (95% CI); N
HSF-siRNA	922	38.42 ± 0.4452 (79.99% [a]); (38.89- 38.00); 30
***β2m*-siRNA**	1, 608	61.85 ±0.3223 (86.67% [b]); (61.85-61.26); 30
No-siRNA control	1, 600	59.26 ± 0.4120 (89.99% [b]); (59.88- 59.10); 30

Data was analysed using the Log-rank test and a one-way ANOVA test (p< 0.001). Letters that differ are statistically significant as determined by a post-hoc Tukey test.

iii. Fertility

Fertility was measured as the mean number of eggs that hatched and the overall vector fertility was significantly reduced in the HSF knockdown *An. funestus* mosquitoes when compared to the two control treatments. *Anopheles funestus* females treated with HSF-siRNA had a 9% decrease in fertility, when compared to the mean of the *β2m*-siRNA and no-siRNA control treatments, and this was statistically significant (one-way ANOVA: p= 0.003, F= 17.55, DF (2, 6)). The control treatments had a mean hatch rate of 76%, while those treated with HSF-siRNA had a mean hatch rate of 63% (Table 2).

iv. Time-to-hatch

All eggs that were oviposited by *An. funestus* females were allowed to hatch over a period of 10 days and the median time-to-hatch values were then compared. When assessing the median time-to-hatch in days (IQR: Q1 – Q3), the eggs laid by *An. funestus* females treated with HSF-siRNA had a hatch time of 5.5 (3.5-5) days post-oviposition. Eggs that were oviposited by *An. funestus* females that were treated with β2m-siRNA had a median time-to-hatch of 6 (5.5-7) days post-oviposition and the no-siRNA control had a median time-to-hatch of 8 (6.5-8.5) days post-oviposition. The median time-to-hatch values were compared between the HSF knockdown samples and the control treatments (Log-rank: $\chi 2$= 2.895, p= 0.235, DF= 2) (Figure 5). This this

translated to a 21.4% significant decrease when compared to the average median time-to-hatch of the controls.

Table 2: Mean fertility values between the An. funestus mosquitoes which ingested three siRNA treatments (HSF-siRNA, β2m-siRNA and no-siRNA control). Results are shown for each treatment, with the average standard deviation (±S.D.) and total sample size (N)

Treatment	Total number of eggs hatched	Mean % of eggs hatched ±S.D.; (95% CI); N	Median time to hatch (Inter-quartile range)
HSF-*siRNA*	630	63 ±0.443; (70.3-68.5); 30[a]	5.5 (3.5-5)
β2m-siRNA	1, 203	75 ±0.567; (75.3- 76.7); 30[b]	6 (5.5-7)
No-siRNA control	1, 237	77 ±0.496; (77.9-78.1); 30[b]	8 (6.5-8.5)

Data was analysed using the Log-rank test and a one-way ANOVA test (p>0.005). Letters that differ are statistically significant as determined by a post-hoc Tukey test.

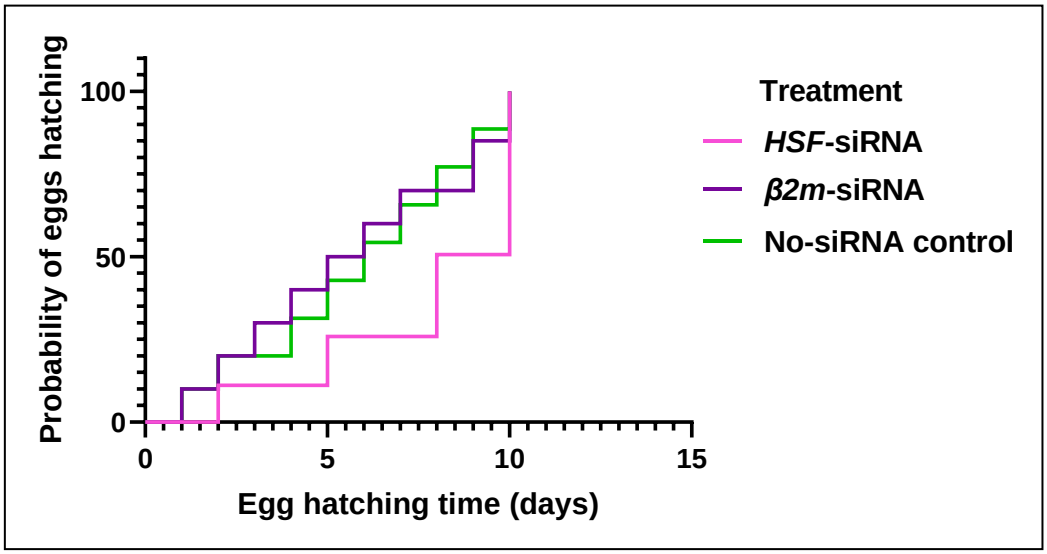


Figure 5: Kaplan-Meier survival analysis of An. funestus fertility (time-to-hatch) assessed after treatment with siRNA. Samples treated with HSF-siRNA (pink) had a time-to-hatch of 5.5 days,

β2m-siRNA had a median time of 6 days (purple) and the no-siRNA control had a median time of 8 days (green).

DISCUSSION

The purpose of this study was to examine the expression of the HSF transcript in the various life stages of *An. funestus* and its biological role in the life table parameters of this species. Because HSF is essential in several physiological and behavioural functions in mosquitoes and little is known about HSF and how it functions in *An. funestus* it was important to study this gene and assess its function in *An. funestus*. HSF was expressed in all life stages of *An. funestus* and therefore is most likely to be a critical molecule in insect development and survival. The *HSF* basal transcript expression in *An. funestus* eggs and pupae was significantly lower when compared to larvae and adults which shows a dynamic flexibility (up and down) as the eggs develop through to the adult. This is not unique to *An. funestus*, and differences in HSF transcript expression have also been observed in *Chilo suppressalis* Walker, a rice pest moth whereby *HSF* expression was highest in the adult male stage (Dong *et al*., 2023) and *Cotesia chilonis*, a parasitoid wasp where *HSF* expression was lowest in the second instar larvae and adults and highest in the third instar larval and pupal stages (He *et al*., 2021).

The complicated life cycle of mosquitoes comprises of both aquatic and terrestrial stages. Temperatures can have an impact on mosquito developmental time and certain life stages are more susceptible to environmental stress than others (Harada and Goto, 2017). Higher temperatures and stressors are combatted in insects using the heat shock response whereby HSF initiates the transcription of genes that code for stress proteins such as molecular chaperones. Therefore, *HSF* transcript expression during periods of high stress and heat may be particularly crucial at certain stages of development (Sørensen and Loechcke, 2002).

The eggs, larvae and pupae of *An. funestus* are found solely in water yet only larvae showed a higher *HSF* transcript expression. This may be due to the fact that eggs have the exochorion, endochorion and serosal cuticle, that allows the egg to be viable

outside of the water (Farnesi *et al*., 2017). In this case HSF may not be required at such large quantities in this life stage due to other mechanisms of protection from the environment. Larvae undergo four developmental instars stages and the larval stage is the longest of all four life stages. The fact that *HSF* transcript expression was highest at this stage suggests a metamorphosis or moulting role and that HSF might be expressed to deal with environmental stress and larval-pupal transition as was seen in *Drosophila* where *HSF* expression was highest in the larval stage (Jedlicka *et al*., 1997). Pupae is the last water stage to be discussed and it does not feed. They are mobile and can dive to avoid predators (Awasthi *et al.,* 2012). The egg and pupal stages are the developmental stages. This suggests that HSF does not play as big a role in the development of *An. funestus* but may have a role in larval and adult development. In other *An. gambiae* transcript studies (whole genome studies) the eggs have the fewest differentially expressed genes, hence during embryo development the insect might put resources into other transcripts that are important for development (Gokhale *et al*., 2013). The adults stage is the only terrestrial stage and had the highest *HSF* expression of the four stages. This suggests HSF plays a crucial role in terms of survival against environmental conditions and regulation of growth and aging. This may further extend to perhaps play a role in germline cell development such as oogenesis and spermatogenesis as seen in *Drosophila* species (Jagla *et al*., 2018) which suggests a reproductive role.

Once the basal transcript expression of HSF was confirmed and that the transcript expression was highest in adults, sugar water containing HSF-siRNA was fed to adult *An. funestus* to knockdown HSF. This method proved suitable due to its ease of use and its benefit of use during downstream HSF studies whereby the effect of HSF was examined on longevity and reproduction.

The longevity of *An. funestus* males and females was significantly decreased by 18.65% after HSF knockdown with HSF-siRNA. Males fed with HSF-siRNA lived shorter than females fed with HSF-siRNA. This is consistent with what is known in the literature as studied in *Ae. albopictus* (De *et al*., 2022) and *An. funestus*, *An. gambiae*, *Ae. aegypti* and *Ae. albopictus* whereby females survived on average 1.2 days longer than males without siRNA feeding (Lambert *et al*., 2022). This disparity between males

and females may be because females generally survive longer since they require time to mate, feed primarily on blood, digest that meal, make eggs, and then lay those eggs in a favourable area (Lambert *et al*., 2022). Males however, are only required to mate and then soon after perish (Barredo and DeGennaro, 2020). Additionally, several different species of mosquitoes' adult females can endure hostile situations, yet when males are faced with such brutal circumstances, they only occasionally persist (Kirby and Lindsay, 2009). The same pattern is seen in this study whereby HSF-siRNA females survived for a median of 25 days and males for only 32 days. A study examined the sugar feeding habits of *Cx. quinquefasciatus* and *Ae. aegypti*. The mean sugar volume in the bodies of female *Aedes* and *Culex* was higher than that of the males. The authors assumed a higher sugar volume suggested a higher volume uptake of sugar bait in females when compared to males (Olson *et al*., 2020). Seeing as the females take more sugar than males, they may have ingested more siRNA. This was an important discovery since *Anopheles* mosquitoes can spread malaria parasites 14 days after gametocyte infection (Bray and Garnham, 1982). The female mosquito must remain alive for at least 14 days after gametocyte infection in order to transmit the parasite. Seeing as *HSF* knockdown reduces *An. funestus* female longevity to a median of 39 days, this approach would not work to eliminate the vector population before the end of the extrinsic incubation period. However, *HSF* knockdown could affect the susceptibility of the female to the parasite and this needs to be investigated.

HSF knockdown in *An. funestus* females resulted in a 36.6% decrease in vector fecundity, and a 9.2% decrease in vector fertility. A disturbance in midgut homeostasis via HSF-siRNA introduction may lessen the availability of nutrients following a blood meal in addition to shortening the mosquito's lifespan. Re-absorption of the growing follicles due to *HSF* knockdown, during the gonotrophic cycle, might limit vector oviposition in *An. funestus*. These observations are seen by Lea et al. (1972) in *Ae. aegypti* whereby the hypothesis that the size of an egg batch is matched by the re-absorption of developing follicles was postulated. In addition, in this study, eggs hatched two days later in HSF-siRNA treated females than in controls. Eggs that remain in the water for longer are more vulnerable and exposed to ovicides such as dinitrophenol compounds and petroleum oils (Smith and Salkeld, 1966). This would ultimately mean the eggs would be targeted and the life cycle would no longer continue. However, one could argue that ovicides in the water poses a deleterious effect on

human health (Agrawal et al., 2010). Eco-friendly tools have been recently implemented against mosquito vectors, including botanical insecticides (Benelli, 2015).

It is true that the almost 20% reduction in longevity, seen in the HSF-siRNA treated *An. funestus* females, will still enable these females to feed and transmit malaria. However, the additional reduction in fecundity (just under 40%) and fertility (almost 10%) seen in *An. funestus* female treated with HSF-siRNA will very likely reduce this vector's population numbers. However, it is possible to use RNAi approaches and combining different target genes in a "super sugar bomb" tactic might have the desired impact of eliminating this vector. To expand on this idea, dsRNA is extremely stable and past studies have shown that dsRNA can last at least 7+ days under insectary conditions (Bennett and Koekemoer, unpublished), hence making this an attractive idea to supplement current sugar toxic baited approaches (Revay *et al*., 2015; Fiorenzano *et al*., 2017; Traore *et al*., 2020; Kumar *et al*., 2023). Other target genes that have been targeted by RNAi and shown to result in reduced reproductive success include the G protein-coupled receptors (GPCRs) (Keyes-Scott *et al.,* 2023), reproductive genes (GAP005958, AGAP011377 and AGAP007280) (Hammond *et al*., 2016), ribosomal proteins (RPS6 and RPL26) (Estep *et al*., 2016), Krüppel homologue 1 (Kr-h1) (Ojani *et al*., 2018), etc. The "super sugar bomb" approach can easily be evaluated under laboratory and semi-field conditions as a proof of principle. Coy *et al.* (2012) employed gene knockdown and mosquito ingestion to investigate the impact of dsRNA introduction into mosquitoes using attractive toxic sugar bait (ATSB) techniques in *Ae. aegypti*. A mixture of two dsRNA was used. Spraying vegetation and bait stations are the two common implementation strategies for ATSB (Kumar *et al*., 2023). The ATSB approach has proven to be quite effective in suppressing the mosquito vector population in sub-Saharan Africa, Israel, and the United States of America among other regions (Müller *et al*., 2010; Revay *et al*., 2015; Fiorenzano *et al*., 2017). For example, ATSB containing the insecticide dinotefuran used against *Anopheles* mosquitoes in Mali drastically reduced the density of mosquitoes, number of older females and sporozoite prevalence demonstrating how ATSB significantly reduces malaria parasite transmission (Traore *et al*., 2020). HSF-siRNA can be used to target other anopheline species as the specific HSF-siRNA is homologous to *An. stephensi*, *An. merus*, *An. gambiae*, *An. coluzzii* and *An. arabiensis.*

In conclusion, *HSF* may be involved in developmental processes and is expressed at different levels across all life stages. The fact that *HSF* is involved in both survival and reproduction suggests that *HSF* has multiple phenotypic expressions in *An. funestus*.

EXPERIMENTAL PROCEDURES

Study samples

Laboratory-reared eggs, larvae, pupae, and adults of *An. funestus* females and males from the FUMOZ colony were used in this research. FUMOZ was established in 2000 using wild-caught *An. funestus* material from southern Mozambique (Hunt *et al*., 2005). The colony is housed in the Botha de Meillon Insectary (Vector Reference Laboratory (VRL), National Institute of Communicable Diseases (NICD), Johannesburg, South Africa), at 80% humidity and 25°C with a 12-hour light; 12-hour dark cycle and 45-minute dusk/ dawn simulation. Mosquito larvae are fed a powdered diet consisting of a mixture of Beeno® dog biscuits (Beeno® South Africa, http://www.beeno.co.za) and Brewer's yeast in a 3:1 ratio (Zengenene *et al*., 2021).

Assessing the *HSF* transcript expression in all the life stages in *An. funestus*

Experimental setup

Experimental setup involved obtaining samples from each stage of the *An. funestus* life cycle at 25°C. Newly emerged *An. funestus* female and male adults were placed in W32.5 X D32.5 X H32.5 cm BugDorm® rearing cages (Megaview Science Co., Ltd, Taichung, Taiwan) in the Botha de Meillon Insectary. The three cages contained 40 female and 40 male adults each to allow for mating for 10 days as this has been shown to be the optimal amount of time for mating in *An. funestus* (Maharaj *et al*., 2022). During this time mosquitoes were allowed to feed *ad libitum* on 10% sucrose solution that was supplied. At day 10 the males were removed.

Obtaining samples from each life stage

At day 13, blood fed females were removed from the cages and placed in separate oviposition cups. The eggs laid in each oviposition cup were removed and then separated by which 300 eggs were removed for RNA extraction and stored in the

laboratory. The remaining eggs were transferred into rectangular larval rearing bowls (120 mm width X 200 mm length X 70 mm height) and filled with 750 ml of distilled water and left to further develop. Larvae were fed twice daily on a mixture described previously. After 13 days, 30 fourth instar larvae were removed from each bowl and sacrificed to be stored in the laboratory for use during RNA extraction. Once the larvae pupated, 30 pupae from each bowl were removed and sacrificed for RNA extraction. The remaining larvae were used to further develop into adults and 20 male and 20 female adults were removed from each bowl for RNA extraction. Three biological replicates were performed and a total of 900 eggs, 60 fourth instar larvae, 48 pupae and 48 newly emerged adults were required for RNA extraction and subsequent cDNA synthesis. It is difficult to sex individual eggs and larvae, although some laboratories use size separation on *Aedes* mosquitoes as a technique. Size separation is not possible for anophelines and therefore, it was assumed that the eggs and larvae were mixed with both males and females in equal ratios as no gender distortion has been reported for this colony. In order to allow for proper comparison, it was decided that the pupae and adults of both genders should be mixed in equal proportion as well.

RNA extraction, Dnase I treatment and cDNA synthesis

RNA was extracted from *An. funestus* using the TRIzol™ extraction method according to the manufacturer's instructions (Invitrogen, 15596018) and treated with Dnase I (New England Biolabs, M03035) The quality and integrity of the RNA was evaluated using a NanoDrop™ spectrophotometer (Thermo Scientific, ND-2000) and RNA native gel respectively. The RNA native gel was viewed using a Molecular Imager Gel Doc XR System (BioRad, 170-8170) RNA was then converted to cDNA using QuanitiNova Reverse Transcription Kit (Qiagen, 205411) according to the manufacturer's instructions. The number of eggs, larvae, pupae, and adults required for RNA extraction differed. RNA was extracted from 300 eggs, 20 larvae, 16 mixed pupae and 16 mixed adults in a 1:1 gender ratio. Due to the size difference between eggs and larvae compared to pupae and adults, more biological material (300 eggs and 20 larvae vs. 16 pupae and 16 adults) was required to ensure sufficient RNA was extracted. In order to determine the genders of the pupae, they were viewed under a microscope to determine the gender of each pupa and pupae of each gender were separated in a 1:1 ratio prior to RNA extraction. The cDNA was then diluted to a concentration of 50 ng/µl in a 100 µl distilled water solution to be used in qPCR.

Real-time Quantitative PCR

Primers targeting the *HSF* gene were designed by Dr. Yael Dahan-Moss using the Vector Base accession number AFUN004137-RA and normalized by Macrogen (Table 3). Real-time PCR amplification was performed according to the instructions of iQ™ SYBR® Green Supermix (dNTPs, iTaq™ DNA Polymerase, $MgCl_2$, fluorescein) (BioRad, 1708882) and was made up to a final volume of 25 µl. The RT-qPCR cycling conditions were as follows: 94°C for 2 minutes and then 94°C for 30 secs, 55°C for 30 secs and 72°C for 40 secs for 42 cycles. The cycling conditions then ended with 72°C for 10 mins and a 4°C hold. qPCR was followed with melt curve analysis for all products and a no-template control (no cDNA) was included to ensure no contamination. Each reaction was run with three biological replicates, each with three technical replicates. The *RPS7* and *GAPDH* genes were used for normalising the data. qPCR data were analysed using the relative transcript expression ratio method whereby the change in Ct (∆Ct) was calculated as ∆Ct = Ct (average Ct of gene of interest) – Ct (average Ct of reference gene) (Livak and Schmittgen, 2001; Pfaffl, 2001). The ∆Ct was subsequently used to calculate the delta-delta Ct (∆∆Ct) value, which is the difference between the aforementioned ∆Ct values. The ∆∆Ct method, also known as the 2–∆∆Ct method, is a simple formula used in order to calculate the relative fold transcript expression of samples when performing real-time PCR. This method gives an output of a fold change value which is an increase or decrease of the gene of interest normalized against a reference gene (Livak and Schmittgen, 2001).

Table 3: Sequences and sequence length of HSF primers.

Primer		Sequence 5'-3'	Amplicon length
HSF	Forward	GCACCCGTAGTAGCAATGGT	206 bp
	Reverse	CCAAGGTTCCTTGATCGTGT	

Assessing the effect of siRNA targeted to the *HSF* gene on life table parameters

Study treatments

Three treatments were included in these experiments. An exogenous gene, mouse beta-2-microglobulin (*β2m*) was used as a non-specific negative control (Da costa *et al*., 2014). The gene, *β2m* is not present in *An. funestus* and therefore feeding this siRNA to mosquitoes should not alter the transcript expression. A no-siRNA control was included, which contains sugar water and green food colouring dye, but no siRNA. The gene of interest, heat shock factor, was included to assess gene transcript expression and life table parameter effects after the use of HSF-siRNA.

Primer	Sequence 5'→ 3'	Amplicon length	Gene sequence
β2m (forward)	GAGAAUGGGAAGCCGAACAUA	21 bp	AH001856.2 (GenBank)
β2m (reverse)	UAUGUUCGGCUUCCCAUUCUC		
HSF (forward)	GACGAUGAAGCAGGAGAAUGA	21bp	AFUN004137-RA (Vector Base)
HSF (reverse)	UCAUUCUCCUGCUUCAUCGUC		

RNA interference

For RNAi experiments, siRNAs were designed by Dr. Yael Dahan-Moss and were synthesised by Ambion (Life Technologies) (Table 4).

Table 4: Sequences and sequence length of HSF and β2m-siRNA

siRNA delivery

A solution of 1 ml of 5% sugar water solution was added directly into each microcentrifuge tube that had the lid removed. The solution was made up of (490 µl) RNA free water, (500 µl) 10% sucrose, 10µl 20ng/µl siRNA solution and a drop of blue gel food colouring (Cake Flora Gel Food Colouring (Forest Green and Navy Blue, www.cakeflora.co.za). These mosquitoes were provided with siRNA-treated sugar water throughout the experiment in order to sustain knockdown. Paper cups with a 280 ml capacity were covered by a 15 cm-by-15 cm piece of gauze that was secured by an elastic band were used and the microcentrifuge tube was fastened upside down into the gauze to allow for feeding.

Determine the role of *HSF* in key life table parameters

i. Longevity

Longevity was evaluated at 25°C and three treatment BugDorm® cages containing a total of 60 newly emerged adult female and male mosquitoes were setup. Each treatment cage was provided with *ad libitum* on the relevant 20 ng/µl sucrose-siRNA-food colouring solution. Three biological replicates were performed. The rate of survival was monitored until 100% mortality was reached for all three treatments.

ii. Fecundity

At day 10, 10 females from each cage were removed, immobilised and spermathecal capsule dissections were performed to assess insemination status. This was implemented to ensure that a change in fecundity, fertility and time-to-hatch were not due to mating success. The terminalia and last abdominal segment of the females were removed in order to expose the spermatheca which was subsequently observed via microscopy at 100X magnification to determine mating status (Methods in Anopheles Research Manual, 2015). The females were either scored “yes” for the presence of spermatozoa (mated) or “no” for the absence of spermatozoa (not mated). The proportion of females mated was calculated as a percentage for each biological replicate.

Mosquito fecundity was analysed using a total of 40 newly emerged virgin female *An. funestus* adult mosquitoes per each treatment. Forty untreated 2-day-old male mosquitoes, as genital rotation of all males reaches the final stage of rotation only 36 hours post emergence (Dahan and Koekemoer, 2013), were introduced to each cage and were left there for 10 days to allow for mating to take place, after which the male mosquitoes were removed from the cages. At day 10, 10 females from each cage were removed to assess mating success as previously described. The remaining females fed *ad libitum* on distilled water which replaced the 10% treated sucrose solution in order to encourage blood feeding at day 11. Two subsequent blood meals were offered to mated females at days 11 and 13 (Munhenga *et al.,* 2016) and the females were

provided with 10% sucrose solution to feed b*ad libitum* throughout this period. After receiving the second blood meal at day 13, each female was transferred into a separate oviposition cup. Mosquitoes were maintained on their respective sucrose solutions by 0.1 g of sterilised cotton wool placed on top of the gauze throughout the experiment until oviposition had taken place and the number of eggs laid were counted by microscopy.

iii. Fertility

Fertility was assessed by determining the number of eggs that hatched from the eggs that were laid. Fertility experimental setup followed on from the fecundity study whereby the laid eggs were monitored to determine the time taken to hatch.

iv. Time-to-hatch

Time-to-hatch was determined by monitoring the hatch time over 10 days. Eggs that did not hatch 10 days post-oviposition were considered infertile.

Statistical analysis

GraphPad Prism was used for all the statistical analyses and creating the graphs (Version 9.0 for Windows, GraphPad Software, USA, www.graphpad.com). In order to assess *HSF* transcript expression in all four life stages, the Shapiro-Wilk test tested data for normality, and those that passed the test were taken into consideration for further analysis. The significance of the differences between treatments was assessed using a one-way ANOVA and Tukey's post hoc test. A Kaplan-Meier survival curve was used to analyse longevity and the Log-Rank test was used to calculate statistical significance of survivability. Fecundity and fertility was determined as the mean number of eggs laid (fecundity) or hatched (fertility) per female which was compared between the treatment and controls, using a one-way analysis of variance (ANOVA), and a Tukey *post-hoc* test. This was done to analyse the differences in means of each variable (Munhenga *et al*., 2016), and report on correlations that were observed. The Kaplan-Meier survival curve was used to analyse fecundity and fertility and the Log-Rank test was used to calculate statistical significance. The Log-rank test was used to

determine whether there was a statistically significant difference in vector time-to-hatch between the various treatments (Log-rank: $p<0.05$).

REFERENCES

Agrawal, A., Pandey, R. and Sharma, B. (2010) Water pollution with special reference to pesticide contamination in India. Journal of Water Resource and Protection, 2(5), pp.432-448.

Akoton, R., Sovegnon, P. M. and Djihinto, O. Y. (2023) Vectorial competence, insecticide resistance in Anopheles funestus and operational implications for malaria vector control strategies in Benin Republic. Malaria Journal, 22, pp.1-12.

Ashu, F. A., Fouet, C., Ambadiang, M. M., Penlap-Beng, V. and Kamdem, C. (2023) Enhancing the efficacy of neonicotinoids against mosquitoes and overcoming resistance issues. bioRxiv [Preprint].

Awasthi, A., Wu, C. and Hwang, J. (2012). Diving as an anti-predator behaviour in mosquito pupae. Zoological Studies, 51, pp.1225-1234.

Bai, J., Liu, Y., Wei, R., Wang, Y., Gong, W. and Du, Y. (2022) Knockdown of heat shock transcription factor 1 decreases temperature stress tolerance in *Bemisia tabaci* MED. Scientific Reports, 12(1), pp.16059-16070.

Barredo, E. and DeGennaro, M. (2020) Not just from blood: mosquito nutrient acquisition from nectar sources. Trends in Parasitology, 36(5), pp. 473-484.

Benelli G. (2015) Plant-borne ovicides in the fight against mosquito vectors of medical and veterinary importance: a systematic review. Parasitology Research, 114(9), pp.3201-3212.

Bray, R.S. and Garnham, P.C.C. (1982) The life cycle of primate malaria parasites. British Medical Bulletin, 38(2), pp.117-122.

Chang, Y. W., Zhang, X. X., Chen, J. Y., Lu, M. X., Gong, W. R. and Du, Y. Z. (2021) Characterization of three heat shock protein 70 genes from *Liriomyza trifolii* and transcript expression during thermal stress and insect development. Bulletin of Entomological Research, 109(2), pp.150-159.

Coy, M. R., Sanscrainte, N. D., Chalaire, K. C., Inberg, A., Maayan, I., Glick, E., and Becnel, J. J. (2012) Gene silencing in adult *Aedes aegypti* mosquitoes through oral delivery of double-stranded RNA. Journal of Applied Entomology, 136(10), pp.741–748.

Da Costa, M., Pinheiro-Silva, R., Antunes, S., Moreno-Cid, J. A., Custódio, A., Villar, M., Silveira, H., de la Fuente, J. and Domingos, A. (2014) Mosquito *Akirin* as a potential antigen for malaria control. Malaria Journal, 13 (470), pp.1-17.

Dahan, Y. L. and Koekemoer, L. L. (2013) Analysis of the genitalia rotation in the male *Anopheles funestus* (Diptera: Culicidae). Acta Tropica, 132, Suppl:S20-5.

De, S., Sharma, G., Bhattacherjee, R., Mandal, U.,Banerjee D. and Suman, D. S. (2022) Life table, survival and fecundity parameters of *Aedes albopictus* (Diptera: Culicidae) strains from desert and coastal regions of India. Acta Tropica, 235, pp. 106625-106639.

Dong, C. L., Feng, Z., Lu, M. X., and Du, Y. Z. (2023). *Chilo suppressalis* heat shock proteins are regulated by heat shock factor 1 during heat stress. Insect Molecular Biology, 32(1), pp.69-78.

Dottorini, T., Persampieri, T., Palladino, P., Spaccapelo, R. and Crisanti, A. (2012) Silencing of the *HSF* gene, the transcriptional regulator of *A. gambiae* male accessory glands, inhibits the formation of the mating plug in mated females and disrupts their monogamous behaviour. Pathogens and Global Health, 106(7), pp.405-412.

Dottorini, T., Persampieri, T., Palladino, P., Baker, D. A., Spaccapelo, R., Senin, N. and Crisanti, A. (2013) Regulation of *Anopheles gambiae* male accessory gland genes influences postmating response in female. The FASEB Journal, 27, pp.86 –97.

Estep, A. S., Sanscrainte, N. D. and Becnel, J. J. (2016) DsRNA-mediated targeting of ribosomal transcripts RPS6 and RPL26 induces long-lasting and significant reductions in fecundity of the vector Aedes aegypti. Journal of Insect Physiology, 90, pp.17-26.

Farnesi, L. C., Vargas, H. C. M., Valle, D. and Rezende, G. L. (2017) Darker eggs of mosquitoes resist more to dry conditions: Melanin enhances serosal cuticle contribution in egg resistance to desiccation in *Aedes, Anopheles* and *Culex* vectors. PLoS Neglected Tropical Diseases, 11(10), pp.e0006063.

Ferguson, H. M., John, B., Ng'habi, K. and Knols, B. G. J. (2005) Redressing the sex imbalance in knowledge of vector biology. Trends in Ecology and Evolution, 20(4), pp.87-95.

Fiorenzano, J.M., Koehler, P.G., Xue, R.D. (2017) Attractive toxic sugar bait (ATSB) for control of mosquitoes and its impact on non-target organisms: a review. International Journal of Environmental Research Public Health, 14(398), pp.345-360.

Gokhale, K., Patil, D. P. and Dhotre, D. P. (2013) Transcriptome analysis of *Anopheles stephensi* embryo using expressed sequence tags. Journal of Bioscience, 38, pp.301–309.

Gomez-Pastor, R., Burchfel, E. T. and Thiele, D. J. (2018) Regulation of heat shock transcription factors and their roles in physiology and disease. Nature Reviews Molecular and Cell Biology 19(1), pp.4–19.

Govoetchan, R., Fongnikin, A., Syme, T., Small, G., Gbego, M., Todjinou, D., Rowland, M., Nimmo, D., Padanou, G. G. and Ngufor, C. (2022) VECTRON™ T500, a new broflanilide insecticide for indoor residual spraying, provides prolonged control of pyrethroid-resistant malaria vectors. Malaria Journal, 21, pp.1-14.

Gross, T. L., Myles, K. M. And Adelman, Z. N. (2009) Identification and characterization of Heat Shock 70 Genes in *Aedes aegypti* (Diptera: Culicidae). Journal of Medical Entomology, 46(3), pp.496-504.

Hammond, A., Galizi, R. and Kyrou, K. (2016) A CRISPR-Cas9 gene drive system targeting female reproduction in the malaria mosquito vector *Anopheles gambiae*. Nature Biotechnology, 34, pp.78-83.

Harada, E. and Goto, S.G. (2017) Upregulation of heat-shock proteins in larvae, but not adults, of the flesh fly during hot summer days. Cell Stress Chaperones, 22(6), pp. 823-831.

He, F., Zhu, F., Lu, M. and Du, Y. (2021) Comparison of morphology, development and transcript expression patterns of *HSF* and *hsp11.0* of *Cotesia chilonis* under normal and high temperature. PeerJ, 9, pp. e11353.

Hightower, L. E. (1991) Heat shock, stress proteins, chaperones, and proteotoxicity. Cell, 66, pp.191-197.

Hunt, R. H., Brooke, B. D., Pillay, C., Koekemoer, L. L. and Coetzee, M. (2005) Laboratory selection for and characteristics of pyrethroid resistance in the malaria vector *Anopheles funestus*. Medical and Veterinary Entomology, 19(3), pp.271-275.

Ibrahim, S. S., Muhammad, A. and Hearn, J. (2023) Molecular drivers of insecticide resistance in the Sahelo-Sudanian populations of a major malaria vector *Anopheles coluzzii.* BMC Biology, 21, pp.125-132.

Jagla, T., Dubińska-Magiera, M., Poovathumkadavil, P., Daczewska, M. and Jagla, K. (2018) Developmental transcript expression and functions of the small heat shock proteins in *Drosophila*. International Journal of Molecular Science, 19(11), pp.3441-3450.

Jedlicka, P., Mortin, M. A. and Wu, C. (1997) Multiple functions of *Drosophila* heat shock transcription factor in vivo. EMBO Journal, 16, pp.2452–2462.

Jin, J., Li, Y., Zhou, Z., Zhang, H., Guo, J. and Wan, F. (2020) Heat shock factor is involved in regulating the transcriptional expression of two potential Hsps (AhHsp70 and AhsHsp21) and its role in heat shock response of *Agasicles hygrophila*. Frontiers in Physiology, 11, pp. 1-10.

Keyes-Scott, N. I., Swade, K. R., Allen, L. R. and Vogel, K. J. (2023) RNAi-mediated knockdown of two orphan G protein coupled receptors reduces fecundity in the yellow fever mosquito *Aedes aegypti*. Frontiers in Insect Science, 3, pp.70-79.

Kirby, M. J. and Lindsay, S. W. (2009) Effect of temperature and inter-specific competition on the development and survival of *Anopheles gambiae* sensu stricto and *An. arabiensis* larvae. Acta Tropica, 109, pp.118-123.

Kumar, G., Gupta, S. K. and Pasi, S. (2023) Attractive toxic sugar baits: a magic bullet for control of malaria and dengue in urban settings of India? Journal of Vector Borne Diseases 60(3), pp.340-341.

Lambert, B., North, A., Charles, H. and Godfray, J. (2022) A Meta-analysis of Longevity Estimates of Mosquito Vectors of Disease. bioRxiv, Cold Spring Harbor Laboratory.

Lea, A.O. (1972) Regulation of egg maturation in the mosquito by the neurosecretory system: the role of the corpus cardiacum. General and Comparative Endocrinology, Supplement 3, pp.602-608.

Livak, K. J. and Schmittgen, T. D. (2001) Analysis of relative gene transcript expression data using real- time quantitative PCR and the 2–ΔΔct method. Methods, 25, pp.402–408.

Maharaj, S., Ekoka, E., Erlank, E., Nardini, L., Reader, J., Birkholtz, L. and Koekemoer, L. L. (2022) The ecdysone receptor regulates several key physiological factors in *Anopheles funestus*. Malaria Journal, 21, pp.1-13.

Methods in *Anopheles* Research - MR4 (2015) Available at: https://www.yumpu.com/en/document/view/49409322/methods-in-anopheles-research-mr4. [Accessed 10 July 2023].

Müller, G.C., Beier, J.C., Traore, S.F. et al. Successful field trial of attractive toxic sugar bait (ATSB) plant-spraying methods against malaria vectors in the *Anopheles gambiae* complex in Mali, West Africa. Malar J 9, 210 (2010).

Munhenga, G., Brooke, B. D., Gilles, J. R., Slabbert, K., Kemp, A., Dandalo, L. C., Wood, O. R., Lobb, L. N., Govender, D., Renke, M. and Koekemoer, L. L. (2016) Mating competitiveness of sterile genetic sexing strain males (GAMA) under laboratory and semi-field conditions: steps towards the use of the Sterile Insect Technique to control the major malaria vector *Anopheles arabiensis* in South Africa. Parasites & Vectors, 9(1), pp.1-12.

N'Dri, B. P., Wipf, N. C. and Saric, J. (2023) Species composition and insecticide resistance in malaria vectors in Ellibou, southern Côte d'Ivoire and first finding of *Anopheles arabiensis* in Côte d'Ivoire. Malaria Journal, 22(93), pp.1-12.

Ojani, R., Fu, X., Ahmed, T., Liu, P. and Zhu, J. (2018), Krüppel homologue 1 acts as a repressor and an activator in the transcriptional response to juvenile hormone in adult mosquitoes. Insect Molecular Biology, 27, pp.268-278.

Olson, M. F., Garcia-Luna, S., Juarez, J. G., Martin, E., Harrington, L. C., Eubanks, M. D., Badillo-Vargas, I. E. and Hamer, G. L. (2020) Sugar Feeding Patterns for *Aedes aegypti* and *Culex quinquefasciatus* (Diptera: Culicidae) Mosquitoes in South Texas. Journal of Medical Entomology, 57(4), pp.1111-1119.

Pfaffl, M. W. (2001) A new mathematical model for relative quantification in real-time RT–PCR. Nucleic Acids Research, 29(9), pp.e45.

Revay, E. E., Schlein, Y., Tsabari, O., Kravchenko, V., Qualls, W., De-Xue, R., Beier, J. C., Traore, S. F., Doumbia, S., Hausmann, A. and Müller, G. C. (2015) Formulation of attractive toxic sugar bait (ATSB) with safe EPA-exempt substance significantly

diminishes the *Anopheles sergentii* population in a desert oasis. Acta Tropica, 150, pp.29-34.

Rogers, D. J. and Randolph, S. E. (2000) The global spread of malaria in a future, warmer world. Science, 289, pp.1763- 1766.

Sinka, M. E., Bangs, M. J., Manguin, S., Coetzee, M., Mbogo, C. M., Hemingway, J., Patil, A. P., Temperley, W. H., Gething, P. W., Kabaria, C. W. and Okara, R. M. (2010) The dominant Anopheles vectors of human malaria in Africa, Europe and the Middle East: occurrence data, distribution maps and bionomic précis. Parasites & Vectors, 3(1), p.1-34.

Smith, E H. and Salkeld, E. H. (1966) The use and action of ovicides. Annual Review of Entomology, 11(1), pp.331-368.

Sørensen, J. G. and Loeschcke, V. (2002) Decreased heat-shock resistance and down-regulation of Hsp70 transcript expression with increasing age in adult *Drosophila melanogaster*. Functional Ecology,16, pp.379–384.

Traore, M. M., Junnila, A. and Traore, S. F. (2020) Large-scale field trial of attractive toxic sugar baits (ATSB) for the control of malaria vector mosquitoes in Mali, West Africa. Malaria Journal, 19(72), pp.1-14.

Tungu, P., Kabula, B. and Nkya, T. (2023) Trends of insecticide resistance monitoring in mainland Tanzania, 2004–2020. Malar Journal, 22(100), pp.1-14.

Ware-Gilmore, F., Novelo, M., Sgrò, C. M., Hall, M. D. and McGraw, E. A. (2023) Assessing the role of family level variation and heat shock gene transcript expression in the thermal stress response of the mosquito *Aedes aegypti.* Philosophical Transactions of the Royal Society of Biological Sciences, 27, pp.378-390.

World Health Organization (1997) Chemical methods for the control of vectors and pests of public health importance (Edited by Chavasse, D. C., and Yap, H. H.). Geneva. Available at: https://www.who.int/whopes/resources/who_ctd_whopes_97.2/en/. [Accessed on 12 December 2022].

World Health Organization (2020) Global Vector Control Response. Available at: https://www.who.int/teams/controlofneglectedtropicaldiseases/interventions/strategies/vector-control. [Accessed 15 August 2023].

World Health Organization (2023) World Malaria Report 2023. Available at: https://www.who.int/publications/i/item/9789240086173. [Accessed on 30 November 2023]

Zengenene, M. P., Munhenga, G., Okumu, F. and Koekemoer, L. L. (2021) Effect of larval density and additional anchoring surface on the life-history traits of a laboratory colonized *Anopheles funestus* strain. Medical and Veterinary Entomology, 36(2), pp.451-459.